Elucidating the mechanism of thymineless death in *Escherichia coli* using global strategies

A Dissertation
SUBMITTED TO THE FACULTY OF
UNIVERSITY OF MINNESOTA
BY

Bree Hamann

IN PARTIAL FULFILLMENT OF THE REQUIREMENTS
FOR THE DEGREE OF
DOCTOR OF PHILOSOPHY

Adviser: Arkady Khodursky, Ph.D.

March 2013

Acknowledgements

I would like to acknowledge the tremendous support I received from my family and friends throughout my years at the University of Minnesota, as well the advice and help from previous lab members over the years. I especially want to thank Aaron for his emotional support which carried me through the most trying circumstances, and I also want to thank Gini & Ray for giving so much of their time and resources to help me raise Elanor during certain challenging times.

The time spent with colleagues and support staff in my program and in Gortner Laboratories made coming to work interesting and fulfilling, and I appreciate all the supportive words and stimulating conversations. I want to especially thank my DGS', Darlene Toedter, and Kristi Lecy for taking me under their wings, helping me mediate problems in the lab, and helping me navigate the intricacies of graduate school bureaucracy. They helped our lab find ways to keep me supported in the program, and I would never have succeeded without their intervention. I'd also like to sincerely thank my committee, especially Janet Schottel who went out of her way to give me explicit guidance in my writing, and advice concerning my work and future plans. Finally, I would never have been able to complete my thesis without the support and guidance of my adviser Arkady Khodursky. In spite the many difficult situations I found myself in, he never judged me, and respected my ideas, interpretations, and plans, while sometimes reserving his personal opinion. This forced me to take more responsibility as a scientist, and I felt more confident to take risks. I learned how to become a critical thinker, an independent researcher and lab manager, which is something I would never have accomplished in a different setting.

Dedication

For my family.

Abstract

Antibiotic resistance is one of the world's most pressing public health problems. An international survey published in 2000 measured the prevalence of antimicrobial resistance to commonly prescribed antibiotics, and found that *E. coli* had developed resistance of between 15-30% to ampicillin and Bactrim©, two of the most commonly prescribed antibiotics (Kahlmeter, 2002). Methotrexate, 5-fluorouracil, and Bactrim© are commonly prescribed antibiotics and cancer treatment therapies which are thought to work by a phenomenon known as thymine-less death. These treatments have been so effective in both bacteria and mammals, in part, because they target the fastest growing cells within the human body killing off cancer and bacterial infections. However, as is the case for all antibiotics eventually, their efficacy is waning. While finding new targets and therapeutic molecules is important in combating multi-resistant microorganisms and cancers, there is no guarantee that such new treatments will be any less toxic to the human host, nor more effective against their targets than what current antibiologicals used to show. Understanding the effects of thymine deprivation on the cell may open new avenues for drug targeting that will bypass current means of survival by the infectious cells resulting in maintaining use of the currently FDA-approved treatments in conjunction with new drug therapies.

In this thesis I discuss work analyzing the mechanism of killing of two types of antibiotics. One is a type II topoisomerase inhibitor, simocyclinone D8, which affects supercoiling of the circular bacterial chromosome. My work described in chapter 1 show that gram negative bacteria are susceptible to the drug when their drug-efflux capacity is compromised via a knock-out of the AcrB efflux pump. Chapters 2 through 5 describe published and unpublished work concerning the mechanism of thymineless death, phenomenon purported to be the mechanism of action for such commonly prescribed drugs as 5-fluoro-2-deoxyuridine, trimethoprim, methotrexate, and other anti-folate drugs.

Table of Contents

List of Tables

Page No.

List of Figures

Chapter 1: Introduction

1.1 An Introduction to the State of DNA in a Living Cell: Replication, Organization, and Repair in *Eschericia coli*

1.1.1. Structure of DNA

All living organisms pass on their traits to their offspring. The molecule which encodes these traits in all free-living organisms, from single to multi-cellular, is deoxyribonucleic acid, or DNA. The central dogma of molecular biology describes how information encoded by DNA becomes transcribed or 'read' into RNA (ribonucleic acid), which in turn is translated into the functional parts or proteins of a living cell. Disrupting the normal information flow may have devastating consequences for the cell.

Bacteria are robust systems in which to study DNA and processes associated with it. The first real evidence that DNA contained the genetic information of the cell was shown in bacteria, when Avery, McCarty and McLeod showed that DNA from a virulent pneumococcal strain of bacteria could 'transform' a non-virulent strain into a virulent one (Mccarty, Avery, & MacLeod, 1944), and since then bacteria have continued to be helpful for the discovery of DNA replication and repair proteins that are highly conserved across all living organisms.

The structure of DNA as first described by James Watson and Francis Crick in 1953, consists of two strands of a sugar-phosphate backbone with nucleotide bases forming a hydrogen-bond ladder up the middle (Figure 1.1)(Watson & Crick, 1953). Inspired by an X-ray diffraction photo taken by Rosalind Franklin and Raymond Gosling, Watson and Crick realized that in order to accommodate the chemistry of the nucleotide bases which make up DNA, the molecule must have the structure of a double-helix (Klug, 1968). Further work done by Meselson and Stahl showed that DNA replicates in a semi-conservative fashion, meaning that parent strands separate, and become the template for synthesis of new daughter strands (Meselson & Stahl, 1958). Therefore, the new DNA duplex consists of one parental strand and one daughter strand. The discovery of

this semi-conservative replication had great implications for DNA replication regulation, as well as DNA repair.

The chemical building blocks that make up DNA and RNA are called deoxyribonucleotides and ribonucleotides respectively (Figure 1.2). These building blocks are made of three parts: a phosphate group, a sugar moiety and one of four types of nitrogenous bases. The ribose sugar which makes up the sugar-phosphate backbone of RNA has one more hydroxyl group at the 2' carbon than the ribose sugar that makes up the backbone in DNA, thus the term '2'-deoxyribonucleotide'. To form a strand of DNA, nucleotides are linked into chains, with the phosphate and sugar groups alternating. This affects the helical geometry of each molecule and helps enzymes which function on either molecule to recognize the proper substrate. While the main purpose of DNA is to store the genetic code and that of RNA is to express it and transfer it to protein making ribosomes, they share most of the same nitrogenous bases. Three of the four canonical bases used in DNA synthesis (cytosine, guanine, and adenine) are utilized in RNA as well, with thymine in DNA and uracil in RNA being the only differing bases. Aside from some rare sugars in the peptidoglycan layer of the bacterial cell wall (He & Liu, 2002), the major role of thymine is as a component of deoxythymidine triphosphate for use in DNA replication in *Escherichia coli*. It is generally well-accepted that DNA is the evolutionary descendant of RNA as a biological information storage molecule, and it has been proposed that it became so due to its sturdier deoxyribose-containing sugar backbone. It is not known, however, whether thymine as a nucleotide constituent is as old. For instance, DNA polymerase has a similar affinity for deoxythymidine-triphosphate, as for deoxyuridine-triphosphate (Warners, 1978), a faculty that would have been unnecessary if DNA began with thymine as one of the constituent nucleotide bases. It has been proposed that thymine is the evolutionary descendant of uracil due to its more stable nature (Jonsson, 1996). Uracil glycosylases are a universal family of enzymes that excise uracil from DNA, and while most uracil

glycosylases will remove uracil from all DNA whether it is base-paired with adenine or guanine, there exist glycosylases which remove uracil specifically from G-U pairings leaving A-U base-pairings intact (Neddermann & Jiricny, 1994). The presence of such a discriminating glycosylase may be because early DNA molecules used uracil rather than thymine as one of the four canonical bases.

1.1.2. Initiation of DNA replication on the bacterial chromosome

In all organisms, DNA replication starts or initiates at a location on the DNA chromosome called an origin. In *E. coli* there is one origin, the *oriC* from which replication proceeds bi-directionally. Because a good deal of energy is required to separate the strands of DNA to begin synthesis, some protein factors exist which help melt the DNA such that replication proteins can access the template. In *E. coli*, an initiator protein DnaA is responsible for the initial melting of DNA near the origin of replication (Figure 1.3). DnaA binds to the energy molecule ATP in the cell as well as it's less energetic, dephosphorylated form, ADP (Kurokawa, *et al.*, 1999). The ratio of DnaA-ATP to DnaA-ADP is one of the regulatory signals controlling initiation of replication. When resources are plentiful, DnaA-ATP concentration is high, and cells initiate replication more frequently. DnaA-ATP has a higher affinity for the *oriC* region than does DnaA-ADP, and ATP hydrolysis must occur to provide the energy for the melting of the DNA strands (Sekimizus, Bramhillq, & Kornberg, 1988). Upon melting the duplex, DnaA then helps direct the loading of the DnaB helicase onto the chromosome near the origin (Marszalek & Kaguni, 1994). DnaB helicase requires the DnaC helicase loader for loading at any site of initiation (Allen & Kornberg, 1991). A helicase uses energy to unwind DNA ahead of replication, and two helicases are loaded at the origin of replication, each proceeding in an opposite direction from the other. The unwinding of the duplex DNA produces a fork-like structure consisting of the duplex parental DNA (the 'stem' of the fork), and the two single DNA strands (the 'prongs' of the fork).

Replication proteins are loaded and proceed along behind this replication fork (Wus, Zechnero, & Marians, 1992).

1.1.3. Role of Topoisomerases

DNA in a cell is organized into a compact, highly coiled structure called a chromosome. Without such compaction, the cell would not be able to contain the vast stretches of DNA within its boundaries (reviewed in Olins & Olins, 2003). However such compaction causes another complication in DNA replication. DNA helicase alone does not have the energy necessary to separate strands of supercoiled duplex DNA, and as DNA helicase pulls a part strands of a duplex, the DNA ahead of a helicase becomes overwound creating an even greater energy barrier to overcome. To aid in alleviating this helical stress, cells have enzymes called topoisomerases which bind to single-or double-stranded DNA, and cut the phosphodiester backbone of the DNA to relieve the helical stress. While maintaining the integrity of the sequence and shape of the strand, the topoisomerase relieves the tension caused by over- or under-winding, and the unwound strand can then be resealed leaving the DNA helix intact for helicases to continue pulling apart ahead of a replication fork. Topoisomerases are differentiated by the number of strands they break, and the coiled structure they target differs. Type I topoisomerases break only one strand of the duplex DNA, allow the unbroken strand to pass through the cut strand, and then reseal the cut (Figure 1.4). This helps alleviate the additional twists that occur ahead of the unwinding of the DNA helicase. However, sometimes the over-twisted DNA doubles up on itself forming a 'supercoil.' Type II topoisomerases relieve this 'supercoil' by breaking both strands of one helix, and passing another unbroken helix through it and resealing the cut (Figure 1.5). This relieves the 'supercoiling' of the DNA ahead of the helicase. The problem of DNA compaction is different in bacteria versus more complex organisms. Nucleosomes in more complex organisms bind to negatively-supercoiled DNA and relieve superhelical

stress (Clark & Felsenfeld, 1991). Positive supercoiling is associated with higher levels of transcription, whereas negative supercoiling is associated with compaction (Lee & Garrard, 1991). The type II topoisomerase gyrase is primarily found in bacteria and is responsible for introducing 'negative supercoils.' This is also helpful for alleviating the positive supercoils generated by the DNA helicase during replication. Bacterial gyrase is quite different structurally than those gyrases that may be present in eukaryotes and therefore is a prime target for a number of commonly used antibiotics including aminocoumarins (which target the ATP hydrolyzing part of gyrase), and quinolones (which target the DNA-binding and cutting portion of gyrase). Chapter 2 of this thesis addresses work that shows the effects of a novel drug which works in a manner different from either of these two classes of gyrase-targeting drugs.

1.1.4. Replication complex components

Other components of the replication machinery are the polymerase (Pol III in *E. coli*) which does the actual DNA synthesis, a clamp which serves as a processivity factor, or helps keep the polymerase bound to the DNA during replication (β), and the clamp loader (γ) (Figure 1.6). DNA strands have a chemical polarity; the nucleotides are strung together by a connection between the 5' hydroxyl end of one sugar molecule and the 3' hydroxyl end of another sugar molecule on each nucleotide via a phosphate bridge moiety (phosphodiester bond)mmmmmmmm,,k. One end of the DNA molecule will have a free 5' phosphate, and is referred to as the 5' end, while the other end will have a free 3' hydroxyl group and is referred to as the 3' end (Figure 1.1). DNA polymerase (Pol III) in *E. coli,* as in all living organisms, requires a primer to begin replication, and only synthesizes DNA in a 5' to 3' direction. To accommodate the requirement for a primer, an enzyme called primase synthesizes a short RNA primer from which DNA Pol III can begin synthesis. The RNA part of this primer must be removed and filled with DNA nucleotides by DNA polymerase I (Pol I) after the Pol III holoenzyme has passed

through. Because the strands of DNA which must be replicated are anti-parallel, that is, one strand runs in a 5' to 3' direction while the other runs in a 3' to 5' direction, replication must accommodate the limitations of DNA Pol III by organizing the 3' to 5' strand in such a way that it can still be replicated in a 5' to 3' direction. DNA helicase DnaB unzips the DNA duplex on the 3' to 5' strand which is then extruded in a loop which provides a stretch of single-stranded DNA to which primase can add primers in a staggered fashion and a second DNA polymerase then hops on in the middle of the loop of unwound DNA and synthesizes in a 5' to 3' direction until it reaches the next RNA/DNA hybrid at which point it ceases replication. That polymerase then dissociates, and binds at the next primed part of DNA within the loop, thus this strand is called the lagging strand, as it can only be synthesized in spurts, or in a discontinuous fashion. The 'leading strand' polymerase can continuously synthesize in a 5' to 3' direction adding nucleotides to the parental strand as fast as the helicase can unwind the duplex. The gaps between the discontinuous fragments of nascent DNA of a lagging strand fragments, also known as 'Okazaki' fragments, are filled by DNA Pol I.

1.1.5. Dealing with DNA replication during exponential growth in bacteria and the role of SeqA protein

E. coli can divide every 20 minutes when in exponential growth, however the bacterial chromosome requires at least 40 minutes to replicate. Nevertheless each daughter cell must contain a whole copy of the parental chromosome to remain viable. Bacterial cells compensate for this by initiating new rounds of replication before previous rounds have finished (Figure 1.7). For this reason, *E. coli* cells can have as many as 8 replication forks proceeding simultaneously (Atlung & Hansen, 1993). These forks must be spatially separated enough such that new forks are not started before previous forks have had a chance to move away from the origin of replication. This is regulated by a number of factors. One of these factors exploits the semi-conservative

nature of the newly synthesized duplex DNA. Newly synthesized DNA is not yet methylated, meaning the new strand of DNA has not had $–CH_3$ groups added to certain nucleotide residues. This methylation is used by the cell for a variety of purposes, including recognizing the new strand as different from the parental strand. Since the older parental strand is methylated, this hemi-methylated DNA becomes the target of certain initiation-inhibiting proteins. For instance, in *E. coli*, SeqA proteins bind and oligomerize on hemi-methylated GATC sequences just behind the advancing fork. This helps block the association of DnaA to the origin of replication until the DNA adenine methyltransferase (Dam methylase) can methylate the daughter strand of DNA giving time for previously loaded forks to move away from the origin. SeqA then dissociates from the fully methylated strand which is now available for new priming complexes formed by DnaA initiator protein.

1.1.6. Types of DNA repair

The hemi-methylated nature of nascent or new DNA is also important in post-replicative repair. While the Pol III holoenzyme has remarkable fidelity, it will occasionally make mistakes incorporating an improper nucleotide base resulting in kinks in the DNA. These mistakes must be repaired by special enzymes in a process called DNA repair. When there is a mismatch in the newly replicated DNA, it is most often repaired by mismatch repair (MMR) enzymes or Mut proteins in *E. coli* (Figure 1.8). These enzymes target the unmethylated strand of DNA since it is likely that the mistake has occurred in the nascent strand of DNA. MutL and MutS proteins travel along the DNA duplex and recognize aberrations in the helical structure of the DNA. The MutH protein then nicks the DNA on either side of the aberration in the unmethylated strand. MutH then unwinds the DNA duplex releasing the nicked region. The gap remaining is then filled by Pol I (Fukui, 2010).

Sometimes interactions with chemicals in the cell or ultraviolet irradiation can damage individual bases or alter their chemical make-up. Other major types of DNA repair processes that target spontaneous damage are base excision repair (BER) and nucleotide excision repair (NER). Base excision repair can be as simple as a particular DNA glycosylase enzyme (which recognizes a certain base, like cytosine or uracil) flipping out bases along the DNA until it reaches a base it recognizes as aberrant and catalyzes hydrolytic removal of the damaged base (Figure 1.9). An AP endonuclease enzyme then cuts the phosphodiester backbone that had been associated with that base, and DNA polymerase fills in the missing nucleotide. DNA ligase then reseals the backbone generating a whole duplex once again (Robertson, *et al.,* 2009). Nucleotide excision repair often handles bulky DNA lesions that cause helical deformities (Figure 1.10). There are many variations of NER, but one of the simplest involves the products of the *uvrA* and *uvrB* genes. UvrA and UvrB form a complex which scans the DNA helix and halts when it detects noticeable distortions in the DNA duplex. The UvrB portion remains at the lesion, and recruits UvrC endonuclease which then makes two cuts on either side of the lesion on the damaged strand. UvrD helicase then binds and separates the damaged strand from the parental strand releasing the segment of damaged single-stranded DNA from the rest of the molecule. At this point, the Uvr proteins dissociate from the DNA, and DNA polymerase and DNA ligase come in to fill the gap (Petit & Sancar, 1999).

Two types of repair rely on homologous recombination of DNA, or the ability of DNA strands to swap between two separate helices as long as the sequence matches between the two. When DNA is damaged such that both strands are compromised or at a single-strand gap in the daughter DNA where the parental DNA has sustained the damage, “swapping” strands with an intact DNA duplex is the best way to ensure DNA polymerase has a correct template on which to perform repair synthesis. One type of repair most often utilized in the case of double-strand breaks utilizes RecBC proteins.

Another less-understood, but equally important pathway for repair is called 'daughter strand gap repair' and is mediated by the RecF pathway in *E. coli*. RecF is essential for post-replicative repair in cells suffering from DNA damaging agents during active growth and replication (Kuzminov, 1999).

Proteins in the RecBCD pathway repair double-strand breaks and require a blunt end to initiate repair (Figure 1.11). RecBCD exonucleolytic enzyme complex (exonuclease V) requires a blunt or nearly blunt double-strand break as a substrate, RecB acts as a helicase, RecC as a 3'->5' exonuclease, and RecD as a 5'->3' exonuclease. This complex loads at a blunt double-strand end, and travels along the DNA degrading both strands. When the enzyme complex encounters an octameric sequence termed 'chi' (5'GCTGGTGG3' in *E. coli*), the 3'-> 5' nuclease activity is attenuated and a 3' single-stranded DNA tail is generated. This tail can then be bound by the primary recombination protein, RecA (the equivalent protein in eukaryotes is called RAD51). RecA then can engage in a homology search, invading neighboring DNA duplexes and base pairing the single strand of DNA it has loaded on with a complete duplex. This reaction generates a physical structure which is recognized by DNA replication complexes which then load and complete repair synthesis. Later these crossover structures are resolved by proteins which cut the DNA at what are termed Holliday junctions, and with or without exchange of strands, the DNA is restored to a whole condition (Kuzminov & Stahl, 1999).

The other form of repair which utilizes recombination as an intermediate is the RecA-dependent RecF pathway of DNA repair. When a single- or double strand break is unavailable, RecA is unable to displace the single-strand binding protein (SSB) which coats single-stranded DNA. RecF binds at the junction of a double-strand, single-strand gap and facilitates the loading of RecA onto the single-strand DNA and removal of SSB

allowing RecA to filament along the single-stranded DNA and initiate recombination-mediated repair (Figure 1.12) (Morimatsu, Wu, & Kowalczykowski, 2012).

1.1.7. Thymineless death in *E. coli* and the SOS DNA damage response.

Thymineless death (TLD) has been studied for decades and yet the mechanism of killing remains elusive. It is the process by which cells of all types, from bacteria to cancer cell lines, lose viability upon starvation for thymine. Thymine is a nucleotide base found only in DNA. Thus its synthesis, catabolism and availability are inextricably linked with DNA metabolism, including replication, repair and recombination.

In 1953 Barner and Cohen observed that starving bacterial cells of thymine, as opposed to xanthine or hypoxanthine (the building blocks of purines like guanine and cytosine), resulted in an exponential drop in viability as measured by colony-forming units of bacteria grown on rich media plates after starvation (Cohen & Barner, 1953). They also found that starving auxotrophic bacteria for other amino acids or pyrimidine bases (phenylalanine, histidine, or uracil) did not result in a drop in viability although their growth flat-lined (Barner & Cohen, 1957; Cohen & Barner, 1956). These thymine-starved cells continued to accumulate "cytoplasmic mass" but DNA replication had abruptly stopped, a set of events termed "unbalanced growth." This definition was further refined to mean limited continuation of protein and RNA synthesis after thymine withdrawal (Gallant & Suskind, 1962; Hanawalt, 1963). Since that time it has been discovered that amino acid starvation elicits a 'stringent response' which results in the up-regulation of nearly a third of the genes in bacteria to protect the cell from starvation conditions, however stringent response results in "balanced growth" as opposed to thymineless death related "unbalanced growth" (Table 1.1). This is likely because the stringent response slows most metabolic functions of the cell (including DNA replication, replication initiation and transcription) which seems to help render the cell more "immune" to the effects of certain antibiotics (Nguyen et al., 2011).

Drugs which are purported to work through thymineless death are most effective in fast-growing cells like bacteria or cancer. The study of thymineless death has been useful for developing therapeutic targets in mammalian cells (Berger & Berger, 2006; Gmeiner, 2005), and also for elucidating the mechanisms of commonly prescribed antibiotics in bacteria (e.g. trimethoprim). Analyzing the effects of thymine starvation in eukaryotic cells is difficult as they are committed to cell death, or apoptosis, upon thymine starvation (Ayusawa, *et al.*, 1983). Apoptosis is a complex phenomenon which can result from the effects of many processes in the cell, and it is often difficult to differentiate between the effects that are simply a by-product of programmed cell death, and those that are thymineless death-specific. The complexity of eukaryotic cells as well as the long history of genetic study in bacterial model organisms has allowed for thymineless death to be most extensively studied in bacteria, particularly the model organism *Escherichia coli*.

The major role of thymine is as one of the four canonical bases used in the synthesis of DNA, and the only nucleotide that does not have a ribonucleotide counterpart. In both prokaryotes and eukaryotes thymidylate synthase catalyzes the reductive methylation of deoxyuridine monophosphate to deoxythymidine monophosphate using a methyl group donated by 5,10-methylenetetrahydrofolate. In fact, dihydrofolate reductase, encoded in E. coli by FolA and FolM , is a target of many antibiotics, and inhibition of this enzyme inhibits thymidylate synthase indirectly. This reaction provides the sole *de novo* source of thymidylate in the cell. Without this enzyme cells must scavenge thymidine from their environment through active transport or diffusion.

While myriad characteristics of cells undergoing thymine starvation have been documented and thoroughly reviewed by others (Ahmad, Kirk, & Eisenstark, 1998; Zaritsky, *et al.*, 2006), those characteristics which have been most consistent over the years, and those which are most relevant in recent developments in the study of thymineless death are summarized here.

The hallmark of thymine-starvation is DNA damage, as measured by transcriptional analyses, pulse-field gel electrophorese (PFGE) and comparative genomic hybridization (CGH) studies (Nakayama, *et al.* 1994). The transcriptional profile of cells undergoing TLD is characterized by up-regulation of the DNA damage, or SOS, response (Sangurdekar *et al*., 2010; Sangurdekar, *et al.*, 2011). SOS response is induced by formation of RecA filaments on single strand DNA. RecA then filaments along the strand encountering LexA-bound *lexA* sequences, and causing the auto-proteolysis of LexA (Nakayama et al., 1994). The RecA-ssDNA filaments may result from single-strand and/or double-strand-breaks (Freifelder, 1969; Hill & Fangman, 1973; Nakayama & Hanawalt, 1975; Gallat & Suskind, 1961; Walker, 1970). Comparative genomic hybridization experiments revealed spatial DNA loss over starvation time (Kuong & Kuzminov, 2012; Sangurdekar et al., 2010) and pulse field gel electrophoresis experiments demonstrated that thymine deprivation results in a progressive increase in DNA fragmentation (Kuong & Kuzminov, 2010).

Thymineless death shares some characteristics with other DNA-damaging agents like UV-radiation (Table 1.1). However, a number of processes that are important for survival of UV-irradiated cells actually confer sensitivity in thymine-starved cells of various types. For instance, RecFOR proteins which are required for post-replicative repair in UV-irradiated *E. coli* reduce viability in thymine-starved cells (Webb, Cox, & Inman, 1997). Also, the highly UV-resistant *Deinococcus radiodurans* is susceptible to thymine starvation, in spite of having a robust RecFOR repair system which is known to repair extensive radiation damage (Satoh et al., 2012). Mutations in nucleotide excision repair (NER) do not appear to have much effect on viability in TLD (Morganroth & Hanawalt, 2006). Chromatographic analysis has shown that thymine-starved DNA has incorporated uracil bases, however the deletion of uracil glycosylase, which excises misincorporated uracils or deaminated cytosines in DNA (and is known to cause single-strand breaks in the process) has no effect on viability in thymine-starved cells (Kunzt*, et*

al., 1985). Our group discovered that DNA is lost symmetrically around the origin of replication, and while stretches of single-stranded DNA have been observed via cryomicroscopy (Nakayama et al., 1994) or detected using enzyme assays (Sangurdekar *et al*., 2010), the single-stranded regions of DNA are not concentrated in any one part of the genome and thus cannot explain the reduction in hybridization at the origin on DNA microarrays.

True repressors of thymineless death are difficult to isolate. Due to the persistent survival of a small fraction of cells in thymine starvation, which upon entering active growth, again become susceptible to thymine starvation, causes a number of false positives in a suppressor screen. The observation that mutations in the RecFORQJ pathway mitigated the killing effects of thymineless death was an unexpected result from a larger experiment where the researcher intended to analyze the effects of thymine-starvation on these and other UV-damage repair gene products (Nakayama, *et al.,* 1988). RecF is a difficult enzyme to study as its effects have thus far only been seen *in vivo*. It has no enzyme activity to measure therefore purification must be done solely by its physical characteristics, and sometimes its effects in a certain *in vitro* condition can be masked by an over-abundance of commonly associated protein partners, like RecOR (Sandler, 2005). Genetic studies have shown that it is involved in inducing the SOS DNA damage response in bacteria but that it requires active replication to do so. In this case it is likely that since there is no free 3' end of DNA available for RecA loading at an active fork, RecF facilitates loading of RecA onto single-stranded, gapped DNA behind replication forks to allow for RecA filmentation on single-stranded DNA-a necessary precursor to SOS response activation (Sassanfar, 1990). Its position in the genome next to the *dnaN* (beta-sliding clamp of DNA polymerase III) which is itself downstream of *dnaA* (replication initiator-protein) may indicate that it has a role in the formation of the replication fork at the origin of replication. The sensitivity of cells to thymine starvation

and the exacerbating role of RecF may indicate that replication initiation, or replication restart at replication forks play a key role in loss of viability.

Figure 1.1 Structure of nitrogenous bases which make up DNA. A 5' phosphate to 3' hydroxyl linked deoxyribose sugar moiety makes up the structural backbone of the helical 'ladder' while hydrogen-bonding between nitrogenous bases (dotted lines) makes up the 'rungs of the ladder.' The four bases making up the alphabet of DNA are Adenine, Thymine, Cytosine, and Guanine where A pairs with T, and C pairs with G.

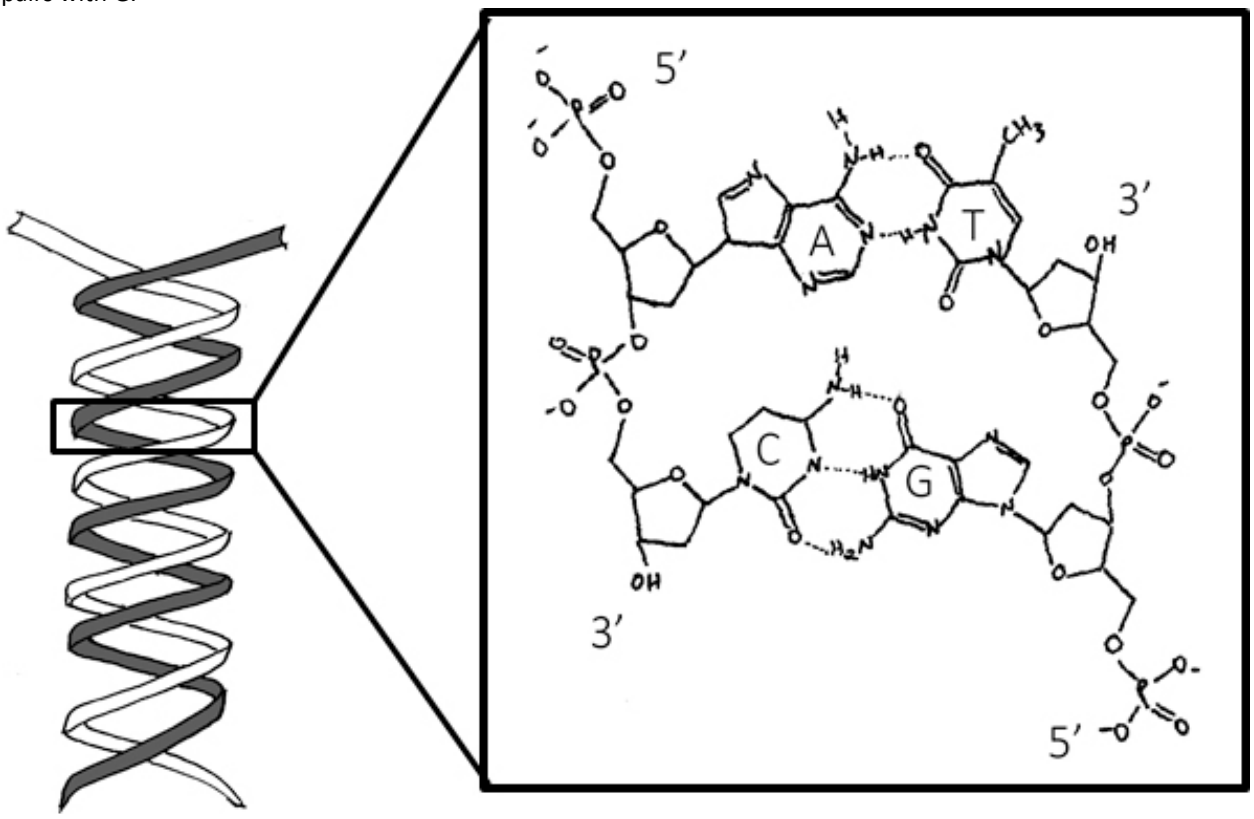

Figure 1.2 Sugar moieties which make up the backbones of RNA and DNA respectively. Numbers with tick marks represent the nomenclature by which the 5 carbons in each sugar are counted. DNA lacks a hydroxyl group at the 2' carbon, and so is referred to as 2'-deoxyribose.

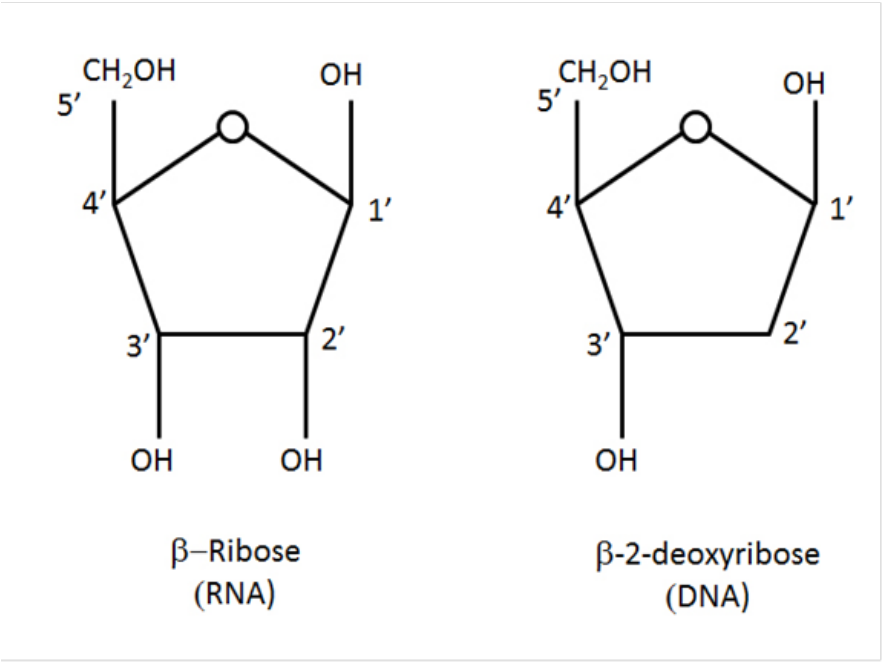

Figure 1.3 Replication initiator protein DnaA (when bound to ATP) binds to special sequences at the origin of replication (*oriC*) called DnaA boxes. When bound to the DNA, the DnaA proteins oligomerize with each other dragging the DNA into a supercoil and then hydrolyze ATP to ADP + phosphate which releases energy causing localized melting of the duplex. At this point replication proteins can load onto the newly formed single-stranded DNA.

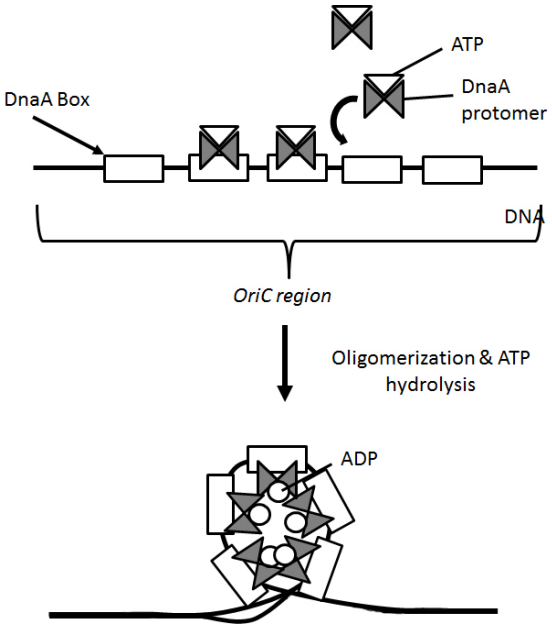

Figure 1.4 Topoisomerase I enzymes relieve the tension of overwound DNA. As DNA helicase pulls apart the strands of DNA at the replication fork, the DNA ahead of the fork compensates by become more twisted (a). A type I topoisomerase, such as Topo I will cut a single-strand of the DNA duplex (b), and then pull the other strand of DNA through the cut (c). Topo I will then reseal the nick leaving behind a more relaxed DNA helix (d).

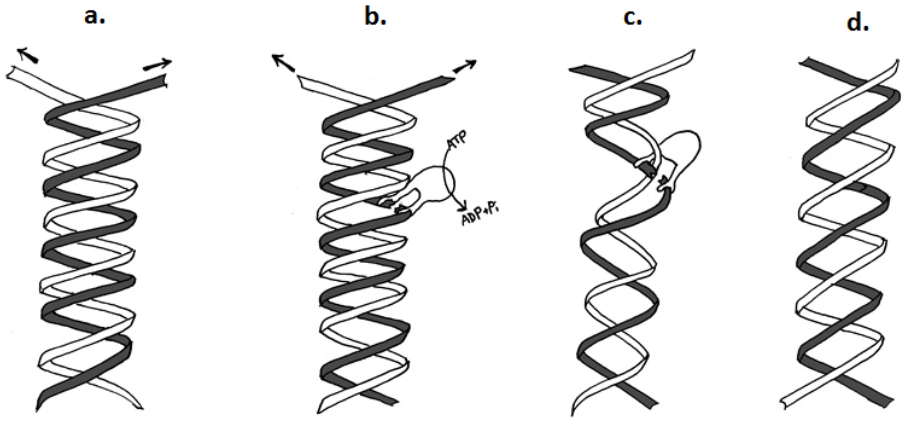

Figure 1.5 Topoisomerase II enzymes relieve supercoils in DNA. During replication, the tension built up along the DNA strand by DNA helicase pulling apart the duplex into single-strands can result in DNA upstream of the fork to begin to double over on itself in what is called a supercoil (a). A topoisomerase II enzyme can cut both strands of the double helix, pull the other double helix in the supercoil through the cut (b), and reseal the cut, leaving behind more relaxed DNA containing one less supercoil.

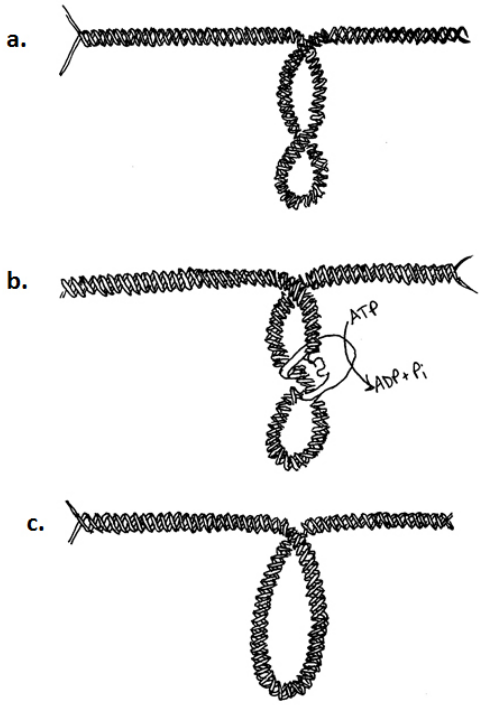

Figure 1.6 Various parts of the replication complex at a replication fork. DnaC helicase loader loads the DnaB helicase which in turn uses ATP to unwind the parental duplex DNA. Primase synthesizes RNA primers which Pol III polymerases use as a starting point to add nucleotides to the single-stranded DNA extruded by the helicase. The τ subunit serves to dimerize the two polymerases, and γ subunit loads the β clamps which help keep the polymerases bound to the DNA. Synthesis is continuous on the leading strand, and discontinuous on the lagging strand (due to the 5'->3' polymerase activity of Pol III) requiring the lagging strand polymerase to dissociate at the end of a short stretch of DNA (called an Okazaki fragment) and bind to the next RNA primer further upstream. Single-strand binding protein (SSB) protects the single-strand DNA from nucleases.

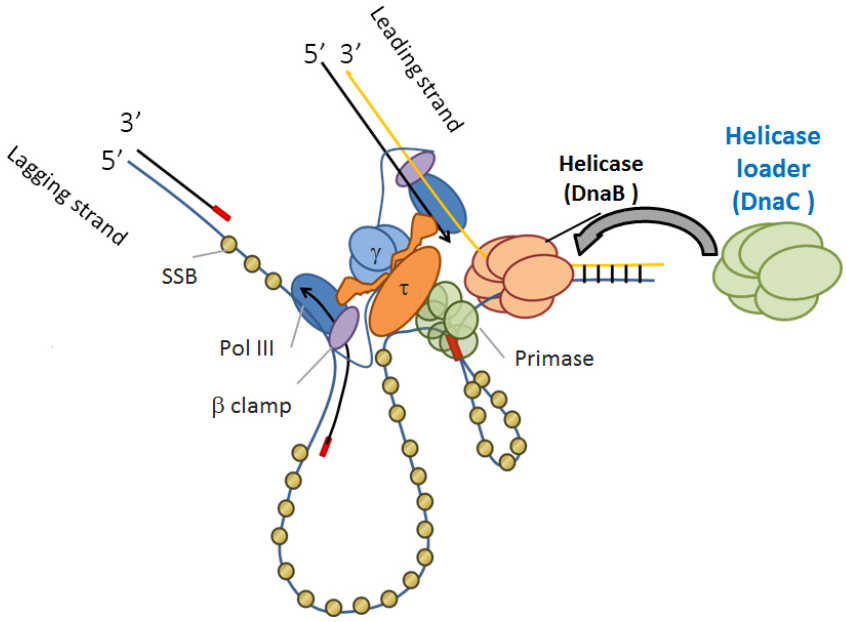

Figure 1.7 Model of the gene-copy number of the bacterial chromosome in stationary and exponential growth. The circular bacterial chromosome has one copy of each gene present during stationary phase when one chromosome is present. When cells enter exponential growth, replication initiates at the origin of replication before the previous rounds of replication have finished. This means that there are more copies of the genes near the origin in exponential growth at any given time but DNA is continuously synthesized such that at least one set of replication forks will have completed replication around the chromosome by the time cells divide.

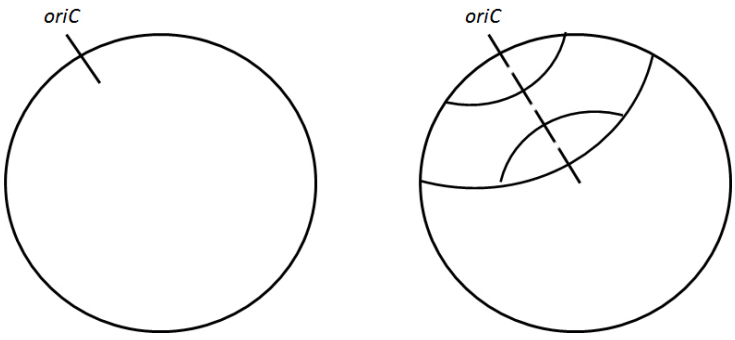

Figure 1.8 Simplistic model of mismatch repair. When part of a nucleotide has been altered, such as the guanine base of dGTP has been oxidized to 8-oxo-7, 8-dihydroguanine by reactive oxygen species, it may cause a disruption in the superhelical nature of the DNA (a). Mismatch repair proteins MutL and H move in a complex along the DNA strands until they reach such an abnormality, at which point MutH protein nicks the sugar backbone of the DNA on either side of the aberration on the unmethylated (or new) strand of DNA. It then unwinds the DNA releasing the nicked region. Polymerase I fills the gap remaining.

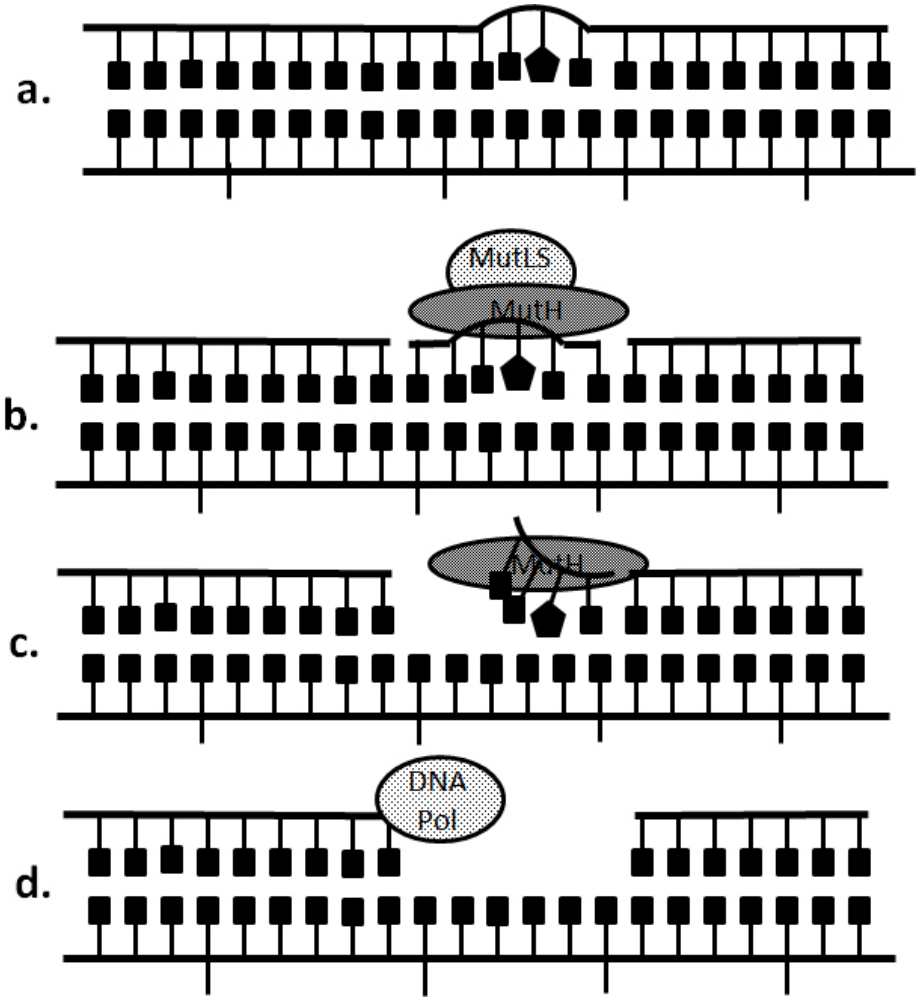

Figure 1.9 Simplistic model of Base Excision Repair (BER). A lesion-specific DNA glycosylase scans the genome by flipping out bases (a). When it reaches the lesion it recognizes specifically, it hydrolyzes the bond between the offending base and its deoxyribose moiety (b). AP Endonuclease then cuts away the sugar backbone (c), and DNA polymerase fills in the gap, and the sugar backbone is sealed by DNA ligase.

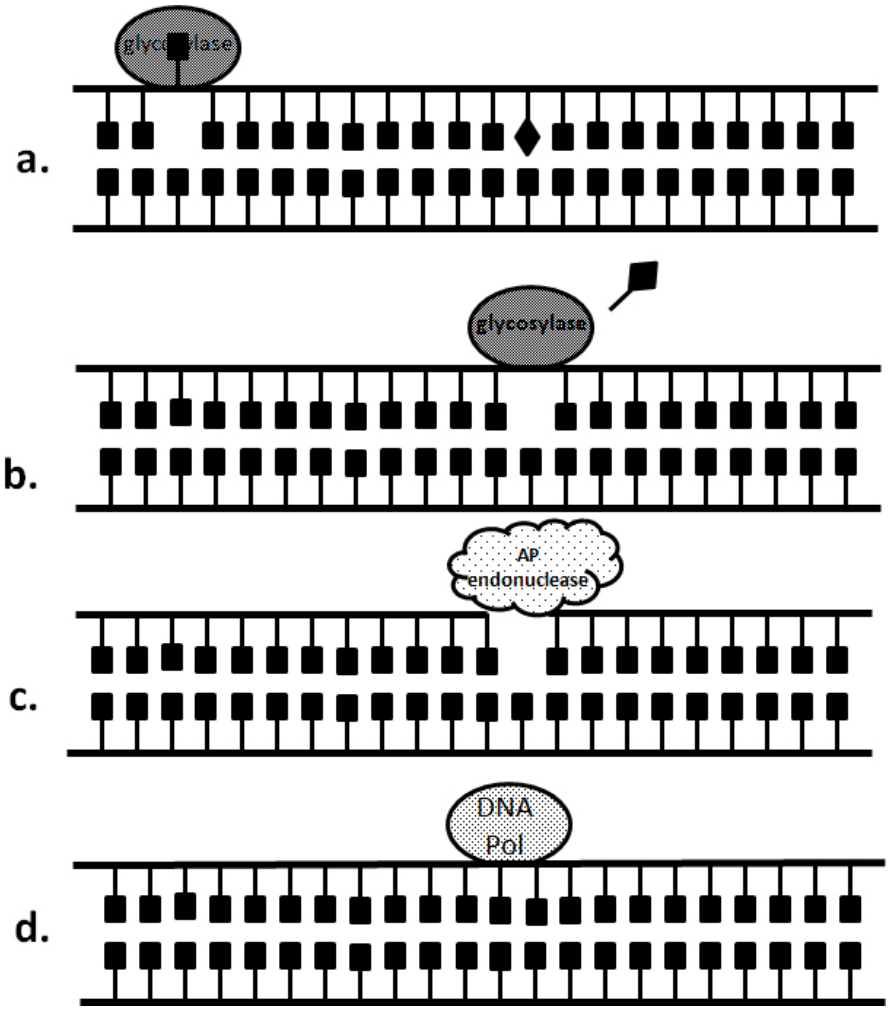

Figure 1.10 Simplistic model of Nucleotide Excision Repair (NER). Bulky damage in fully methylated DNA which distorts the superhelical structure of the DNA is recognized by UvrA and B proteins. The UvrB subunit remains at the lesion and attracts UvrC endonuclease that nicks the DNA on either side of the distortion. UvrD helicase then unwinds the nicked DNA releasing it from the DNA duplex along with the other Uvr proteins. DNA polymerase then comes in to fill the gap, and the sugar backbone is sealed by DNA ligase.

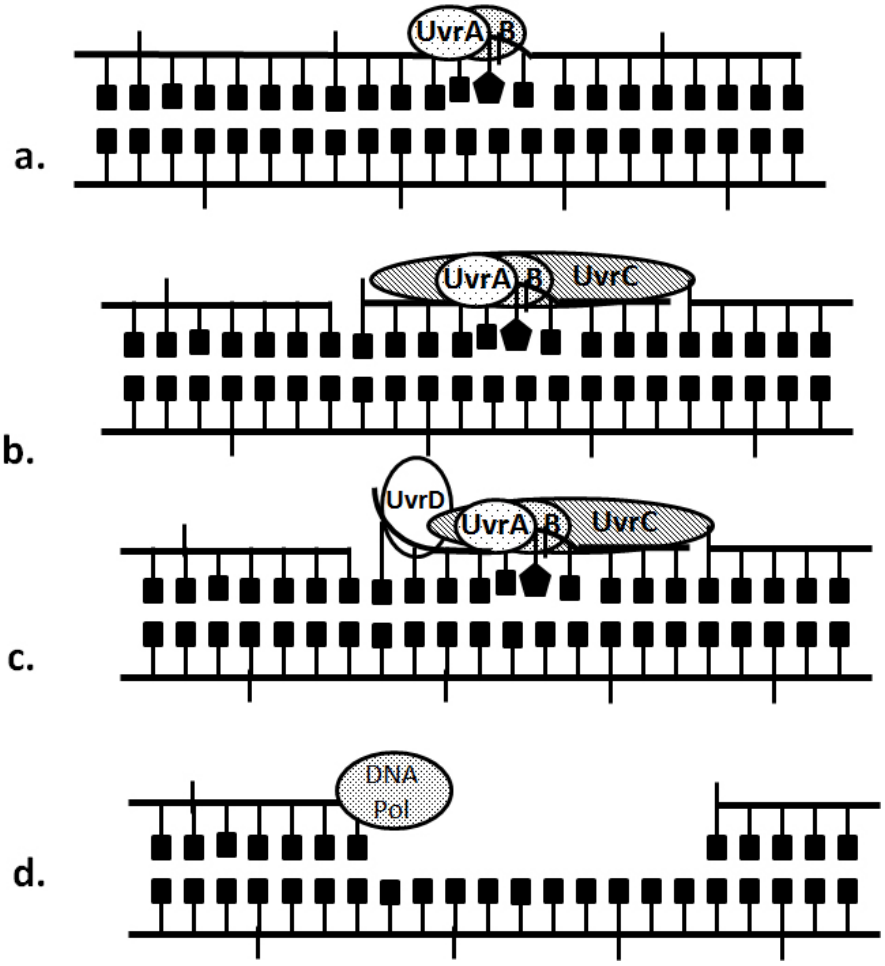

Figure 1.11 Simplistic model RecBCD processing of a double-strand break. RecBCD enzymes load onto a blunt or almost blunt double-strand end of DNA (a). RecB acts as a helicase pulling apart the strands of DNA so they can be degraded by either RecC (3'->5' exonuclease) or RecD (5'->3' exonuclease) (b). When the complex encounters a unique octomeric sequence called a *chi* sequence, the activity of the RecCD subunits change (c). The RecC activity is diminished allowing for a 3' free end to be formed on which recombination protein RecA can be loaded (d). RecA can then undergo homology searches and invade neighboring whole DNA duplexes for recombination events or repair synthesis (e).

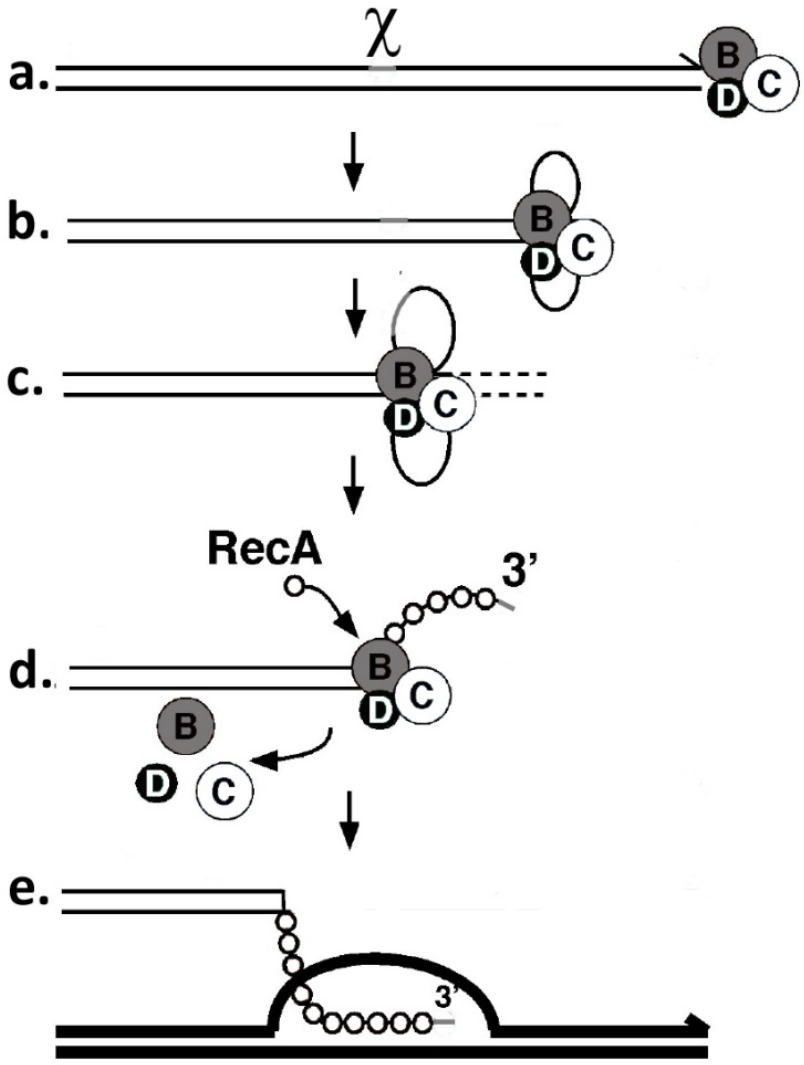

Figure 1.12 Simplistic model of how RecA-dependent RecFOR pathway can be used to fill daughter-strand gaps. Short dotted lines represent nascent DNA, and solid lines represent parental DNA. Example: A lesion in the DNA that passes through the helicase can result in a stalled polymerase in the lagging strand, the polymerase then dissociates and rebinds further upstream leaving behind a daughter-strand gap (a). RecFOR proteins are recruited to the daughter-strand gap junction and facilitate loading of RecA recombination protein onto the single-strand DNA (b). RecA filaments along the strand and invades a neighboring DNA duplex. DNA polymerase is recruited to this recombination structure and repair synthesis takes place (c). Ruv enzymes resolve the recombination structure resulting in a crossover event and the gap has been filled with new DNA (long dashes).

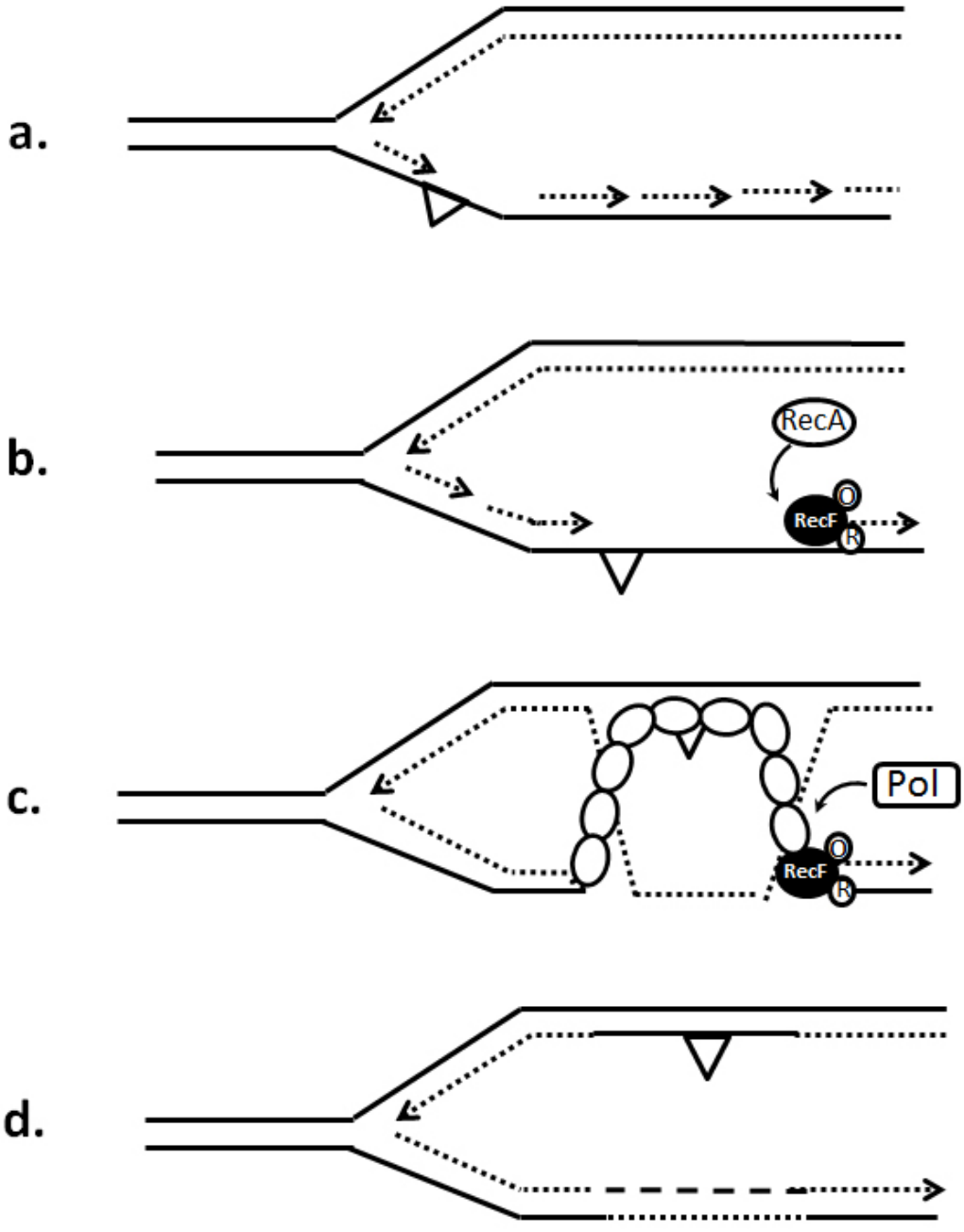

Table 1.1 Characteristics of thymine starvation in comparison to other types of starvation or cellular stresses

Thymineless death	UV irradiation	Amino acid starvation
• Halt to DNA replication elongation	• Temporary arrest of DNA replication elongation	• Slowed DNA replication
• Limited initiation	• Continued productive initiation	• NO new initiation (inhibition of lagging strand synthesis)
• "Unbalanced growth" – Transcription & translation continue for several generation times	• "Balanced"+ – Transcription &translation continue	• "Balanced" – -Most transcription & translation halts (stringent response)
• SOS (DNA damage) response	• SOS (DNA damage response)	• Unknown
• ss-ds breaks	• ss-ds breaks	
• Increased recombination	• Increased recombination	
• *Aggravated* by actions of RecF pathway during active growth	• *Requires* action by RecF pathway for survival during active growth	
• Bacteriocidal	• Bacteriostatic (contingent on repair)	• Bacteriostatic

Transition to Chapter 2

The work presented in Chapter 2 was published in the journal of *Antimicrobial Agents and Chemotherapy* (*53*(5), 2110-2119) in 2009. My role in this study was to analyze the effects of the antibiotic, simocyclinone D8 (simo D8) in *Eschericia coli.* Simocyclinone D8 was identified as a novel antibiotic from *Streptomyces* antibioticus Tü 6040 and has structural similarities to aminocoumarin antibiotics which target the ATP-hydrolyzing portion of bacterial gyrase. Simocyclinone D8 has a novel function in that it prevents the binding of gyrase to DNA. This antibiotic is effective against Gram positive bacteria, but it has little to no activity against Gram-negative bacteria such as *E. coli* (Schimana, *et al*, 2000). Using a drug-efflux-pump deficient *acrB::KAN* mutant of *E. coli,* I was able to measure loss of viability in *E. coli* cells treated with varying concentrations of antibiotic (Figure 2.5). I also purified RNA from treated and control cells to be labeled in a reverse transcription reaction with Cy3- and Cy5-labeled dUTPs for measurement of gene expression using cDNA microarrays. I learned to do basic data analysis of large datasets by centering data, and using the Significance Analysis of Microarrays (SAM) extension in Microsoft Excel to identify genes which were significantly up- or down-regulated in antibiotic treated cells as opposed to control cells. Professor Arkady Khodursky then further processed the data removing noise and smoothing the output from the microarray scanner. The data from those microarray experiments are shown in Figures 2.6-2.9. To verify gene expression from microarray data I performed quantitative PCR on RNA isolated from treated and untreated cells to measure transcriptional levels of the subunits of the type II topoisomerases in the cell (both gyrase subunits), and topoisomerase I. Finally, I visualized the nucleoids of simoD8-treated *E. coli* cells at varying times during drug treatment using DAPI-stain.

In vitro work showing the inhibitory effect of Simocyclinone D8 on purified topoisomerase was performed by Lisa M. Oppegard, Hans-Peter Fiedler, and Professor Hiroshi Hiasa. Simocyclinone D8 was synthesized by Professer Keith Ellis. The results of this study showed that the targets of simocyclinone D8 in Gram-negative bacteria (type II topoisomerases) are susceptible to the antibiotic *in vitro*. *In vivo, E. coli* cells were affected when the drug-efflux pump AcrB was compromised.

Chapter 2: In Vivo and In Vitro Patterns of the Activity of Simocyclinone D8, an Angucyclinone Antibiotic from *Streptomyces antibioticus*

Simocyclinone D8 (SD8) exhibits antibiotic activity against gram-positive bacteria but not against gram-negative bacteria. The molecular basis of the cytotoxicity of SD8 is not fully understood, although SD8 has been shown to inhibit the supercoiling activity of *Escherichia coli* gyrase. To understand the mechanism of SD8, we have employed biochemical assays to directly measure the sensitivities of *E*. *coli* and *Staphylococcus aureus* type II topoisomerases to SD8 and microarray analysis to monitor the cellular responses to SD8 treatment. SD8 is a potent inhibitor of either *E*. *coli* or *S*. *aureus* gyrase. In contrast, SD8 exhibits only a moderate inhibitory effect on *S*. *aureus* topoisomerase IV, and *E*. *coli* topoisomerase IV is virtually insensitive to SD8. The antimicrobial effect of SD8 against *E*. *coli* has become evident in the absence of the AcrB multidrug efflux pump. As expected, SD8 treatment exhibits the signature responses to the loss of supercoiling activity in *E*. *coli*: upregulation of gyrase genes and downregulation of the topoisomerase I gene. Unlike quinolone treatment, however, SD8 treatment does not induce the SOS response. These results suggest that DNA gyrase is the target of SD8 in both gram-positive and gram-negative bacteria and that the lack of the antibacterial effect against gram-negative bacteria is due, in part, to the activity of the AcrB efflux pump.

2.1 Introduction

All type II topoisomerases, except *Sulfolobus shibatae* topoisomerase VI, are well conserved and belong to a large protein family, the type IIA topoisomerases (Champoux, 2001; Wang, 2002). They are essential for DNA replication and chromosome segregation, as well as for the maintenance of chromosome structure and DNA superhelicity. Although these enzymes share common biochemical properties, each enzyme exhibits a distinct catalytic preference, which reflects its specialized function in vivo (Champoux, 2001; Wang, 2002). For instance, DNA gyrase is the only enzyme that can introduce negative supercoils into DNA, whereas topoisomerase IV (Topo IV) is an efficient decatenase that is responsible for segregating daughter chromosomes. DNA gyrase and Topo IV consist of GyrA and GyrB subunits and ParC and ParE subunits, respectively. GyrA and ParC subunits are responsible for catalyzing the strand breakage and

religation reactions, whereas GyrB and ParE subunits bind and hydrolyze ATP. The active forms of gyrase and Topo IV are an $\alpha_2\beta_2$ tetramer (Champoux, 2001; Wang, 2001).

Both DNA gyrase and Topo IV are the cellular targets of the quinolone and coumarin antibacterial drugs (Drlica & Malik, 2003; Maxwell, 1999). The quinolones, such as norfloxacin and ciprofloxacin, are poisons of gyrase and Topo IV, which can trap either gyrase or Topo IV in a topoisomerase-drug-DNA ternary complex. In contrast, the coumarins, such as novobiocin and coumermycin A1, are competitive inhibitors of the ATPase activity. Interestingly, gyrase has been shown to be the primary target of quinolone drugs in *Escherichia coli*, whereas Topo IV becomes the primary target in *Staphylococcus aureus* and *Streptococcus pneumoniae* (Drlica & Malik, 2003; Ferroro, *et. al.*, 1994; Khodursky, Zechiedrich & Cozzarelli, 1995; Maxwell, 1999; Pan & Fisher, 1997). These observations have suggested that gyrase and Topo IV are the primary targets in gram-negative and gram-positive bacteria, respectively. It has been demonstrated, however, that each quinolone drug has a preferred target and the target selection can be altered by changes in quinolone structure (Pan & Fisher, 1997; Pan & Fisher, 1999). Thus, it remains unclear exactly what determines the primary target of a quinolone drug in cells.

Simocyclinone D8 (SD8) belongs to a new class of angucyclinone antibiotics isolated from *Streptomyces antibioticus* Tü 6040 (Holzenkämpfer, *et. al.,* 2002; Holzenkämpfer & Zeeck, 2002; Schimana, *et. al.,* 2000; Theobald, Schimana & Fiedler, 2000). SD8 contains a halogenated aminocoumarin moiety (Figure 2.1), a unique feature of the -coumarin drugs. However, in addition to the coumarin moiety, SD8 contains an angucyclic polyketide core, a deoxyhexose, and a tetraene side chain. An agar plate diffusion assay and a broth dilution method have shown that SD8 exhibits antibiotic activity against gram-positive bacteria, such as *S. aureus*, *Bacillus brevis*, *Bacillus subtilis*, and *Streptomyces viridochromogenes*, and little to no activity against gram-negative bacteria, such as *E. coli*, *Proteus mirabilis*, and *Pseudomonas fluorescens* (Schimana, *et. al.,* 2000).

Despite the potential importance of SD8, only one study has been conducted on the mechanism of SD8 (Flatman, *et. al.,* 2005). Although the coumarin drugs and SD8 share an aminocoumarin moiety, unlike the coumarins, SD8 does not inhibit the ATPase activity of gyrase. Instead, it inhibits the supercoiling activity of *E*. *coli* gyrase by interacting with the GyrA subunit and preventing gyrase from binding to DNA (Flatman, *et. al.,* 2005). However, the effects of SD8 on topoisomerases from gram-positive bacteria have not been examined. In this study, we conducted a comprehensive analysis of the activity of SD8 to understand the mechanism of its action in both gram-positive and gram-negative bacteria. We decided to use two distinct approaches, biochemical assays and microarray analysis, to achieve our objective. Biochemical assays showed that SD8 was a potent inhibitor of both *E*. *coli* gyrase and *S*. *aureus* gyrase but a much less potent inhibitor of Topo IVs. We took advantage of our finding that a bacteriostatic effect of SD8 against *E*. *coli* became evident in a Δ*acrB* strain and monitored the transcriptional response to SD8 treatment in *E*. *coli*. SD8 treatment led to the signature response to the loss of supercoiling activity. Unlike quinolone treatment, however, SD8 treatment did not induce the SOS response. Thus, in vivo and in vitro patterns of the activity of SD8 suggested that DNA gyrase is the target of SD8 in both gram-positive and gram-negative bacteria and that the activity of the AcrB multidrug efflux pump is, at least in part, responsible for the ineffectiveness of SD8 against gram-negative bacteria.

2.2 Materials and Methods

2.2.1. DNAs and proteins.

Negatively supercoiled pBR322 DNA was purchased from New England Biolabs, and relaxed DNA was prepared by incubating the negatively supercoiled DNA with human topoisomerase I (Topogen). Kinetoplast DNA was purchased from Topogen. The subunits of *E*. *coli* gyrase, *E*. *coli* Topo IV, *S*. *aureus* gyrase, and *S*. *aureus* Topo IV were expressed and purified, and the active enzymes were reconstituted as described previously (Hiasa, 2002; Hiasa, DiGate & Marians, 1994; Hiasa & Shia, 2000; Hiasa, *et. al.*, 2003; Peng & Marians, 1993).

2.2.2. Fermentation, isolation, and purification of SD8.

The fermentation of *S*. *antibioticus* Tü 6040 was carried out at the University of Minnesota Biotechnology Resources Center following previously described procedures (Schimana, *et. al.,* 2000). We found that the choice of carbon and nitrogen sources was critical to the production of SD8. Production of SD8 was monitored by analytical reversed-phase high-performance liquid chromatography (HPLC) (analytical HPLC with a photodiode array detector; Waters Alliance) on a C_{18} column (5 µm; 4.6 by 150 mm; Restek) using acetonitrile and 0.1% formic acid as the mobile phase. Separation was achieved using a linear gradient from 50:50 acetonitrile-0.1% formic acid to 60:40 acetonitrile-0.1% formic acid over 30 min.

After completion of the fermentation, cells were separated from the broth by passing the culture through a 150 US mesh sieve. Packed cells (665 g) were processed as described previously (Schimana, *et. al.,* 2000). The combined methanol extracts (wet with water) were concentrated to a dark orange crude solid (20.2 g) on a rotary evaporator. HPLC analysis of this crude extract showed SD8 to be the least polar constituent (comparison to HPLC of the original preparation by H.-P. Fiedler and his colleagues). HPLC analysis of an ethyl acetate extract of the fermentation broth, as well as a lyophilized sample, showed that the broth did not contain SD8.

The crude natural product was purified using catch-and-release solid-phase extraction on diol-modified silica gel. Attempts to purify SD8 on normal silica gel using standard chromatography failed with a range of solvents. A ~5-g sample of the crude product was dry loaded (50 g of diol-modified silica) onto a 400-g diol-modified silica gel column prepared with 100% dichloromethane. Dry loading of the sample was imperative given that the crude material is only sparingly soluble in dichloromethane and had to be loaded in methanol. Solid-phase extraction purification of the crude product on diol-modified silica gel at 1.25% (5 g crude product on 400 g matrix) allowed elution of SD8 as the first yellow band off the column with 1% methanol-dichloromethane. The fractions from this first band were combined, and analysis by HPLC and nuclear magnetic resonance showed them to contain only SD8.

Extensive analytical chemistry and biological activity testing was performed on this “current” preparation of SD8 to ensure that it is identical to the “original” preparation of SD8 that was

isolated from *S*. *antibioticus* Tü 6040. Details of these experiments and their results are included in the supplemental material.

2.2.3. Supercoiling assay.

Standard reaction mixtures (20 µl) contained 50 mM Tris-HCl (pH 8.0 at 23°C), 10 mM $MgCl_2$, either 100 mM (for *E*. *coli* gyrase) or 600 mM (for *S*. *aureus* gyrase) potassium glutamate (KGlu), 10 mM dithiothreitol, 50 µg/ml bovine serum albumin, 1 mM ATP, 0.3 µg of the relaxed DNA, either 10 fmol (as a tetramer) of *E*. *coli* gyrase or 50 fmol (as a tetramer) of *S*. *aureus* gyrase, and various concentrations of either SD8 or ciprofloxacin (a generous gift from the Bayer Corporation). Reaction mixtures were incubated at 37°C for 15 min and terminated by adding EDTA to 25 mM and further incubating at 37°C for 5 min. The DNA products were analyzed by electrophoresis through vertical 1.2% SeaKem ME agarose (Lonza) gels (14 by 10 by 0.3 cm) at 2 V/cm for 15 h in a running buffer of 50 mM Tris-HCl (pH 7.9 at 23°C), 40 mM sodium acetate, and 1 mM EDTA (TAE buffer). Gels were stained with ethidium bromide (EtBr), then photographed, and quantified using an Eagle Eye II system (Stratagene).

2.2.4. Decatenation assay.

Reaction mixtures (20 µl) contained 50 mM Tris-HCl (pH 8.0 at 23°C), 10 mM $MgCl_2$, either 100 mM (for *E*. *coli* Topo IV) or 400 mM (for *S*. *aureus* Topo IV) KGlu, 10 mM dithiothreitol, 50 µg/ml bovine serum albumin, 1 mM ATP, 0.3 µg of kinetoplast DNA, 50 fmol (as a tetramer) of either *E*. *coli* Topo IV or *S*. *aureus* Topo IV, and various concentrations of either SD8 or ciprofloxacin. Reaction mixtures were incubated at 37°C for 15 min and terminated by adding EDTA to 25 mM and further incubating at 37°C for 5 min. The DNA products were analyzed, and the gels were photographed and quantified as described in the preceding paragraph.

2.2.5. Two-step DNA cleavage assay.

Reaction mixtures (20 µl) contained 50 mM Tris-HCl (pH 8.0 at 23°C), 10 mM $MgCl_2$, the indicated concentrations of KGlu (only when indicated in the figure legends), 10 mM dithiothreitol, 50 µg/ml bovine serum albumin, 1 mM ATP, 5 µg/ml tRNA, 0.3 µg of either the

supercoiled or relaxed DNA (as indicated in the figure legends), and the indicated amounts (as a tetramer) of various topoisomerases. The indicated concentrations of either SD8 or ciprofloxacin were incubated in the first stage for 5 min at 37°C. Then, the indicated concentrations of either ciprofloxacin or SD8 were added, and the reaction mixtures were incubated during the second stage for 10 min at 37°C. Sodium dodecyl sulfate was added to a concentration of 1%, and the reaction mixtures were further incubated at 37°C for 5 min. EDTA and proteinase K were then added to 25 mM and 100 µg/ml, respectively, and the incubation was continued for an additional 15 min at 37°C. The DNA products were purified by extraction with phenol-chloroform-isoamyl alcohol (25:24:1, vol/vol) and then analyzed by electrophoresis through vertical 1.2% agarose gels at 2 V/cm for 15 h in TAE buffer that contained 0.5 µg/ml EtBr (unless otherwise indicated). After destaining in water, gels were photographed and quantified using an Eagle Eye II system.

2.2.6. SD8 treatment of *E. coli*.

E. coli MG1655 (wild-type) cells were grown to mid-exponential phase in 10 ml of LB medium in Erlenmeyer flasks at 37°C. The cells were then reinoculated into 96-well plates at a dilution in LB medium such that cells were at a concentration giving an optical density at 600 nm (OD_{600}) of 0.1. Various concentrations of SD8 (0 µM [dimethyl sulfoxide {DMSO}, the solvent for the drug], 5 µM, 10 µM, 20 µM, and 40 µM) were added to the wells. The OD_{600} of the culture was measured every 4 minutes (with a 30-s shaking period before measurement) over the course of 3 hours at 37°C in a Wallac 1420 plate reader (Perkin Elmer). In a separate assay, cells were grown in LB medium up to exponential phase and reinoculated into Erlenmeyer flasks containing 10 ml of fresh LB medium, at which point drugs of various concentrations (identical to the concentrations listed above) were added to the medium, and the cells were grown for 2 hours at 37°C, then diluted, and plated on LB agar plates containing no antibiotic. The plates were incubated overnight at 37°C, and the number of CFU was determined the following day.

The *E. coli* Δ*acrB* strain, a direct mutant of the wild-type MG1655 strain, was obtained from the Keio collection (Baba, *et. al.*, 2006). *E. coli* Δ*acrB* cells were treated in a manner similar to that described above, except that the drug concentrations used were from 10 nM to 40 µM for the growth assay and the cells used for viability counts were grown with higher concentrations

of drug (0 μM [DMSO], 20 μM, and 80 μM) for 2 hours before diluting and plating on LB agar plates.

2.2.7. Microarray and real-time PCR (RT-PCR) analyses.

Relative mRNA abundances between treated and nontreated cells, or a mutant and the wild type, were compared using *E*. *coli* whole-genome DNA microarrays containing 99% of all annotated open reading frames and the stable RNA genes. The protocols for slide preparation, RNA purification, reverse transcription with the Cy dyes, hybridization, and image scanning were described previously (Khodursky, *et. al.,* 2003).

The RNA samples were extracted from the cultures grown in triplicate from single isolates to an OD_{600} of 0.5 to 0.6 using the hot-phenol method (Khodursky, *et. al.,* 2003). After treatment with 20 μM SD8 or an equivalent volume of DMSO as a control for 2 hours, cells were fixed with a 10% solution of ethanol and phenol (95%/5%, vol/vol), and total RNA was extracted using an RNeasy minikit (Qiagen).

Portions of the control and treated sample RNA were reverse transcribed using Superscript II reverse transcriptase (Invitrogen) and labeled for microarray hybridization using Cy3 and Cy5 dyes (Amersham Biosciences), and the dyes were swapped for one of the replicates. Arrays were hybridized for 6 h at 65°C, scanned, and then analyzed using the GenePix Pro 3.0 software. Intensities in both channels were smoothed using the lowess method, and dye- and array-specific noise was removed using the analysis of variance error model (Kerr, Martin & Churchill, 2000). In pairwise comparisons, differentially expressed genes were identified at a false discovery rate of less than 5% using the SAM package (Tusher, Tibshirani & Chum, 2001).

The remaining RNA was reverse transcribed to cDNA using Superscript II, and the RT-PCR for RNA quantification was carried out using Sybr green kit and ABI Prism 7900 (Applied Biosystems) according to the manufacturer's protocol. The absolute change in gene expression was calculated based on the method described by Livak and Schmittgen (Livah & Schmitten, 2001). The primers used for RT-PCR were as follows: *topA* forward, 5’-CGGCCCGATCGTTGAGTGTGA-3’; *topA* reverse, 5’-GTGGTGCCACTTCGCCGTTAC-3’; *gyrA* forward, 5’-GTTCGCGGTATTCGCTTAG-3’;

gyrA reverse, 5′-GCGACTTGGTTGGGTATTC-3′; *gyrB* forward, 5′-AACGAACTGCTGGCAGAATAC-3′; *gyrB* reverse, 5′-TAAGTCGAGCGCACCTTTAC-3′; 16S rRNA forward: TGGCAAGCTTGAGTCTCGTA-3′; and 16S rRNA reverse, 5′-ACCTGAGCGTCAGTCTTCGT-3′.

Microarrays and the RT-PCR analyses for Δ*acrB* cells were performed in a similar fashion, except that cells were treated with either 5 μM of D8 or an equivalent volume (25 μl) of DMSO for 2 hours.

2.2.8. Visualization of nucleoids using DAPI staining.

A 10-ml culture of Δ*acrB* cells was grown to mid-exponential phase in LB medium at 37°C, then split into two cultures, one treated with 20 μM SD8 and the other with DMSO (the solvent for the drug) for 30 min at 37°C. Cells were harvested and washed with 1× phosphate-buffered saline. 4′,6-Diamidino-2-phenylindole (DAPI) (Promega) was added to a concentration of 5 μg/ml, and the cells were incubated at room temperature for 10 min. After the cells were washed twice with 1× phosphate-buffered saline, they were placed under the glass coverslips coated with poly-l-lysine solution and visualized using a BH-2 Olympus fluorescence/differential interference contrast microscope.

2.3. Results

2.3.1. In vitro pattern of SD8 activity.

SD8 inhibits *E*. *coli* DNA gyrase in vitro (Flatman, *et. al.,* 2005) but has no antibacterial effect against *E*. *coli* (Schimana, *et. al.,* 2000). At the same time, SD8 inhibits *S*. *aureus* growth via an unknown mechanism (Schimana, *et. al.,* 2000). To develop a consistent picture of SD8's antibacterial effects, we set out to determine SD8 activity against representative gram-negative and gram-positive topoisomerases. We first investigated which topoisomerases are more likely to be targeted by SD8 on the basis of its inhibitory effects on *E*. *coli* and *S*. *aureus* type II topoisomerases.

2.3.1.1. SD8 inhibits the supercoiling activity of *S. aureus* gyrase.

As described previously (Blanche, *et. al.*, 1996; Hiasa, *et. al.,* 2003; Tanaka, *et. al.,* 1991), *S. aureus* topoisomerases require high concentrations of KGlu for their optimal catalytic activities. We found that the optimal KGlu concentrations for the supercoiling activity of *S. aureus* gyrase and the decatenation activity of *S. aureus* Topo IV were 600 to 800 mM and 400 mM, respectively (Hiasa, *et. al.,* 2003; data not shown). Almost no activity of either *S. aureus* enzyme was detected under the conditions (50 to 100 mM KGlu) used in the catalytic assays for *E. coli* topoisomerases. Accordingly, the supercoiling assay for *S. aureus* gyrase was performed in the presence of 600 mM KGlu. Under these conditions, 50 fmol of *S. aureus* gyrase was capable of completely supercoiling 100 fmol of the relaxed DNA. The supercoiling activity of *S. aureus* gyrase was measured in the presence of various concentrations of either SD8 or ciprofloxacin (Figure 1.2). Unlike ciprofloxacin, SD8 was a potent inhibitor of *S. aureus* gyrase (50% inhibitory concentration [IC_{50}] of 1.45 µM; Table 2.1), suggesting that gyrase is an effective target of SD8 in *S. aureus*.

It required only 10 fmol of *E. coli* gyrase to completely supercoil 100 fmol of the relaxed DNA under our standard reaction conditions (100 mM KGlu). Therefore, the supercoiling assay for *E. coli* gyrase was performed using 10 fmol of *E. coli* gyrase (Figure 2.2) The IC_{50} of SD8 for *E. coli* gyrase was 0.41 µM, whereas that of ciprofloxacin was 2.35 µM (Table 1). Thus, SD8 was a more potent inhibitor of *E. coli* gyrase than ciprofloxacin was.

We also employed a two-step DNA cleavage assay to assess the differences, if any, in the SD8 sensitivity between *S. aureus* gyrase and *E. coli* gyrase (Figure 2.3). This assay allowed us to measure the ability of SD8 to block the binding of gyrase to DNA as the inhibition of ciprofloxacin-induced covalent topoisomerase-DNA complex formation. On the basis of the comparable effects of SD8 on the supercoiling activities of *S. aureus* gyrase and *E. coli* gyrase (Table 2.1), we had expected to observe results with *S. aureus* gyrase at levels of SD8 similar to those seen with *E. coli* gyrase (Figure 2.3A). Instead, significantly higher concentrations of SD8 were required for the inhibition of ciprofloxacin-induced covalent *S. aureus* gyrase-DNA complex formation (Figure 2.3B). One possible explanation was that the high concentrations of KGlu present in the supercoiling assay for *S. aureus* gyrase could affect the apparent SD8 sensitivity of

S. *aureus* gyrase by changing the conformation of *S*. *aureus* gyrase and/or the interactions among SD8, *S*. *aureus* gyrase, and DNA. To test this possibility, the two-step DNA cleavage assay was performed in the presence of a high concentration of KGlu (Figure. 2.3C). To accommodate the inhibitory effect of KGlu on the stimulation of the cleavage activity of bacterial type II topoisomerases by ciprofloxacin (Blanche, *et. al.,* 1996; Hiasa, *et. al.,* 2003; Pfeiffer & Hiasa, 2004), 400 fmol (instead of 50 fmol) of *S*. *aureus* gyrase and 400 mM KGlu (we could not detect the DNA cleavage activity in the presence of 600 mM KGlu) were used in this assay. The presence of 400 mM KGlu significantly increased (about fourfold) the ability of SD8 to inhibit the formation of ciprofloxacin-induced covalent *S*. *aureus* gyrase-DNA complexes (Figure. 1.3C). These results suggest that SD8 can inhibit the supercoiling activity of *S*. *aureus* gyrase by interfering with its DNA binding, as was shown with *E*. *coli* gyrase (Flatman, *et. al.,* 2005).

2.3.1.2. Topo IVs are poor targets of SD8.

Because of the high degree of similarity between gyrases and Topo IVs, many gyrase inhibitors also inhibit Topo IV, although the sensitivities of gyrase and Topo IV from a particular bacterium to each drug are usually different (Drlica & Malik, 2003; Ferroro, *et. al.*, 1994; Khodursky, Zechiedrich & Cozzarelli, 1995; Maxwell, 1999; Pan & Fisher, 1997). Thus, we examined whether SD8 could also inhibit the decatenation activity of either *S*. *aureus* Topo IV or *E*. *coli* Topo IV.

Again, because of the differences in optimal salt concentrations, the decatenation assays for *S*. *aureus* Topo IV and *E*. *coli* Topo IV were performed in the presence of 400 mM and 100 mM KGlu, respectively, using 50 fmol of either *S*. *aureus* Topo IV or *E*. *coli* Topo IV (Figure. 2.4). SD8 exhibited a moderate inhibitory effect on *S*. *aureus* Topo IV, but *E*. *coli* Topo IV was essentially insensitive to SD8 (Table 2.1). The IC_{50} of SD8 for *E*. *coli* Topo IV (270 μM) was almost 20-fold higher than that for *S*. *aureus* Topo IV (14.5 μM) and almost 8-fold higher than the IC_{50} of ciprofloxacin for *E*. *coli* Topo IV (34 μM). On the basis of the differences in SD8 sensitivity between gyrases and Topo IVs, gyrase appeared to be the target of SD8 in both *S*. *aureus* and *E*. *coli*.

The two-step DNA cleavage assay for *S*. *aureus* Topo IV was also performed in the absence (see Figure S3A in the supplemental material) or presence of 400 mM KGlu (see Figure S3B in the supplemental material). Again, the IC_{50} of SD8 was reduced about fourfold by the presence of 400 mM KGlu. The IC_{50} for *E*. *coli* Topo IV was 200 to 400 μM (see Figure S3C in the supplemental material), which was close to the value seen in the catalytic assay (Table 1 and Figure 4).

2.3.2. In vivo pattern of SD8 activity.

The data presented above essentially ruled out Topo IV as an SD8 target in *E*. *coli*. They also suggested that the inhibitory effect of SD8 against *E*. *coli* gyrase and *S*. *aureus* gyrase was comparable and that it was better than the antisupercoiling activity of ciprofloxacin against either enzyme. If the in vitro effective concentrations are any indication, then the enzymatic activities of *E*. *coli* gyrase and *S*. *aureus* gyrase in vivo should be as susceptible to SD8 as they are to ciprofloxacin. Thus, the effect of SD8 on *S*. *aureus* is mediated, at least in part, by targeting DNA gyrase. On the other hand, the lack of SD8 antibacterial activity against *E*. *coli* could be due to the low effective concentration of the drug in vivo, the tolerance of the specific bacterial system to the inhibition of supercoiling activity (as can be inferred from a study by Jensen et al. [Jensen, *et. al.,* 1999]), or a combination of both factors.

2.3.2.1. The AcrB multidrug efflux pump affects the efficacy of SD8 against *E*. *coli*.

SD8 did not affect the growth of the wild-type MG1655 strain at any concentration up to 80 μM (Figure. 2.5 and data not shown). It has been shown that *E*. *coli* type II topoisomerases can be inhibited in vivo by coumarin antibiotics in mutants with deficient efflux (Hardy & Cozzarelli, 2003; Khodursky, *et. al.,* 2000). To test whether efficient efflux also protects the *E*. *coli* target(s) from SD8, we examined the effect of SD8 on growth of a Δ*acrB* mutant. The AcrB protein is one of the resistance-nodulation-division family of multidrug efflux pumps (Murakami, *et. al.,* 2002; Nikaido & Zgurskaya, 2001; Tikhonova & Zgurskaya, 2004). SD8 inhibited bacterial growth of the Δ*acrB* strain at a concentration as low as 5 μM (Figure. 2.5). SD8 treatment of Δ*acrB* cells also resulted in the elongation of the cells (see Figure. S4 in the supplemental material). Despite clear bacteriostatic effects across a range of concentrations, SD8 treatment did not result in

more than a 50% reduction in viability counts, even at 80 μM (data not shown). These results showed that the resistance of wild-type *E*. *coli* to SD8 was, at least in part, due to efflux of the drug from the cell. In the absence of AcrB-mediated efflux, SD8 effectively inhibited bacterial growth at concentrations comparable to the effective concentration of novobiocin (data not shown), and as with novobiocin, the effect of SD8 was largely bacteriostatic.

2.3.2.2. The SD8 treatment causes the loss of supercoiling activity, but not DNA damage, in *E. coli*.

The results presented above point toward the existence of an intracellular target(s) for SD8. Because the drug does not fully inhibit bacterial growth in liquid medium or on plates, it was not feasible to set up a positive genetic screen to identify the target(s). On the other hand, it has been repeatedly demonstrated that genome-wide transcriptional profiles can reliably capture regulatory patterns associated with molecular mechanisms of drug activity (Cheung, *et. al.,* 2003; Gmuender, *et. al.,* 2001; Jeong, Hiasa & Khodursky, 2006; Peter, *et. al.,* 2004; Tikhovona & Zgurskaya, 2004). Therefore, we proceeded to assess the nature of the SD8 target by examining the regulatory consequences of the drug treatment on the transcriptional activity of the entire genome. An "SD8 expression profile" was constructed from the set of genes most significantly affected by SD8. When we compared the SD8 profile with the expression profiles, for the same set of genes, from almost 200 conditions of normal growth, growth arrest, and killing by antibacterial drugs and conditional mutations (Sangurdekar, Srienc & Khodursky, 2006), we found that the SD8 expression profile was most similar to the profiles that were observed under conditions of gyrase inhibition, either by a mutation or by norfloxacin or novobiocin treatment (Figure. 2.6). The probability of observing such similarities by chance, estimated by bootstrapping, was less than 1 in 1,000.

In 30 min of SD8 treatment, twice as many genes were significantly upregulated as were downregulated (132 versus 64 with a 95th percentile false discovery rate of 5%; see Table S2.2 in the supplemental material). The most downregulated gene (*topA*) encodes for topoisomerase I. Additionally, eight genes were downregulated at least twofold. The products of three of these genes, *topA*, *hns*, and *fis*, are known to be involved in removal of negative supercoils, either directly by the reaction of relaxation, as with topoisomerase I, or by constraining free supercoils,

as with H-NS and FIS (Bliska & Cozzarelli, 1987). The most downregulated genes also included *cspA*, a positive regulator of *hns*.

Of the 22 most upregulated genes (twofold or more), the products of 5 genes are associated with the control of initiation of chromosomal DNA replication, including the *gyrA* and *gyrB* genes, *dnaA*, *mioC*, and *gidA*. Importantly, the upregulation of DNA gyrase genes *gyrA* and *gyrB* was consistent with the downregulation of the *topA* gene, demonstrating that SD8 treatment activated the supercoiling-dependent regulatory loop, in which reduction in the supercoiling activity of DNA gyrase leads to downregulation of *topA* transcription and upregulation of transcription of the gyrase genes (Menzel & Gellert, 1983). The changes in the transcript levels of *topA* and the gyrase genes were confirmed by the RT-PCR experiments. The changes in the gyrase and *topA* transcripts in *E. coli* Δ*acrB* cells treated with SD8 were 0.31-fold ± 0.14-fold for *topA*, 8.21-fold ± 2.76-fold for *gyrA*, and 5.55-fold ± 5.55-fold for *gyrB* compared to a solvent-treated control.

More formal analysis of gene sets revealed that two classes of genes were overrepresented among the genes significantly upregulated by SD8, genes encoding surface antigens (enterobacterial common antigen and the O antigen of LPS) (*P* value corrected for multiplicity of measurements < 10^{-3}) and genes encoding DNA replication proteins ($P < 0.02$). Both sets of genes were affected to a similar extent by SD8 and novobiocin treatment (Figure. 2.7), whereas norfloxacin had a smaller effect on these sets of genes (data not shown). We carried out a similar analysis with the characteristic profiles of norfloxacin and novobiocin treatments. The transcriptional signature of the norfloxacin effect was the induction of the SOS response (adjusted *P* value < 10^{-11}), induction of the tricarboxylic acid (TCA) cycle genes ($P < 10^{-18}$), and downregulation of genes encoding components of the citrate-dependent iron transport system ($P < 10^{-7}$) (Jeong, Hiasa & Khodursky, 2006; Sangurdekar, Srienc & Khodursky, 2006). We found that the downregulation profiles of the iron transport cluster were similar in norfloxacin and SD8 treatments (Figure. 2.8). However, SD8 treatment did not result in significant induction of the SOS and TCA genes compared to norfloxacin treatment (Figure. 2.8). The transcriptional signature of the novobiocin effect was induction of RpoH targets ($P < 10^{-8}$), induction of relaxation-sensitive genes ($P < 10^{-5}$), and downregulation of supercoiling-sensitive genes (*P* <

10^{-10}) (Peter, *et. al.,* 2004; Sangurdekar, Srience and Khodursky, 2006). In SD8 treatment, relaxation-sensitive genes as a group were similarly affected, but not the RpoH and supercoiling-sensitive genes (Figure. 2.9). It must be pointed out that similar differences can be seen between the effects of norfloxacin and novobiocin.

2.3.2.3. Effect of SD8 on the state of the bacterial nucleoid.

The data presented above showed that SD8 affected the state of DNA supercoiling in vivo, likely by inhibiting the supercoiling activity of gyrase. Since the level of superhelicity is an essential attribute of the bacterial nucleoid, which contributes to chromosome organization (Postow, *et. al.,* 2004) and packing (Stuger, *et. al.,* 2002), we hypothesized that the inhibition of supercoiling by SD8 in vivo should result in at least partial unraveling of the nucleoid. This unraveling could be visualized by fluorescence microscopy as characteristic changes in the nucleoid morphology. We examined the morphology of the *E. coli* nucleoid following SD8 treatment of Δ*acrB* cells using DAPI staining. SD8 treatment resulted in detectable changes in the morphology of the nucleoid, such as a noticeably larger area occupied by the nucleoids, as well as the unusual shape of the nucleoid contour (Figure 2.10). Such an outcome, which may be indicative of reduced DNA scaffolding by gyrase, can be explained by the inhibition of gyrase biding to DNA by SD8 (Flatman, *et. al.,* 2005). Consistent with these observations, we found that SD8 interfered with the cleavage activity of gyrase in vitro (see Figure S5 in the supplemental material). This may also explain the lack of the DNA damage response (Figure. 2.8).

2.4. Discussion

DNA gyrase and Topo IV are essential enzymes that display distinct cellular functions (Champoux, 2001; Wang, 2002). Gyrase is the only topoisomerase that introduces negative supercoils into DNA, whereas Topo IV is responsible for decatenation of sister chromosomes. The importance of bacterial type II topoisomerases is underscored by the fact that both gyrase and Topo IV are the cellular targets of clinically important antibacterial agents, the quinolones and the coumarins (Drlica & Malik, 2003; Maxwell, 1999). The quinolone drugs poison gyrase and Topo IV, whereas the coumarins inhibit their ATPase activities. Interestingly, each quinolone drug selects one of two topoisomerases as its primary target in vivo, and the primary target

changes depending on the drug, as well as the bacterium (Drlica & Malik, 2003; Ferroro, *et. al.,* 1994; Khodursky, Zechiedrich & Cozzarelli, 1995; Maxwell, 1999; Pan & Fisher, 1997). For instance, ciprofloxacin targets gyrase in *E*. *coli* and Topo IV in *S*. *aureus*. In our catalytic assays (Table 2.1), the primary targets, *E*. *coli* gyrase and *S*. *aureus* Topo IV, are at least fivefold more sensitive to ciprofloxacin than the secondary targets, *E*. *coli* Topo IV and *S*. *aureus* gyrase.

It has been shown that SD8 inhibits *E*. *coli* gyrase by a novel mechanism, by binding to the catalytic domain of the GyrA subunit and preventing gyrase from binding to DNA (Flatman, *et. al.,* 2005). SD8, however, exhibits antibiotic activity against gram-positive, but not gram-negative, bacteria (Schimana, *et. al.,* 2000). We examined the effects of SD8 on the catalytic activities of *S*. *aureus* topoisomerases in order to determine the target of SD8 in gram-positive bacteria. We found that SD8 could inhibit the supercoiling activity of *S*. *aureus* gyrase, as well as that of *E*. *coli* gyrase (Table 2.1). In addition, we found that, as was the case with *E*. *coli* gyrase (Flatman, *et. al.,* 2005), SD8 could interfere with the binding of *S*. *aureus* gyrase to DNA (Figure. 2.3). In contrast, SD8 had only a modest inhibitory effect on *S*. *aureus* Topo IV, and *E*. *coli* Topo IV was not sensitive to SD8. Thus, gyrase seems to be the target of SD8 in both gram-positive and gram-negative bacteria, suggesting that the differences in the susceptibilities of gram-positive and gram-negative bacteria to SD8 are not due to large differences in the sensitivities of topoisomerases to SD8.

DNA gyrases and Topo IVs share extensive homologies, and their differences in susceptibilities to various inhibitors are determined by subtle differences in the amino acid residues of the drug binding pockets (Champoux, 2001; Drlica & Malik, 2003; Maxwell, 1999; Wang, 2002). Although the binding pocket of SD8 has yet to be determined, it appears that SD8 binds to the GyrA subunit through a bipartite interaction (A. Maxwell, personal communication). Such an interaction might explain the differences in the susceptibilities of gyrase and Topo IV to SD8. For instance, although SD8 interacts with the GyrA subunit at two binding sites, SD8 might be able to bind to the ParC subunit only at one of the two binding sites. Of course, the determination of the SD8 binding pockets on gyrase and Topo IV is required to understand the molecular basis of the different susceptibilities of gyrase and Topo IV to SD8.

The DNA cleavage assays for *S*. *aureus* topoisomerases revealed an interesting effect of KGlu on the SD8 sensitivity (Figure 2.3). *S*. *aureus* gyrase can bind and cleave DNA in the absence of KGlu but requires high concentrations of KGlu to catalyze the supercoiling reaction (Hiasa, *et. al.,* 2003). The concentrations of SD8 required to inhibit the formation of ciprofloxacin-induced *S*. *aureus* gyrase-DNA complexes in the absence of KGlu were significantly higher than those in the presence of KGlu. Thus, KGlu affected the apparent SD8 sensitivity of *S*. *aureus* gyrase. This could be due to the accessibility of SD8 to its binding pocket in different conformations of the topoisomerase. It is possible that SD8 can interact with *S*. *aureus* gyrase effectively when *S*. *aureus* gyrase is in an active conformation for supercoiling (in the presence of high concentrations of KGlu), but not when *S*. *aureus* gyrase is in an inactive conformation for supercoiling (in the absence of KGlu).

Genome-wide transcriptional profiles can reliably capture regulatory patterns associated with molecular mechanisms of drug activity (Cheung, *et. al.,* 2003; Gmuender, *et. al.,* 2001; Jeong, *et. al.,* 2006; Peter, *et. al.,* 2004; Tikhonova & Zgurskaya, 2004). The transcriptional response of *E*. *coli* to SD8 treatment mimics the profiles of gyrase inhibition. It also has certain unique characteristics that suggest that SD8-treated cells are not as stressed (limited DNA damage response, no heat shock response, and general stress response) as cells treated with either norfloxacin or novobiocin. It is possible that these differences are due to the fact that SD8 does not reach sufficiently high concentration in the cell to produce those secondary effects. However, because the effects of norfloxacin and novobiocin are also different and because the intracellular SD8 concentration appears to be high enough to elicit certain characteristic responses, it is also quite possible that the observed transcriptional variations are due to SD8's unique mechanism of gyrase inhibition, which does not involve conversion of gyrase into a poison. These results also suggest that the main target for SD8 in vivo is indeed gyrase.

There are many possible reasons why SD8 is effective against gram-positive bacteria, but not against gram-negative bacteria. It is possible, although unlikely, that a modest inhibition of the *S*. *aureus* Topo IV activity by SD8 could contribute to the effectiveness of SD8 against *S*. *aureus*. However, since SD8 was capable of inhibiting both *S*. *aureus* gyrase and *E*. *coli* gyrase, the lack of inhibition of *E*. *coli* gyrase is highly unlikely to be the reason why SD8 is ineffective against *E*. *coli*.

Multidrug efflux pumps, especially those belonging to the resistance-nodulation-division family, play an important role in establishing the resistance of gram-negative bacteria to a number of agents (Poole, 2001; Ramos, *et. al.,* 2002). The *acrB* deletion affected the sensitivity of *E*. *coli* to SD8 (Figure. 2.5). Thus, the AcrB multidrug efflux pump is partially responsible for the ineffectiveness of SD8 against gram-negative bacteria.

Antibiotics have been life-saving interventions for decades. Infections of gram-positive bacteria, particularly methicillin-resistant *S*. *aureus*, are often considered life threatening, and drug development tends to focus on gram-positive pathogens. However, the recent emergence of drug-resistant gram-negative bacteria presents an equally, if not more, important challenge to public health (Roberts & Simpson, 2008; Taubes, 2008). Unfortunately, the development of drug-resistant bacterial pathogens seems to occur faster than the development of new antibacterial drugs by pharmaceutical companies. One approach to develop a drug that is effective against gram-negative pathogens is the co-optation of drugs that are active against gram-positive bacteria but not against gram-negative bacteria. This process of co-optation would involve creating artificial conditions where gram-negative bacteria could become susceptible to the drugs, investigating mechanisms of action, and tailoring chemical structures of the drugs to overcome nonspecific defensive mechanisms of gram-negative bacteria if such targets can be found. This work presents a case study, using SD8 as a model drug, of the first two steps. Efforts are under way to identify chemical modifications that improve the potency of SD8 and to broaden its spectrum.

Figure 2.1. Structure of SD8. Two functional groups, the aminocoumarin and the glycone, are shown. The calculated molecular mass of SD8 is 932.2169, whereas the molecular masses, determined by mass spectrometry, of the original and current preparations of SD8 are 932.2134 and 932.2139, respectively. Me, methyl.

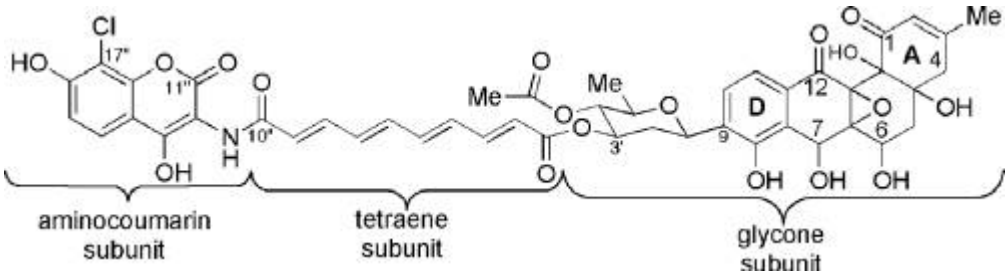

Figure 2.2. SD8 is a potent inhibitor of *S. aureus* gyrase. The supercoiling reaction mixtures containing the relaxed DNA, either 50 fmol of *S. aureus* (Sa) gyrase (A) or 10 fmol of *E. coli* (Ec) gyrase (B), and the indicated concentrations of either SD8 or ciprofloxacin (Cipro) were incubated, and the DNA products were analyzed as described in Materials and Methods. Lanes 1 and 2 contain controls with gyrase and drug present (+) or absent (−). The arrows in panels A and B show that gyrase was present in lanes 3 to 13.

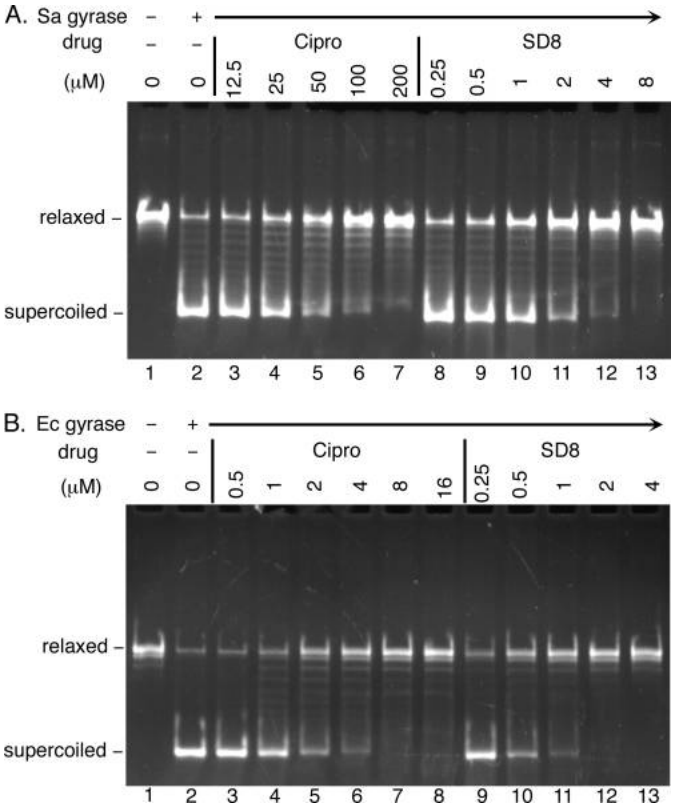

Figure 2.3. The presence of KGlu affects the apparent SD8 sensitivity of *S*. *aureus* gyrase in the DNA cleavage assay. The two-step DNA cleavage assay was performed as described in Materials and Methods. (A) For *E*. *coli* (Ec) gyrase, 50 fmol of *E*. *coli* gyrase, the supercoiled DNA, and the indicated concentrations of SD8 were first incubated, and then 10 μM of ciprofloxacin (Cipro) was added to the reaction mixtures. (B and C) For *S*. *aureus* (Sa) gyrase, 400 fmol of *S*. *aureus* gyrase, the supercoiled DNA, and the indicated concentrations of SD8 were first incubated in the absence (B) or presence (C) of 400 mM KGlu, and then 50 μM of ciprofloxacin was added to the reaction mixtures. No EtBr was included in the TAE buffer. Lanes 1 and 2 contain controls with gyrase and drug present (+) or absent (− and 0). The arrows in panels A, B, and C show that gyrase was present in lanes 3 to 9 or 10.

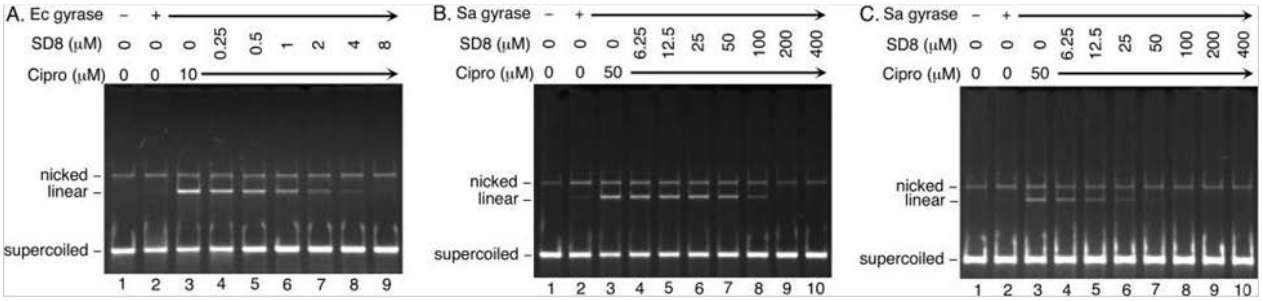

Figure 2.4. Effects of SD8 on the decatenation activity of Topo IV. The decatenation reaction mixtures containing kinetoplast DNA, 50 fmol of either *S*. *aureus* (Sa) Topo IV (A) or *E*. *coli* (Ec) Topo IV (B), and the indicated concentrations of either SD8 or ciprofloxacin (Cipro) were incubated, and the DNA products were analyzed as described in Materials and Methods. Lanes 1 and 2 contain controls with Topo IV and drug present (+) or absent (− and 0). The arrows in panels A and B show that Topo IV was present in lanes 3 to 12.

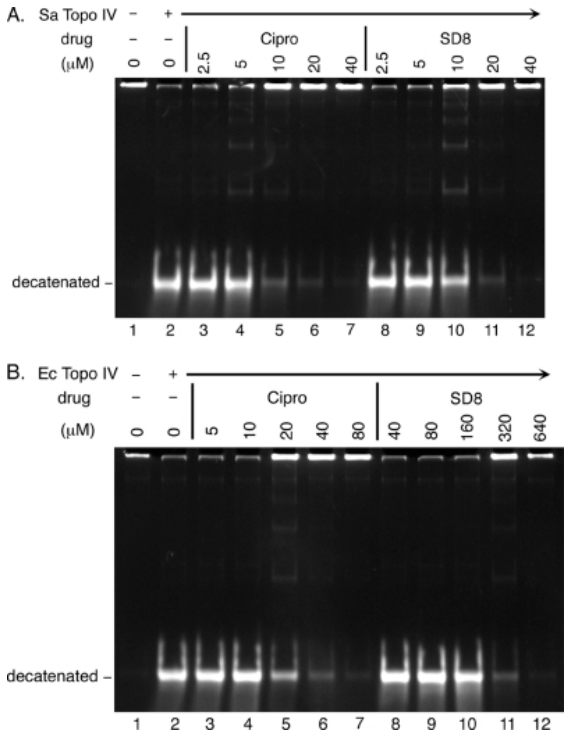

Figure 2.5. Effect of SD8 on growth of wild-type and Δ*acrB* strains. Absorbance (Abs) over time at 600 nm of wild-type (A) and Δ*acrB* (B) cultures treated with various concentrations of SD8 recorded in a 96-well format. The error bars represent 1 standard deviation of measurements done in triplicate. The cells were treated with SD8 (D8) concentrations ranging from 10 nM to 50 µM; however, only results from 1 µM to 50 µM are depicted, as there was little difference in the growth pattern of cells treated with <1 µM SD8.

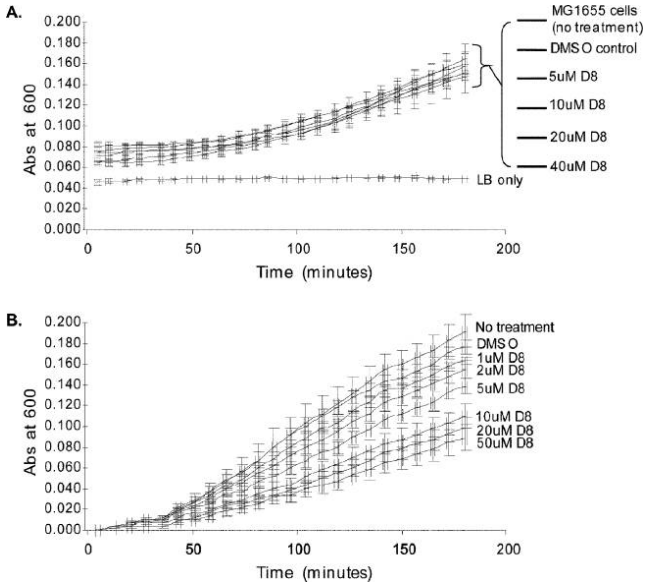

Figure 2.6 Transcriptional profile of SD8 treatment is most similar to the profile of gyrase inhibition. For the set of genes significantly affected by SD8 treatment, the Pearson correlation coefficients between the vector obtained in SD8 treatment and each of the 198 microarray conditions were calculated and plotted in descending order.

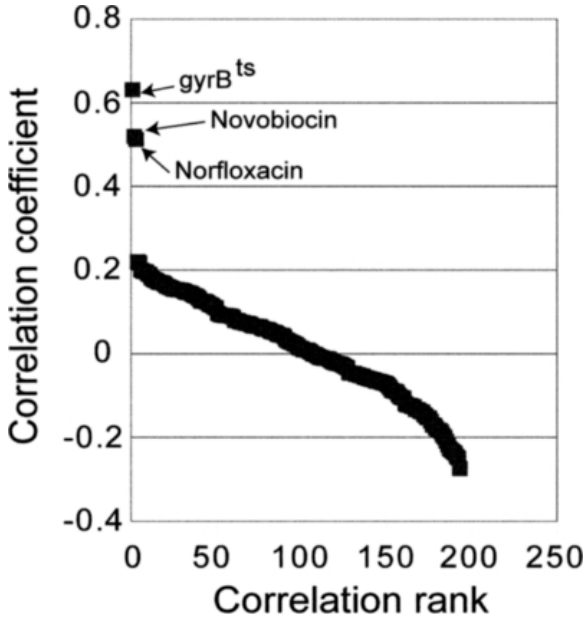

Figure 2.7 Surface antigen and DNA replication genes are similarly upregulated by SD8 and novobiocin. Pairwise correlations between profiles (expressed as one-dimensional vectors of log-transformed ratios of transcript abundances) of genes encoding DNA replication proteins and of genes encoding surface antigens. The reference treatments are indicated along the *x* axes. In Figure 7 to 9, only the genes that were identified as significantly affected at a median false discovery rate of 5% or less are labeled.

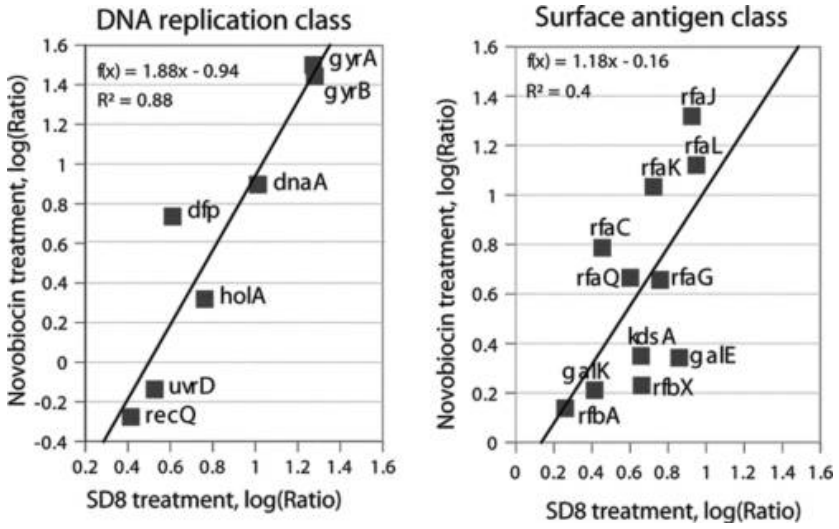

Figure 2.8 The pattern of SD8 activity shares limited similarity with transcriptional patterns of the norfloxacin effect. The characteristic profiles of norfloxacin treatment, the induction of the SOS response, upregulation of the TCA cycle genes, and downregulation of genes encoding components of the citrate-dependent iron transport system, were compared with those of SD8 treatment. Pairwise correlations between profiles of gene classes are shown as described in the legend to Figure 2.7.

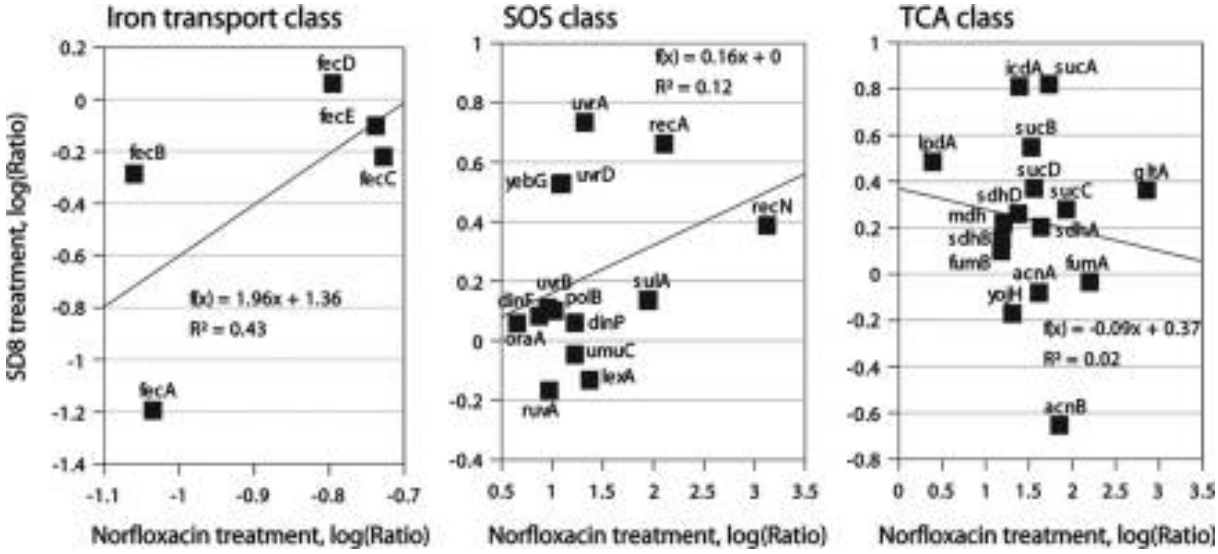

Figure 2.9 The pattern of SD8 activity shares limited similarity with transcriptional patterns of the novobiocin effect. The transcriptional signatures of the novobiocin effect, the induction of RpoH targets, upregulation of relaxation-sensitive genes, and downregulation of supercoiling-sensitive genes, were compared with those of the SD8 treatment. Pairwise correlations between profiles of gene classes are shown as described in the legend to Figure 2.7.

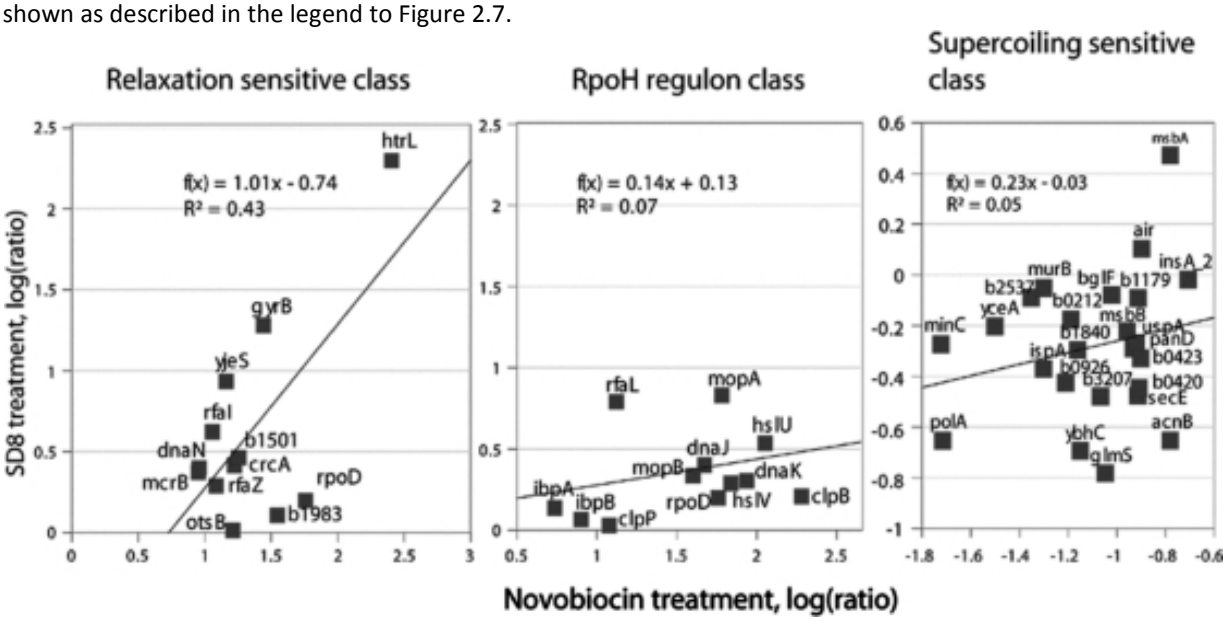

Figure 2.10. Effect of SD8 on nucleoid morphology. Exponentially grown Δ*acrB* cells were treated with either SD8 or DMSO, the solvent of SD8, stained with DAPI, and visualized by fluorescence (A, B, E, and F) and phase-contrast (C, D, G, and H) microscopy.

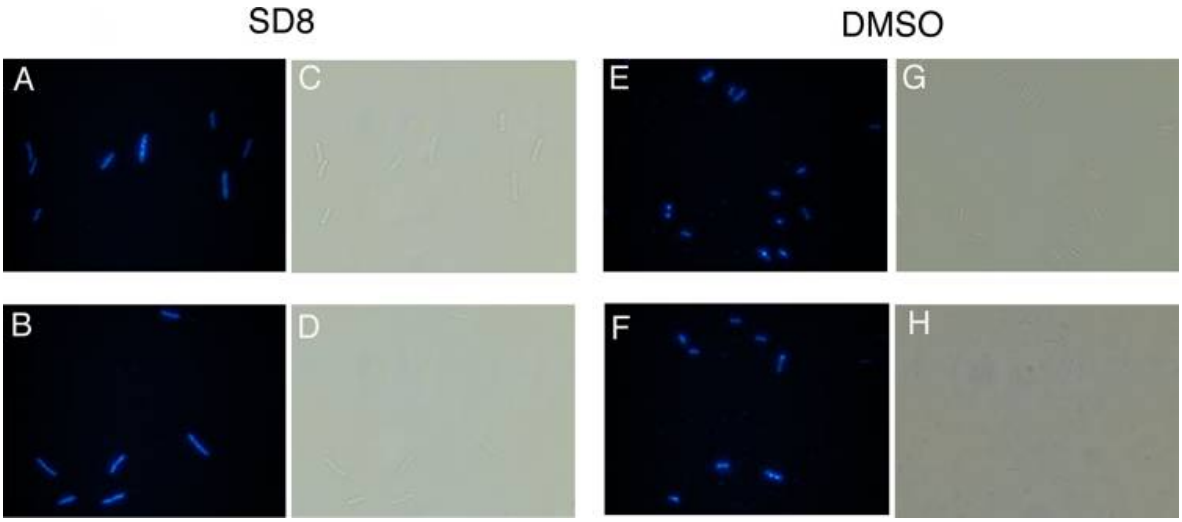

Table 2.1.

Drug sensitivities of *S. aureus* and *E. coli* topoisomerases

Topoisomerase	IC_{50} (μM) of topoisomerase	
	SD8	**Ciprofloxacin**
S. aureus gyrase	1.45 ± 0.35	48 ± 9
E. coli gyrase	0.41 ± 0.03	2.35 ± 0.55
S. aureus Topo IV	14.5 ± 0.5	8.4 ± 0.1
E. coli Topo IV	270 ± 10	34 ± 1

[a]The drug sensitivities of gyrases and Topo IV

Chapter 2: Supplementary Information

S.2.1. Characterization of SD8

Analysis by reversed phase-HPLC and mass spectrometry of the 'current' preparation of SD8 produced for this study showed it to be identical to the 'original' preparation of SD8 isolated from *S. antibioticus* Tü 6040 (Figure S2.1). We also analyzed both the current and the original preparations of SD8 by NMR. Our 1- and 2-D studies allowed us to further assign the proton and carbon spectra of the natural product. In the proton spectra, we were able to assign all but two of the hydrogens (the C4a and C12b OH's), and we were able to assign all of the peaks in the carbon spectra (Figure S2.1 and Table S2.1). This represented a significant improvement over the initial analysis of SD8 (38) where only one of the seven alcohol peaks were assigned and the carbons at position 12 (δ65.9 ppm) and 12a (δ190.4 ppm) could be assigned only after isotopic enrichment by ^{13}C feeding experiments.

Next, we assessed the effects of the current preparation of SD8 on Ec gyrase and compared them with those of the original preparation of SD8. We performed the supercoiling and DNA cleavage assays to compare the effects of the two preparations of SD8 on Ec gyrase (Figure S2). Both the original and current preparations of SD8 inhibited the supercoiling activity of Ec gyrase (Figure S2.2A). In addition, an approximately equimolar ratio of SD8 to ciprofloxacin abolished ciprofloxacin-induced covalent gyrase-DNA complex formation (Figure S2B). These results were essentially identical to those reported previously (8) and demonstrated that the current preparation of SD8 exhibited the same activity as the original preparation of SD8. All experiments except those shown in Figs. S1 and S2 were conducted using the current preparation of SD8.

Table S2.1. ^{1}H NMR signals of the SD8 hydroxyl protons

Proton	δ_H (ppm, J in Hz)
6-OH	5.63[a] (d, 6.7)
7-OH	6.91[b] (s)
8-OH	9.59[c] (s)
13-OH	12.60[d] (br s)
16”-OH	9.69[e] (br s)
4a-OH	4.85[f] (br s) or 5.27[g] (br s)
12b-OH	4.85[f] (br s) or 5.27[g] (br s)

[a, c, e-f]Peaks shifts were previously reported but assignments were not. (10).
[a]Previously reported as 5.58 ppm.
[b]Peak not previously reported.
[c]Previously reported as 9.58 ppm.
[d]Previously reported as 12.60 and assigned as 13-OH.
[e]Previously reported as 9.85 ppm.
[f]Previously reported as 4.82 ppm.
[g]Previously reported as 5.27 ppm.

Table S2.2. The list of genes significantly (median FDR of 5% or less) affected by SD8 treatment

Down regulated genes	Fold change	Log(base2) of fold change	Error	Upregulated genes	Fold change	Log(base2) of fold change	Error
topA	0.31	-1.69	0.45	b3618	4.92	2.3	0.21
yggH	0.42	-1.25	0.22	pstB	2.69	1.43	0.19
fecA	0.44	-1.18	0.23	argS	2.57	1.36	0.26
hns	0.45	-1.15	0.16	b3618	2.52	1.33	0.21
cspA	0.47	-1.09	0.19	udhA	2.49	1.32	0.3
b0805	0.49	-1	0.15	ycfC	2.44	1.29	0.29
b1452	0.5	-1	0.33	gyrB	2.43	1.28	0.21
fis	0.5	-1	0.45	gyrA	2.42	1.28	0.12
ompC	0.56	-0.84	0.15	prsA	2.41	1.27	0.19
accC	0.56	-0.84	0.09	b0955	2.39	1.26	0.25
rnb	0.56	-0.84	0.14	yebC	2.38	1.25	0.15
dksA	0.57	-0.81	0.1	fnr	2.35	1.23	0.13
b2007	0.58	-0.79	0.15	ycaJ	2.28	1.19	0.23
accB	0.6	-0.74	0.07	pstS	2.27	1.18	0.31
valS	0.61	-0.71	0.12	rnpA	2.26	1.18	0.33
tonB	0.61	-0.71	0.17	gidA	2.19	1.13	0.11
rpsQ	0.64	-0.64	0.3	kbl	2.14	1.1	0.18
fimI	0.64	-0.64	0.07	b2532	2.11	1.08	0.12
ybhA	0.65	-0.62	0.09	mioC	2.1	1.07	0.19

fimC	0.68	-0.56	0.09
b1641	0.69	-0.54	0.05
yjgF	0.69	-0.54	0.02
b0877	0.7	-0.51	0.02
pta	0.7	-0.51	0.05
rpsO	0.7	-0.51	0.08
b4395	0.7	-0.51	0.1
mscL	0.72	-0.47	0.01
yaaC	0.73	-0.45	0.09
yiaV	0.73	-0.45	0.04
yhbG	0.73	-0.45	0.11
surA	0.74	-0.43	0.05
csrB	0.74	-0.43	0.1
ybhA	0.75	-0.42	0.09
srmB	0.76	-0.4	0.04
b1112	0.76	-0.4	0.06
fabA	0.76	-0.4	0.08
yjeA	0.76	-0.4	0.07
ygiM	0.77	-0.38	0.09
hupB	0.77	-0.38	0.08
apt	0.78	-0.36	0.04
yaaD	0.79	-0.34	0.06
yggE	0.79	-0.34	0.07
ytfM	0.8	-0.32	0.07
ispB	0.8	-0.32	0.02
glnA	0.81	-0.3	0.06
rfe	0.81	-0.3	0.05
aceE	0.82	-0.29	0.05
gcd	0.83	-0.27	0.14
b2673	0.83	-0.27	0.05
b2174	0.83	-0.27	0.05
b2771	0.84	-0.25	0.05
rplN	0.84	-0.25	0.05
nrdB	0.85	-0.23	0.02
gshB	0.85	-0.23	0.04
yidA	0.85	-0.23	0.04
pcnB	0.85	-0.23	0.03
b1193	0.85	-0.23	0.03
yfiC	0.86	-0.22	0.04
xseA	0.87	-0.2	0.03
yi21_2	0.89	-0.17	0.03
yhbP	0.89	-0.17	0.03
mscL	0.91	-0.14	0.01
ribE	0.91	-0.14	0.02
ydiE	0.93	-0.1	0.01
yidC	2.05	1.04	0.04
nhaA	2.05	1.04	0.16
dnaA	2.02	1.01	0.1
ruvC	1.99	0.99	0.18
aspS	1.98	0.99	0.12
deoC	1.94	0.96	0.26
rfaL	1.93	0.95	0.2
ychM	1.92	0.94	0.1
yjeS	1.91	0.93	0.16
rfaJ	1.9	0.93	0.16
b3838	1.89	0.92	0.14
potD	1.86	0.9	0.21
gidB	1.85	0.89	0.18
ycfB	1.85	0.89	0.19
b0660	1.84	0.88	0.24
galE	1.81	0.86	0.17
sucA	1.77	0.82	0.13
yejM	1.76	0.82	0.14
b3472	1.74	0.8	0.18
phoB	1.74	0.8	0.19
rfaL	1.73	0.79	0.2
b3836	1.71	0.77	0.05
holA	1.7	0.77	0.15
rfaG	1.69	0.76	0.06
yibO	1.69	0.76	0.17
fldA	1.67	0.74	0.13
pckA	1.67	0.74	0.07
rfaK	1.65	0.72	0.23
tdh	1.64	0.71	0.16
lysS	1.63	0.7	0.13
yi52_9	1.62	0.7	0.11
add	1.61	0.69	0.18
b2299	1.59	0.67	0.08
rpsU	1.59	0.67	0.07
b1777	1.59	0.67	0.08
gnd	1.59	0.67	0.11
hrpA	1.58	0.66	0.11
recA	1.58	0.66	0.06
rfbX	1.58	0.66	0.07
kdsA	1.58	0.66	0.06
b0619	1.57	0.65	0.06
b1778	1.57	0.65	0.12
yigC	1.56	0.64	0.14
nagC	1.55	0.63	0.09
b3837	1.54	0.62	0.09
dfp	1.53	0.61	0.02

rfaQ	1.52	0.6	0.15
yi52_2	1.51	0.59	0.09
speG	1.51	0.59	0.14
yi52_10	1.5	0.58	0.06
hepA	1.49	0.58	0.12
b1630	1.48	0.57	0.15
b2286	1.47	0.56	0.09
yi52_3	1.46	0.55	0.07
rpmB	1.46	0.55	0.14
greA	1.45	0.54	0.1
ysdA	1.44	0.53	0.14
yebG	1.44	0.53	0.06
yefJ	1.44	0.53	0.11
uvrD	1.44	0.53	0.1
rfaB	1.44	0.53	0.19
sapA	1.43	0.52	0.07
b0658	1.43	0.52	0.13
lolA	1.43	0.52	0.13
purL	1.41	0.5	0.11
yi52_11	1.4	0.49	0.1
b2530	1.39	0.48	0.12
phoU	1.39	0.48	0.12
cydD	1.39	0.48	0.04
msbA	1.39	0.48	0.12
rfaC	1.37	0.45	0.07
yigO	1.37	0.45	0.1
yfhF	1.36	0.44	0.11
leuS	1.35	0.43	0.11
sseB	1.35	0.43	0.11
rph	1.34	0.42	0.04
recQ	1.33	0.41	0.06
galK	1.33	0.41	0.1
cydC	1.32	0.4	0.1
ttk	1.31	0.39	0.07
b1171	1.3	0.38	0.08
yebB	1.3	0.38	0.05
aroC	1.29	0.37	0.09
phnA	1.29	0.37	0.07
prfB	1.29	0.37	0.08
nuoG	1.29	0.37	0.06
gltA	1.29	0.37	0.04
b3570	1.28	0.36	0.06
b1628	1.27	0.34	0.07
truA	1.27	0.34	0.07
b1629	1.27	0.34	0.09
b2343	1.25	0.32	0.08

yjeB	1.25	0.32	0.08
fdx	1.22	0.29	0.21
b1786	1.22	0.29	0.02
b2028	1.2	0.26	0.08
b3015	1.2	0.26	0.05
rfbA	1.2	0.26	0.04
ybaJ	1.2	0.26	0.04
b2258	1.19	0.25	0.1
yigW_2	1.18	0.24	0.04
pheT	1.18	0.24	0.05
yrbB	1.16	0.21	0.03
yheS	1.16	0.21	0.05
o161	1.15	0.2	0.03
metJ	1.14	0.19	0.02
yjaG	1.14	0.19	0.02
yagX	1.13	0.18	0.04
b0669	1.13	0.18	0.03
fliE	1.12	0.16	0.03
yhfK	1.1	0.14	0.01
b2788	1.1	0.14	0.02
b1036	1.1	0.14	0.02

Figure S2.1. NMR studies of SD8. PanelA. Top: Proton NMR Spectra (400 MHz, d^6-DMSO) of the original preparation of SD8 isolated from *S. antibioticus* Tü 6040. Bottom: Proton NMR Spectra (400 MHz, d^6-DMSO) of the current preparation of SD8 prepared for this study. **Panel B.** Carbon NMR Spectra (100 MHz, d^6-DMSO) of the current preparation of SD8, where C-12 (δ65.9 ppm) and C-12a (δ190.4 ppm) can be observed.

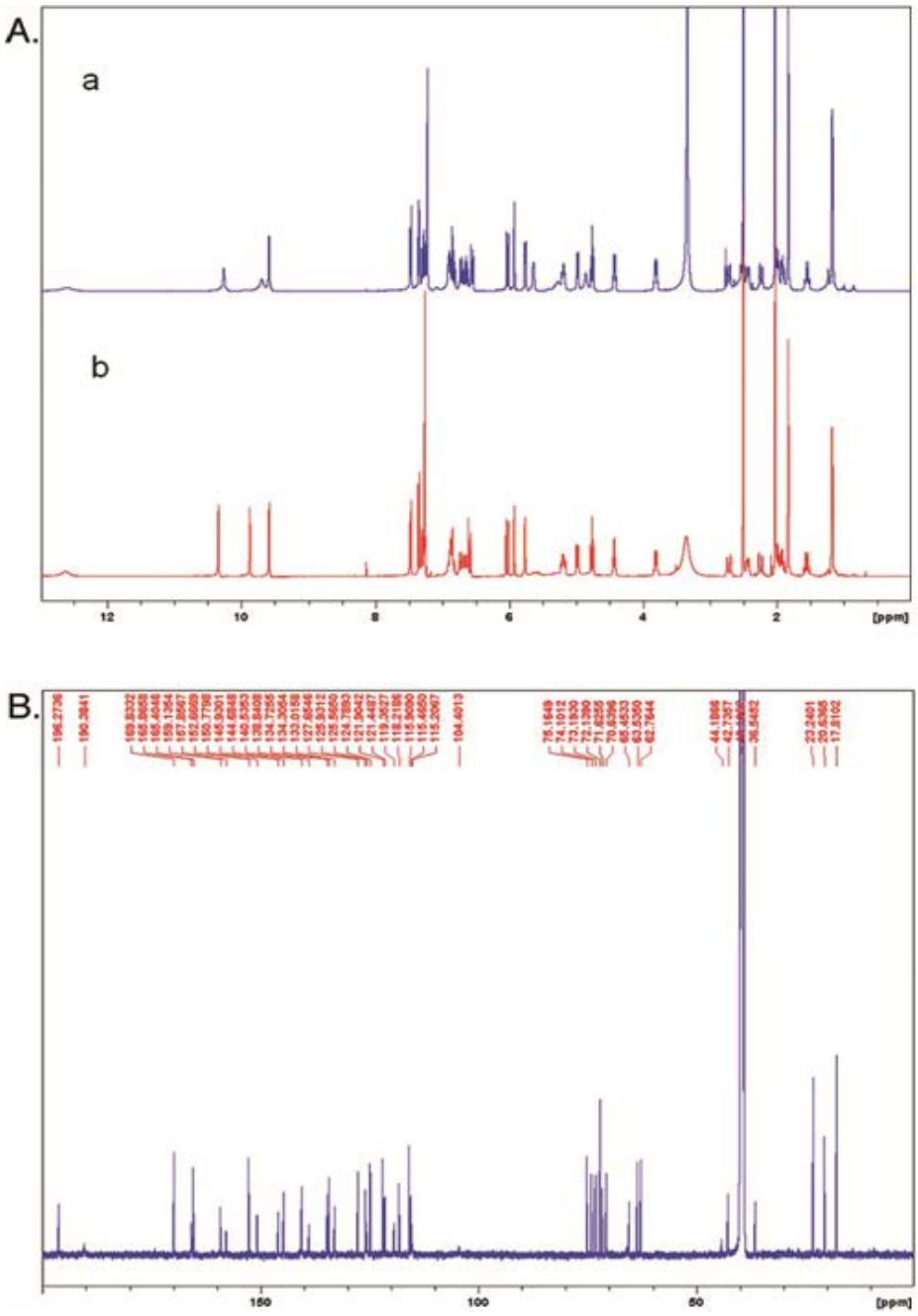

Figure S2.2. Effects of SD8 on Ec gyrase. Panel A. The supercoiling reaction mixtures containing the relaxed DNA, 10 fmol of Ec gyrase, and the indicated concentrations of either the original or current preparation of SD8 were incubated and the DNA products were analyzed as described in "MATERIALS AND METHODS". **Panel B.** Standard DNA cleavage reaction mixtures (20 μL) containing 50 mM Tris-HCl (pH 8.0 at 23°C), 10 mM $MgCl_2$, 10 mM dithiothreitol, 50 μg/mL bovine serum albumin, 1 mM ATP, 5 μg/mL tRNA, 0.3 μg of the relaxed DNA, 100 fmol of Ec gyrase, 10 μM ciprofloxacin, and the indicated concentrations of either the original or current preparation of SD8 were incubated were incubated at 37°C for 10 min. SDS was added to a concentration of 1%, and the reaction mixtures were further incubated at 37°C for 5 min. EDTA and proteinase K were then added to 25 mM and 100 μg/mL, respectively, and the incubation was continued for an additional 15 min at 37°C. The DNA products were purified by extraction with phenol/chloroform/isoamyl alcohol (25:24:1, v/v) and then analyzed by electrophoresis through vertical 1.2% agarose gels at 2 V/cm for 15 hours in TAE buffer that contained 0.5 μg/mL EtBr. After destaining in water, gels were photographed and quantified using an Eagle Eye II system. For both panels: SD8 #1, the original preparation; SD8 #2, the current preparation.

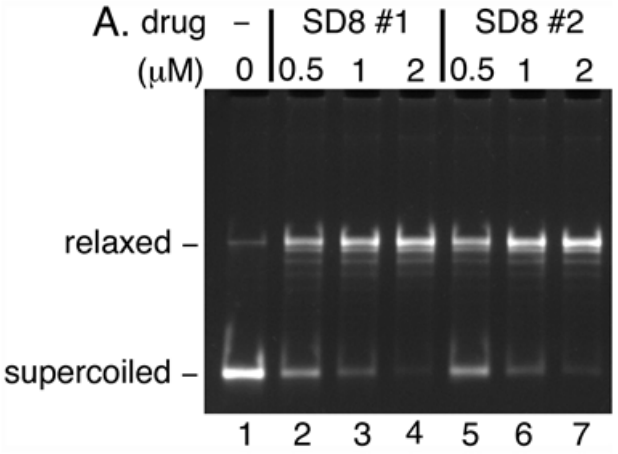

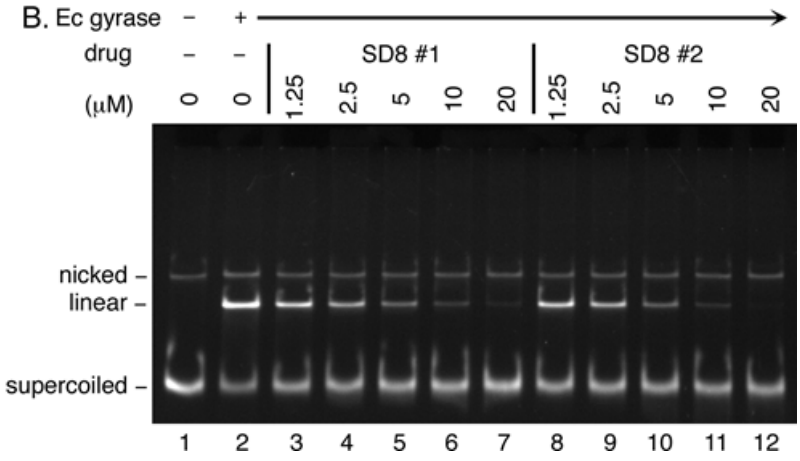

Figure S2.3. The presence of KGlu affects the apparent SD8 sensitivity of Sa Topo IV in the DNA cleavage assay. The 2-step DNA cleavage assay was performed as described in "Materials and Methods". For Sa Topo IV, 50 fmol of Sa Topo IV, the relaxed DNA, and the indicated concentrations of SD8 were first incubated in the absence (**Panel A**) or presence of 400 mM KGlu (**Panel B**) and then 50 μM of ciprofloxacin was added to the reaction mixtures. For Ec Topo IV (**Panel C**), 50 fmol of Ec Topo IV, the relaxed DNA, and the indicated concentrations of SD8 were first incubated and then 50 μM of ciprofloxacin was added to the reaction mixtures. EtBr present in the TAE buffer converted the relaxed DNA into the supercoiled form during gel electrophoresis.

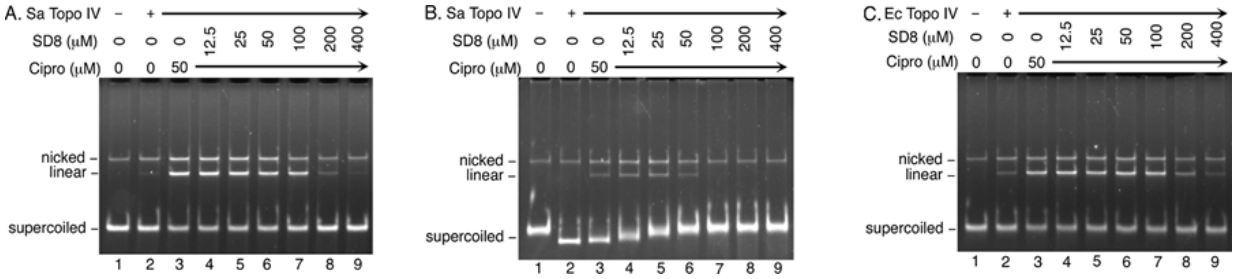

Figure S2.4. The SD8 treatment causes the elongation of Δ*acrB* cells. Δ*acrB* cells were visualized by the direct contrast confocal microscopy after treatment with varying concentrations of SD8 for 2 hours in LB media.

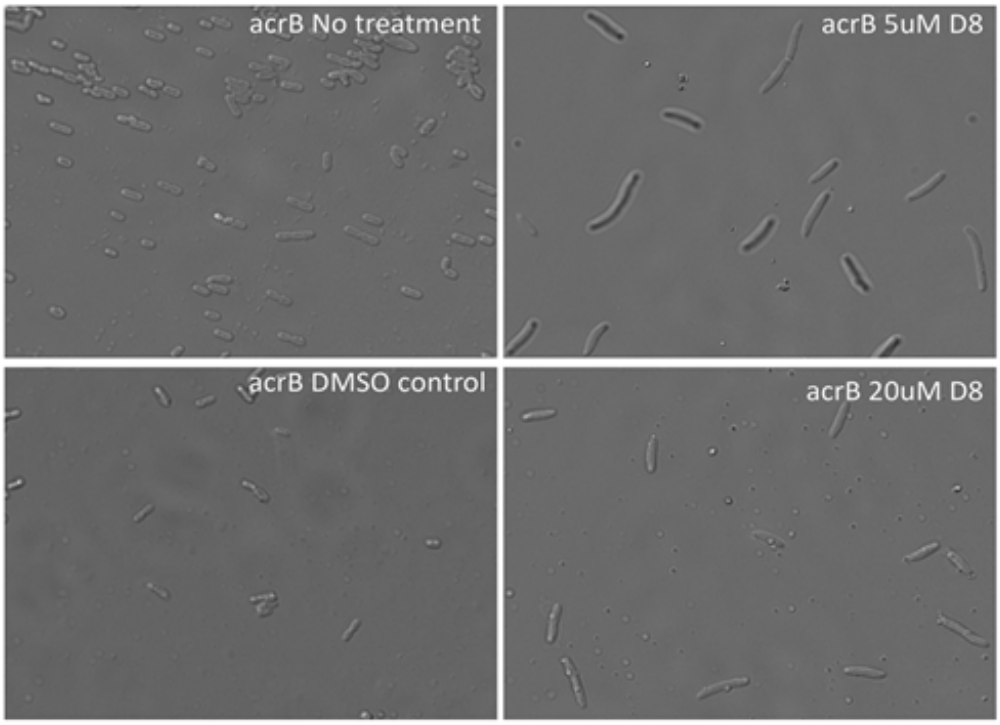

Figure S2.5. SD8 inhibits the cleavage activity of DNA gyrase *in vitro*. The 2-step DNA cleavage assay was performed as described in "Materials and Methods", except that no EtBr was included in the TAE buffer. In this experiment, 200 fmol of Ec gyrase was incubated in the first step with the supercoiled DNA and 10 μM of either ciprofloxacin (C) or SD8 (S), followed by the second step of incubation with 10 μM of either SD8 or ciprofloxacin. Lanes 3 and 6 show the DNA products after the first step of incubation.

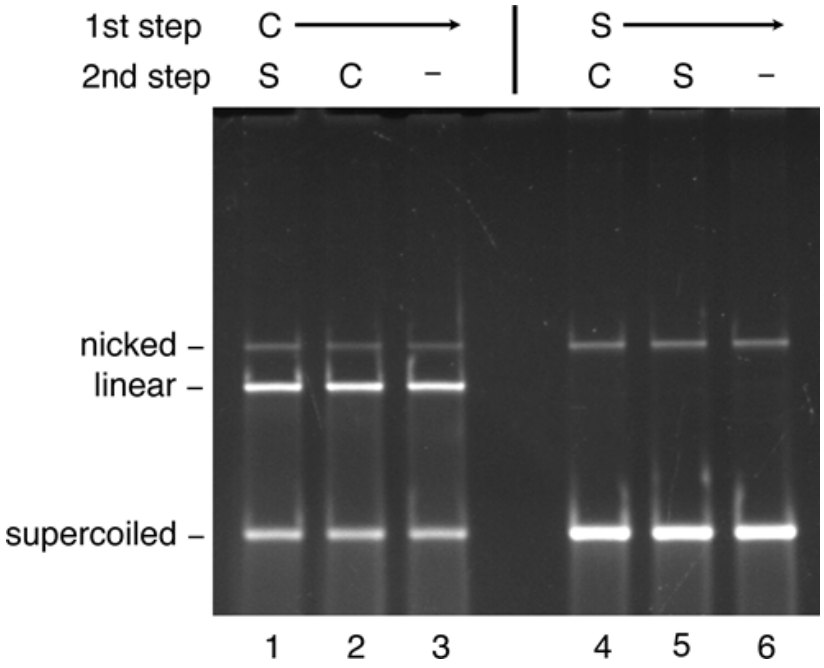

Transition to Chapter 3

The work presented in chapter 3 was published in the journal of *Molecular Microbiology* (75(6), 1455-1467) in 2010. My work in this study showed that the loss of genetic information surrounding the origin of replication was mitigated in mutants defective in the auxiliary recombination proteins ReF, O, Q, and J, and that viability was directly correlated with genetic loss in these mutants (data shown Figures 7 & 8). I purified DNA from thymine-starved *E. coli* cells, labeled the DNA with Cy3- and Cy5- dUTPs for approximation of gene-copy number using comparative genomic hybridization to DNA microarrays.

Other experiments and data analysis performed in this paper were done by Drs. Dipen Sangurdekar, Dmitri Smirnov, and Professor Arkady Khodursky.

Chapter 3: Thymineless Death is Associated with Loss of Essential Genetic Information from the Replication Origin

Thymine starvation results in a terminal cellular condition known as thymineless death (TLD), which is the basis of action for several common antibiotics and anticancer drugs. We characterized the onset and progression of TLD in *Escherichia coli* and found that DNA damage is the only salient property that distinguishes cells irreversibly senesced under thymine starvation from cells reversibly arrested by the nucleotide limitation. The damage is manifested as the relative loss of genetic material spreading outward from the replication origin: the extent of TLD correlates with the progression of damage. The reduced lethality in mutants deficient in the RecFOR/JQ repair pathway also correlates with the extent of damage, which explains most of the observed variance in cell killing. We propose that such spatially localized and persistent DNA damage is the consequence of transcription-dependent initiation of replication in the thymine-starved cells and may be the underlying cause of TLD.

3.1 Introduction

Escherichia coli thymidylate (dTMP) auxotrophs, *thyA*− mutants, when grown in a medium that is devoid of thymine, but which contains other essential nutrients, undergo filamentation and loss of viability. The phenomenon, termed 'thymineless death (TLD)', which was first reported by Barner and Cohen in *E. coli* over 50 years ago (Barner and Cohen, 1954), has also been observed in other prokaryotes, yeasts, mammalian cells (reviewed in Ahmad *et al.*, 1998) and even in the UV and Gamma-radiation hyper-resistant *Deinococcus radiodurans* (Little and Hanawalt, 1973). *E. coli* cells synthesize dTMP from dUMP in a reaction catalysed by the *thyA* encoded thymidylate synthase. Mutants that have lost *thyA* function cannot grow without externally supplied thymine or thymidine, and when the nucleotide is removed from the growth medium, they gradually lose the ability to form colonies. After thymine withdrawal, DNA replication ceases (Barner and Cohen, 1954; Hanawalt *et al.*, 1961; Maaløe and Hanawalt, 1961). As thymine is found only in DNA, thymine deprivation does not affect other genetic information processing reactions in the cell, at least for some time after commencement of starvation

(Barner and Cohen, 1954; Hanawalt *et al.*, 1961; Maaløe and Hanawalt, 1961; McFall and Magasanik, 1962). This phenomenon of ongoing RNA and protein synthesis in the absence of DNA replication is known as unbalanced growth (Barner and Cohen, 1954). The paradigm of unbalanced growth has been fruitful for generating and testing a multitude of hypotheses addressing the molecular nature of the effects of thymine starvation.

The first tenet of the unbalanced growth induced by thymine starvation is the cessation of replicative DNA synthesis, brought about by depletion of the dTTP pool. Accompanying that are the observations of extensive DNA damage (Freifelder, 1969; Nakayama and Hanawalt, 1975; Guarino *et al.*, 2007) and DNA repair synthesis (Pauling and Hanawalt, 1965) in cells undergoing TLD. Damaged DNA is a probable root cause of the increased frequency of mutations (Adelberg and Coughlin, 1956; Pauling and Hanawalt, 1965) and recombination (Gallant and Spottswood, 1964) in the thymine-starved cells. Incorporation of uracil into DNA (Warner *et al.*, 1981) as a function of available dUTP, followed by its removal by dedicated uracil-N-glycosylases, may also contribute to increased mutagenesis and DNA fragility.

The second principal element of unbalanced growth is the continuation of RNA and protein synthesis, which have been viewed as necessary conditions for TLD, in cells deprived of thymine (Gallant and Suskind, 1962; Hanawalt, 1963). Indeed, depriving cells of an energy source or inhibiting transcription or translation rescues the cells from TLD (Nakayama and Hanawalt, 1975). Although inhibition of RNA or protein synthesis may have wide-ranging consequences, only once during the cell cycle do those processes dynamically interact with DNA replication (i.e. when initiation of chromosomal DNA replication requires de novo transcription and to some extent translation) (Kornberg and Baker, 1992). The preponderance of evidence, stemming from experiments in which TLD was examined in the context of DNA replication status of the cell, points to the critical role of initiation of DNA replication in TLD: (i) cells which have completed ongoing rounds of DNA replication are immune to killing as long as no further rounds are initiated (Maaløe and Hanawalt, 1961); (ii) temperature-sensitive mutants in *dnaA* and *dnaC*, whose products are required for normal initiation of chromosomal DNA replication (Lark, 1972), do not undergo TLD when starved for thymine under non-permissive conditions (Bouvier and Sicard, 1975; Nakayama *et al.*, 1994; P.A. Morganroth and P.C. Hanawalt, unpubl. results); (iii)

once DNA replication is initiated, inhibition of elongation by mild hydroxyurea treatment (Morganroth and Hanawalt, 2006), which inhibits nucleotide synthesis but not transcription, or by temperature-sensitive mutations in *dnaB* or *dnaE* which affect replication elongation but not initiation, does not rescue cells from TLD (P.A. Morganroth and P.C. Hanawalt, unpubl. results). Although contributions to TLD from other specialized pathways that can be induced by DNA damage and/or metabolic dislocation caused by thymine starvation (which by definition would require de novo mRNA and protein synthesis), should not be discounted, the initiation of chromosomal DNA replication appears to be an essential condition for TLD.

Double mutants that are more resistant or susceptible than a *thyA*− parent to TLD have also been identified. Most of those mutations were found to be in genes whose products are involved in DNA recombination and repair pathways (listed in Ahmad *et al.*, 1998). Of particular interest is the observation that mutations in enzymes involved in the repair of double-strand breaks (*recBC*) increase the sensitivity of cells to TLD (Anderson and Barbour, 1973; Nakayama *et al.*, 1982), whereas mutations in those enzymes that process single-strand DNA or repair single-strand gaps (*recFORJQ*) rescue TLD (Anderson and Barbour, 1973; Nakayama *et al.*, 1982; Nakayama *et al.*, 1984). Although genes with roles in the SOS response to DNA damage (*lexA*) and in nucleotide excision repair (*uvrA*) were found to have no role in mitigating TLD (Morganroth and Hanawalt, 2006), a recent study, using different strains, has shown that the SOS response and *sulA*, in particular, can contribute to lethality (Fonville *et al.*, 2010).

Extant theories for the mechanism of TLD allude to irreparable DNA damage due to: single-strand (Nakayama and Hanawalt, 1975) or double-strand (Yoshinaga, 1973) DNA breaks, stalling of replication forks (Nakayama, 2005) or DNA degradation in proximity of replication forks (Reiter and Ramareddy, 1970), accumulation of a toxic metabolite(s) (Cohen and Barner, 1954; Freifelder and Maaløe, 1964), induction of the bacterial programmed cell death (Sat *et al.*, 2003), structural defects caused by perturbed cell wall and nucleoid organization (Ohkawa, 1975; Zaritsky *et al.*, 2006), and lethal filamentation (Bazill, 1967). However, the relative contribution of these factors, individually or in combination, to the dramatic reduction in colony formation in populations of *E. coli* cells starved for thymine remains to be determined. On the other hand, the existence of a multitude of explanations for the TLD phenomenon is testimony

to the pleiotropic consequences of perturbations in thymine metabolism. Pleiotropic perturbations, genetic and environmental, have been successfully tackled by systemic analysis of genomic activity (e.g. Jeong *et al.*, 2006; Sangurdekar *et al.*, 2006; Faith *et al.*, 2007). In the present study, we have tracked temporal genome-wide transcriptional responses in *E. coli* cells undergoing TLD using cDNA microarrays. We compared these responses to those under a thymine-limiting condition, wherein cells do not lose viability (Zaritsky *et al.*, 2006), to identify specific transcriptional signatures associated with cell death.

We found that the DNA damage response is the most pronounced characteristic that sets apart thymine-starved cells from thymine-limited (TLM) cells. Furthermore, comparative genomic hybridization of chromosomal DNA during the course of TLD revealed progressive loss of genetic material at the origin of replication and in its vicinity in association with TLD. Double mutants in DNA repair and recombination: *thyA recF*, *thyA recJ*, *thyA recO* and *thyA recQ* (in the closely related parental strain W3110) mitigated cell viability loss to varying degrees, and were correspondingly associated with a reduced loss of genetic information. We conclude that populations of *E. coli* cells undergoing TLD can be characterized by spatially localized persistent DNA damage, emanating bi-directionally from the origin of replication. As initiation of DNA replication from the origin is a necessary condition for TLD, we believe that the *ori*-centred DNA loss is fundamentally linked to the underlying cause of the phenomenon.

3.2 Materials and Methods

3.2.1. Strain, media and growth conditions

Escherichia coli K12 strain MG1693 (MG1655 *thyA, lam, rph*) was obtained from Coli Genetic Stock Center (CGSC 6411), and has a thymine requirement of 20 μg ml^{-1}. Limiting thymine concentration for this strain was observed to be 5 μg ml^{-1} (concentration at which cell division is affected, but viability is not). *E. coli* strains W3110 for *thyA* (*thyA36 deoC*), *thyA recO* (*thyA deoC recO6218 sub tet 857 for cdn3-240*) and *thyA recF* (*thyA36, deoC, recF6206 sub tet857 for cdn4-295*) were kindly provided by J. Courcelle, and a *thyA recQ* double mutant was obtained from the Yale Coli Stock Center (CGSC 7702). These strains were found to have a thymine requirement of 1–2 μg ml^{-1}. Prior to any experiment, cells were streaked on LB plates, and

colonies were inoculated in M9 minimal medium + 0.4% glucose and 20 μg ml^{-1} of thymine depending upon the requirement of the strain. The overnight inoculum was resuspended in fresh M9-glucose medium containing thymine and incubated at 37°C and maintained in exponential phase for at least six doublings. Media shifts during thymine starvation or limitation were done by harvesting cells at mid-exponential phase – washing twice with M9-glucose at room temperature and resuspending in pre-warmed M9-glucose (with no or limiting thymine).

For viability counts, samples were diluted in 0.9% NaCl, plated on LB agar plates and incubated for 12–16 h at 37°C. For microarray hybridizations, control samples were prepared by resuspending a fraction of spun cells in pre-warmed M9-glucose containing 20 μg ml^{-1} thymine for 15 min. Starved/limited samples were collected at 15, 30, 45, 60 and 90 min after resuspension. All samples were fixed using Ethanol/Phenol (95%/5%, v/v) solution, spun down and snap frozen in liquid nitrogen. For transcription inhibition studies, rifampicin was purchased from Sigma-Aldrich (St Louis, MO). For hybridizations of the W3110 strain, control samples were washed twice with thymineless media after being grown for six doublings in 2 μg ml^{-1} thymine M9-glucose media before starvation. Starved samples were collected 3 h after resuspension, spun down and frozen.

3.2.2. Microarray hybridization

RNA was extracted using Qiagen RNeasy Mini kit (Qiagen Valencia, CA; Cat # 74104). Whole genome microarrays were printed as described elsewhere (Khodursky *et al.*, 2003). RNA samples were labelled, purified and hybridized as described (Khodursky *et al.*, 2003). Technical duplicate samples for each time point were hybridized with a dye-swap, and array data were collected, normalized using print-tip Lowess, and anova model was fitted using maanova package in R (Wu *et al.*, 2003). Transcription data is available at NCBI GEO, Accession No. GSE19879.

3.2.3. DNA damage mapping

DNA was extracted from samples using silica-gel based QiaAMP DNA mini kit (Qiagen Valencia, CA; Cat # 51304). Extracted DNA was checked for RNA contamination by gel electrophoresis, and purified DNA was sonicated using Branson Digital Sonifier (30% power, 3 pulses of 10 s each, final size range 200–1000 bp). Re-purified and concentrated DNA was labelled using BioPrime Array Labeling Kit (Invitrogen, Carlsbad, CA) for cDNA microarray hybridizations. A representative sample was hybridized in triplicate on high-resolution 385K arrays from Roche Nimblegen (http://www.nimblegen.com), which have 385 000 probes located at every 25 bp of the *E. coli* genome. For quantitative PCR, primers were designed to query genes that are in the vicinity of *oriC* and *ter* regions. Purified DNA from 0 h and 3 h samples (after RNAse treatment) was used as template. Data were collected using the SYBR green QPCR technology. C_t data for *oriC* proximal genes was normalized to genes in the *ter* region and was converted to log ratio format.

3.2.4. ExoIII-S1 nuclease assay

Genomic DNA from *E. coli* was prepared using DNeasy Tissue kit according Qiagen protocol. Purified DNA was treated with or without exoIII exonuclease. Five micrograms of genomic DNA in 25 µl of 1× ExoIII buffer was mixed with equal volume of 1× ExoIII buffer supplemented (or not supplemented) with 100 units of Fisher BioReagents Exonuclease III (Fisher Scientific, Pittsburgh, PA, USA). Samples were incubated for 10 min at 37°C. Immediately after the end of reaction, samples were transferred on ice. Two hundred microlitres of 1× S1 buffer with 60 units of S1 nuclease (Promega, Madison, WI, USA) was added to the sample and reaction was performed for 30 min at 25°C. To stop reaction 25 µl of stop solution (0.3 M Tris base, 0.05 M EDTA) was added and mixed. DNA after enzymatic treatment was purified by phenol/chloroform extraction and ethanol precipitation.

3.2.5. Data analysis

Data from RNA and DNA hybridizations were analysed for significance in a standard manner (see *Supporting information* for details).

3.3 Results

The effects of thymine starvation and limitation on cell viability in exponentially growing cells of *E. coli* K12 *thyA*– are illustrated in Figure 1A. Under the starvation condition, the drop in cell viability, as measured by the number of colonies appearing on nutrient agar plates after 16 h incubation, was about 20% in the first 60 min, followed by a more rapid reduction to less than 10% of the original cell count by 3 h of starvation. This observation is consistent with the previously reported kinetics of viability loss in different *thyA*– strains (Ahmad *et al.*, 1998) (see *Experimental procedures* for details). Under thymine-limitation conditions (growth in suboptimal 5 μg ml^{-1} of thymine), cells divided at a slower rate but did not lose viability, as exemplified by a moderate increase in colony count.

For microarray experiments, cells undergoing thymine starvation were collected at 15 min intervals during the first 90 min after thymine withdrawal. Control samples were treated similarly to starved or limited samples (*Experimental procedures*). Transcript abundance data were collected after hybridization, normalized and analysed as described in *Experimental procedures*. Significance analysis of microarray data was performed assuming duplicate samples at 30, 45, 60 and 90 min time points as replicates.

By using a threshold of 1.5-fold differential expression and a false discovery rate of less than 5%, 138 genes were found to be upregulated and 91 genes to be downregulated during starvation (top 30 from each set are listed in Table 3.1). Genes belonging to the LexA controlled SOS regulon (Courcelle *et al.*, 2001) constituted 11 of the top 13 upregulated genes, including *recN*, *recA*, *sulA* and *lexA*. Those four were the most affected genes in the genome at 15 min of starvation, and the magnitude of induction doubled over time (Figure 3.1B). Other significantly induced LexA targets were *cho*, *uvrA*, *uvrD*, *dinD*, *dinI*, *dinP*, *yebG*, *sbmC*, *umuDC*, *ysdA*, *recX* and *ftsK*. This corroborates earlier observations that thymine starvation induces the DNA damage response (Ahmad *et al.*, 1998; O'Reilly and Kreuzer, 2004). Expression of genes belonging to the deoxyribose salvage pathway (*deoCABD*) was also upregulated, indicating increased salvaging of thymine from the medium. The primary downregulated genes included genes involved in pyrimidine synthesis, Krebs cycle and energy metabolism.

3.3.1. Similarity of transcriptional responses under conditions of thymine limitation and starvation

Some of the transcriptional responses detected in cells undergoing TLD may not be directly associated with thymine starvation, but could reflect non-specific effects such as growth rate adjustment. We investigated whether these responses could be reproduced in a TLM condition wherein cells are limited for growth by suboptimal thymine concentrations. Under such conditions, cell growth is affected (data not shown) but not cell viability, as measured relative to viable counts in the culture before thymine was limited in the medium (Figure 3.1A) (Zaritsky *et al.*, 2006). Genome-wide transcriptional data were analysed as for TLD samples and the cellular response to thymine limitation was verified with the upregulation of *deoCABD* operon which is responsible for thymine scavenging.

The global gene expression response to TLD and TLM was strikingly similar (Figure 3.1D and Figure S3.1). The average of gene expression profiles at similar time-points between the two conditions had a correlation of 0.50 (Figure 3.1D). However, a prominent difference was induction of SOS genes in TLD, but not in TLM (Figure 3.1B–D, Figure S3.1 and Table S3.2). When pre-classified gene sets were compared (*Experimental procedures*; Sangurdekar *et al.*, 2006), the difference in average expression of gene sets between the two conditions was limited to the sets overlapping with the SOS pathway: LexA regulon and DNA damage inducible pathway (Figure S3.2, Table S3.2). Moreover, at the level of individual genes, which cannot be unambiguously assigned to well-defined regulons, we also observed that thymine starvation, but not thymine limitation, likely induces changes in DNA structure, which in turn result in characteristic transcriptional patterns. For example, the *ssb* gene, which codes for a single-stranded DNA binding protein and that is required for protecting single-strand DNA during DNA replication, repair and recombination (Meyer and Laine, 1990), was significantly upregulated (an average of 30% induction with a false discovery rate of 0%) in thymine-starved but not limited cells (Table S3.1), suggesting an increase in the concentration of single-strand DNA in the cells undergoing TLD, whereas the *hns* and *stpA* genes encoding nucleoid-associated proteins were significantly downregulated during TLD, indicative of nucleoid unfolding. Thus, rapid depletion of the dTTP pool, which occurs when cells are moved into thymine-free medium, generates the signal for SOS induction, whereas reduction or slow depletion of the nucleotide pool, which

occurs when cells are limited for thymine, does not. Of note is that induction of the SOS regulon reached its peak within an hour and the response became significant as early as 15 min after thymine withdrawal (Figure 1B). At the same time, the viable cell count dropped by less than 25% during the first hour of starvation. Thus, full mounting of the DNA damage response precedes the major loss of viability but does not rescue the cells. If we assume that the viability is lost during the course of thymine starvation and that the pattern of transcriptional regulation in thymine-starved cells is informative, as was shown in a multitude of other conditions (Sangurdekar *et al.*, 2006; Faith *et al.*, 2007), then at least one of the following should be true: (i) the DNA damage response is overwhelmed by the amount of damage; (ii) the type of damage that is induced by thymine starvation cannot be efficiently repaired, if at all, although it (or its component) can trigger the SOS response; (iii) thymine starvation triggers other irreversible processes, unrelated to DNA damage (cf. Kohanski *et al.*, 2007). As we did not see any indication of induction of any other general damage process, such as oxidative damage or membrane leakage, in our comparison with a thymine limited culture, we could rule out the third option. Because inability to induce SOS response did not affect either TLD kinetics or its extent (Morganroth and Hanawalt, 2006; B.L. Hamann and A.B. Khodursky, unpubl. data), it is unlikely that an inequity between the repair capacity of the cell and the extent of DNA damage significantly contributes to TLD. Therefore it seemed plausible to us that the outcome of thymine starvation is determined, at least in part, by the nature of DNA damage.

3.3.2. Comparative analysis of the state of DNA

Nakayama *et al.* proposed that DNA surrounding the origin of replication, 160 kb on both sides of the origin, was likely to have been damaged during TLD, as measured by its resistance to digestion by a restriction endonuclease (Nakayama *et al.*, 1994). It was also reported (Nakayama *et al.*, 1994) that DNA from thymine-starved cells had extensive single-strand (ss) character, which rendered it hyper-sensitive to digestion by S1 nuclease. We hypothesized that the location of such damaged DNA could be mapped more precisely using genome-wide microarrays. This hypothesis was based on the assumption that the regions of single-strand DNA would be similarly distributed in a measurable fraction of cells undergoing TLD. Following S1 endonuclease digestion, we should be able to identify such regions as ‘deletions’ in the

comparative genomic DNA hybridizations relative to the control DNA. DNA samples isolated from the thymine-starved cells were treated with S1 endonuclease and visualized in agarose gel following electrophoresis (Figure 3.2, lane 6). Compared with the 0 h control (lane 7), S1 treatment of DNA from the 3 h sample resulted in pronounced degradation of a relatively high-molecular-weight chromosomal DNA band, confirming results reported by other groups that DNA from thymine-starved cells is more sensitive to S1, presumably due to more extensive single-strand character, than DNA from non-starved cells. The difference between DNA from starved and non-starved cells was even more pronounced following S1 digestion of ExoIII pre-treated DNA (lanes 4 and 5).

To map the location of ssDNA along the chromosome, we treated chromosomal DNA extracted from pre-starvation and starved cells with S1 nuclease and looked for changes in gene copy number as a function of chromosomal position (*Experimental procedures*). Normally growing cells exhibit a gene copy number gradient that peaks at the origin of replication, indicative of a measurable proportion of cells initiating new rounds of replication before division (Figure 3.3A). If DNA from starved cells had a locus-specific single-stranded character, different patterns of DNA damage could be expected depending upon the distribution and extent of localized damage in genomes across a population of cells (Figure 3.3B and C). Genomic DNA from normally growing cells in exponential phase and from cells starved for thymine for 3 h was extracted, treated with S1 nuclease, sheared and hybridized against similarly treated genomic DNA from stationary phase cells, which have a uniform gene copy number distribution. Cells undergoing thymine starvation showed a similar gradient to that in pre-starvation cells. However, there was a significant drop in gene copy number ratio that peaked at the origin of replication (*oriC* – 3.92 Mb) and was symmetrical around the origin (Figure 3.4). The spread and twofold magnitude of the drop was confirmed using high-resolution microarrays with strand-specific oligo probes every 25 bp along the genome (Figure S3.3). Surprisingly, this pattern was observed even when the 3 h sample DNA was not treated with S1 nuclease. Further, there was no difference in the profiles of S1-digested and non-S1-digested DNA with respect to the slope of the gradient, or the depth and spread of damage around the origin (data not shown). Therefore, the S1 treatment was omitted from further experiments. Two conclusions can be drawn from this finding. First, the distribution of single-strand DNA in the chromosome of

thymine-starved cells is likely to be uniform or at least insufficiently spatially biased in order for the bias to be detected by available genomics means. Second, the observed variation of DNA copy number in the vicinity of the origin is not due to single-strand DNA character in that region of the chromosome. When the difference in copy numbers in pre-starvation and starvation stages was fit in a linear model, the damage was observed to be localized symmetrically around the *oriC* region between 3.7 and 4.2 Mb (Figure S3.4). There was no difference between the gradients in gene copy number in pre-starvation and starved cells. As the gradient reflects average DNA dosage (across the cell population) of chromosomal loci in replicating cells relative to non-replicating stationary cells (Khodursky *et al.*, 2000), the similarity between the two gradients indicates that the majority of loci, outside of the origin-proximal area, along the chromosome are replicated to the same extent (have the same dosage) in the starved culture as in the pre-starvation culture. The amplitude of the peak in Figure 3.4 also indicates that genetic loci at *oriC* were twofold less abundant than expected in normally growing cells.

The damage profile was tracked over time by taking samples from the culture undergoing TLD at 30 min (at which point little to no death was observed), 1 and 2 h (Figure 3.5). When compared with the 0 min control, no significant change was observed in the damage profile at 30 min. At 1 h, some evidence of damage could be seen, whereas by 2 h the damage was completely established and it did not change further at a later time point. This profile also correlated qualitatively with the TLD viability curve (Figure 3.1) where an exponential rate of cell death was observed after 1 h following the onset of starvation. This observation was further supported by quantitative PCR of gene markers selected in proximity of the origin and terminus of replication (Figure S3.5), confirming that in cells undergoing TLD the DNA dosage in the origin-proximal region was less than that in the terminus-proximal region. The observed copy number loss could not be attributed to the cessation of initiation of DNA replication in cells lacking thymine. Indeed, when initiation of replication was inhibited by rifampicin in exponentially growing *thyA*– cells, a different relative copy number profile emerged (Figure3. 6) which was indistinguishable from the profile of stationary cells, consistent with the role of transcription in replication initiation but not in elongation.

3.3.3. Mitigation of chromosomal loss in TLD-resistant DNA repair mutants

Mutants in the repair/recombination pathway catalysed by *recJQ*, *recFOR* were reported to be more resistant to TLD in *thyA*– background, and in fact the original *recQ* mutant was selected in a search for mutants that were resistant to TLD (Nakayama *et al.*, 1982; Nakayama *et al.*, 1984). To determine if DNA loss is correlated with the loss of viability, mutants in *thyA, thyA recF*, *thyA recJ*, *thyA recO* and *thyA recQ* in W3110 background (see *Experimental procedures* for strain description) were starved for thymine and viability was measured and DNA damage was mapped to the chromosome. W3110 *thyA*– was more sensitive to TLD than MG1655, with 3.3 ± 0.4% survival 3 h post starvation. A mutant in *thyA recF* was significantly more resistant, with 38 ± 10% survival at 3 h. Mutants *recJ*, *recO* and *recQ* were also more resistant at 32 ± 9%, 27 ± 7% and 25 ± 4% survival at 3 h respectively (Figure 3.7A). DNA damage in these mutants following thymine starvation was mapped to the chromosome using comparative genomic hybridizations (Figure 3.7B–F). The extent of DNA damage in *thyA*– parental strain appears qualitatively higher than that in double mutants. To evaluate DNA loss quantitatively, a score equal to the ratio of two parameters were considered: (i) slope of gene copy number from the boundary of damage to the midpoint of damage and (ii) global slope of gene copy number from the proximity to the terminus to the boundary of damage (Figure 3.8A). This score captures the extent of DNA loss as the rate of loss of chromosomal loci relative to the natural gradient in the *oriC*-distal genome. As seen in Figure 8B, the DNA damage score was significantly correlated (Pearson $R^2 > 0.9$) with the extent of killing in the different strains.

3.4 Discussion

Loss of cell viability during thymidylate depletion is a phenomenon observed in many diverse organisms and this has been exploited for treatment of infections (by means of trimethoprim and sulphamethoxazole) (Amyes and Smith, 1974) as well as to curb the growth of cancerous cells (by means of methotrexate and 5-fluorouracil) (Longley *et al.*, 2003). Despite the extensive and insightful history of research in this field, the precise events leading to the loss of viability remained elusive. As thymine metabolism directly affects DNA synthesis and maintenance, several hypotheses have been proposed to explain the loss of DNA integrity during TLD, and

there is a volume of evidence (summarized for *E. coli*) that corroborates this line of thought (Ahmad *et al.*, 1998).

In this study, we aimed to report an orthogonal set of observations: those of transcriptional responses during TLD using DNA microarrays. We were motivated by other successful applications of genomics to studies of pleiotropic genetic and physiological effects as well as by molecular conditions that were not easily tractable by conventional, single gene centric techniques (e.g. Jeong *et al.*, 2006; Faith *et al.*, 2007). We surmised that a genome-wide survey of a transcriptional state of the cell developed in response to thymine starvation would be indicative of molecular processes taking place in the cells undergoing TLD and that, by extension, might provide complementary information about mechanisms behind the phenomenon. The primary transcriptional response during TLD was the rapid induction of SOS response genes, consistent with the generation of a DNA damage signal early in the starvation. We also observed that pyrimidine synthesis genes were significantly downregulated. Synthesis of pyrimidines is feedback controlled by pyrimidine and purine levels within the cell, and it is likely that perturbed rate of DNA replication and/or RNA synthesis leads to repression of nucleotide biosynthesis. To ascertain the specificity of these and other responses, we compared transcriptional states of thymine-starved and -limited cells. We observed that whereas DNA damage response genes were differentially expressed between the two conditions, pyrimidine synthesis and galactitol metabolic genes were repressed to different degrees. Thus we have concluded that on a molecular level, TLD must be associated, at least in part, with DNA damage.

To probe the state and location of DNA damage, we determined the relative abundance of individual loci across the chromosome in a population of cells starved for thymine for 3 h. A region of aberrant gene copy distribution was identified around the origin of replication. Beyond this region, the distribution assumed a regular gradient which is expected from normally growing exponential phase cells in minimal medium, indicating that either there is some DNA replication activity in the average population even after 3 h of thymine starvation or that DNA replication elongation ‘freezes’ immediately after thymine starvation due to the precipitous drop in dTTP levels (Neuhard, 1966) and the gradient is preserved for the duration of starvation (Figure 3.5). To confirm that the profile of gene copy loss around the origin was not an artefact

of arrested DNA replication initiation, we assessed the profile of cells growing with thymine and treated with rifampicin (Figure 3.6) and demonstrated that lack of DNA replication initiation does not explain the profile observed during TLD.

Thus, not only do the transcriptional responses during TLD point towards DNA damage, but also the DNA itself appears to be in an aberrant state in the vicinity of the replication origin. While DNA in the starved cells may also be damaged elsewhere along the chromosome, concentrated and persistent damage at the replication origin was observed and the shape and location of the lesion strongly implicates the process of initiation of DNA replication in its formation: in a population of thymine-starved cells the frequency of the damage is the highest at the origin and lowest 250 kb away from it.

To establish a causative link between DNA loss and lethality, we controlled the former factor by using different mutants, which had been reported to be resistant to TLD (Nakayama *et al.*, 1982; Nakayama *et al.*, 1984). After verifying that the extent of killing is diminished in these mutants, we proceeded to measure the extent of DNA degradation, or loss, in them after starvation. We devised a simple score to measure the extent of DNA loss, as the ratio of slopes of gene copy number around the boundary of damage. The extent of DNA degradation was found to be directly correlated with cell killing. As S1 nuclease treatment of DNA from thymine-starved cells did not degrade the origin-proximal DNA any further, DNA in the damaged region must be either double-stranded or missing all together, or some combination of both. For example, if 50% of cells in a thymine-starved population lost a segment of origin-proximal DNA on both strands, and 50% did not, that would result in a twofold DNA copy number reduction at the origin, as observed in our study. However, if only 50% of cells are missing an essential piece of genetic material, the expected reduction in viability should also be only 50% and not several orders of magnitude which is characteristic of TLD. However, if the loss of any particular DNA segment is a probabilistic phenomenon and because there is a multitude of essential DNA segments in the vicinity of the origin, one can envision a situation in which any one of the essential segments is missing in no more than half of the DNA molecules but each chromosome molecule is missing at least one of them, resulting in a cumulative loss of viability in more than 90% of cells (see Figure 9A for a schematic illustration; essential segments are discretized and

uniformly spatially distributed for the ease of illustration). Alternatively, the S1 nuclease-resistant confirmation of the observed DNA 'lesion' may have resulted from the origin-centric degradation of nascent DNA followed by re-annealing of template strands (see Figure 3.9B for visualization). As the relative extent of DNA degradation explains more than 90% variance in viability of *thyA*– strains deficient or proficient in the RecFOR repair pathway, it follows that the observed DNA degradation is a quantitative attribute of TLD, which results, at least in part, from the activity of the *rec* products. It remains to be seen whether our observation can be explained by such an activity targeting only nascent DNA, as was demonstrated by Courcelle *et al.* (2006) in the case of RecJ and RecQ, or through degradation of both template and nascent DNA, as was hypothesized by Belle *et al.* (2007). Whereas a model postulating degradation of both template and nascent strands (Figure 3.9A) can at least partially explain loss of viability based on first genetic principles, a model postulating degradation of only nascent DNA cannot explain viability loss without making additional assumptions about the fate of a 'two-bubble' chromosome structure (Figure 3.9B).

In summary, we have shown that the phenomenon of TLD, which had been functionally linked to replication initiation, is quantitatively linked to the physical state of the DNA surrounding the origin of replication. The observed degradation of the origin-proximal DNA is a probable basic mechanism for TLD.

Figure 3.1. Cell viability and gene expression responses during thymine starvation (TLD) and limitation (TLM). A. Thymine starvation leads to an exponential drop in cell viability after a lag period, as measured by plating (cfu, colony-forming units). In thymine limitation, cells were resuspended in a medium containing 5 μg ml^{-1} thymine causing slowing of growth but not killing. Cells were grown in M9 minimal medium + 0.4% glucose and 20 μg ml^{-1} thymine prior to starvation. Error bars correspond to standard error of the mean of measurements. Growth of cells in non-limiting thymine is also indicated. B and C. Transcription profiles of SOS response genes. The profiles of SOS genes were tracked in cultures undergoing thymine starvation leading to TLD (B) or thymine limitation, TLM (C). During TLD, several SOS genes, indicated on the right-hand side of B, are induced more than twofold (log ratio of fold change > 1) whereas during TLM these genes remain unperturbed. Relative mRNA abundances of individual genes were measured at indicated time points (connected by lines for ease of visualization) following thymine withdrawal or limitation using cDNA microarrays. RNA samples isolated from cells immediately before thymine perturbations were used as references in two-colour microarray hybridizations. D. Similarity in expression responses of genes of the *E. coli* genome during thymine starvation (TLD) and limitation (TLM). Gene expression at 45, 60 and 90 min under TLD and TLM conditions were averaged and plotted. The correlation of the scatter is 0.51. SOS response genes were differentially expressed in TLD and are represented as filled squares.

Thymineless death is associated with loss of essential genetic information from the replication origin

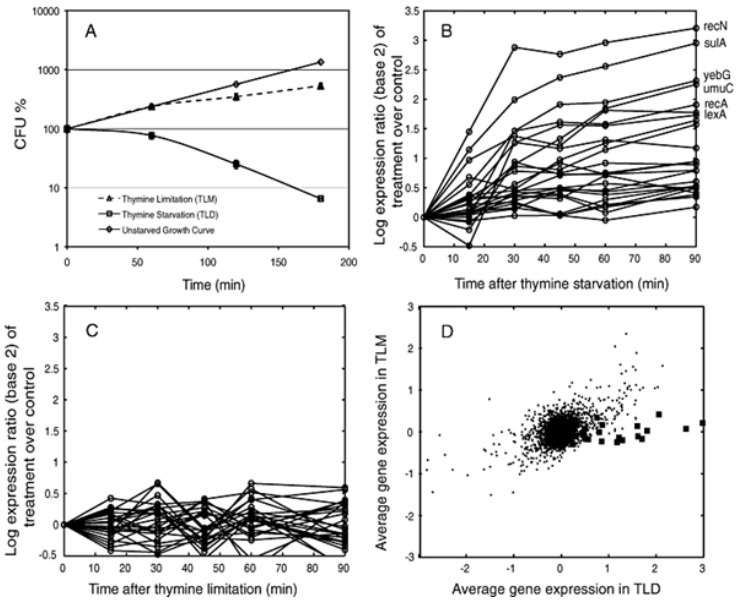

Figure 3.2. Nuclease sensitivity of DNA from thymine-starved cells. DNA from non-starved (0 h) and starved (3 h) samples was extracted. Lanes 1 and 2: Untreated DNA from both samples shows a similar pattern indicating DNA is not more degraded at 3 h than at 0 h. Lane 6 and 7: S1 nuclease treatment of both samples results in visible degradation of 3 h sample relative to 0 h. Lane 4, and 5: Treatment with ExoIII and S1 significantly degrades 3 h sample as compared with the control.

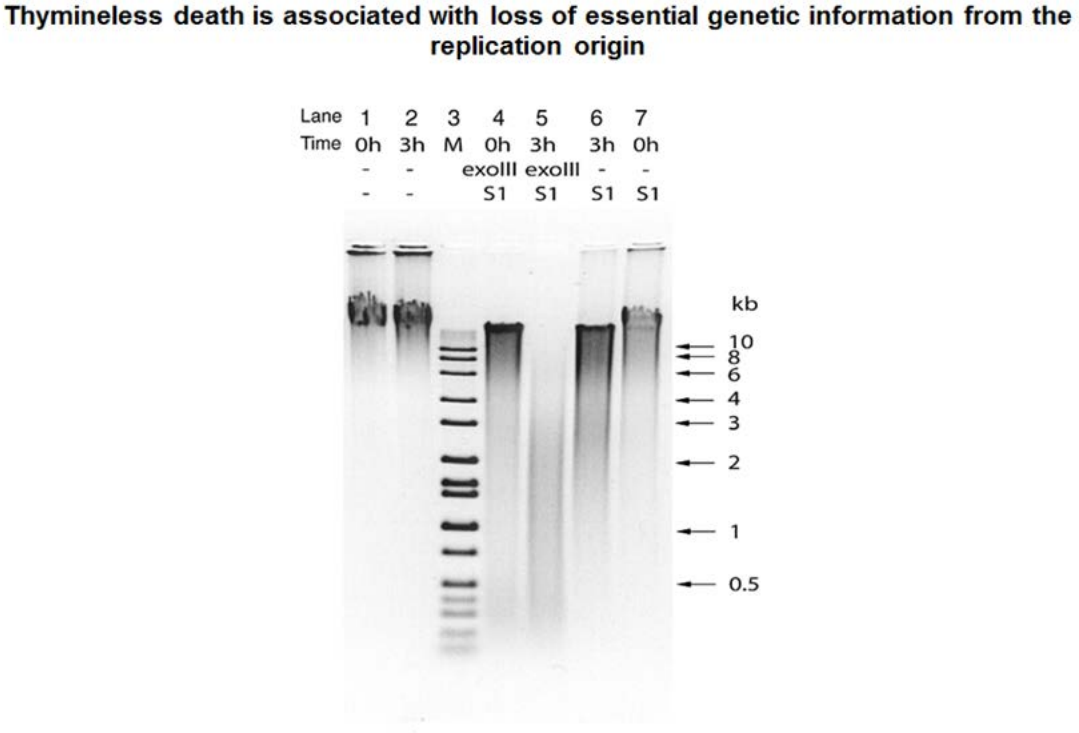

Figure 3.3. Distribution of gene copy number along the chromosome in dividing cells and localization of spatially biased copy number variation caused by DNA damage. Cells undergoing normal growth initiate multiple rounds of replication. Such cells when compared with stationary phase cells on a microarray exhibit a characteristic copy number distribution along the length of the chromosome (A). The terminus region will have the equivalent of one copy per dividing chromosome. The height of the peak depends on the number of dividing cells in the population and is limited by the resolution of the microarray detection. If the chromosome in TLD cells is damaged at multiple non-random sites, and the damage can be mapped by nuclease digestion, the profile of gene copy number will be as shown in B. The extent of drop in gene copy number from normal will depend on the distribution of the damaged sites in the population. If the damage is at multiple random locations, the differences will average out and no significant change will be detected in the profile. If the damage occurs at the growing replication forks and grows inward (C), the gradient is expected to flatten around the origin of replication if the density of replication forks in that region is higher than elsewhere in the chromosome. The grey dashed line in the right panel of C indicates the original undamaged profile for comparison.

Thymineless death is associated with loss of essential genetic information from the replication origin

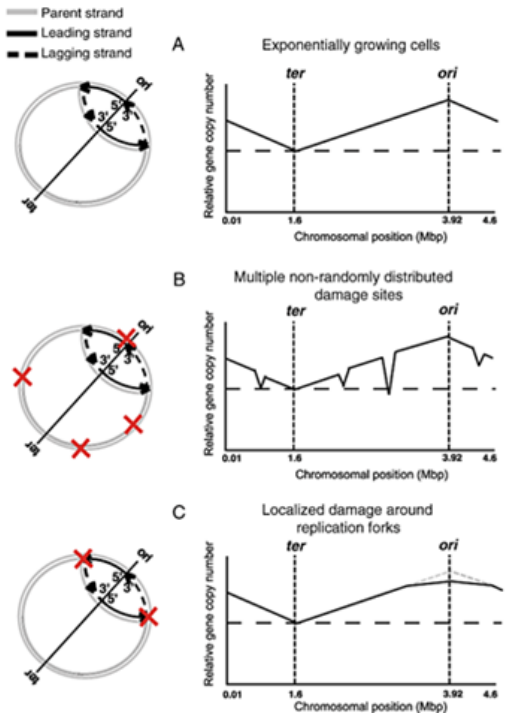

Figure 3.4. Chromosomal map of DNA damage during TLD (black) and before starvation (grey). DNA copy number shows a significant dip between 3.5 and 4.2 Mb along the chromosome. Before starvation, the graph indicates the expected replication-induced gradient of DNA dosage of chromosomal loci. The data were normalized to the *ter* region and smoothed using the loess smoothing algorithm in MATLAB (span 0.01).

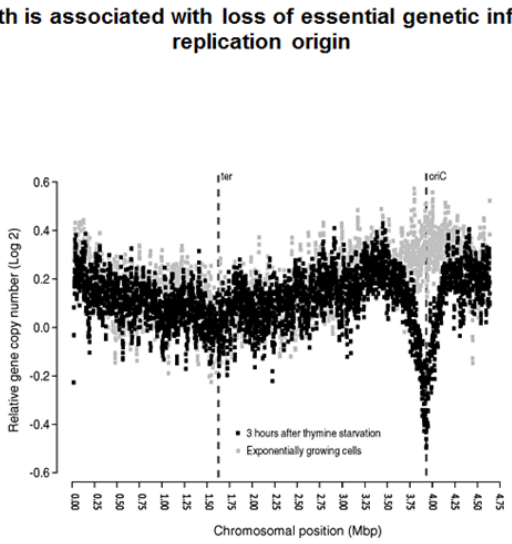

Figure 3.5. Temporal profile of DNA degradation induction around the replication origin during TLD. Loss in gene copy number at the origin was studied as a time series after thymine withdrawal. Curves correspond to 0 h (black), 30 min (blue), 1 h (cyan), 2 h (green) and 3 h (red) of starvation. Significant damage is seen at 2 and 3 h time points. Data from microarray hybridization was normalized to *ter* and smoothed using loess smooth algorithm in MATLAB (span 0.3).

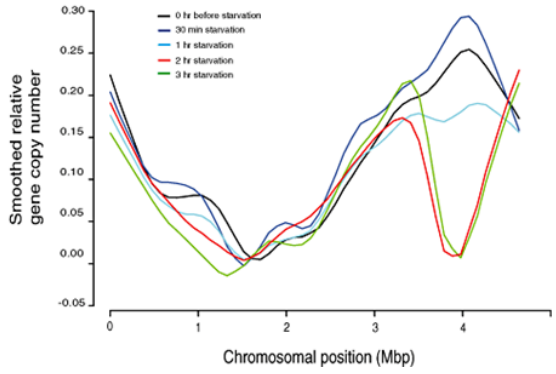

Figure 3.6. Chromosomal gene copy number profile after rifampicin treatment. Rifampicin-treated cells (200 μg ml^{-1} for 1 h) showed a similar gene copy number distribution (black) as stationary cells; no trend was observed in the vicinity of the origin. Smoothed data are plotted as a continuous line. Data were smoothed using MATLAB smoothing algorithm (loess, span 0.3).

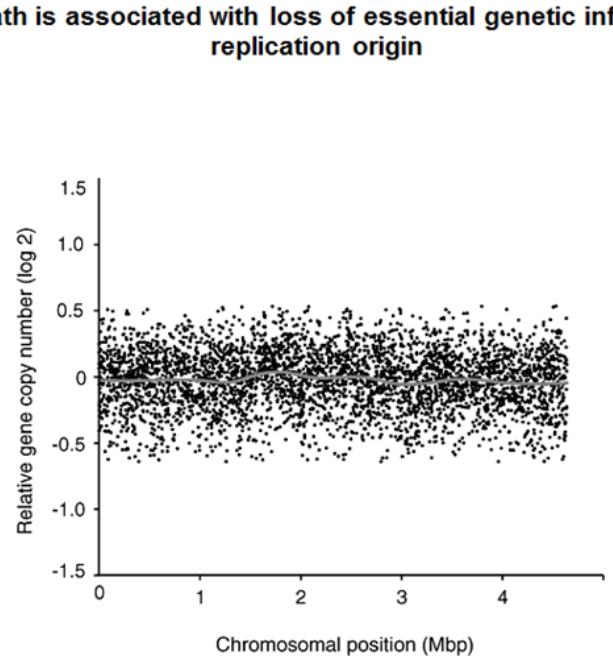

Figure 3.7. Cell viability (A) and comparative genomic hybridization profiles of *rec* mutants (B) *thyA*–, (C) *thyA recF*, (D) *thyA recJ*, (E) *thyA recO*, (F) *thyA recQ*, obtained relative to respective DNA sample of non-starved cultures grown into stationary phase. Cell viability and comparative genomic hybridization data from DNA repair mutants were collected after thymine starvation and analysed as described in *Experimental procedures*. Viability of DNA repair mutants is significantly higher than that of parent *thyA*– strains (W3110 background) post starvation (A). The nature of DNA loss in the terminus proximal region observed in a sample from the *thyA recO* strain is under further investigation.

Thymineless death is associated with loss of essential genetic information from the replication origin

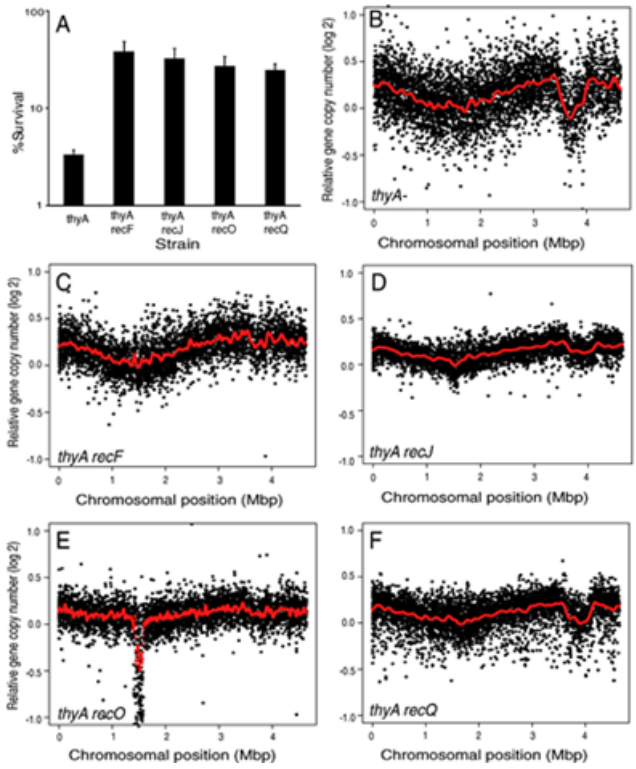

Figure 3.8. Correlation of viability and DNA damage in DNA repair mutants. A. DNA damage score is a ratio of slopes of gene copy number. B. DNA damage is correlated with cell killing in *rec* mutants.

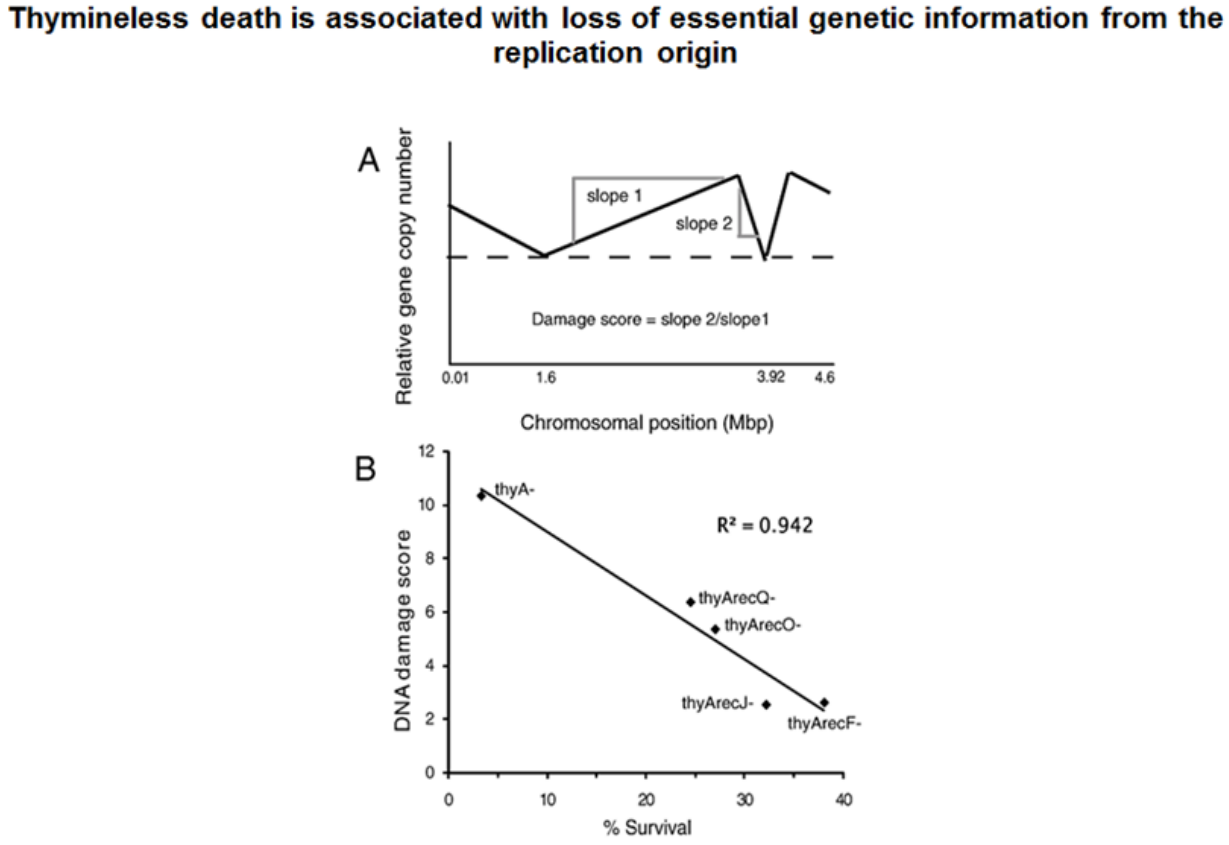

Figure 3.9. Models of DNA degradation following thymine starvation. A. Irreversible loss of both template and nascent DNA strands resulting from processing of (stalled) replication intermediates in the vicinity of the origin. The area is divided into 10 hypothetical genetically essential segments (1–10 above top line, segment '5' would overlap with the position of the origin in such a layout). Each horizontal line with a Roman numeral on the left-hand side corresponds to a DNA degradation outcome on any given chromosome. Note that not a single essential segment is missing from more than 50% of outcomes, while each outcome has at least one essential segment missing. B. A possible S1 resistant confirmation of the replicon that may result from degradation of only nascent DNA strands following thymine starvation.

Thymineless death is associated with loss of essential genetic information from the replication origin

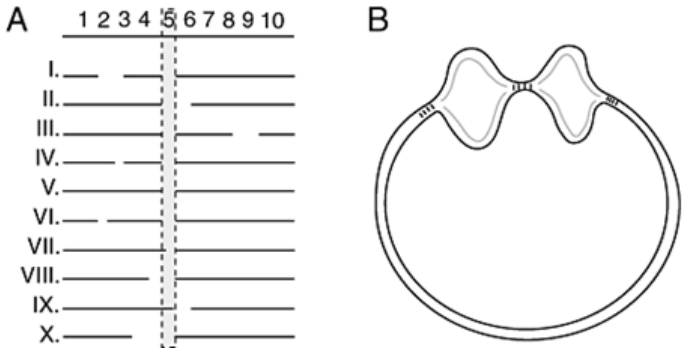

Table 3.1

Upregulated genes in TLD		Downregulated genes in TLD	
Gene name	Fold change	Gene name	Fold change
recN*	8.0	uraA§	0.2
sulA*	5.7	pyrB§	0.2
b1741*	2.2	pyrI§	0.2
uvrA*	2.9	codB§	0.2
dinD*	2.3	yjgF§	0.2
lexA*	2.9	codA§	0.2
yebG*	3.5	carA§	0.3
yiaG	2.7	carB§	0.3
sbmC*	2.2	pyrC§	0.3
recA*	2.9	sdhD	0.4
deoC	2.9	ftn	0.4
dinP*	1.7	fdoG	0.4
ysdA*	3.0	sdhB	0.4
deoA	2.6	hns	0.4
msyB	2.7	ompT	0.4
b1683	3.5	sdhA	0.4
sodC	2.5	sdhC	0.4
b1783	3.1	argG	0.4
hdeA	2.7	argG	0.4
tktB	2.7	gdhA	0.4
nfo	1.6	gatB	0.5
dinI*	2.2	malE	0.5
b3012	3.5	gatA	0.5
b2665	2.3	pyrD§	0.5
wrbA	2.2	gatY	0.5
b1681	2.8	gatC	0.5
b2464	2.0	gatZ	0.5
deoB	1.8	lamB	0.5
oraA*	1.6	oppB	0.5
ycgB	2.7	sdhB	0.5

Gene expression values during time points 45 min, 60 min and 90 min were treated as replicates and significance analysis of microarrays (Tusher *et al*., 2001) was done to identify top differentially expressed genes. Fold-change refers to ratio of gene expression with respect to 0 min reference. All genes have a *q*-value (False Discovery Rate) of 0. Genes belonging to the SOS regulon are marked with (*) and are over-represented in top upregulated genes. Other significant genes include the *deoCABD* operon, which is responsible for thymine scavenging. Among downregulated genes, those belonging to pyrimidine synthesis pathways (marked with §) are over-represented.

Chapter 3: Supplementary Information

S3.1. Supplementary Methods

S3.1.1. Data analysis

For RNA hybridizations, the log-ratio values obtained from MAANOVA analysis were then analyzed to identify significantly differentially expressed genes using Significance Analysis of Microarrays (SAM)(Tusher *et al.*, 2001). SAM was done on fitted values after gene, dye and array specific effects were removed and experimental noise was added to the biological effects(Kerr *et al.*, 2000). To analyze responses using pathway/gene set information, the methods of Tian et al (Tian *et al.*, 2005) and Sangurdekar et al(Sangurdekar *et al.*, 2006) were used. The former method calculates pathway activity score based on average amplitude of expression within a gene set and the distribution of randomized background expression data. The latter method (EntropyReduce) calculates gene set activity in time series data, based on a measure of increased coherence and amplitude in the data. Gene set information for classifying genes was collated from GenProtEC (Serres *et al.*, 2004), Ecocyc (Keseler *et al.*, 2005) and RegulonDB (Gama-Castro *et al.*, 2008). For CGH arrays, log ratios of intensities of treated sample and sample from stationary phase were taken and arranged by chromosomal position of gene center (for cDNA arrays) or by probe position (for 385 K arrays). Smoothing of data was done using Lowess smooth method in Matlab.

S3.1.1.1. Extended list of differentially expressed genes

The list of significantly up-regulated genes also included *deoCABD*, encoding components of a deoxyribose salvage pathway, as well as several genes involved in iron transport and iron-sulfur metabolism and in response to stresses (pH, osmotic and growth). Among the downregulated genes, the top 9 genes were those involved in pyrimidine de novo synthesis and transport. Additionally, among the downregulated genes we found those that encode components of the Krebs cycle (*sdhCABD, sucBCD, acnB*), arginine metabolism (*argDG,artJ*), ATP synthesis (*atpABCDEFH*), cytochrome *bo*

oxidase (*cyoAB*), formate dehydrogenase (*fdoGI*), iron storage (*ftn*), nucleoid maintenance (*hns,stpA*), pyrimidine transport and inter-conversion (*ndk, adk, upp, tsx*), cell division (*minCD*), sugar transporters (*gatABCDYZ*, *malEMT*, *manXYZ*, *rbsD*, *ptsG*, *lamB*, *sfcA*) and other transporters (*ompFT*, *oppBD*). Nucleotide reductase *nrdB* was upregulated 2-fold indicating its derepression by reduction in dTTP pools. A recurring feature in the list of differentially expressed genes was their function in iron or ironsulfur metabolism (among upregulated genes) and association with iron-sulfur clusters in the proteins encoded by the genes (downregulated).

We also tracked cellular responses using annotated gene sets, considering the temporal profiles of genes within the set (EntropyReduce,(Sangurdekar et al., 2006)}) or the average of fully induced expression values (Tian et al., 2005) at the later time stages. Gene sets related to LexA mediated DNA repair and SOS response constituted the top induced responses as indicated by EntropyReduce (Supplementary File). Other pathways which were active but whose members were not enriched in the significant genes category included OxyR targets (oxidative stress response, induced), PurR targets (purine biosynthesis, repressed) and targets of zinc uptake regulator Zur and global regulators CRP, H-NS and IHF.

Fig. S3.1: Clustering diagram of gene expression profiles observed in a thyA- mutant during thymine starvation (TLD) and thymine limitation (TLM) .

Relative transcript abundance data obtained during time courses of TLD and TLM were concatenated and visualized using hierarchical clustering. Genes (defined in rows) that show significant similarities in temporal expression profiles across the data points (defined in columns) are clustered together. Expression levels of upregulated genes are shown in yellow, and those of downregulated genes are in blue. Many of gene clusters are enriched for genes that are either coregulated or whose products are involved in the same molecular function, biological process or cellular compartment. Clustering can be used to qualitatively compare expression activity of groups of genes between TLD and TLM conditions. Iron metabolism, pyrimidine metabolism and general stress response genes were similarly affected during the two conditions, while SOS response was induced only in TLD but not in TLM. Genes belonging to Group 1 and Group 2 were also differentially induced in TLM but could not be described by any single functional category. Detailed lists of significant genes and gene sets are given in Supplementary Tables 1-3.

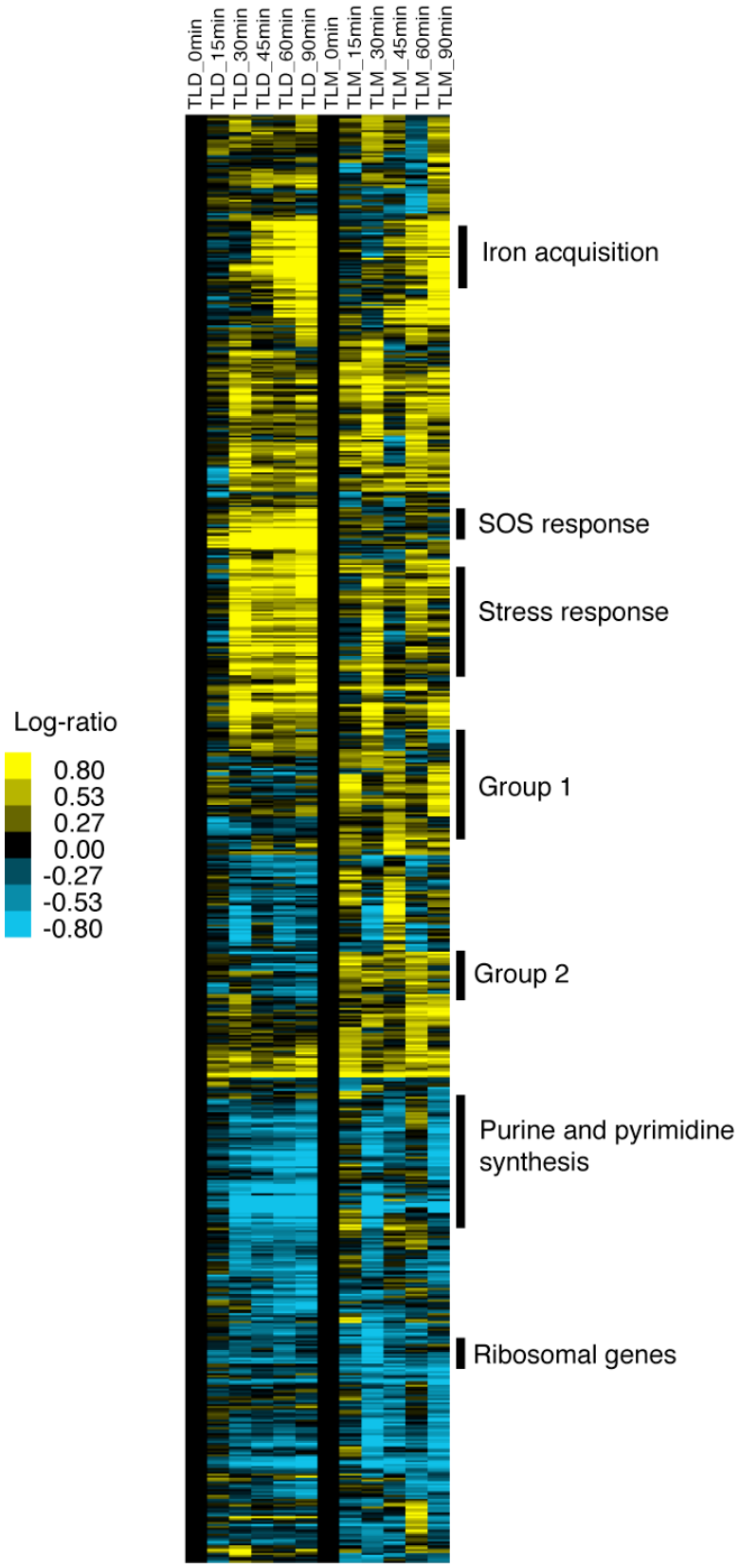
TLD_0min
TLD_15min
TLD_30min
TLD_45min
TLD_60min
TLD_90min
TLM_0min
TLM_15min
TLM_30min
TLM_45min
TLM_60min
TLM_90min
Iron acquisition
SOS response
Stress response
Group 1
Group 2
Purine and pyrimidine synthesis
Ribosomal genes
Log-ratio
0.80
0.53
0.27
0.00
-0.27
-0.53
-0.80

Fig S3.2. Similarity in responses of classified gene sets between TLD and TLM.
Transcriptional responses of
gene sets are strongly correlated between TLD and TLM conditions. Gene sets were compiled from available ontology databases; the sets reflect current gene assignments according to functional categories and/or regulons. The correlation coefficient is 0.71. As in Fig. 1 of main article, gene expression ratios for 45, 60 and 90 minutes were averaged for every gene in a set and the averages of members within a set were plotted. Gene sets related to SOS response (multifunctional categories 5.8 (SOS response), and LexA regulator targets) are marked with filled squares; pyrimidine synthesis (multifunctional category 1.5.2.2 (pyrimidine synthesis) and de novo pyrimidine synthesis - filled circles); galactitol metabolism (GatR targets and multifun category 4.S.65 (galactitol) - filled triangles). Refer to Table S2 for a listing of gene sets used in the analysis

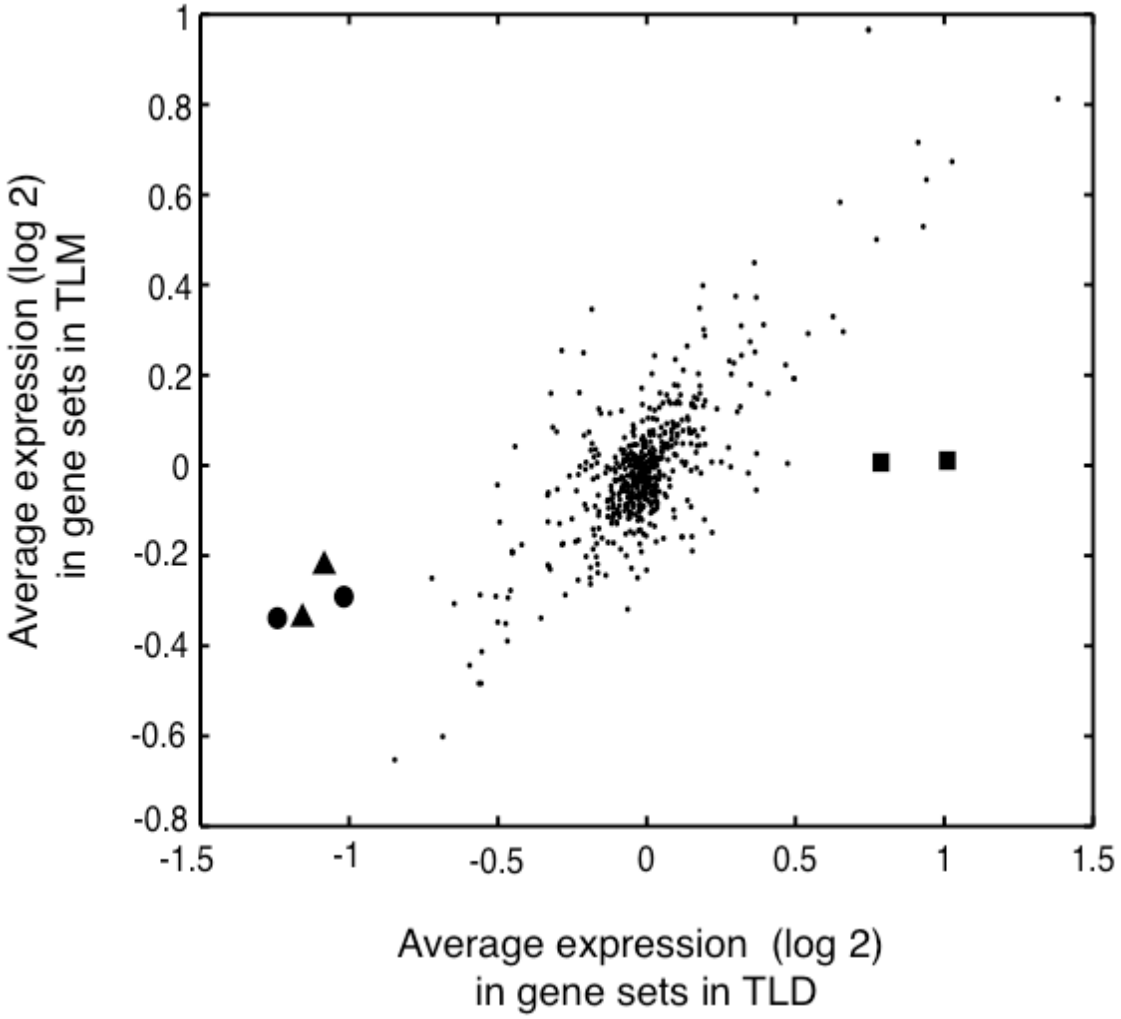

Fig. S3.3: High resolution chromosomal map of degradation of DNA surrounding the origin during TLD. Arepresentative sample was analyzed using Nimblegen's 385K array platform, with neighboring probe distance of 25 bp. The plot reproduces the results obtained from a lower resolution DNA microarrays.

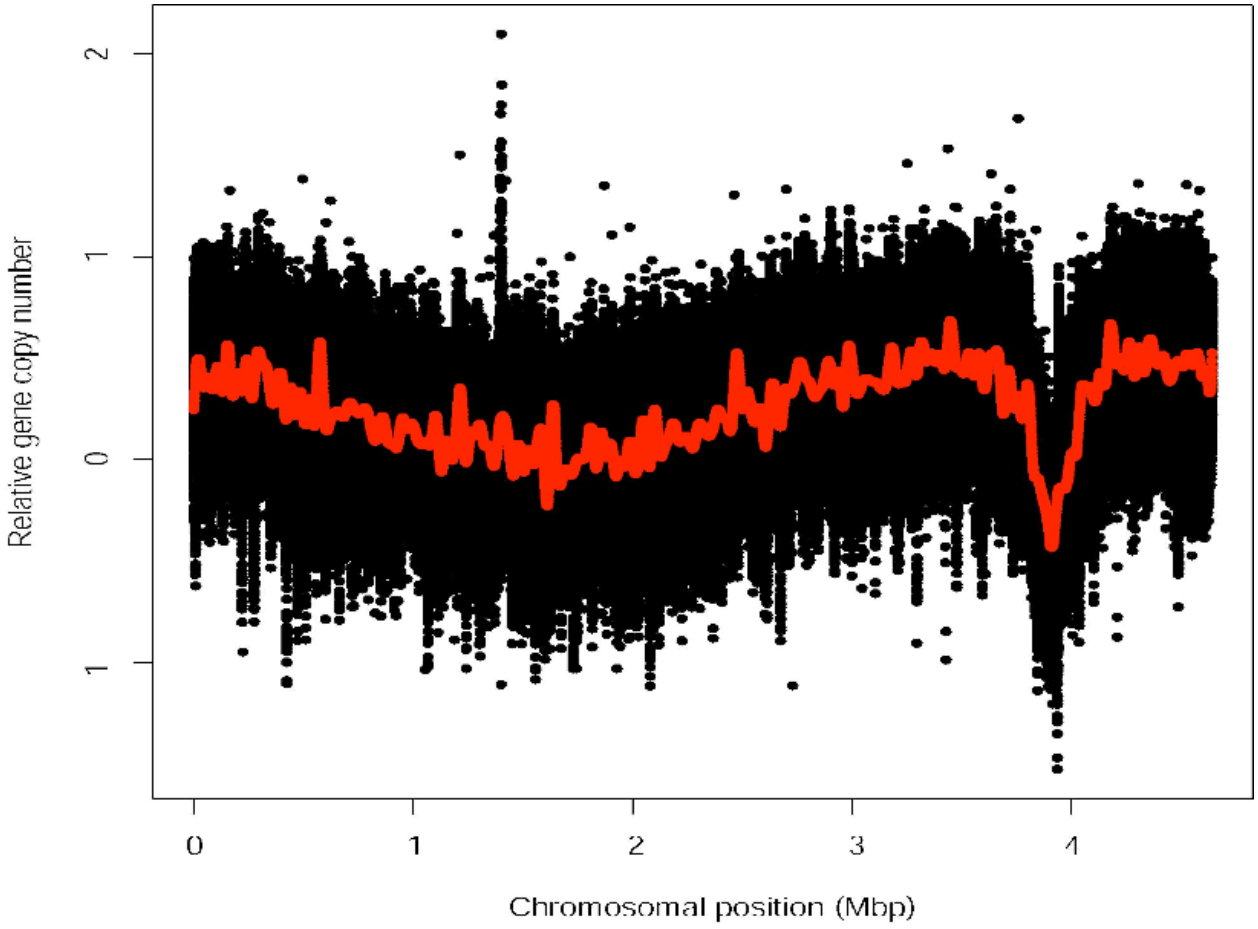

Fig. S3.4: Linear fit of gene copy number profile between 0 hr and 3 hr. Identical gene copy number profiles for 0 hr and 3 hr were observed along the chromosome except in the proximity to the origin. Data from individual replicate microarray hybridizations was fit to a linear model (Limma) (Smyth, 2004) and Fvalues representing a measure of log odds score were calculated and plotted along the chromosome. Pvalues of the F-score were also calculated using the same method, and p-value-gram indicates that significant and contiguous differences between the two conditions (0 and 3 hr) were close to the origin. Data was smoothed using loess smoothing algorithm in MATLAB (span 0.05).

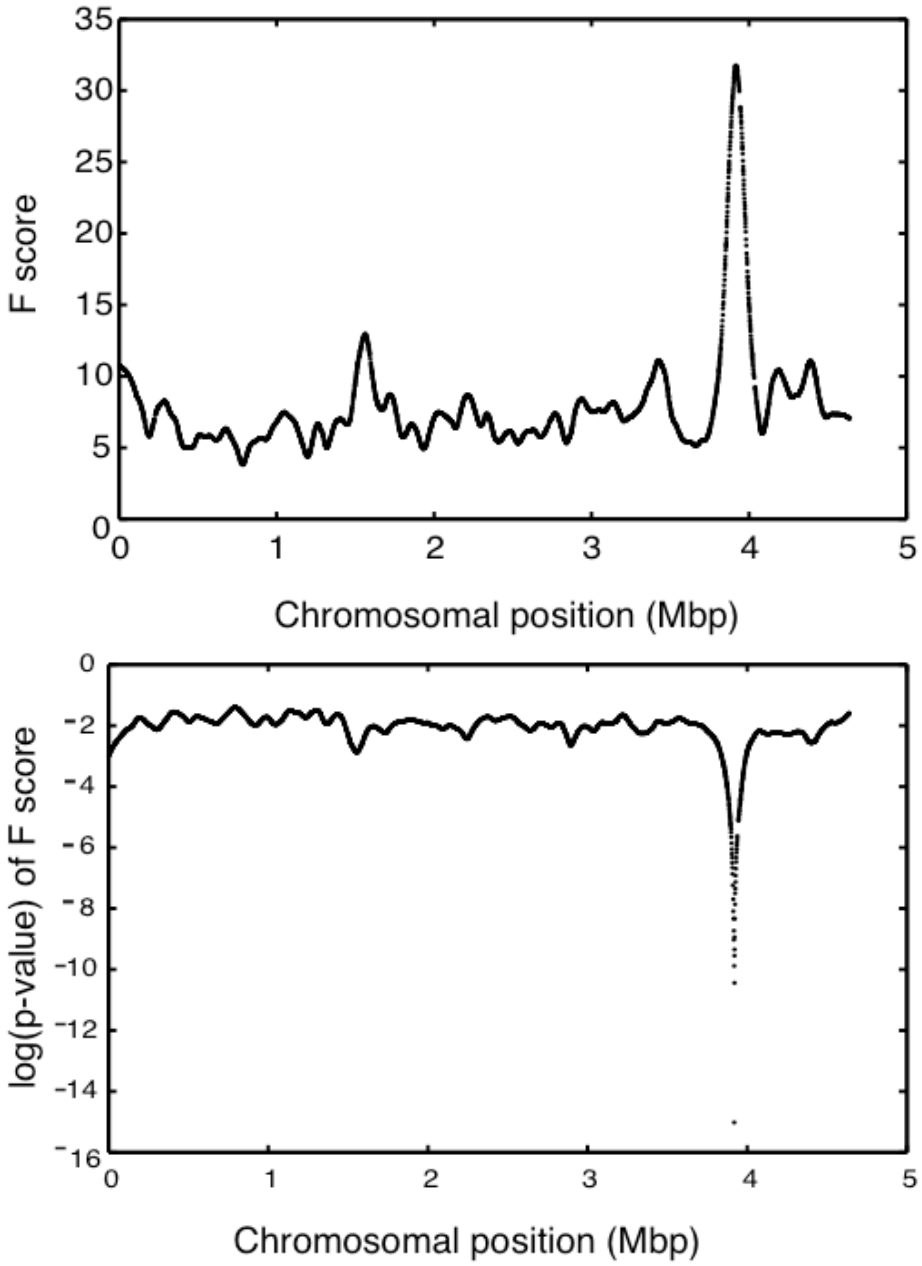

Fig. S3.5: Quantitative PCR of gene markers along the chromosome. Genes closer to the origin exhibit 2-fold loss in copy number compared to those closer to the terminus at 3 hr of starvation. Primers were designed to query genes that are in the vicinity of *oriC* and *ter* regions,and qPCR was performed using SYBR green dye as per manufacturer directions.

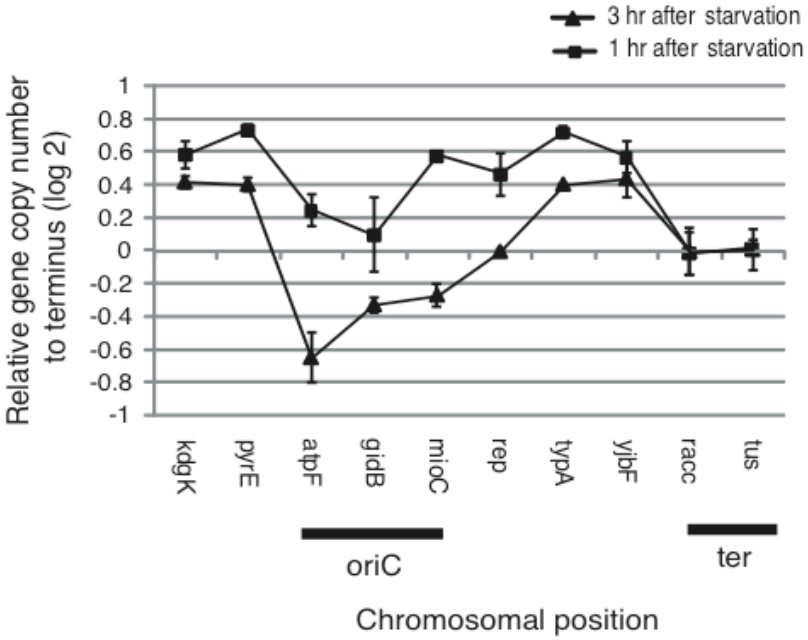

Gene marker

Marker	Chromosomal position of gene center (Mb)
kdgK	3.68
pyrE	3.81
atpF	3.92
gidB	3.92
mioC	3.92
rep	3.96
typA	4.06
yjbF	4.23
racc	1.42
tus	1.68

Transition to Chapter 4

Our comparative genomic hybridization studies showed a loss of hybridization of DNA from around the origin of replication in thymine-starved cells, and my work, which showed that a 'DNA damage score' is directly proportional to loss of viability in thymine-starved cells. Those results lead to the hypothesis that either the DNA loss itself is responsible for the loss of viability, or the mechanism of cell death that eventually results in DNA degradation, subsequently results in loss of viability. In either scenario, loss of DNA around the origin implies that either initiation of chromosomal replication itself or events concerning replication forks near the origin are responsible for the loss. Since both phenomena are closely related, I wanted to determine whether: 1) a portion of the chromosome within the span of the lesion, which was observed after three hours of thymine starvation in *E. coli*, is uniquely fragile and prone to degradation, or 2) the process of initiation of replication is detrimental in and of itself, or 3) the proximity of replication forks to the origin of replication have an effect on DNA degradation in TLD.

To address the first question, I made a *thyA*$^-$ strain of *E. coli* with two functional origins of replication, one native to the cell and one from a naturally occurring F-factor (F-fertility). That work shows that DNA degradation can occur from any functional, DnaA-dependent origin of replication, and that if there is some property of DNA that makes this particular segment susceptible to degradation, it is neither sequence specific outside of the core of the origin nor dependent on the genetic context (as there is nothing in common between the genes inside two lesions or surrounding them).

To address the 2nd question I investigated *thyA*$^-$ temperature-sensitive replication initiation mutants of *E. coli* in various stages of growth, replication-synchronization, and conditions of thymine deprivation to determine whether and to what extent initiation of chromosomal replication affected viability of cells deprived of thymine. The results of that work seem to show that replication initiation is either fully decoupled from the state of replication elongation or allowed to continue (as opposed to other functions which halt when DNA damage is sense,

like cell division) as a means by which cells attempt to rescue their genetic material when elongating forks are arrested. In UV-irradiation, increasing numbers of initiated replication forks means that as stalled forks are dismantled, at least one set of replication forks will progress to completion on a whole, repaired chromosome. The same situation correlates with increasing loss of viability in cells starved for thymine.

To answer the 3rd question, I used a genetic system that allows for only one-directional replication of the chromosomal DNA. In this strain, a piece of DNA containing a cassette with TetO operator sites is integrated into the genome just counter-clockwise of the origin of replication. Such design is expected to block progression of counter-clockwis forks which were initiated at the *oriC* when TetR repressor is present. I also wished to use temperature-sensitive initiation of replication mutants for synchronization of the replication cycle to better understand the relationship between proximity of replication forks to the origin of replication and the extent of the DNA degradation around the origin. Results of these studies showed that repressor bound DNA in thymine starved cells renders the cells exceptionally sensitive to thymine starvation (although I am uncertain whether this is due to blocking of replication fork progression at the bound site, or inhibition of cell activities), but more importantly, proximity of replication forks to the origin of replication may have an effect on the degradation of DNA. Synchronized cells that are allowed to initiate replication have less degradation when they are starved immediately upon return to permissive temperature as opposed to those cells which had time to deplete thymine in chain elongation during restrictive temperature before return to permissive temperature. Also, the ability of the cells to re-initiate in thymine starvation seems to precipitate the significant degradation around the origin of replication.

Chapter 4: Using Temperature-sensitive Replication Initiation mutants to observe the effects of replication initiation on viability and DNA degradation around the origin of replication

4.1. Introduction

4.1.1. Determining Whether DNA Degradation Can Occur Proximal to Ectopic Origins of Replication During Thymine Starvation

To determine whether the DNA surrounding the origin is more sensitive to thymine starvation and therefore degradation during growth I constructed a thymidylate deficient strain carrying an ectopic origin of replication in addition to its native oriC. This has been accomplished in some studies by the cloning and re-insertion of the native OriC origin of replication elsewhere in the genome (Wang, *et al.*, 2011), however naturally occurring *E. coli* containing more than one DnaA-dependent origin of replication are available.

The F-factor is a large plasmid or episome which is a 'fertility factor' in *E.coli* cells. Its presence allows the cell to become a donor during the process of conjugation with another cell. This factor can also incorporate into the bacterial chromosome forming a region known as an Hfr region. All Hfr strains arise from the integration of a conjugative plasmid into the bacterial chromosome by any number of possible recombinational events (reviewed in Ippen-Ihler & Minkley, Jr., 1986). As an episome, the F-factor replicates from one of two origins (OriV) which is DnaA-dependent, and ensuing initiation results in bi-directional replication. The other origin (oriT) is used during conjugative transfer between cells where the F-factor undergoes rolling circle replication. When the F-factor recombines into the chromosome, and the native *E. coli* origin is removed, replication may occur from the bi-directional OriV (Low, 2010). In this work I utilized an Hfr strain KL16 of *E. coli* wherein the fertility factor had incorporated near the 65' position in the chromosome (Figure 4.1 from Low, 2010) but the native oriC was intact.

4.1.2. The Role of Replication Fork proximity to the Origin of Replication in DNA Degradation During Thymine Starvation

While many studies have manipulated DNA replication and RNA transcription via chemical means, the results are difficult to interpret as drugs can have a variety of effects in cells. For instance hydroxyurea, a commonly used ribonucleotide reductase inhibitor, tends to degrade in solution releasing even more toxic compounds which act in a manner independent from ribonucleotide reductase inhibition (Kuong & Kuzminov, 2009).

Mild heat-shock also causes drastic changes in cell physiology, but is a condition that cells have evolved to cope with. Viability assays in thymine starved cultures showed that cells deprived of the nucleotide during heat-shock did not have significantly different rates of survival over the duration of starvation compared to cells starved at 37°C. Hence I proceeded to investigate the effects of thymine deprivation on temperature-sensitive replication initiation mutants.

E. coli DnaC protein is an essential component of the replication loading machinery. I transferred a *thyA*$^{-}$ allele into a K-12 strain of *E. coli* used in other studies which also contains a *dnaC(1)*^{ts} mutation. DnaC is a helicase loader protein that loads the DnaB replicative helicase onto duplex DNA. DnaB is necessary for processive unwinding of DNA ahead of DNA polymerase in DNA replication. With primase DnaB is necessary for initiation of replication at the origin of replication, for continued priming of lagging-strand synthesis, and has been shown to be necessary for restart at stalled replication forks (Marszalek & Kaguni, 1994; Wahles, Laskenb, & Kornberg, 1989).

Unlike other temperature-sensitive DnaC mutants, *dnaC1*(ts) does not show residual replication elongation at non-permissive temperatures (Sicard & Bouvier, 1975; Wechsler, 1975; Wechsler & Gross, 1971). At first this was interpreted to mean that *dnaC1*(ts) was a chain elongation mutant. Later studies into the nature of DnaC function showing its role as a helicase loader, and its ability to suppress primosome double mutants *priBC,* it became more apparent that replication restart is affected in this mutant, and the faulty 'elongation' in this mutant is due to replication fork stalling, and subsequent DnaB loss on the DNA strand (Maisnier-Patin, Nordström & Dasgupta, 2001; Sandler *et al*., 1999).

Although *dnaC*^{ts} strains are ideal for synchronization, since they are required for both origin-dependent replication complex loading and replication restart, I found, similarly to other groups that the *dnaC1*^{ts}-containing PC1 cells did not complete replication upon shift to restrictive temperature during starvation based on comparative genomic hybridization analysis. Since I wasn't certain that the inability to complete replication was due to cells running out of thymine for replication, or whether encounters with lesions uncoupled polymerases and kicked off DnaB helicase (as seen in McInerney & O'Donnell, 2007), I decided to try another temperature-sensitive replication initiation temperature-sensitive strain that specifically targeted *oriC*-dependent replication initiation. DnaA is a membrane-bound replication initiator protein at the pole of the cell, and binds specific sequences termed DnaA boxes near the origin of replication resulting in unwinding of the DNA duplex allowing access for replication complex loading. It is required for OriC-based DNA replication in *E. coli*, but not lagging strand priming or replication restart and so its effects can be differentiated from those of DnaC.

4.1.3 Manipulating the Direction of Replication Forks During Thymine-less Death

In addition to using replication synchronization to manipulate the position of replication forks (how far forks could progress before starving cells of thymine) I also tried to create a 'uni-directional' strain which curbed replication in the counter-clockwise direction by means of repressor-bound *tetO* cassettes**.**

Under the assumption that the span of DNA degradation seen during TLD is directly correlated to replication fork position, I attempted to manipulate the direction of replication forks proceeding from the origin of replication. I obtained a strain of *E. coli* from the lab David Sherratt engineered to contain a *tetO* array proximal to the origin of replication (3.910Mbp) and *lacO* array near the replication terminus (1.381 Mbp, 208 kbp anticlockwise of *dif*)(Lau et al., 2004). On a separate plasmid are encoded the genes for TetR-EYFP and LacI-ECFP repressors. Each array is organized as 200 *lacO* or *tetO* operator sites separated by a unique 10bp sequence between each and every binding site to prevent recombination events out of the genome. When transcription of the respective repressors is induced at a low concentration of arabinose, the array can be visualized within the cell as low quantities of fluorescently-tagged repressor

bind at the targeted sequences at concentrations that do not appear to inhibit replication. At higher concentrations of repressor, however, replication can be stalled, effectively blocking progress of the replication fork at that repressor site (Possoz, Filipe, Grainge, & Sherratt, 2006). Using CGH arrays, I wanted to observe whether the loss of DNA symmetric to the origin of replication shifts in *tetO+* cells in comparison to the origin when repressor is induced and replication progress counterclockwise of the native origin is blocked.

4.2 Methods

4.2.1. Strains Obtained and Constructed

KL16 Hfr strain was obtained from the Yale Coli Genetic Stock Center (CGSC #4245; Hfr(PO45), λ^-, *e14-*, *relA1*, *spoT1*, *thi-1*).

KL16 Δ*thyA* was made by using the Red recombinase method described in (Datsenko & Wanner, 2000). Briefly, primers homologous to 50 base-pairs both upstream and downstream of the thyA gene in the *E. coli* genome along with 20 base-pairs of homology to the beginning and end of the kanamycin cassette in plasmid pKD13 were used to amplify the kanamycin cassette region (F: GGTCATCAGATGCGTTTTAACCTGCAAGATGGATTCCCGCTGGTGAcAACGTGTAGGCTGGAGCTGCTTC; R: CGCACACTGGCGTCGGCTCTGGCAGGATGTTTCGTAATTAGATAGCCACCATTCCGGGGATCCGTCGACC). This linear DNA was gel-purified, and transformed into electro-competent MG1655 cells expressing the Red helper recombinase from a pKD46 plasmid. Colonies were selected on rich LB plates supplemented with 10μg/mL thymine, and 30μg/mL kanamycin. The *thyA*$^-$ phenotype was verified on M9 minimal plates with and without thymine. The kanamycin cassette was then repaired via FLP recombinase expressed on a transformed pCP20 plasmid (Amp^R). All plasmids for this procedure are available from the Yale Coli Genetic Stock Center.

E. coli strain PC1 (F-, *leuB6*(Am), λ^-, *thyA47*, *rpsL153*(strR), *dnaC1*(ts), *deoC3*) was obtained from the Yale Coli Genetic Stock Center. Attempts to generate a MG1655 Δ*thyAdnaC1(ts)* proved unsuccessful. I managed to couple the *dnaC1(ts)* allele to an intergenic kanamycin cassette by means of linear recombination using the Red recombinase method described in

making KL16*thyA::KAN.* This KAN cassette is located within the ~200bp non-coding intergenic space between opposing operons containing genes *yjjQ* and *yjjP* (primers used for amplifying the KAN cassette from plasmid pKD13: F: 5'-TGCAAAATCACACAACCAATATTTATTCAATGAAATCTGATGGATTCCGGGGATCCGTAC-3';R: 5'-ATCATCATAATGAATTTATTGTTTGGCCTTTACGAATCAGGGTGTAGGCTGGAGCTGCTT-3'). I successfully transferred the now KAN-coupled *dnaC1(ts)* into MG1655 and W3110 wild-type backgrounds which tested positive both for temperature-sensitivity as well as kanamycin resistance. However, I was unable to transfer this allele into either an MG1655*recF*$^{-}$ or MG1655*thyA*$^{-}$ background, nor was I able to transfer a *recF::KAN* or *thyA::KAN* allele into the MG1655 *dnaC1(ts)* background via P1-transduction or linear recombination using the Red recombinase system (utilizing primers with 50 base pairs of homology both upstream and downstream of the genes targeted for knock-out), no matter what order I attempted the knock-outs. There is a possibility that during the process of aminopterin selection, *thyA*$^{-}$ mutants which arose also acquired secondary mutations, or decades of use of this strain before deposit in the Yale Coli Genetic Stock Center also resulted in secondary mutations which may mitigate the effects of a *thyA*$^{-}$ allele in a *dnaC(ts)* background (which is likely still suboptimal for DnaC function at permissive temperature).

MG1655 *dnaA5*^{ts} was made by transferring the *tnaA300::Tn10*-coupled temperature-sensitive allele from a strain kindly donated by Steven Sandler (University of Massachusetts , Amherst) into the MG1655Δ*thyA* strain (made similarly as described previously for the KL16 strain) by P1 transduction. The *dnaA*5 allele has two missense mutations, one of which results in a reduced DNA-binding affinity for the replication origin (G426S), and the other (A184V) results in the proteins' heat sensitivity, and lag in DNA synthesis due to lower ATP binding in a reconstituted system with purified proteins (Carr, 1996).

I created an MG1655Δ*thyAtetO*$^{+}$*tus::KAN* strain out of the MG1655Δ*thyA E. coli* strain I made (described above). Using P1-transduction, I moved a *tus::KAN* allele from the Keio collection into the MG1655Δ*thyA* strain. The native *tus* gene encodes for a protein that binds at *ter* regions near the replication terminus of *E. coli* and is involved in facilitating replication fork slow-down and eventual resolution of replication between oncoming forks which initiated at the

OriC at the opposite end of the circular bacterial chromosome. Removing Tus would ensure there were fewer obstacles to clockwise-moving replication forks which must pass beyond the *ter* region to replicate the rest of the genome for which replication is blocked in the counter-clockwise direction. I then made a P1-lysate of the original MG1655 *tetO*$^{+Gm}$ strain I obtained from Sherratt, and using this lysate, transduced the MG1655 Δ*thyAtus::KAN* strain selecting for the gentamycin-resistance marker which is placed in the middle of the origin-proximal *tetO* array. This strain would tolerate growth in M9 media supplemented with casamino acids and thymine as well as LB rich media when transformed with the plasmid encoding the TetR repressor in the presence of gentamycin and ampicillin to select for the *tetO* array and TetR-repressor encoding plasmid respectively. A *tetO*$^{+}$ *thyA*$^{+}$*tus::KAN* strain transformed with the *tetR* containing plasmid under the control of an arabinose promoter was induced over-night in glycerol media containing gentamycin and ampicillin, and fluorescence identifying the location of the cassette was observed as a punctuate dot via fluorescent microscopy.

4.2.2. Growth conditions

Non-temperature-sensitive strains were grown overnight at 37°C with agitation in M9 minimal media supplemented with 0.4% glucose, 0.2% casamino acids (Difco Bacto Casamino Acids Technical, 223120), 1μg/mL thiamine, 5μg/mL uracil, and 20μg/mL thymine. The following morning, the cultures were diluted in the same media to an OD600 of approximately 0.05, and grown for at least six generations before thymine starvation.

Temperature-sensitive strains were grown in the same media at 20°C overnight (to prevent entry into deep stationary phase which takes a much longer time to recover from and enter exponential growth the next day) and then diluted those cells to an OD600 of approximately 0.025 into 30°C media the next morning for growth of at least six divisions before heat-shock and/or starvation.

4.2.3. Starvation and heat-shock treatment

For non-temperature-sensitive strains, cells were starved in exponential growth (after approximately five divisions) via pelleting by centrifugation (6 minutes at 6,000rpm) and then re-suspension in media of the same constitution without thymine supplementation.

For temperature-sensitive strains, starvation and heat-shock were performed as follows: The period of 90 minutes heat-shock for replication run-out was optimized by determining the minimum amount of time necessary for cells in exponential growth (with an OD600 lower than 0.2 to avoid any possibility of early entry into stationary phase) in M9 minimal media to run-out replication such that cells fixed while still in heat-shock showed a flat line in CGH arrays (the ratio of DNA from exponential to stationary phase cells was equal across the genome), and 15 minutes return to permissive temperature produced a plateau centering around the origin of replication indicating an increase in gene-copy number at the origin. This time matched well with what has been used for synchronization in literature (Withers & Bernander, 1998).

To determine whether any changes in genomic integrity were innately due to unknown factors in the genotype of the tested strains, *dnaA*^{ts} and *dnaC*^{ts} cells were starved at permissive temperature without heat-shock, and DNA integrity was measured by comparative genomic hybridization (CGH) arrays. After six generations at 30°C, an aliquot of cells from the exponential culture was washed via centrifugation and re-suspension in thymine-less media. Cells were kept at permissive temperature (30°C) for three hours in starvation.

To determine whether heat-shock itself had an effect on genomic integrity an aliquot of cells was heat-shocked for 180 minutes in the presence of thymine, and a sample was harvested just before return to permissive temperature for DNA purification, and subsequent CGH analysis.

The amount of thymine readily available upon return from restrictive temperature to permissive temperature for replication initiation was controlled in part by heat-shock with and without thymine. It is known that the 'lag period' from the time the cells are initially starved for thymine to the point where they encounter exponential decline in viability is correlated to the concentration of thymine present in the media upon starvation implying that cells have an

internal reserve of thymine that must be utilized before the true effects of starvation are noticeable (Ahmad et al., 1998). Cells starved during shift to heat-shock hypothetically utilize their thymine reserves during heat-shock until ongoing replication cycles have been completed and so may have little to no thymine left for DNA replication upon downshift to permissive temperature. Cells heat-shocked in the presence of thymine have adequate internal thymine with which to complete chromosomal replication, and enough to allow longer tracts of DNA to be replicated upon downshift to permissive temperature. In essence, cells which are allowed to re-initiate after incubation in thymine have replication forks capable of traveling farther than cells which were allowed to re-initiate after 90 minutes of starvation. To determine whether this variance in thymine utilization affected the dynamics of thymine starvation, samples were harvested from cultures that had been heat-shocked with and without thymine for 90 minutes and various time-points after synchronization by heat-shock. The DNA purified from cells subjected to these two treatments was analyzed by CGH array. In the former instance, cells were spun down, re-suspended in 42°C media supplemented with thymine and incubated at that temperature for 90 minutes. At 90 minutes heat-shock, the cells were filtered and re-suspended in 30°C media without thymine. Cells that were starved of thymine throughout heat-shock were starved by washing via centrifugation and re-suspension in 42°C thymine-less media. These cells were then harvested at the following time-points: after 90 minutes heat-shock (while cells were still in heat-shock); just after return to permissive temperature (0 minutes permissive- this sample was to determine whether initiation had occurred during the downshift); within 20 minutes of return to permissive temperature (in the presence of thymine, 20 minutes is adequate for some replication to have occurred at the origin); and 180 minutes at permissive temperature (270 minutes thymine starvation).

4.2.4. Viability

To measure viability of cells subjected to thymine starvation I took 100µL of culture at various starvation time points and plated the cells in serial dilution (in 0.2µM filtered 0.9% NaCl) on LB-rich agar plates supplemented with 10µg/mL thymine. For temperature-sensitive strains, these plates were incubated 16-20 hours at 30°C until homogenous colonies of approximately 1-2mm appeared and colonies were visually counted. For all other strains incubation was done at 37°C

until colonies 1-2mm diameter appeared. Viability was determined to be the percent survival during starvation as compared to 0 minutes starvation.

4.2.5. DNA purification and labeling for CGH analysis

Samples of culture at various points in starvation were harvested by fixation in 15% stop solution (5% phenol and 95% ethanol) for 30 minutes with agitation on ice. Samples were then spun down by ultracentrifugation (6 minutes, 6,000rpm), media poured off, and cell pellet frozen at -80°C until genomic DNA purification.

Due to low yields using QIAGEN genomic DNA purification kits, I used Promega's Wizard Genomic DNA Purification kit (Catalog no. A1120). This yielded a high quantity of nucleic acid which was used in downstream applications (if purity was above 1.7 A260/280 in 10mM Tris-HCl, 1mM EDTA, pH 8.0 [TE], otherwise DNA was extracted once with an equal volume of phenol-chloroform [50/50%), pH 8.0, precipitated with 1/10 volume of 3M sodium acetate and equal volume of isopropyl alcohol, washed with 70% ethanol, air-dried, and resuspended in 500µL of 10mM Tris-HCl, pH 8.0). All DNA was sonicated for 4 pulses, 12 seconds each at 25% amplitude with 30 seconds rest on ice between pulses using a Branson Digital Sonifier Model 250 to shear DNA to sizes running between 0.5-3 kilobases on a 1% agarose gel. This mixture was then precipitated with 1/10 volume of 3M sodium acetate and equal volume of isopropyl alcohol, washed with 70% ethanol, air-dried, and resuspended in 25µL of 10mM Tris-HCl, pH 8.0. DNA concentration was measured by spectrophotometer, and labeled with Cy3 or Cy5-dUTP (Agilent technologies) using the BioPrime DNA Labeling System (Cat No. 18094-011). Labeling reactions were cleaned using E.Z.N.A. MicroElute DNA Clean-Up Kit (Omega Biotek Cat No. D6296-01). Microarray production and hybridization followed a protocol described elsewhere (Khodursky, *et al.* 2003).

4.2.6. Replication Run-out

To determine whether there is a noticeable difference in the number of viable replication forks, as well as total duplex nucleic acid content, I treated cells in various stages of growth and starvation for replication run-out. Replication run-out is a commonly used method which entails

treating cells with replication initiation- and cell division-inhibiting drugs. This treatment allows for completion of replication of chromosomes, but such cells are unable to undergo initiation of new rounds of replication nor divide. RNA synthesis has been shown to be a pre-requisite for replication initiation in *E. coli* (Lark & Afol, 1972; Lark, *et al.*, 1963), and so drugs such as chloramphenicol or rifampicin are used. Drugs like cephalexin are used to prevent septum formation necessary for cell division. These cells are then permeabilized (usually via fixation by alcohol) and stained with nucleic acid specific dyes. In my case, the most readily available dye was propidium iodide which, when bound to the minor groove of DNA can be excited by 488nm wavelength light, and has an increase in emitted fluorescence of approximately 50-fold (in the 605nm range) as compared to free-dye or dye bound to single-stranded nucleic acids (Sklar, 2005).

For replication run-out analysis, cells were split into two aliquots, one for fixation (pelleting and resuspending cells in a 30/70 solution of 1X PBS [pH 8.0] and ethanol) to represent the beginning of replication run-out, and the second for replication run-out which was done by treating cells with 100µg/mL cephalexin (to inhibit cell division), and 200µg/mL rifampicin (to sufficiently inhibit RNA transcription necessary for replication initiation from the OriC) for three hours.

After the period of replication run-out, cells were fixed in the same manner as the non-run-out treated cells, and kept at 4°C until staining for nucleic acid content. Since propidium iodide does not have a preference for either single or double-stranded nucleic acid, cells needed to be treated with RNase to remove most of the contaminating nucleic acid (Bernander, Stokke, & Boye, 1998). Before staining for nucleic acid, cells were pelleted, resuspended in 1X PBS (pH 8.0) and treated with 100µg/mL of RNase A (Invitrogen cat no. 12091-021) for two hours at 37°C. Cells were then treated in the presence of the enzyme with 5µg/mL propidium iodide (courtesy of the Srienc Lab) for one hour before nucleic acid content was measured by flow cytometry. Non-RNase-treated cells were also run as a control to determine the efficacy of the RNase treatment. These fixed cells (stained and unstained, RNase-treated and non) were ran on a FACsCalibur flow cytometer. A flow cytometer transports cells in a fluid jet stream through through a focal plane of a monochromatic light beam. It can simultaneously measure size (light

scatter), fluorescence (through the use of filters), and number of cells. With RNase treatment, the fluorescence is a measure of DNA content per cell and is a linear parameter (Bernander et al., 1998).

Flow cytometry data was analyzed using FlowJo 7.6 software (this is explained in more detail in Appendix A). Viable replication forks were interpreted to be represented by distinct peaks as measured by flow cytometry after replication-run-out treatment. DNA content per cell was estimated, whenever possible, from the most representative peaks of PI fluorescence distributions of cells that were not subjected to replication run out.

4.3 Results

4.3.1. DNA Degradation Occurs Around any DnaA-dependent Origin of Replication During Thymine Starvation

KL16Δ*thyA* cells maintained in exponential growth for five generations in the presence of adequate thymine and then starved for thymine for 3 hours had a viability of 5.8±1.5% as compared to the beginning of starvation which confirmed a *thyA*$^-$ phenotype.

The native origin of replication was replaced with a chloramphenicol resistance (Cm) cassette to determine whether DNA degradation could occur without the native origin however, removal of the native origin (KL16Δ*thyAoriC::Cm*) resulted in a growth rate three times as slow as the parental KL16Δ*thyA* strain. Comparative genomic hybridization did not show degradation around either origin but it is not certain whether this is due to the type of origin of replication in use, or whether such degradation would be unnoticeable considering the slow growth of the *oriC::Cm* strain (such as in W3110*thyA*$^-$*recO*$^-$ strains which also had a shallow CGH gradient of exponential growth over stationary phase DNA indicating slow replication). Other studies using a strain of *E. coli* with an additional OriC elsewhere in the genome (called OriZ) showed a C (replication) period similar to that of wild-type cells with only the native origin, however having only the OriZ origin without the native origin significantly slowed the division period (D period (Wang et al., 2011), which corresponds to the slower rate of growth seen here with only the Hfr origin. Unlike the *oriC::Cm* strain, the OriC$^+$ strain appears to show decreased level of

hybridization to the probes representing ORFs surrounding the two origins (Figure 4.2). There may be a possibility that a strain with two origins initiates from both origins simultaneously as seen in the OriC-OriZ study, but if so, such firings do not result in viable replication forks as KL16Δ*thyA* cells have on average about half as many viable replication forks (based on replication run-out) than do Hfr$^-$Δ*thyA* cells (Figure 4.3) although this might be due to the slightly slower growth rate of KL16 cells as compared to Hfr$^-$ cells. It is possible that a combination of slower growth as well as collisions between opposing replication forks results in fewer viable replication forks. If both origins fired, and resulted in two sets of viable replication forks, one would expect the Hfr+ strain to have more viable replication forks than the wild-type strain which can only initiate from one origin. A different possibility is that the clockwise-moving fork of the Hfr origin collides with the counterclockwise-moving fork of the native origin rendering both inviable, but even in this case, one would expect the two replication run-out peaks to overlap since two viable forks would remain, moreover such a collision event (without the mediating effects of the normal Tus/Ter interaction which normally resolves oncoming replication forks at the replication terminus of the cell) would be catastrophic. Alternatively, a different origin is used in different cells.

Overall, the loss of hybridization around both origins of replication indicates that DNA degradation can occur at any DnaA-dependent origin of replication within the cell, and since the sequence of the DNA within the Hfr region is very different from that around the native origin, I conclude that the sequence of the DNA symmetric to the native origin is no more sensitive to degradation than other DNA in the cell.

4.3.2. Temperature-Sensitive Strains of *E. coli* can Continue to Have Initiation Events Which Result in Viable Replication Forks, and Loss of Viability in Starvation Correlates with Increased Number of Viable Replication Forks.

I wanted to understand whether replication of initiation, or replication fork proximity affected the degradation of DNA symmetric to the origin of initiation, and cell viability in thymine starvation.

To determine whether DNA degradation correlated with proximity of replication forks to the origin of replication, I treated cells under varying conditions of thymine starvation and synchronization by heat-shock to compare the viability and DNA integrity of cells which have just initiated replication and those whose forks were allowed to progress further along the chromosome. If close proximity of replication forks is necessary for DNA degradation then I would expect cells which were allowed to initiate and replicate for at least 20 minutes before starvation to have higher viability, and less DNA degradation than those cells which were starved immediately upon return to permissive temperature, or those starved while still in heat-shock. The CGH profiles shown in Figure 4.4 show that DNA degradation is not necessary for loss of viability (Figure 4.6), although degradation is associated with a greater loss of viability and that there is no significant difference in viability between cells that have been starved coming out of heat-shock and those which were allowed to initiate replication in the presence of thymine for 20 minutes before starvation. Figure 4.5 shows that there is little loss of viability of cells starved for thymine in heat-shock as compared to cells heat-shocked with adequate thymine. The higher viability in the thymine-supplemented strain may be an indication that replication progressed to completion for most cells and they succeeded in dividing which would result in more colony forming units upon plating at the end of heat-shock. The lack of killing may be due either to lack of initiation of replication, as has been implicated in other studies (Martín & Guzmán, 2011), or lack of replication re-start (due to a lack of viable DnaC protein which is required for loading of DnaB helicase for replication events). To identify which of these two possibilities explains the lack of killing, I performed these same experiments with another temperature-sensitive replication initiation strain, MG1655 *dnaA*^{ts}*thyA* which would eliminate the possibility of replication restart playing a role.

Figure 4.6 shows that initiation of replication may help mitigate killing in thymine starvation, and may be a defense mechanism used by cells in thymine starvation although Figure 4.7 implies that chronic starvation leads to catastrophic loss of DNA symmetric to the origin of replication (4.7A has been starved in heat-shock but does not show a 'dip' around the origin, however 4.7C & D which have been allowed to initiate after starvation begins show signs of a 'dip' indicating DNA degradation). Based on the CGH analysis of those cells which spend most of their time in heat-shock with starvation, without initiation, quality of DNA suffers near the origin

of replication resulting in poorer hybridization to microarrays. This may indicate that multiple chromosomes are necessary to repair and maintain at least one viable chromosome or that events in heat-shock lead to lesions which result in poorer quality DNA.

Stresses like nucleic acid synthesis targeting drug treatment (hydroxyurea) and DNA damaging agents like UV-irradiation of *E. coli* cells result in initiation of newrounds of replication initiation when forks from previously started rounds are still arrested, which is thought to be a defense mechanism by the organism to allow at least one viable replication fork to complete replication (Odsbu, Morigen, & Skarstad, 2009; Rudolph, Upton, & Lloyd, 2007). To determine whether new initiations took place after start of thymine starvation, I compared the number of viable replication forks over the course of starvation in each strain using replication run-out.

Figure 4.8 shows that in both temperature-sensitive replication initiation mutant strains of *E. coli* that there is an initiation event that occurs in heat-shock when cells are starved of thymine that does not occur in heat-shocked cells supplemented with adequate thymine (Figure 4.8A). This implies that cells experience issues in DNA replication early in thymine starvation, which, despite mild heat-shock, still results in an initiation event whereas in adequate thymine cells do not initiate. It must occur early enough in thymine starvation such that active DnaA or DnaC protein is still present for successful replication initiation. After synchronization by heat-shock, and return to permissive temperature with simultaneous thymine starvation there is one more initiation event which occurs between 0 minutes and 60 minutes starvation. Interestingly, replication run-out shows that there is no initiation event between end of heat-shock ('90min HS') and beginning of starvation (15 minutes), however an average of comparative genomic hybridizations CGH) indicate that an initiation event does occur at this timepoint and produces some increase in gene copy number at the origin of replication (Figure 4.4B). This can be interpreted to mean that the initiation event that results in the peak in the CGH arrays does not complete replication and at some point before completion, those replication forks become inviable. It is probable that the events that lead to inviability of the replication forks also leads to the degradation of DNA near the forks and thereby the origin of replication. The extent of the 'dip' in the CGH arrays may show the point at which such replication forks become inviable, and degradation begins.

The MG1655Δ*thyAdnaA*^{ts} strain results are difficult to interpret. On one hand this strain behaves consistently with the *dnaC*^{ts} strain in that it experiences additional initiation events during starvation. On the other hand it apparently loses DNA over heat-shock as well as viable replication forks as the samples heat-shocked with thymine have flow cytometry peaks which shift to lower fluorescence corresponding to half the number of chromosomes as compared to the exponential time point (beginning of heat-shock) based on the values of the modes of the peaks. This is not an isolated incident as Figure 4.9 shows averages of the most populous peaks (peaks containing the majority of the events in a flow experimental sample) amongst biological replicates and such results are consistent among the replicates. While *dnaA*^{ts} strains are used for DNA replication synchronization in *E. coli*, no literature exist that studies what happens to the DNA in these strains during heat-shock. It is likely that the loss of nucleic acid and viable replication forks in heat-shock has something to do with the nature of this mutant. DnaA is a transcriptional regulator of a number of genes, but not all of its targets are known. The irregularities in the CGH arrays for the *dnaA*^{ts} may be explained by something other than thymine starvation. For instance, thymine starvation results in changes in the levels of other deoxyribonucleoside triphosphate (dNTP) pools (reviewed in Ahmad et al., 1998), and DnaA is known to be a transcriptional regular of ribonucleotide reductase in *E. coli*, and without active DnaA protein, the cell may not be able to maintain adequate levels of nucleotides for replication under these circumstances. This may also explain why the *dnaA*^{ts} strain shows poorer viability in thymine starvation in heat-shock (Figure 4.10A). It does not explain, however why *dnaA*^{ts} cells have significantly higher viability than PC1 (*thyA*$^{-}$*dnaC*^{ts}) cells upon reentry to permissive temperature. One explanation is that PC1 cells have adequate DnaA protein available upon return to permissive temperature to allow for immediate initiation of replication, and based on the comparison replication run-out (Figure 4.8) have more viable replication forks per cell as compared to *dnaA*^{ts} cells (with relatively similar amount of nucleic acid content). OriC initiation complexes have been seen to form at the origin of replication, even if no further attempt at initiation is attempted in PC2 (*dnaC(2)*^{ts}) cells of *E. coli* at restrictive temperature, and such complexes were not seen when cells were treated when rifampicin or chloramphenicol were added (Gayama, Kataoka, Wachi, Tamura, & Nagai, 1990). Upon return to permissive temperature, cells with such complexes already formed will be able to complete initiation

before other cells. This would mean more initiation events than cells without such complexes. More viable replication forks may mean more sister chromosomal arms and more locations where thymine can be utilized and thus exhausted at a faster rate than if only one viable replication fork existed. This implies that viability is most likely correlated with the number of replication forks available during thymine starvation, although it is difficult to say whether some loss of viability is attributable to newly loaded replication forks progressing and encountering previously stalled replication forks resulting in some sort of irreparable damage. One would have to understand what kind of event resulted in previously loaded forks to stall in the absence of thymine while new forks progress unhindered.

4.3.3. Repressor-Bound DNA Proximal to the Origin of Replication is Toxic to Thymidylate-Synthase-Compromised Cells.

The MG1655Δ*thyAtetO*$^{+}$*tus::KAN* strain tolerated the pLAU63 plasmid containing the arabinose-inducible *tetR-EYFP* gene under selection pressure in M9 media supplemented with gentamycin and ampicillin. However, the strain rapidly lost viability when induced with 0.01% arabinose (the concentration optimal for good visualization, 0.05% is deemed necessary to block replication) in exponential growth in the presence of thymine, and would not grow when arabinose was present in the media at time of inoculation. Sherratt showed that when Tus is present, induction at 0.05% arabinose resulted in rapid decrease in plating efficiency, which is thought to be due to replication forks running into Tus-Ter complexes and being unable to complete replication of the genome. I had hoped to improve viability of cells by removing the Tus-encoding gene, and allowing for movement of replication forks past the anti-fork oriented Tus-*ter* complexes. While the cells appeared to be able to survive and grow without an identifiable *tus* gene (as measured by internal and external PCR amplifications as compared to control cells), and with an array present near the origin of replication (in *tetO*$^{+}$*thyA*$^{-}$*tus*$^{-}$ cells transformed with pLAU63 [*tetR*^{ara}] plasmid), inducing this strain with even low amounts of arabinose (0.001-0.01%) resulted in rapid decline in viability independent of thymine starvation. Because *thyA*- strains have less internal dTTP than *thyA+* strains even with adequate supplementation of thymine or thymidine (Ahmad et al., 1998), it is possible that the killing lesion in thymineless death is increased in strains that have a replication-fork blocking lesion or

construct. It is also possible that having a repressor-bound piece of DNA mimics the condition in the cell during thymine starvation where the replication fork is stalled or blocked, and unable to progress.

Figure 4.1. Chromosomal map of known Hfr strain integration positions. KL16 Hfr strain of *E. coli* has an Hfr region around 65 minutes between *serA* and *lysA* genes.

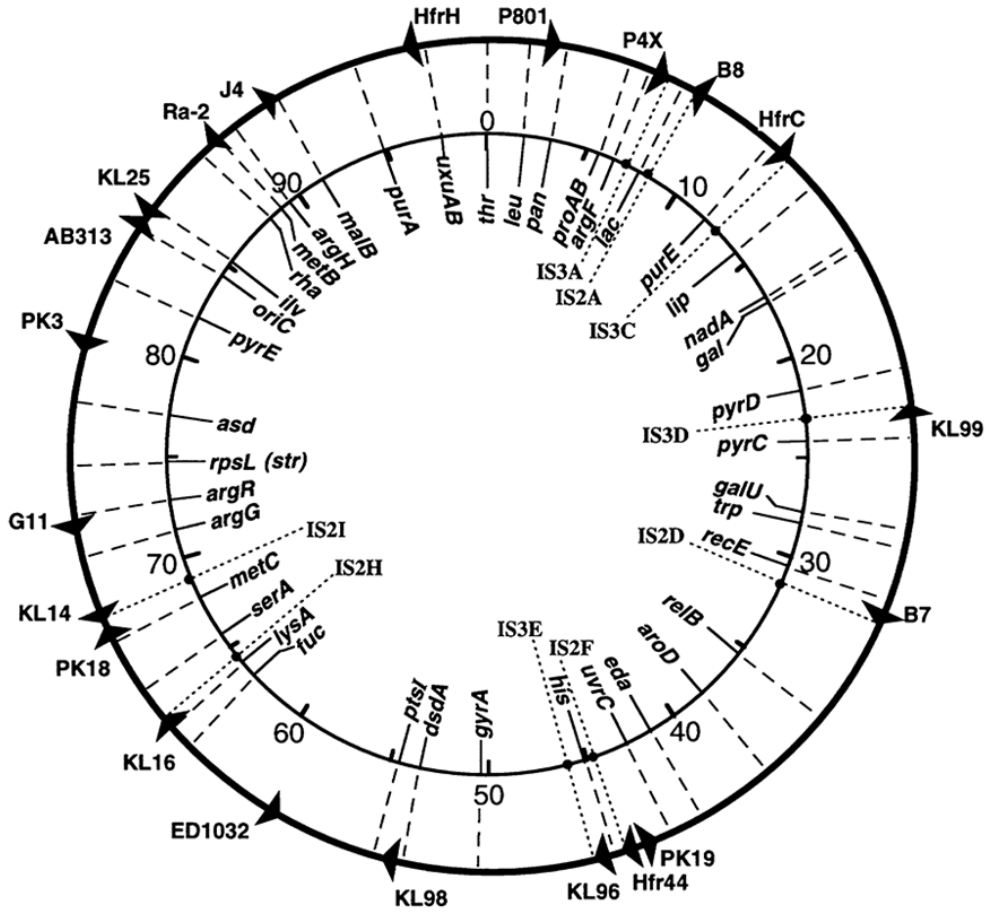

From Low, B.K. 2010 Posting Date. Chapter 127. Hfr Strains of *E. coli.* In A. Böck, R. Curtiss III, J. B. Kaper, P. D. Karp, F. C. Neidhardt, T. Nyström, J. M. Slauch, C. L. Squires, and D. Ussery (ed.), *EcoSal-Escherichia coli and Salmonella: Cellular and Molecular Biology. http://www.ecosal.org. ASM Press, Washington, DC.*

Figure 4.2. Ratio of gene copy number of DNA from KL16Δ*thyA* cells '3 hours starved'/'stationary phase'. Vertical dotted lines represent the two origins of replication.

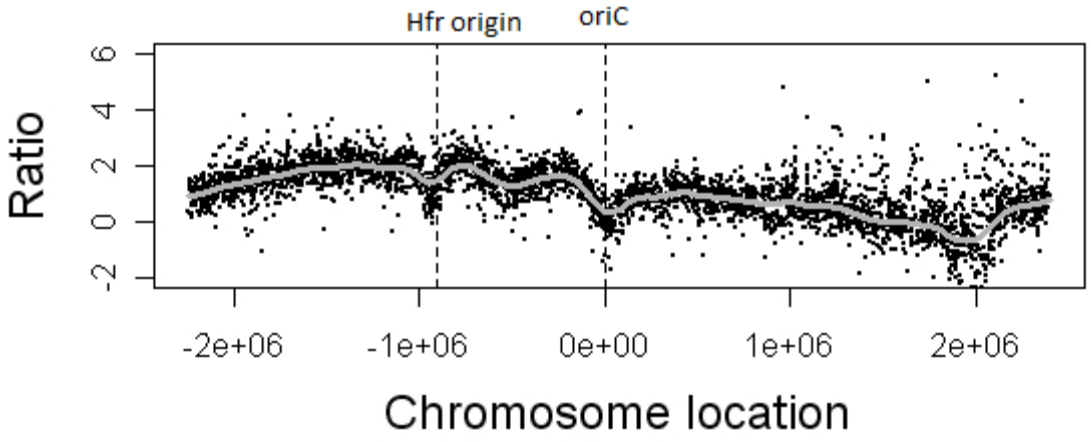

Figure 4.3. Replication-runout results of K-12 *E. coli* Δ*thyA* strains with and without an integrated Hfr in exponential growth. Values of fluorescence of modes are shown above the dotted line they represent. Hfr^- strains appear to have twice the chromosomal equivalents as do Hfr^+ strains.

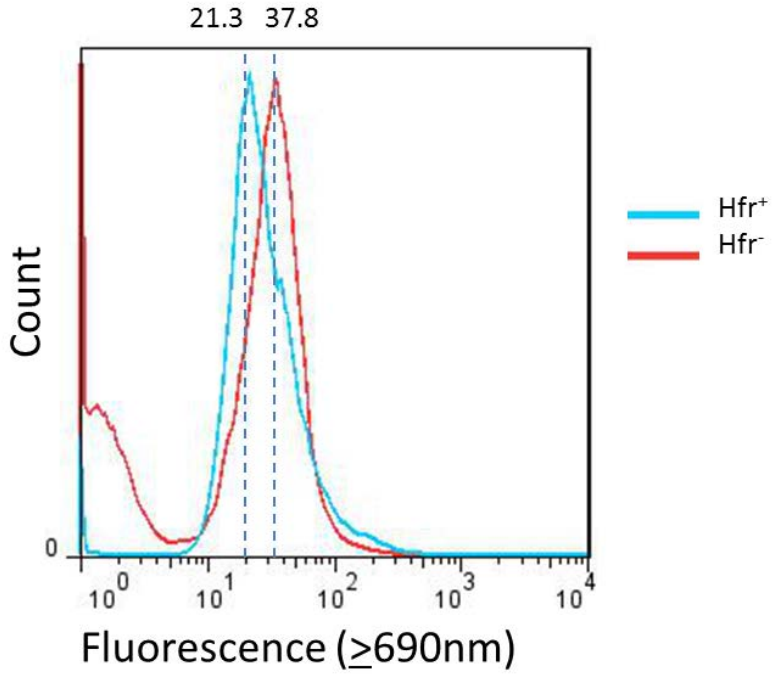

Figure 4.4. Overlapping graphs of comparative genomic hybridizations of PC1 (*thyA*$^{-}$ *dnaC*^{ts}) cells in varying conditions of starvation and heat-shock. The ratio shown is the gene copy number of experimental (starved and or heat-shocked cells) over a reference sample, in this case stationary phase cells. A flat line indicates a homogenous gene copy number throughout the genome, similar to what can be seen in stationary cells which have completed replication. Peaks indicate a higher gene copy number in the experimental sample than in the reference stationary phase sample. In **A.** cells that were heat-shocked with adequate thymine, were starved of thymine upon downshift to permissive temperature. '0 minutes' indicates the time into starvation which was simultaneous with downshift to permissive temperature; the flat-line at '0 minutes' indicates that PC1 cells can complete replication in heat-shock in the presence of adequate thymine. Likewise, '20 minutes' also refers to time into permissive temperature and starvation. Initiation has occurred at 20 minutes indicating there was adequate thymine for cells to initiate new rounds, however by 180 minutes starvation, it appears that the replication forks did not proceed very far before stalling although it is uncertain whether this is due to loss of thymine substrate or fork stalling at lesion. DNA degradation cannot be detected under this condition of starvation. In **B.** cells were starved throughout heat-shock. The '0 minutes' line is not flattened indicating that replication forks did not succeed in running out during heat-shock. The line at '20 minutes' into permissive temperature shows a new initiation event occurring, and by three hours starvation, DNA degradation seems to have occurred. These two graphs suggest that replication fork proximity to the origin (controlled by thymine access during heat-shock) is a pre-requisite for DNA degradation.

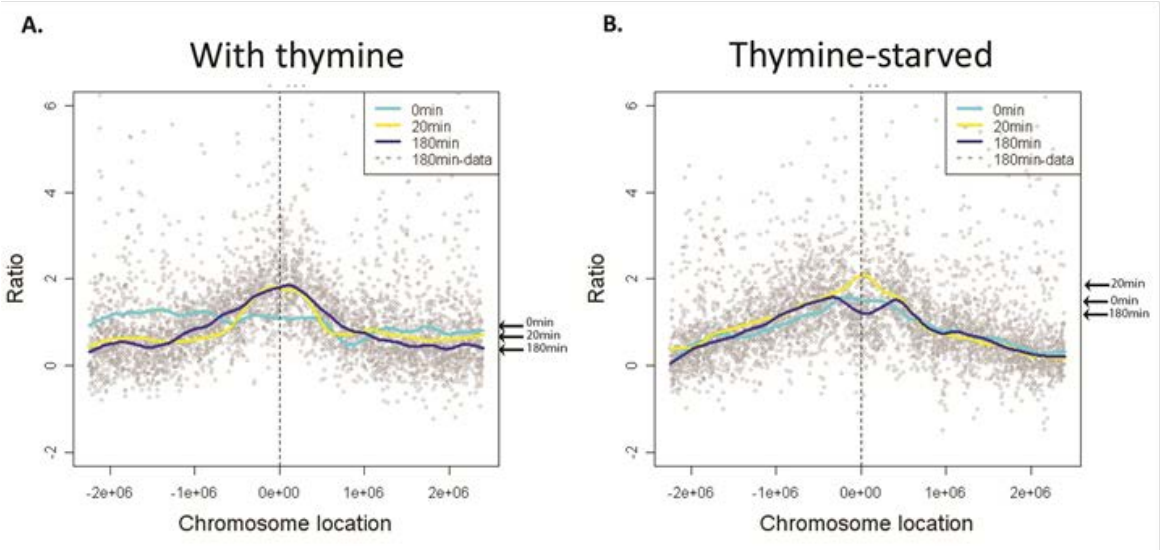

Figure 4.5. Presence of thymine during heat-shock does not appear to greatly affect viability indicating that most loss of viability occurs when cells are allowed to initiate replication, or allowed to undergo replication restart in the presence of viable DnaC protein. This graph shows viability of PC1 (*thyA⁻dnaC^{ts}*) *E. coli* cells after 90 minutes heat-shock with and without thymine starvation (as compared to beginning of heat-shock).

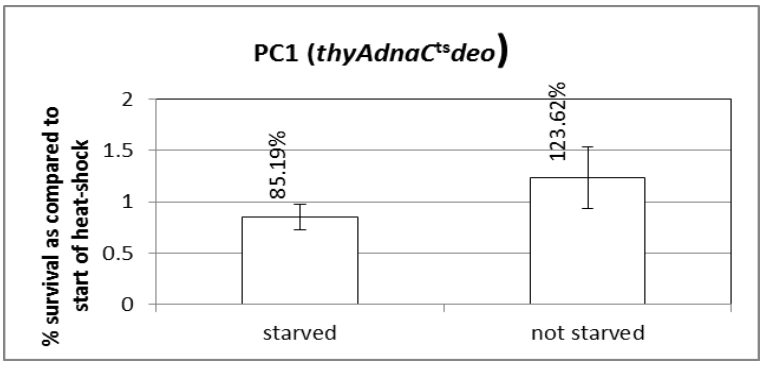

Figure 4.6. This graph shows average viability of PC1 (*thyA⁻dnaC^{ts}*) cells after 180 minutes thymine starvation under varying conditions of replication synchronization. A 'Exponential' cells indicates that cells were starved without synchronization in exponential growth.

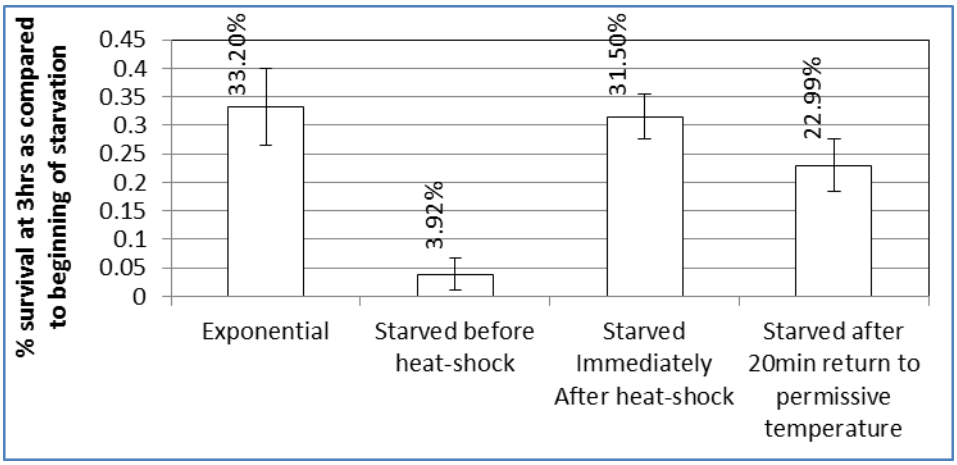

Figure 4.7. Overlapping graphs of comparative genomic hybridizations of MG1655Δ*thyAdnaA*^{ts} cells in varying conditions of starvation and heat-shock (OriC-centered). The graphs are an average of three biological replicates, and all replicates were split and subjected to all of the conditions within the same experiment. The ratio shown is the gene copy number of experimental (starved and or heat-shocked cells) over a reference sample, in this case stationary phase cells. A flat line indicates a homogenous gene copy number throughout the genome, similar to what could be seen in stationary cells which have completed replication. Peaks indicate a higher gene copy number in the experimental sample than in the reference stationary phase sample. In **A.** cells were heat-shocked with adequate thymine, and returned to permissive temperature for 15 minutes with thymine. This graph represents the 'control' behavior of this strain upon return to permissive temperature. The lack of a plateau in the middle at the OriC indicates that inadequate functional DnaA protein is present for normal OriC-dependent replication initiation. In **B.** cells were starved throughout heat-shock. The plateau and sharp drop-off towards the replication terminus (at the sides) may indicate that cells ran out of all nucleotides and not just thymine. Nevertheless, the plateau present symmetric to the OriC shows that replication forks do not stall in the same way as in PC1 cells indicating that replication restart is viable in this strain during thymine starvation. Graphs **C.** and **D.** are of cells starved upon entry to heat-shock, and either returned to permissive temperature (**C**.) or for the duration of starvation (**D**.).

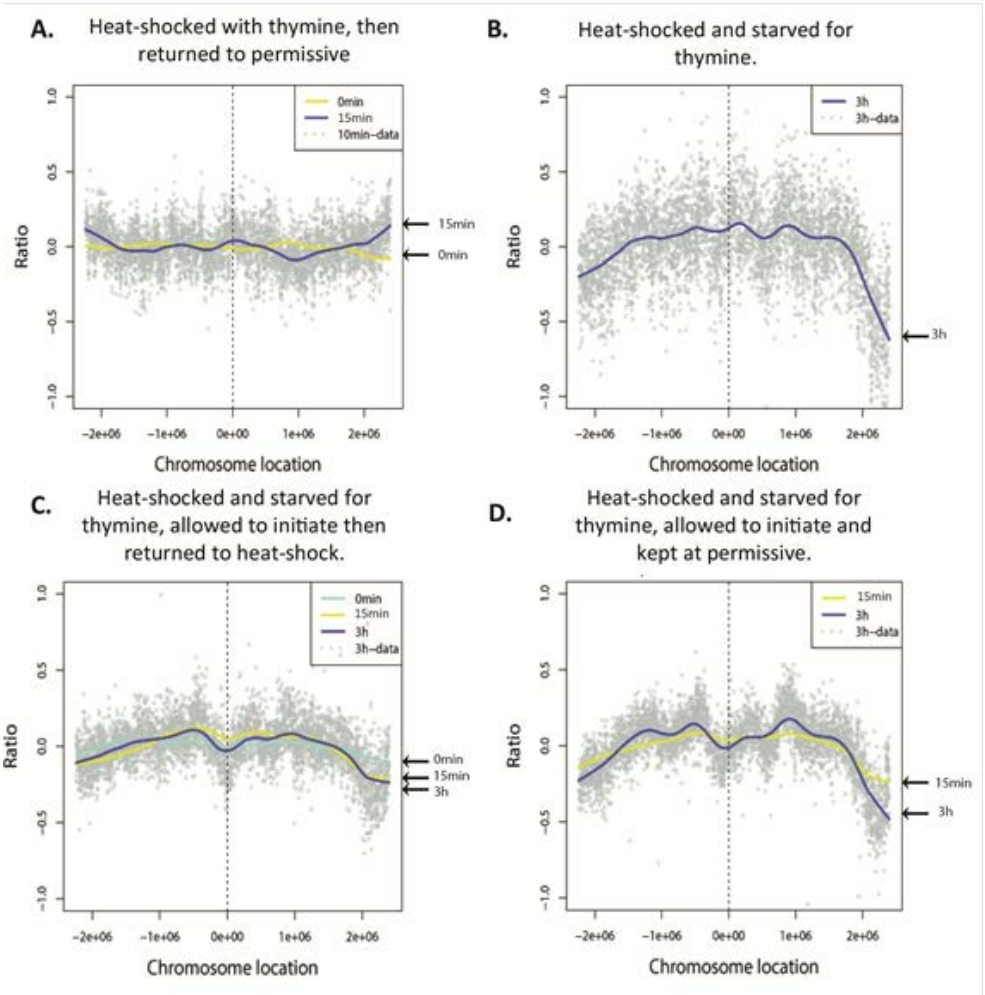

Figure 4.8. In both temperature-sensitive replication initiation mutant strains of *E. coli* that there is an initiation event that occurs in heat-shock when cells are starved of thymine that does not occur in heat-shocked cells supplemented with adequate thymine. The peaks in each graph represent a population of cells with a similar fluorescence value. The fluorescence results from excitation of a nucleic acid specific dye, which, after RNase treatment is indicative of DNA content per cell. When cells are allowed to undergo 'replication run-out' in the presence of adequate thymine, the viable replication forks form complete chromosomes. When cells are fixed before replication run-out, the DNA content is indicative of the amount of DNA present at that starvation timepoint. The higher the fluorescence value, the more DNA content or chromosomes per cell in that population of cells. After starvation cells continue to initiate new rounds of replication resulting in new viable replication forks (as indicated by peaks of higher fluorescence), although DNA content does not increase in a similar fashion indicating elongation is stalled.
A shows a direct comparison of PC1 (*thyA*$^{-}$*dnaC1*^{ts}) and MG1655Δ*thyAdnaA*^{ts} cells over time with and without synchronization by heat-shock. 'Viable replication forks' is flow data from cells treated for replication run-out. 'Total nucleic acid' is flow data from cells fixed just before replication run-out treatment.
B shows a direct comparison of PC1 (*thyA*$^{-}$*dnaC1*^{ts}) and MG1655Δ*thyAdnaA*^{ts} cells over starvation after synchronization by heat-shock.

A.

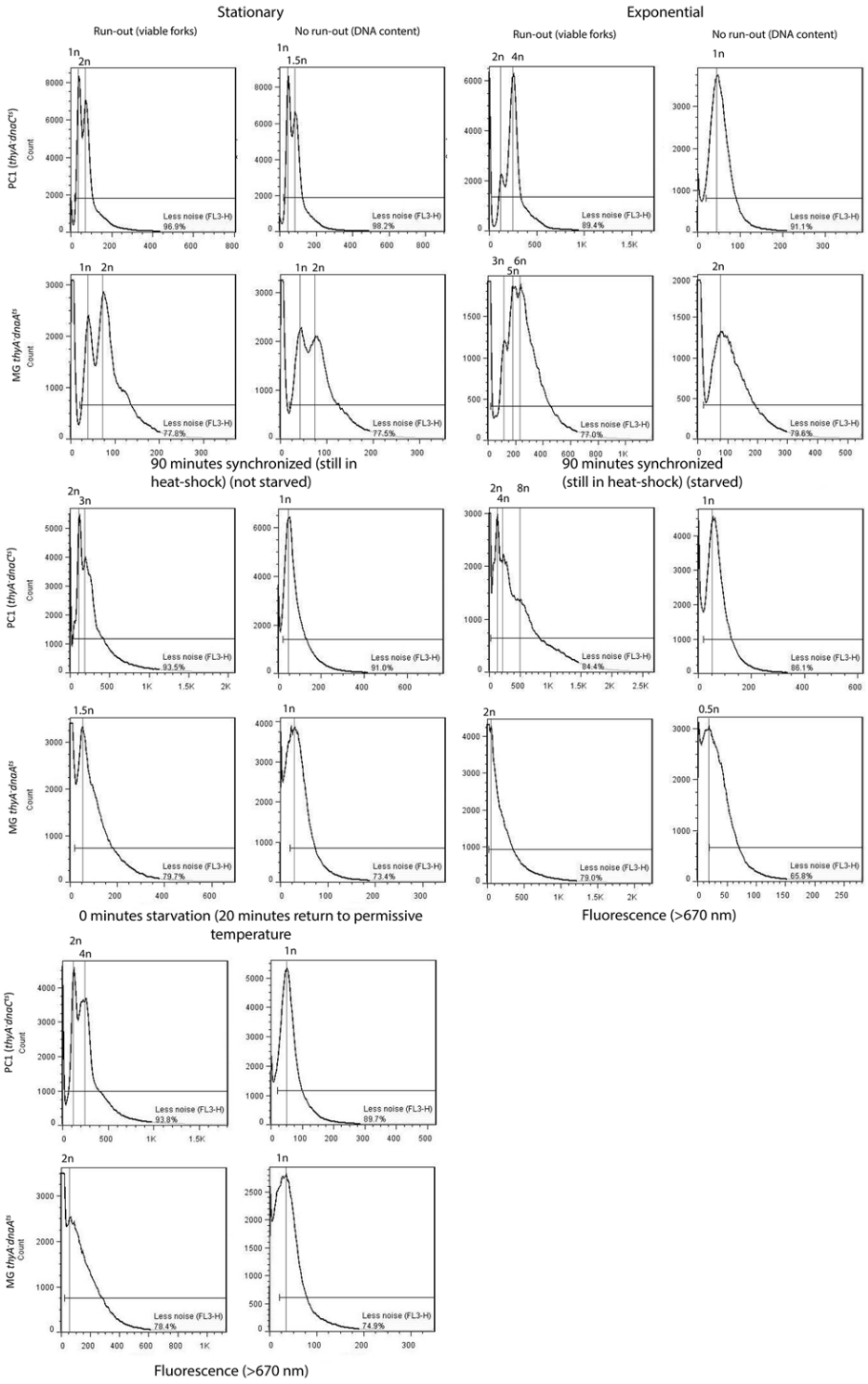
Stationary
Exponential
Run-out (viable forks)
No run-out (DNA content)
Run-out (viable forks)
No run-out (DNA content)
PC1 (thyA dnaC^ts)
MG thyA dnaA^ts
Count
Less noise (FL3-H)
90 minutes synchronized (still in heat-shock) (not starved)
90 minutes synchronized (still in heat-shock) (starved)
0 minutes starvation (20 minutes return to permissive temperature
Fluorescence (>670 nm)
Fluorescence (>670 nm)

B.

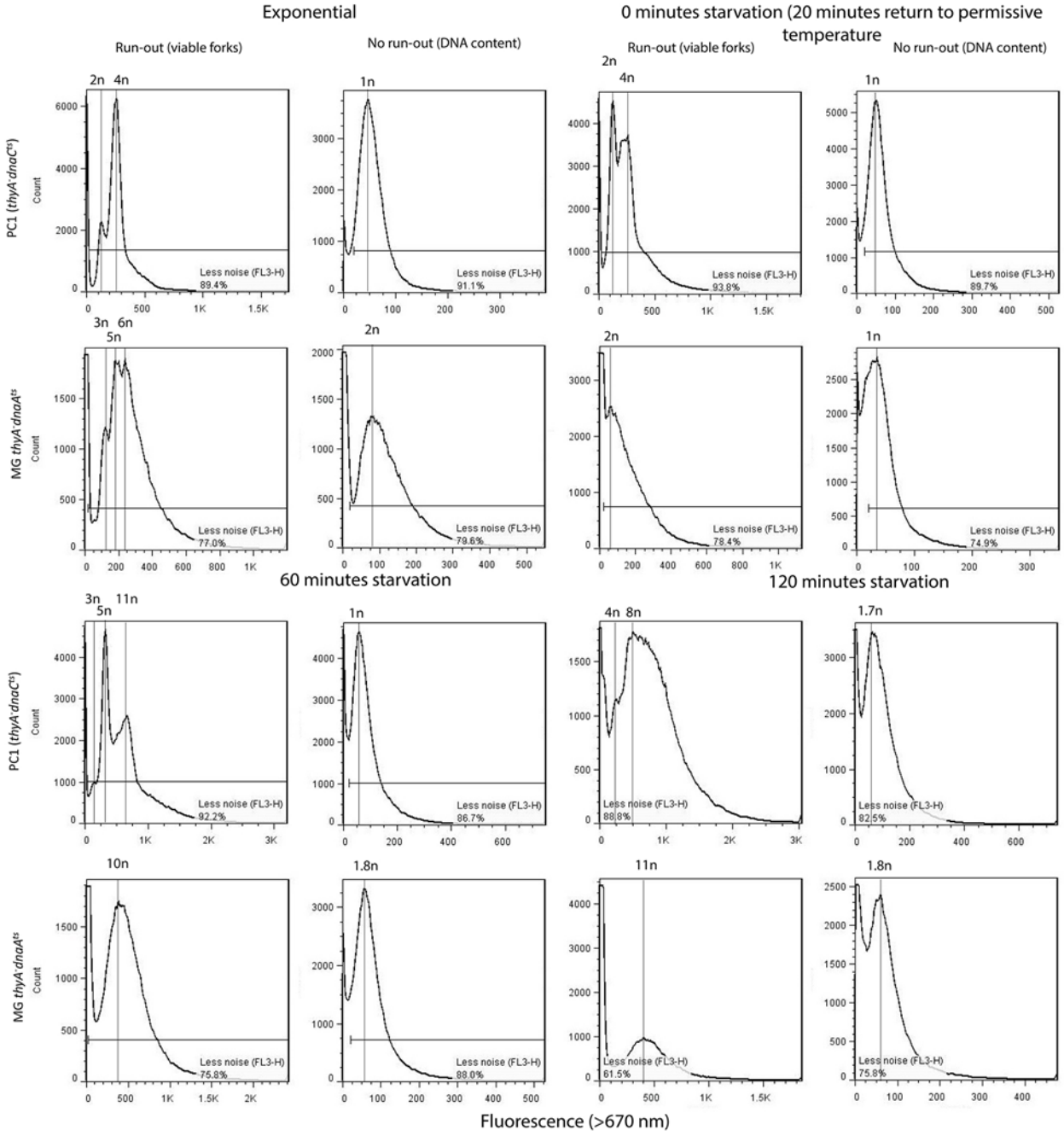
Exponential
0 minutes starvation (20 minutes return to permissive temperature
Run-out (viable forks)
No run-out (DNA content)
Run-out (viable forks)
No run-out (DNA content)
PC1 (thyA dnaC^ts)
MG thyA dnaA^ts
Count
2n 4n
1n
3n 6n
5n
2n
60 minutes starvation
120 minutes starvation
3n 11n
4n 8n
1.7n
10n
1.8n
11n
Less noise (FL3-H)
89.4%
91.1%
93.8%
89.7%
77.0%
79.6%
78.4%
74.9%
92.2%
86.7%
88.8%
82.5%
75.8%
88.0%
61.5%
75.8%
Fluorescence (>670 nm)

Figure 4.9. The average of the modes of the most populous peaks in flow cytometry samples. a.) represents those samples treated for replication run-out (3 hours replication run-out). b.) represents those samples fixed before replication run-out (0 minutes replication run-out).

A.

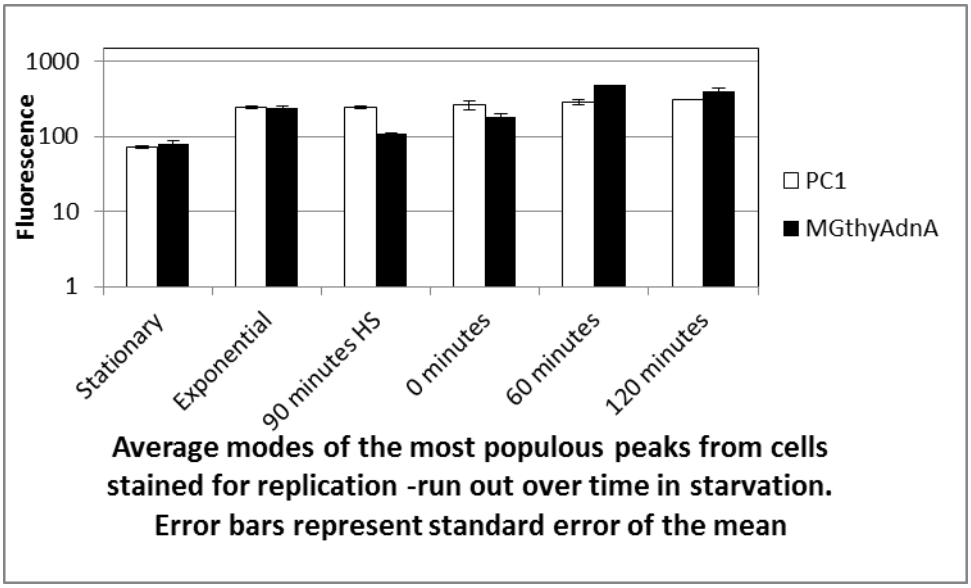

B.

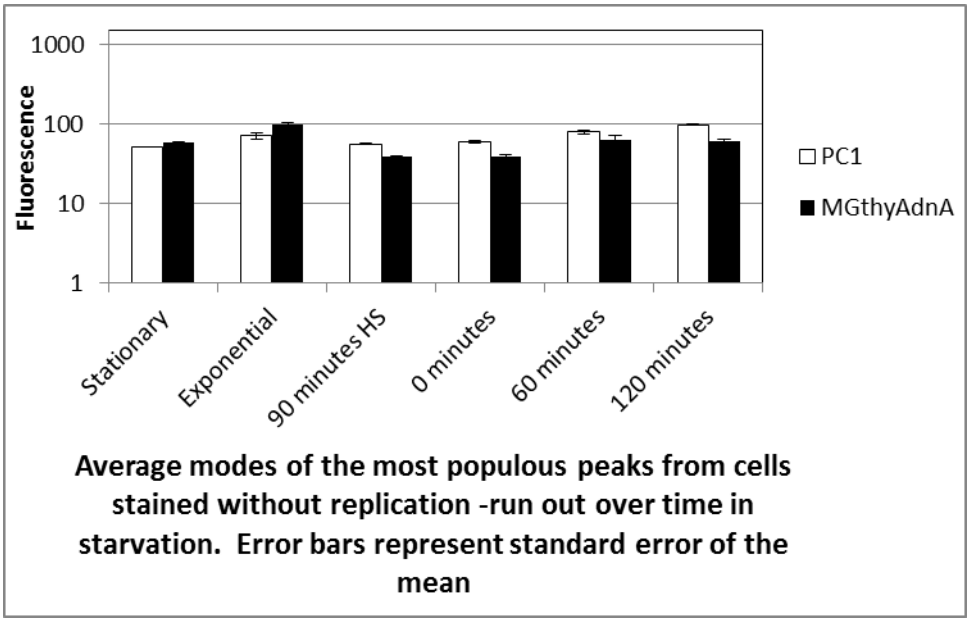

Figure 4.10. Comparison of viability between *dnaA*^{ts} and *dnaC*^{ts} (PC1) *E. coli* cells. **a.)** Viability of cells still in heat-shock after 90 minutes of starvation in heat-shock. **b.)** Viability of cells 3 hours after return to permissive temperature as compared to 0minutes return to permissive temperature. Cells were starved of thymine and heat-shocked for 90 minutes, and then underwent temperature-downshift simultaneously with thymine starvation.

A.

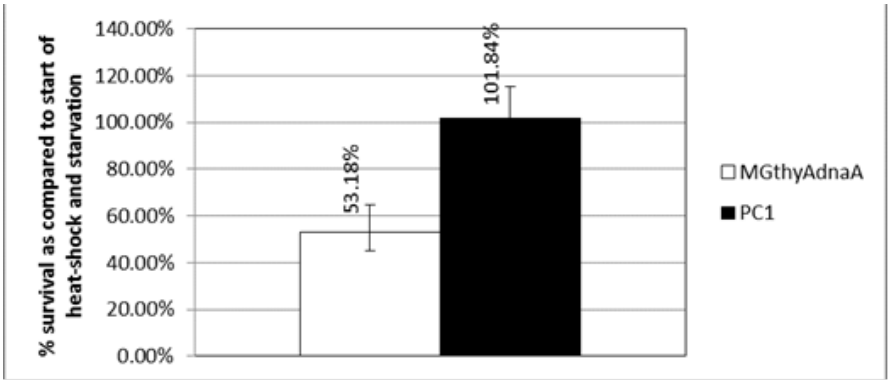

B.

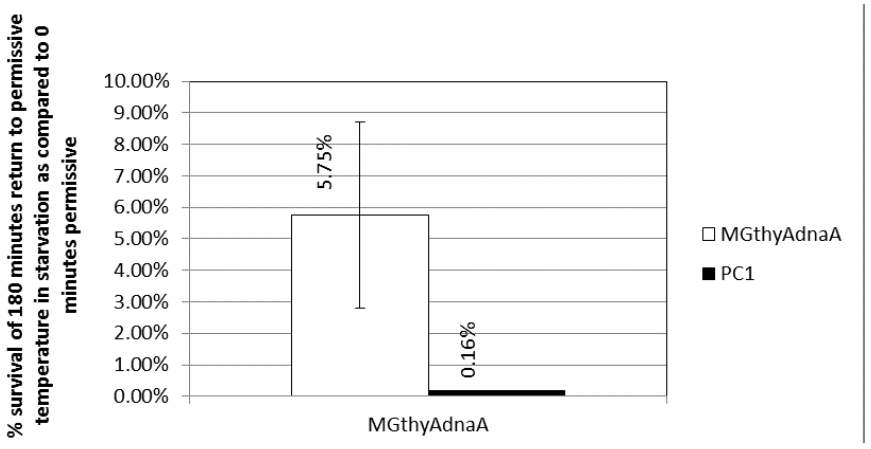

Transition to Chapter 5

My work published in 2010 (Sangurdekar et al., 2010) showed that of the RecFOJQ proteins mutants used in our thymine-starvation studies, RecF showed the most antagonistic effect in TLD. In other words, the absence of RecF rescued viability as well as mitigated the DNA damage score better than the other mutants tested, including RecQ the only TLD suppressor selected for by traditional screening methods (H Nakayama & Hanawalt, 1975; Hiroaki Nakayama, 2005). For this reason I focused on the effects of RecF in thymine starved cells treated for replication run-out as RecF has been associated with replication fork maintenance, rescue, and post-replicative repair (Chow & Courcelle, 2004; Steven J Sandler, 2005). Since work with the temperature-sensitive replication initiation mutants showed that number of viable of replication forks is higher in cells more susceptible to killing by thymine starvation (chapter 4 of this thesis), and also because viability is higher in *recF*$^-$ cells during thymine starvation (Kuong & Kuzminov, 2010; Sangurdekar et al., 2010), I was interested in knowing whether there is a difference in viable replication forks between RecF$^+$ and RecF$^-$ *E. coli* in thymine starvation. To understand this I performed replication run-out in two different RecF$^-$ background strains. I also wanted to know whether de-regulating the initiation of replication process would increase the rate of killing in thymine starvation and for that work I constructed a *thyA*$^-$ strain of *E. coli* wherein one of the suppressors of replication initiation, *seqA*, was removed to allow accelerated replication initiation.

Thesis Chapter 5: Replication Fork Viability in *recF*$^-$ Strains and the Effects of Unregulated Replication Initiation During Thymine Starvation

5.1 Introduction

5.1.1. What is the Variation in Viable Replication Forks as Measured by Replication Run-out in RecF$^+$ as compared to RecF$^-$ *E. coli*

RecF is an auxiliary protein in recombination repair to RecA, the main recombination protein which is required for recombination in all phases of growth of *E. coli*. The role of RecF in this capacity is limited to post-replicative repair, specifically daughter-strand gap repair (Sandler, 2005). Cells lacking RecF protein are more sensitive to UV-irradiation during exponential growth, and the role of RecF is thought to be involved in filling gaps in newly replicated DNA behind replication forks (Courcelle, Crowley, & Hanawalt, 1999). Although *in vitro* studies have shown that RecF is not necessary for loading RecA onto single-stranded regions of DNA (in fact it appears to have an inhibitory effect on RecOR recruitment of RecA to ssDNA regions [McInerney & O'Donnell, 2007]), it has some role in recruiting RecA to daughter strand gap junctions (where double-stranded and single-stranded DNA meet). RecF accelerates loading of RecA at that junction, although it is not necessary (Handa, *et al.* , 2009; Sakai & Cox, 2009). RecF has also been shown to protect nascent DNA at stalled replication forks (Chow & Courcelle, 2004; Courcelle & Hanawalt, 2003). All of the effects described here may have a role in TLD. For instance, large multi-kilobase lengths of single-stranded DNA has been observed in thymine starvation. Complex DNA structures are formed during TLD (probably resulting from homologous recombination) which can be trapped in agarose plugs during pulse-gel electrophoresis, and that knocking out recombination proteins like RecF alleviates this phenomenon (Nakayama, *et al.,* 1994). The homologous structures could be a result of RecF-mediated recombination at daughter-strand gap junctions.

The location of *recF* in the genome is also interesting as it is placed in the same operon as *dnaA* and *dnaN* which encode the replication initiator protein DnaA and the beta subunit (sliding clamp) of DNA polymerase III respectively. It has been suggested that RecF may be a replication

protein due to its location in the genome (Kogoma, 1997)(Figure 5.1). In my work I have been unable to create a double Δ*recF dnaC*^{ts} mutant in the same background. Although I have been able to couple the *dnaC2* mutation from PC1 (*dnaC2*) *E. coli* background to a kanamycin resistance cassette in the genome, transfer it by P1 transduction into a RecF+ background, and also been able to transfer the *recF::KAN* allele into a *dnaA*^{ts} background, I have never succeeded in transferring that *recF::KAN* allele into PC1 cells or the MG1655 *dnaC*^{ts} background either by P1 transduction or Red recombinase-mediated linear recombination into the genome. Although experimental incompetence may play a role, while doing many of these assays simultaneously where transfer works in one background but not another leads me to believe that perhaps a *recF*$^{-}$ *dnaC*$^{-}$ double-mutant is synthetic lethal, even if it is only a temperature-sensitive *dnaC* allele.

The *recF* gene is located directly upstream of another essential gene, *gyrB* (Figure 5.1) which encodes the ATPase subunit of a bacterial type-2 topoisomerase, DNA gyrase. To be sure that the effects of RecF on viability in thymine starvation was due to the action of the RecF enzyme and not polar effects that may be affecting the transcriptional regulation of the essential downstream gene, I complemented the CL579 strain used in this chapter and my 2010 Molecular Microbiology paper with a *recF*-containing constitutively expressing plasmid. Figure 5.2 shows that RecF protein expressed from a pBRBB plasmid (constitutive expression and 10-20 copies per cell) can functionally rescue *recF*$^{-}$ cells from UV irradiation as well as sensitize those cells to thymine starvation.

5.1.2. The Effects on Viability When Initiation Regulation is Disrupted in Thymine Starvation

Unlike eukaryotic cells, many bacteria are capable of initiating new rounds of DNA replication before previously loaded replication complexes have finished synthesizing the chromosome (Kubitschek & Freedman, 1971). This is thought to be a means for cells, which can replicate the entire chromosome in 40 minutes, to be able to divide within 20 minutes during exponential growth. Once one round of replication has completed, that chromosome can segregate into a daughter cell, and there is less than 20 minutes remaining for the subsequent set of replication

forks to reach completion so that another daughter cell can undergo division. This process must be carefully regulated to allow for the optimal number of replication forks to be progressing at the same time, yet temporally separating the initiation sufficiently so as to avoid co-directional collisions of replication complexes due to natural pauses and restarts in replication processes. The bacterial origin of replication (OriC) contains a number of unique sequences called "DnaA boxes" which, when fully methylated, are bound by the replication initiator-protein DnaA. The monomers of DnaA form a complex wrapping the DNA in a kind of protein core, and then engage in local melting of the DNA duplex allowing access for DnaC to load DnaB helicase, which becomes the basis of the replisome-the complex of enzymes including DNA polymerase which replicate DNA.

Unlike eukaryotes which have a number of cell cycle regulators and checkpoints to ensure that replication is coupled with division, in *E. coli* and other bacterial cells, replication initiation appears to be primarily coupled to growth, and growth-dependent accumulation of ATP-bound DnaA protein. Specifically the ratio of ATP to ADP is critical as DnaA can bind both molecules equally well, but only DnaA-ATP is active in replication initiation and regulation of ribonucleotide reductases(Kaguni, 2006). To prevent the immediate re-initiation of DNA replication in cells growing in rich media, the freshly replicated, still hemi-methylated DNA is sequestered by SeqA protein which binds hemi-methylated GATC sequences within this DNA (Guarné, *et al*., 2005) . Since a viable *seqA::KAN* strain is available in the Keio collection, I wished to see the effect of removing this form of suppression on cells suffering from thymine starvation, since other work has shown that initiation of replication is important for loss of viability in thymine starvation (Hanawalt, 1963; Martín & Guzmán, 2011; Morganroth & Hanawalt, 2006).

5.2 Methods

5.2.1. Strains

The strains used in this study are the same as those used in the 2010 Molecular Microbiology paper published by my group as well as the temperature-sensitive strains utilized in the preceding chapter.

CL001 (λ⁻ *thyA*36, *deoC*2, in(rrnD-rrnE)1, *rph*) and CL579 (derived from CL001 except P1 phage transduced with an *recF*6206 allele (sub *tet*857 for cdn4-295)) share the same parental strain of *E. coli*. W3110 is very similar to MG1655 in terms of a wild-type K-12 strain excepting a few point mutations and an inversion between *rrnE* and *rrnD* ribosomal RNA regions (which are highly homologous regions)(Hill & Harnish, 1981). A *recA::KAN* allele was verified by sequencing from an MG1655 *recA::KAN* strain created by Kyeong Jeong who studied previously in the lab, and then introduced into the CL001 strain by linear recombination using the Red recombinase method described in the methods of chapter 4 of this thesis (Datsenko & Wanner, 2000). The CL001 *seqA::KAN* strain was made by transferring the *seqA::KAN* allele from the Keio collection into CL001 cells by P1 phage transduction.

The *recF* gene was cloned from the MG1655 genome into a pBRBB plasmid kindly donated by Sarah Bloch of the Schmidt-Dannert lab, and freshly transformed into CL579 cells before each experiment. Transformed cells were selected by ampicillin resistance on thymine-supplemented plates, and colonies less than 2 days old were used for starvation experiments.

The MG1655Δ*thyAdnaA*^{ts} strain was P1 tranduced with a *recF::KAN* allele from the Keio collection (Baba, *et al*., 2006), and the position of the gene replacement was verified by PCR using primers for outside and inside the kanamycin cassette as suggested in the Datsenko & Wanner study (Datsenko & Wanner, 2000).

5.2.2. Growth, Viability, and Replication Run-out

All strains were grown in M9 minimal media (0.4% glucose, 0.2% casamino acids, 10µg/mL thiamine) and supplemented with either 10 or 20µg/mL of thymine depending on strain requirement. Temperature-sensitive strains were grown at 30°C and heat-shocked at 42°C whereas W3110 strains were all grown and treated at 37°C. *SeqA::KAN* cells did not grow well at 37°C on kanamycin, forming small, heterogeneous colonies, therefore these cells were treated at though they were temperature-sensitive and cultivated and treated at 30°C.

Viability was assayed by plating and approximating the number of viable cells in a suspension by colony forming units (CFU) of thymine-starved cells on LB plates. Replication run-out was performed similarly as was described in chapter 3 of this thesis.

Replication run-out of Δ*seqA* cells in other studies results in ill-defined peaks similar to what I observe in this study (Ferullo & Lovett, 2008), indicating that the lack of definite peaks in *seqA::KAN* cells is due to the nature of replication initiation in the absence of the functional SeqA protein and not due to issues with the replication run-out assay.

5.3. Results

5.3.1. Absence of RecF protein results in a massive drop in nucleic acid content late in thymine starvation as well as fewer viable replication forks per cell.

Similar to other groups studying TLD, I have found that *recF*$^-$ cells have higher viability than *recF*$^+$ strains over time, and *recA*$^-$ cells have lower viability over time in thymine starvation (Figure 5.3), although unlike other groups my Δ*thyArecA::KAN* strain did not have higher viability later in starvation (Fonville, *et al.,* 2010; Kuong & Kuzminov, 2010). There are some possibilities as to why, for instance strain background (some strains have a higher number of persister cells which never enter exponential growth with active replication, and can thus escape the effects of thymine starvation), and medium used (other groups described used a medium richer in casamino acids. My work described in the Appendix shows that casamino acids affect viable replication fork number beyond growth rate, which may indicate why viability is so much lower in casamino-acid supplemented experiments versus non-supplemented experiments). I am also interested in knowing the relationship between viable replication forks and presence and absence of RecA protein, however previous studies with *recA*$^-$ mutants of *E. coli* showed that chromosomal degradation occurs in the absence of the RecA protein as measured by replication run-out (Skarstad & Boye, 1988, 1993; Zahradka, *el.*, 2009), and since I am also using this technique, measuring replication run-out in *thyA*$^-$*recA*$^-$ cells would be difficult to interpret as it is difficult to differentiate between thymine-starvation-dependent nucleic acid changes due to *recA*$^-$, and *recA*$^-$dependent changes independent of nucleotide starvation.

In *thyA*$^{+}$ cells, RecF protein appears to play a role in replication fork maintenance as *recF*$^{-}$ (CL579) cells cultured in exponential growth have fewer viable replication forks per cell while maintaining virtually identical amounts of chromosomes (Figure 5.5) as compared to *recF*$^{+}$ (CL001) cells. This may indicate that these cells have the capability to initiate rounds of replication resulting in the same number of viable replication forks as wild-type cells but under some conditions, these replication forks fail. Because both RecF+ and RecF- cells maintain approximately the same number of chromosomes in exponential growth (based on nucleic acid content Figure 5.4), cells where viable forks are lost may have the event occur at particularly vulnerable parts of the genome, like the origin of replication. Replication near the origin of replication requires transcription according to studies which have shown irrespective of the genes proximal to the origin of replication, transcription must take place near the origin for replication to progress beyond the point of initiation (reviewed in Katayama, *et al.*, 2010; Sclafani & Holzen, 2007). Replication run-out treatment inhibits transcription meaning that any replication fork collapse near the origin would be unable to be restarted without initiation. If RecF is needed to maintain the DNA structure at troubled replication forks, it is possible that RecF is necessary for resumption of troubled forks near the origin of replication. This activity would complement the hypothetical role of RecF in replication fork maintenance and protection of nascent DNA at replication forks in *E. coli* (Chow & Courcelle, 2004).

In *thyA*$^{-}$ cells, even with adequate thymine, the *thyA*$^{-}$*recF*$^{-}$ strain has a higher portion of its population with *more* replication forks per cell even while maintaining the same amount of nucleic acid content (Figure 5.5A, exponential growth and 0 minutes starvation). Whereas the population of run-out *thyA*$^{-}$ (RecF^{+}) cells appear to continually shift to the right over starvation, *thyA*$^{-}$ *recF*$^{-}$ cells continue to maintain a population of cells within the original 1n (n=chromosome number) until late into starvation (approximately 120 minutes) which coincides with the time point at which this particular background of *E. coli* shifts from lag loss of viability to rapid loss of viability in thymine starvation. The observation that DNA content without run-out remains unchanged up until approximately 120 minutes in both RecF^{-} and RecF^{+} cells seems to indicate that in spite of the additional viable replication forks appearing, replication is stalled and no new nucleotides can be successfully incorporated into the chromosome. Interestingly, Figure 5.5B

shows that it is at that exact time that the cells have a large jump in size indicating filamentation, a hallmark of the SOS DNA damage response. In *thyA*$^{-}$*recF*$^{-}$ cells, however, the total nucleic acid content dramatically diminishes between 120 and 180minutes as compared to *thyA*$^{-}$ cells which may indicate more DNA degradation, although perhaps not all in one place when looking at CGH arrays.

Some catastrophic event which occurs between the 120-180 minute time point in both RecF^{-} and RecF^{+} cells (As *thyA*- cells also show a large jump in size right before the exponential loss of viability phase occurring after 120 minutes starvation) may likely prime the cell for the massive degradation observed in DNA CGH arrays (Kuong & Kuzminov, 2012; Sangurdekar et al., 2010).

One way to explain the contradictory observations that *recF*$^{-}$ cells have higher viability than *recF*$^{+}$ cells in spite of seeing more DNA degradation in replication run-out but not in CGH array analysis is that these starved *recF*$^{-}$ cells are degrading DNA from collapsed forks while simultaneously initiating new rounds of replication. Those new forks may progress further due to nucleotides from degraded DNA being recycled to provide substrate for newly loaded and still viable replication complexes, and also the idea that the fewer the number of viable replication forks, the fewer locations for incorporation of nucleotides allowing further progression of the forks that remain. Nevertheless, based on the same CGH data (Figure 5.2A), both *recF*- and *recF+* cells experience a massive loss of DNA hybridized around the origin of replication therefore the event which primes these cells for such degradation is occurring in both backgrounds. Without viable RecF protein protecting the nascent DNA at stalled replication forks, *recF*$^{-}$ cells may at least be able to recycle some nucleotide which can be used to make viable template for rescue efforts in the cell.

5.3.1. Allowing for initiation of replication in thymine-starved *E. coli* cells increases the rate of killing, and filamentation.

Based on viability assays and size measurements from flow cytometry data (Figures 5.7 and 5.8B), CL001-*seqA::KAN* cells lose viability and experience a large jump in size more quickly than do CL001 cells in the same media and culture conditions. This on its own seems to indicate that

more frequent replication initiation accelerates the events which result in killing of thymine-starved cells. One explanation would be that replication initiation is a key factor in loss of viability in thymine starvation, and increasing replication initiation increases killing (Martín & Guzmán, 2011). Another explanation may be that the presence of more replication forks provides more sites for thymine incorporation which exhausts the levels of dTTP in the cell faster.

Late in starvation, there appears to be a tight peak representing a single chromosome upon replication run-out in these *seqA::*KAN cells at 120 minutes starvation and 180 minutes in $SeqA^+$ cells. The appearance of this peak also coincides with a drop in the value of fluorescence representing DNA content. I interpret it to mean one of two possibilities: One possibility is that before the effects of replication run-out drugs take effect these cells can initiate one round of replication, and in the presence of adequate thymine run those replication forks to completion. Such an initiation event is much more likely in *seqA::KAN* cells which cannot regulate their replication initiation efficiently. However this peak manifests in $SeqA^+$ cells later in starvation. If lack of regulation of replication initiation was the only reason for this peak, then I would expect to see it in other time points of thymine starvation in *seqA::KAN* cells.

Another possibility is that a DNA degradation event occurs, releasing nucleotide which can be recycled and incorporated at a new viable initiation event. The same time that this single-chromosome peak appears there appears to have been been a loss of total nucleic acid content in the cells. This seems to indicate that even late in thymine starvation cells retain the ability to initiate replication, and in the presence of adequate thymine run to completion. This means that without adequate thymine, the replication forks in these cells become stalled or involved in some process which makes incorporation of new nucleotide impossible after some point.

Figure 5.1. Local genomic map of *recF* gene

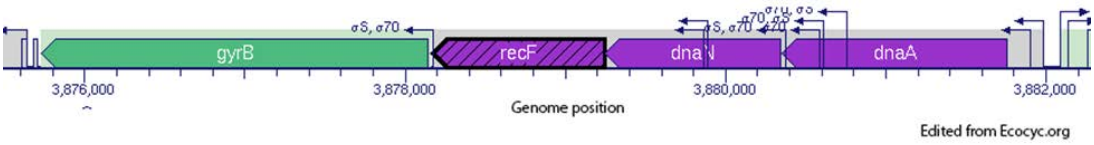

Figure 5.2. A.) Comparative genomic hybridizations of the following strains after 3 hours of thymine starvation: CL001 (W3110 *thyA*$^-$), CL579 (W3110*thyA*$^-$*recF*$^-$), CL579 with pBRBB vector (dsRed insert), CL579 with pBRBB vector (*recF* insert). The y-axis is the ratio of experimental sample gene copy number to reference (stationary phase sample). The x-axis represents gene position (OriC-centered). B.) Complementation assays show that CL579 cells (*thyA*$^-$*recF*$^-$) complemented with *recF* on a plasmid suffer a similar loss of viability as CL001 (*thyA*$^-$recF$^+$) cells. C.) Complementation assays show that CL579 cells (*thyA*$^-$*recF*$^-$) complemented with *recF* on a plasmid can rescue viability after 20 seconds of UV irradiation in a sterile hood.

A.

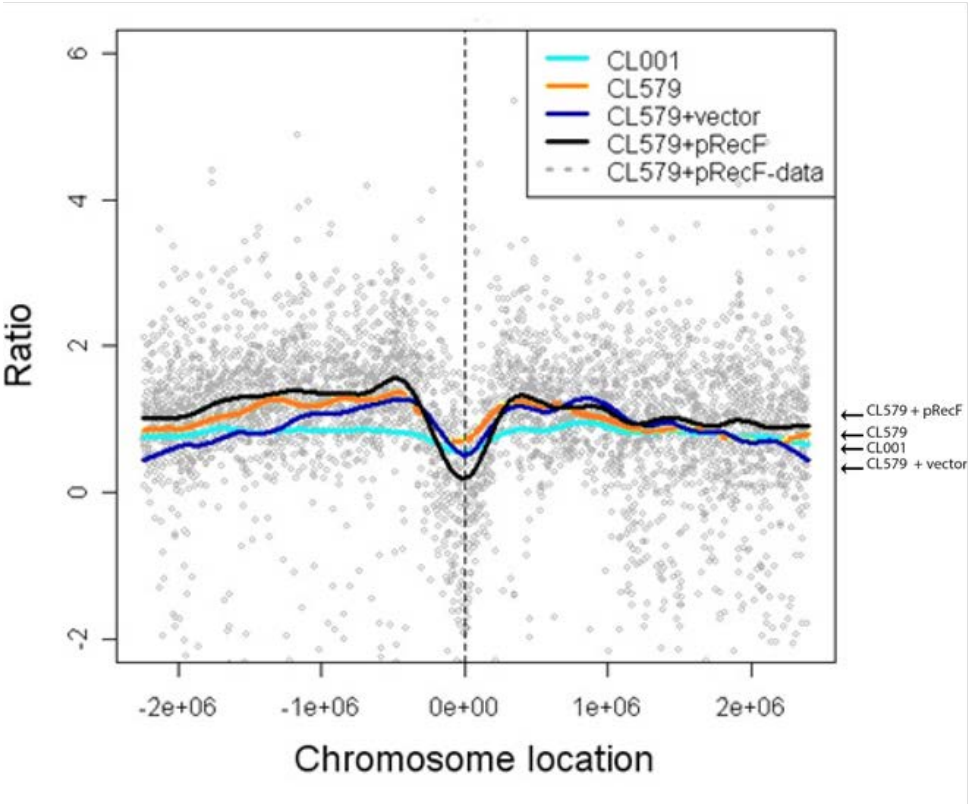

B.

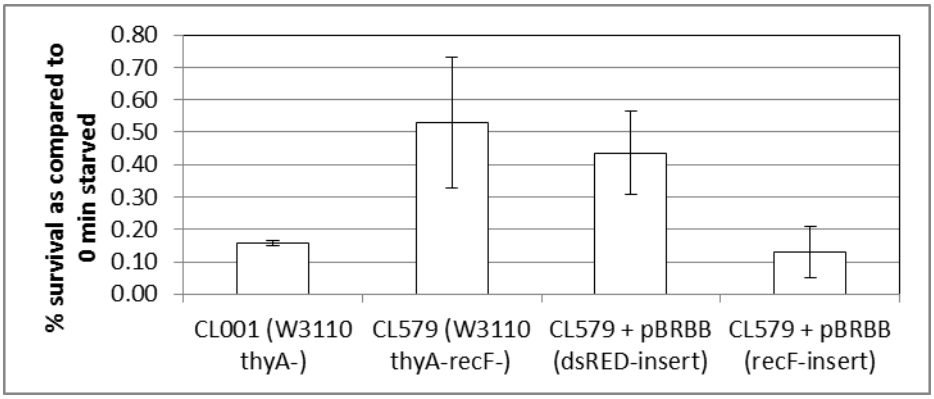

C.

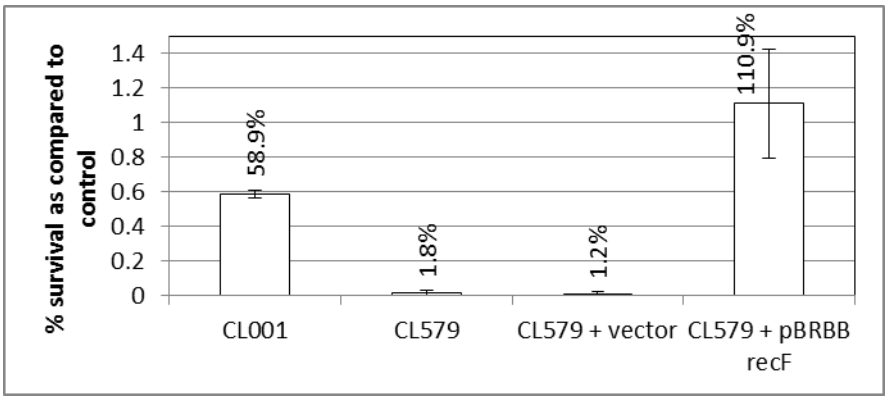

Figure 5.3 Viability of various *thyA*⁻ strains over time in thymine starvation: CL001 (W3110*thyA*⁻), CL579 (W3110*thyA*⁻*recF*⁻), and CL001-recA (W3110*thyA*⁻*recA::KAN*)

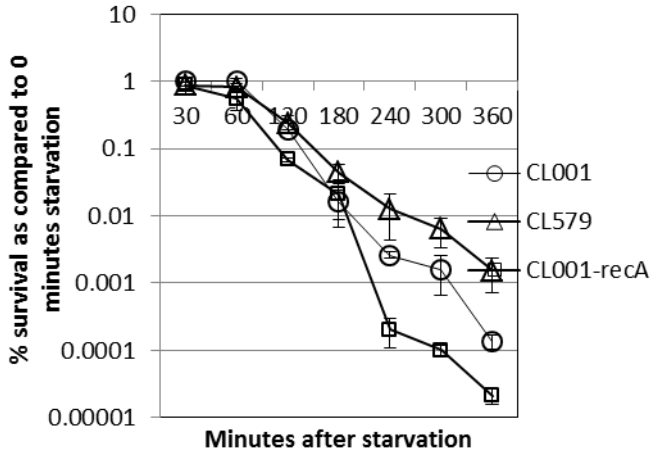

Figure 5.4. Replication run-out of *thyA*$^{+}$ strains with and without a *recF::KAN* gene replacement for cells in exponential growth in M9 media. Wild-type cells with a *recF::KAN* allele have fewer viable replication forks per cell than *recF*$^{+}$ cells in spite of retaining approximately the same amount of DNA content. Numbers above vertical lines represent the chromosomal equivalent within the population for that peak (n=1 chromosome). A chromosome from replication run-out represents 1 pair of viable replication forks. A chromosome without run-out represents the DNA present upon start of replication run-out.

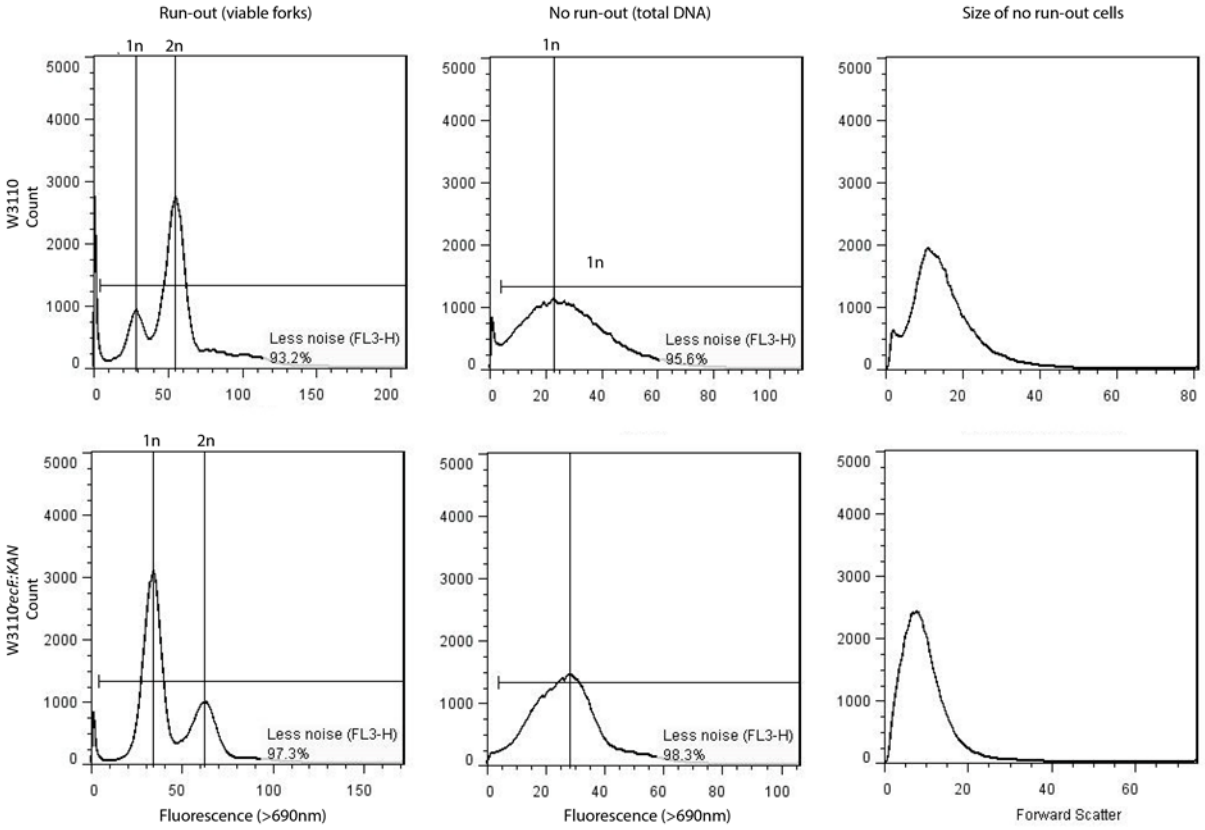

Figure 5.5. A Replication run-out of *thyA*$^{-}$ strains with and without a functioning *recF* allele show that *recF*$^{-}$ cells are unable to maintain the same number of viable replication forks as *recF*$^{+}$ cells. Replication run-out of *thyA*$^{+}$ strains with and without a *recF::KAN* gene replacement for cells starved of thymine in exponential growth in M9 media. Minutes represent time into starvation. Numbers above vertical lines represent the chromosomal equivalent within the population for that peak (1n = 1 chromosome). A chromosome from replication run-out represents 1 pair of viable replication forks. A chromosome without run-out represents the DNA present upon start of replication run-out. In **B.** the forward scatter (size) is shown across time for each strain compared against itself.

A.

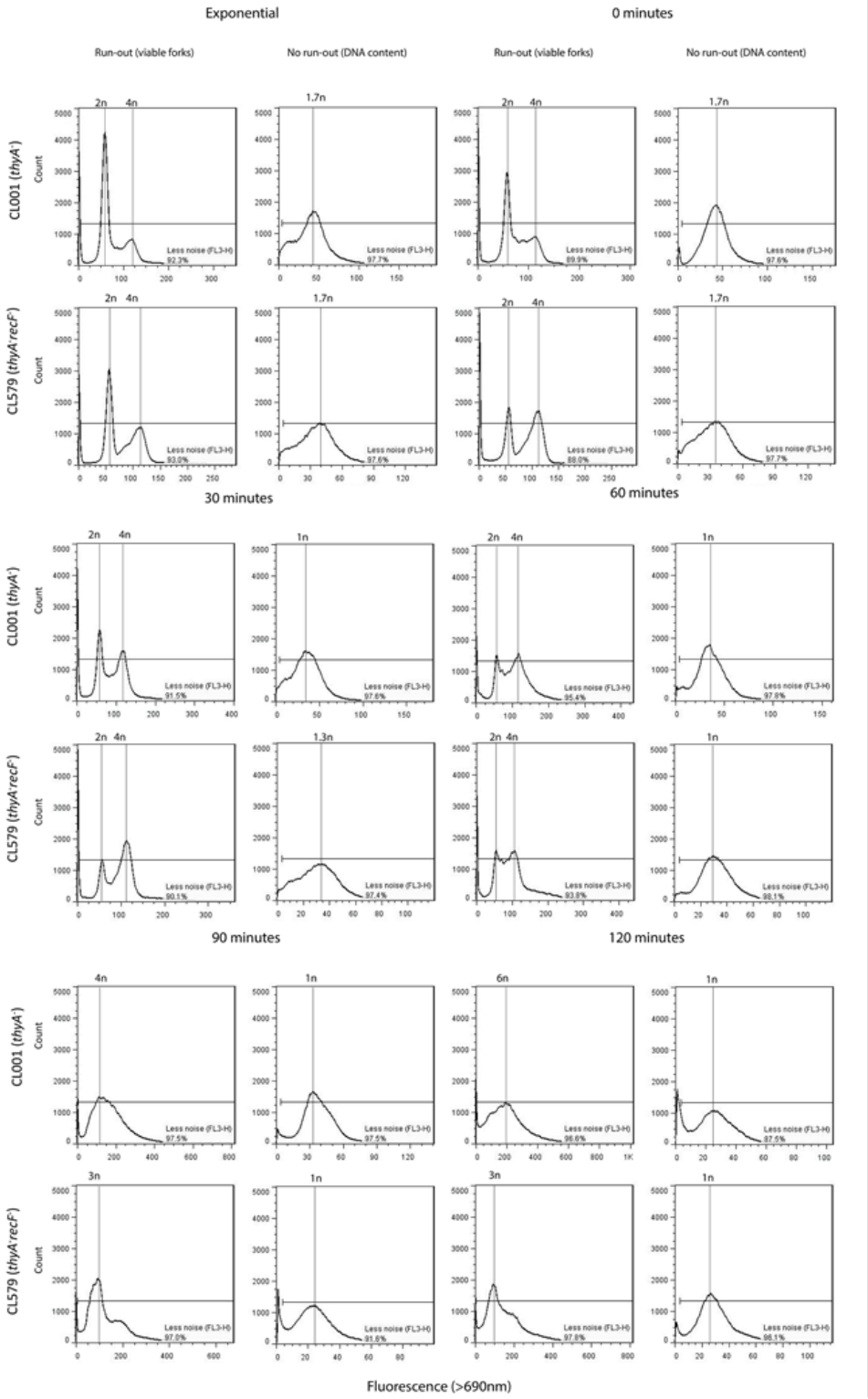
Exponential
0 minutes
Run-out (viable forks)
No run-out (DNA content)
Run-out (viable forks)
No run-out (DNA content)
CL001 (thyA-)
CL579 (thyA-recF-)
Count
30 minutes
60 minutes
90 minutes
120 minutes
Fluorescence (>690nm)

B.

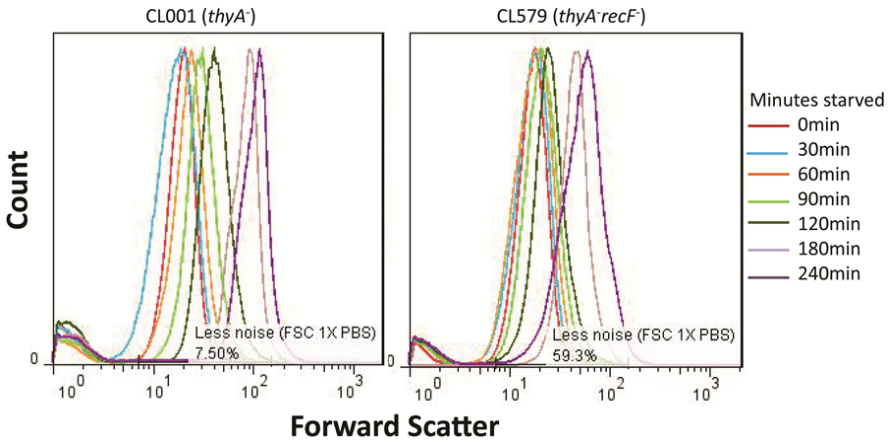

Figure 5.6. Loss of viability of CL001 and CL001 *seqA*::KAN strains as compared to beginning of starvation where percent survival is calculated by the number of colony-forming-units (CFUs) at a certain time point in starvation as compared to the number of CFUs measured at the beginning of starvation. Error bars represent standard error of the mean.

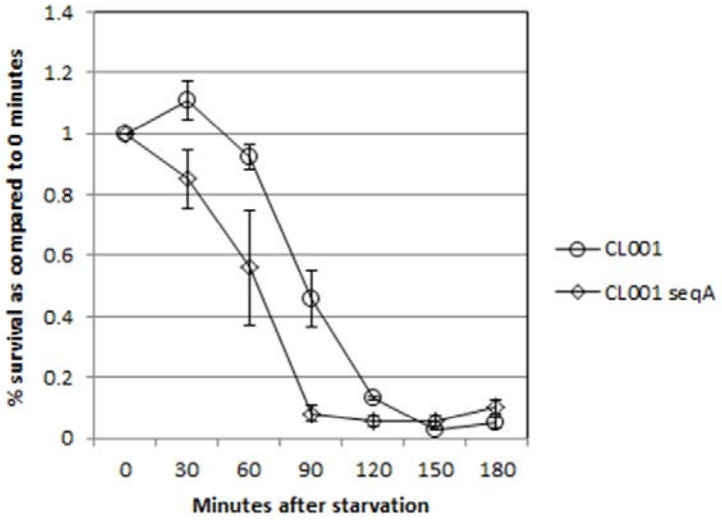

Figure 5.7. Replication run-out of *thyA*$^+$ strains with and without a *seqA::KAN* gene replacement for cells starved of thymine in exponential growth in M9 media. The events occurring in *seqA::*KAN cells appear to be similar to events occurring in *seqA*$^+$ strain only at an accelerated rate. Minutes represent time into starvation. Numbers above vertical lines represent the chromosomal equivalent within the population for that peak (1n = 1 chromosome). A chromosome from replication run-out represents 1 pair of viable replication forks. A chromosome without run-out represents the DNA present upon start of replication run-out. In **B.** the forward scatter (size) is shown across time for each strain compared against itself.

A.

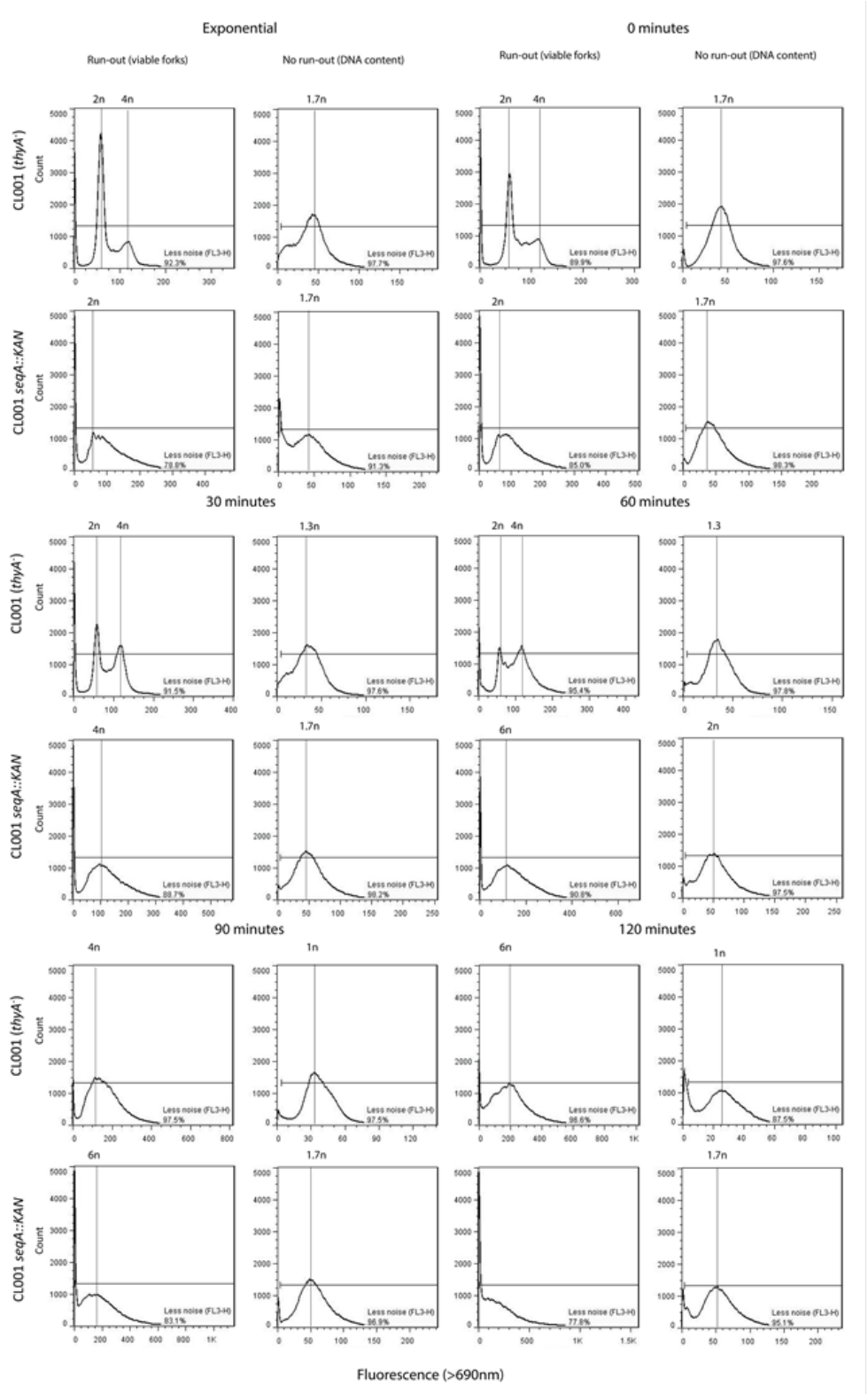
Exponential
0 minutes
Run-out (viable forks)
No run-out (DNA content)
Run-out (viable forks)
No run-out (DNA content)
CL001 (thyA-)
CL001 seqA::KAN
Count
2n
4n
1.7n
30 minutes
60 minutes
1.3n
1.3
6n
90 minutes
120 minutes
1n
Less noise (FL3-H)
92.3%
97.7%
89.9%
97.6%
79.8%
91.3%
85.0%
90.3%
91.5%
97.6%
95.4%
97.8%
89.7%
90.2%
90.8%
97.5%
97.5%
97.5%
96.6%
87.5%
83.1%
96.9%
77.8%
95.1%
Fluorescence (>690nm)

C.

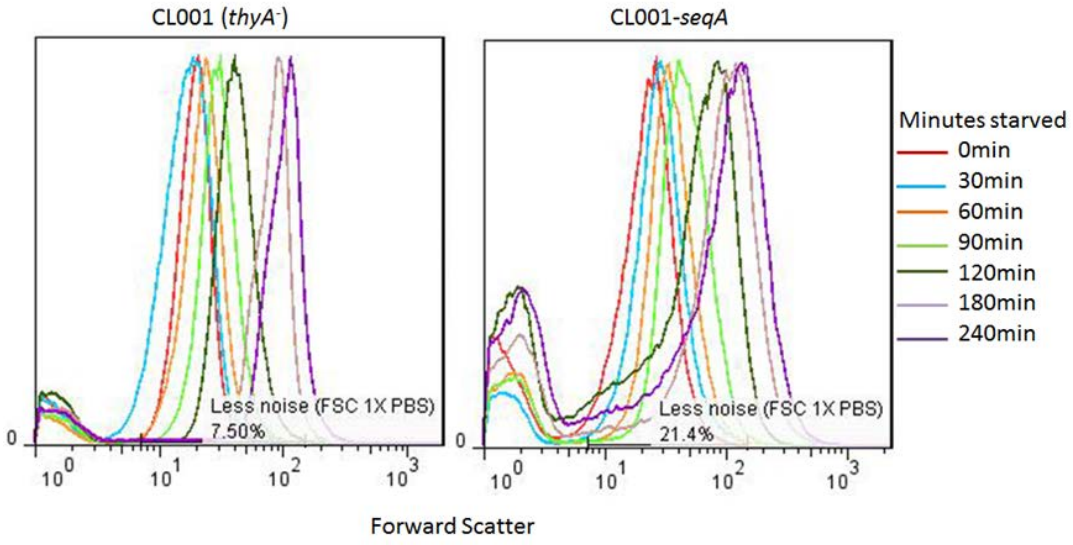
CL001 (thyA-)
CL001-seqA
Minutes starved
0min
30min
60min
90min
120min
180min
240min
Less noise (FSC 1X PBS)
7.50%
Less noise (FSC 1X PBS)
21.4%
0
0
Forward Scatter

Chapter 6: Summary of Results and Discussion

The work showing that viability in thymine-starved *E. coli* is directly proportional to a massive loss of DNA around the origin of replication was an important breakthrough in what had become a puzzling, and stagnant field. This observation naturally led to the next most obvious question: what causes the massive loss? In performing the experiments described in the previous chapters of this thesis, I wanted to answer this question, and in doing so discovered many new and perplexing characteristics of thymine starvation.

I utilized a variety of background strains, experimental conditions and drug treatments to find a system that would best illustrate the events leading to the DNA loss. While results were consistent within an experimental set-up, I was often perplexed as to why I saw a set of results that fell outside the outcomes I thought possible. For instance, in the case of synchronizing replication initiation in temperature-sensitive thymine-requiring mutants of *E. coli* I expected to see a variation in the 'dip' or DNA degradation around the origin. I expected to see a narrowing of the dip in synchronized cells if replication fork proximity set the boundaries of the degradation, or I expected a deepening of the dip if replication initiation was the key factor (since simultaneous mass initiation events should lead to more damage). The last thing I expected was to see little to no change regardless of synchronization status yet continued loss of viability. Many experimental set-ups I attempted resulted in such convoluted results, and it seemed that no matter what experimental set-up I tried, the results couldn't be fit into any sort of consistent model. The more I learned about thymineless death the more I realized it had an intrinsic link to several vital processes in the cell. I worried that this meant there would be too many unknowns beyond my control, or obstacles to overcome in interpreting my results. Nevertheless, I trusted that if the data is consistent, it must have a valid explanation; the difficulty lay in trying to find the common link between all of these perplexing observations.

Here I reiterate conclusions from the experiments described earlier in this thesis, directly compare them to illustrate how they fit into an overall model.

6.1. Summary of conclusions from analyzing and comparing results from chapters 3, 4, and 5.

6.1.1. Results showing the role of replication restart and replication initiation in thymineless death

6.1.1.1. There are futile initiation events which do not result in complete replication of the chromosome

Comparative genomic hybridizations of *thyA*$^{-}$*dnaC*^{ts} mutants show that gene copy number increases by 20 minutes return to permissive temperature (at which point cells are starved)(Figure 6.1A), however the majority of replication run-out of cells (most populous peak in run-out) under the same condition do not have variation in the number of viable replication forks between 0 minutes and 20 minutes return to permissive temperature (0 minutes starvation) (Figure 6.1B). This implies that not every initiation event results in viable replication forks capable of completing replication.

6.1.1.2. There are productive initiation events later in thymine starvation (60-120 minutes)

In all strains studied, replication run-out shows additional initiation events which result in viable replication forks (contingent on return of thymine to media during replication run-out) as far along as 120 minutes into starvation (Figure 6.2). This is interesting as other studies have shown that replication slows to as much as 10% of original synthesis rate as compared to growth with adequate thymine(Kuong & Kuzminov, 2012). This implies that the nucleotide concentration requirement for initiation is different from replication elongation. It also implies that provided adequate thymine, these replication forks will progress to completion, indicating that as late as 120 minutes starvation, the catastrophic events which seem to target new replication forks have not yet occurred.

6.1.1.3. Replication initiation becomes uncoupled from normal cell processes early in thymine starvation

Strains of *E. coli* which cannot initiate replication in heat-shock (either *dnaC*^{ts} or *dnaA*^{ts} backgrounds) have additional initiation events during starvation in heat-shock as compared to when grown with adequate thymine (Figure 6.3). These events must occur early in starvation when there is still enough viable DnaC or DnaA to allow for the events to occur. Such an initiation event likely occurs outside of the natural cycle of *E. coli* cells in heatshock. The continual increase in viable replication forks while total DNA content remains the same in replication run-out also indicates that replication initiation is uncoupled from replication elongation (Figure 6.2).

6.1.1.4. Replication initiation is required for DNA degradation at the origin of replication

Starving Δ*thyAdnaA*^{ts} cells results in degradation at the origin of replication when such cells are allowed to return to permissive temperature as opposed to remaining in heat-shock (Figure 6.4). In either scenario, cells continue to lose viability indicating that the killing lesion is not isolated at the origin of replication.

6.1.1.5. Origin proximal degradation includes nascent and parental DNA

In *thyA*$^{-}$*dnaC*^{ts} cells starved for thymine in heat-shock, gene copy number increases by 20 minutes return to permissive temperature as compared to 0 minutes return to permissive temperature (cells were harvested at the point of temperature shift), but that gene copy number drops below the value seen at 0 minutes when cells have been starved for 180 minutes. This indicates that the parental DNA present at 0 minutes starvation has also been degraded by 180 minutes along with the nascent DNA synthesized at 20 minutes permissive temperature (Figure 6.5). Since it is known that degradation happens elsewhere in the genome during thymine starvation (Kuong & Kuzminov, 2012; Sangurdekar et al., 2010), but that it does not result in duplex disintegration, and also the observation that DNA degradation can occur from origins of different sequence composition (chapter 4 of this thesis) it seems likely that either

replication forks proximal to the origin or the DNA synthesized from those forks proximal to the origin are somehow unique.

6.1.1.6. Replication restart likely plays a role in the killing lesion during thymine starvation

The two conditional mutants defective in replication initiation in this study function in different ways. Cells with a *dnaA*^{ts} mutation cannot initiate replication from the *oriC* during heat-shock, but cells with the *dnaC*^{ts} mutation cannot initiate replication from the *oriC* or from any other location (such as collapsed forks in the case of replication restart). There is a variation in viability of these mutants depending on whether they are starved in heat-shock, or at permissive temperature (Figure 6.6). Cells capable of replication restart but not initiation from the origin of replication (*dnaA*^{ts} mutants*)* lose viability during thymine starvation to a greater extent than do cells which cannot start replication from any location (*dnaC*^{ts} mutants) during heat-shock. Meanwhile, those cells which can pre-prime the origin of replication with DnaA complexes and thus have more initiation events upon return to permissive temperature in starvation (*dnaC*^{ts} mutants), show higher loss of viability during starvation at permissive temperature. This implies that the ability to undergo replication restart sensitizes cells to thymine starvation, and the more replication forks present during thymine starvation, the more quickly cells lose viability. More replication forks mean having more locations to incorporate dTTP, which in turn will accelerate thymine depletion.

6.1.1.7. DNA is partially single-stranded in character late in thymine starvation.

Replication run-out of *dnaA*^{ts} cells heat-shocked and starved for 90 minutes shows cells which have what seems like 80% of a chromosome worth of deoxyribonucleic acid (Figure 6.7). In spite of the initial DNA content, these cells complete 1-2 chromosomes worth of DNA synthesis in replication run-out indicating at least 1 pair of viable replication forks were present at the beginning of replication run-out. Cells must have a complete template for a complete chromosome to be replicated. A cell can contain less than a full chromosome, and yet have a complete template for replication run-out if part of the chromosome is single-stranded in nature. Cells with a *dnaC*^{ts} mutation do not appear to have this same phenotype. This may

indicate that DnaC-dependent replication restart during thymineless death results in single-stranded DNA.

6.1.2. Role of RecF protein in thymineless death

Another point of interest in studying thymineless death is the role of RecF protein during thymineless death and why *recF*$^-$ cells remain viable longer into thymine starvation than their *recF*$^+$ counterparts.

6.1.2.1. RecF may play a role in the viability of replication forks proximal to the origin of replication

Figure 6.3 shows that in W3110 RecF$^+$ cells new initiation events (which, in the presence of sufficient thymine, produce viable replication forks) occur well into thymine starvation. However, W3110 *thyA*$^-$*recF*$^-$ cells appear to lose viable replication forks over time in thymine starvation (Figure 6.8A-B). When MG1655 temperature-sensitive cells are synchronized for replication in heat-shock, returned to permissive temperature, and begin replication from a single chromosome (as in *dnaA*^{ts} mutants), regardless of the presence of a *recF* allele, cells have a dramatic increase in viable replication forks during starvation (Figure 6.8C-D). This brings forth another puzzling problem. With this experimental set-up, it cannot be determined whether wild-type cells actually initiate replication as often as *dnaA*^{ts} cells but fail to maintain those resulting replication forks, or whether wild-type cells simply initiate replication less often than *dnaA*^{ts} cells due to some deficiency in the mutant DnaA protein. Nevertheless, the irregular number of chromosomes in Δ*thyArecF::KANdnaA*^{ts} cells as compared to *recF*$^+$ cells suggests that RecF has a role in either maintenance of replication forks near the origin of replication or in replication initiation itself.

Previous studies have shown that RecF plays a role in protecting nascent DNA at UV lesions, and may be involved in replication restart (Chow & Courcelle, 2004; Courcelle et al., 1999). Since RecF has been implicated in replication restart, and cells with compromised replication restart ability have higher viability (Figure 6.6), along with the observation that RecF$^-$ cells often

contain odd numbers of chromosomes during starvation (Figure 6.8) it is possible that the exacerbating role of RecF in thymine starvation is the facilitation of replication restart at fragile replication forks. This role is most significant when multiple chromosomal arms and or replication forks are present at the start of starvation also indicating that recombination likely plays a role.

6.2. Discussion and Future Directions

6.2.1. Discussion

Several conclusions can be drawn from the experiments described in the chapters of this thesis, which suggest that during thymineless death, catastrophic events occur at replication forks in actively growing cells which result in eventual degradation of DNA at those regions. In particular, replication forks newly formed during thymine starvation eventually result in loss of duplex DNA around the origin of replication suggesting that either the DNA that is synthesized at these forks, or the structure of the forks themselves is compromised in some way. The presence of incomplete chromosomes in replication initiation-deficient cells indicates that degradation may occur in other parts of the chromosome but only in a single-stranded fashion. The role of RecF appears to be in the maintenance of new replication forks. More replication forks mean more locations for incorporation of thymine and a faster depletion of thymine reserves. Using up thymine at many replication forks means there is less likelihood that a one replication fork will have enough substrate to complete replication around the chromosome. This by itself may be enough to explain the difference in rate of loss of viability between *recF*$^-$ and *recF*$^+$ cells.

These conclusions correlate with what has been observed in scientific literature concerning thymineless death, replication restart, and the role of RecF protein in the cell. The discovery of massive DNA degradation symmetric to the origin of replication correlating directly with loss of viability in thymine-starved cells explained a number of phenotypes. For instance, it explained the immunity of origin-proximal DNA to endonucleases (Nakayama et al., 1994) and the seeming immunity of DNA from starved cells to methylases (Freifelder, 1967). It also explained the loss of high-molecular-weight DNA from thymine starved cells (McFall & Magasanik, 1962), and

easily explained the induction of the SOS DNA damage response in bacteria. The loss of DNA around the origin made it clear that either replication initiation or replication fork-related events are involved with the loss of viability in thymine-starved cells, and my work described in this thesis as well as by others supports this idea. My work shown in chapter 5 with *thyA⁻seqA⁻ E. coli* cells shows that deregulating replication initiation led to an increased loss of viability during thymine starvation. This indicates that either the replication initiation event itself is lethal, or the increase in the possible locations for dTTP incorporation accelerates the depletion of thymine and therefore the onset of the detrimental effects of thymineless death. My work as well as others show that replication initiation occurs well into thymine starvation (Martín & Guzmán, 2011), and does not stop until the point where origin-proximal degradation takes place. In spite of this, replication elongation does not proceed to any real extent either due to slowed nucleotide incorporation as suggested by Kuong, *et al* (2012) where radiolabeled nucleotide incorporation slowed to 10% of wild-type rate, or due to stalled replication forks as is indicated by my *dnaC^{ts}* replication run-out and comparative genomic hybridization data. This indicates that the thymine requirement for replication initiation differs from the requirement for replication elongation. This might explain why some initiation events resulting in some increase in gene copy number in *dnaC^{ts}* cells do not run out complete chromosomes in replication run-out. The observation by Kuong, *et al.* that degradation of nascent DNA occurs in thymine-starved cells corroborates the observation made in chapter 4 of this thesis that there is extensive single-stranded character to the chromosome in late starvation, and may help explain what appears to be less than a full chromosome in thymine-starved, replication-restart proficient, but replication initation-deficient *dnaA^{ts}* cells. The loss of viability in cells with no DNA degradation at the origin of replication during thymine starvation indicates that some killing likely results from catastrophic events at previously established replication forks. Understanding the difference between replication forks resulting from 'new' initiation events and 'older' forks established before thymine starvation, as well as the condition of the DNA synthesized by each may illuminate the events that result in killing.

This loss of genetic material had a direct correlation with viability in *thyA⁻,* and in known suppressor double-mutants such as *thyA⁻recF⁻, thyA-recO⁻, thyA⁻recJ⁻* and *thyA⁻recQ⁻*. However, Kuong *et. al.* discovered that *recA* mutants not only lack this characteristic degradation but they

and others found that *thyA*$^{-}$*recA*$^{-}$ cells are more susceptible to thymine-starvation during the early phase of TLD and show a reduced rate of killing during exponential killing (Fonville, *et al.*, 2010; Kuong & Kuzminov, 2012). The difference between their results and mine shown in this thesis (Chapter 5) is that there may exist other processes in the cell that can affect *recA*$^{-}$ related outcomes. One possibility is that decrease in the rate of killing in *recA*$^{-}$ could be due to so-called reckless degradation of DNA (Clark, *et al.,* 1966; Skarstad & Boye, 1988, 1993) and the supply of dTTP in such mutants may never be sufficiently exhausted to prevent the cells from successfully preserving the integrity of at least one chromosome before thymine is made available again. Moreover, it has been shown that the rate of TLD depends on availability of dTTP, with the rate increasing dramatically when cells are starved when being grown in progressively lower concentrations of thymine (Beacham, *et al.*, 1971; Ohkawa, 1975). Another possibility is that RecA may be involved in damage accumulation in the cells over the starvation time and without RecA DNA somehow would not be damaged as much. RecA does not generate reactive recombinational intermediates on its own, it requires loaders or licensing factors: RecFOR on single strand gaps, presumably behind the fork, RecBC on double strand breaks, and possibly DnaQ at stalled forks (Pohlhaus, *et al.*, 2008). If these RecA^{-}formations proceed in the absence of adequate dTTP, rather than engaging in DNA repair, these structures may instead become substrates for nucleolytic degradation. Therefore, in the absence of RecA such degradation will be diminished and removal of individual licensing factors will have only fractional effect on the degradation, as was observed in *recBC*$^{-}$ and *recF*$^{-}$ single mutants.

All of these characteristics make the circumstances surrounding thymine starvation difficult to interpret. Thymineless death has been notable in that the DNA damage occurring during thymine starvation appears to localize near active 'growing points' or replication forks in the form of chromosomal fragments (Ayusawa et al., 1983), and around the origin of replication in the form of massive degradation of DNA (Kuong & Kuzminov, 2012; Sangurdekar et al., 2010). This fits well with the observation that cells in stationary phase or between rounds of replication are immune to thymine starvation (Barner & Cohen, 1957; Cummings & Kusy, 1970; Hanawalt, 1963). Since the RecFOR pathway is required in post-replication repair (Cox, 2001; a Kuzminov, 1999), and has been implicated in replication fork reversal, and restart (Courcelle & Hanawalt, 2003; Handa, *et al.*, 2009; Morimatsu, *et al.*, 2012), as well as the observation that chromosomal

fragmentation occurs near the 'growing points' or active replication forks in thymine starvation (Ayusawa et al., 1983; Kuong & Kuzminov, 2010), it is probable that the lethal action of RecF occurs at active replication forks during thymineless death. My work shown in chapters 4 and 5 of this thesis also imply that RecF has a detrimental effect at new replication forks from initiations occurring during thymine-less death.

My work shown in chapters 4 and 5 of thesis shows that replication restart is probably occurring in thymine-starved cells. The process of replication restart stems from a need for DnaC helicase loader to re-load the DnaB helicase in *E. coli*. The *in vivo* work of Rudolph, *et al.* and the *in vitro* work of McInerney & O'Donnell show that bypass of lesions in DNA synthesis requires DnaC protein, which is a DnaB helicase loader (McInerney & O'Donnell, 2007; Rudolph, et al, 2007). McInerney and O'Donnell showed that helicase unwinding continued regardless of lesions in either the leading or lagging strand template, and the two replication complexes uncoupled when one was blocked resulting in the DnaB helicase (PCNA in eukaryotes) falling off of the strand (McInerney & O'Donnell, 2007). It is thought that replication forks bypass very few lesions, and often stall at the first one. The stretch of single-stranded DNA produced before the uncoupling ranges from 500-4000 base pairs on a plasmid substrate, such single-stranded DNA would likely be a substrate for RecA recombination protein. The *in vitro* work by McInerney & O'Donnell (as well as others) indicates that RecA (along with at least RecFO) is necessary for the removal of the replication complex and processing the DNA into a D-loop structure which can then be used as a loading substrate for replication restart. In the course of uncoupling of the polymerases from one another (caused by the continuation of the lagging strand polymerase while the leading strand polymerase is blocked at least 4 kilo-bases), the DnaB helicase dissociates and must be reloaded by DnaC. Since all recombinational-repair resulting in stretches of single-stranded DNA requires replication to occur, and requires adequate substrate to do so, the lack of dTTP may render this activity unstable, and susceptible to degradation when the process collapses.

Other groups have suggested that upon encountering a lesion, replication polymerases can essentially 'slip past' the lesion. Replication restart is avoided and in the process a stretch of single-stranded DNA is left, and must be subjected to daughter-strand gap repair (Heller &

Marians, 2006; Hoffmann et al., 1996; Lopes, *et al.*, 2006). This process involves the leading strand polymerase stalling allowing for a stretch of DNA to be unwound at the helicase which is subjected to a lagging-strand type of primase-dependent RNA priming allowing the replication complex to bind to the newly primed location (Figure 6.9). This results in a stretch of single-stranded DNA to fall behind. The recent discovery that three polymerases are most likely associated together at the replication fork (Georgescu, *et al.*, 2012; Reyes-Lamothe, *et al.*, 2010) could explain the tolerance of *E. coli* replication complexes for bypassing lesions in such a manner. Both of these processes would result in substrates for RecF protein which has been seen to interact with double-strand/single-strand junctions in DNA *in vitro*.

6.2.2. Model

If replication forks undergo restart during thymineless death, either due to a replication fork stall due to lack of substrate, or due to uncoupling of helicases caused by replication 'slippage,' this would explain why certain mutations of thymine-requiring strains are more resistant or more sensitive to thymine starvation depending on their role in replication restart.

RecA is thought to be necessary for all replication restart. Multiple sister chromosome arms are necessary for RecA-associated recombination and RecA appears to be necessary for DNA degradation to occur (Kuong & Kuzminov, 2012), however the DNA degradation does not appear to be a direct cause of death as is apparent by viability measurements of *thyA⁻recF⁻, thyA,⁻* and *thyA⁻recA⁻* double-mutant studies (Fonville et al., 2010; Fonville, et al, 2011; Kuong & Kuzminov, 2010; Sangurdekar et al., 2010). Also, many active replication forks at the start of thymine starvation result in increased loss of viability, although this may be due to cells running through their supply of thymine faster than would occur should fewer replication forks exist at the time of starvation.

Aside from replication initiation temperature-sensitive mutants, *recF⁻* is the *E. coli* mutant which most rescues the effects of thymineless death, and RecF may be involved in 'poisoning' of replication forks (Figure 6.10). While DNA degradation seems to be an important element of survival during thymine starvation, any new thymine released from possible degradation events

gets incorporated at the origin of replication; not at pre-existing, and most likely stalled forks (the gene-copy ratio of thymine starved cells remained unchanged during starvation of *thyA*$^-$ *recA*$^-$ cells except at the OriC [Kuong & Kuzminov, 2012]). It is likely that the role of RecA and RecBC is to degrade DNA at the site of replication fork collapse to allow for recycling of nucleotide substrate which can then be made available at other viable replication fork sites.

RecF has never been implicated in the loss of parental DNA, and further work investigating the binding partners of RecF protein at this critical time point in thymine starvation may illuminate the role of RecF in normal replication and growth.

My replication run-out, viability, and microarray data examined in this thesis indicate that replication initiation occurs after withdrawal of thymine, and even later than that recorded in recent studies looking at cells starved for only 10 minutes (Martín & Guzmán, 2011) (Figures 5.5 & 5.7). Similarly, my results indicate that the more replication forks that are present during starvation, the greater the loss of viability (Figure 6.11A). Nucleic acid content does not increase markedly while the number of viable replication forks increases over time in thymine starved cells (Figure 6.11B). This indicates that replication initiation and replication elongation are uncoupled. Interestingly, although these forks are stalled, they appear to remain viable and can resume replication pending return of adequate thymine until at least two hours of starvation (peaks in replication run-out remain tight and distinct until after 2 hours starvation). This time point coincides with a large drop in viability, and the beginning of the loss of nucleic acid content based on both CGH microarrays and replication run-out data. RecF protein has been shown to have a role in maintaining stalled replication forks and protecting nascent DNA. My work shows that when starved cells lack functional RecF protein, those cells have a markedly higher viability than RecF$^+$ cells, particularly in poor medium (not supplemented with casamino acids). RecF$^-$ cells also appear to lack the ability to initiate or maintain new rounds of replication. RecF cannot induce homologous recombination on its own and must interact with RecA to allow for RecA filaments to form on daughter-strand gaps. However RecA is part of the protection mechanism utilized by cells in thymineless death based on the high sensitivity of *thyArecA* double mutants. It is possible that the lesions which are induced by RecFORA are mitigated by the actions of RecABCD, however it may be even more likely that RecF has unique

attributes *in vivo* which cause the repair processes that the cell normally induces under such DNA-damaging conditions like UV-irradiation to fail when inadequate substrate is available for repair polymerases. Nevertheless, replication run-out indicates that such lethal repair processes likely occur at around two hours starvation since from that point replication forks fail to run out in distinct peaks during replication run-out (distinct peaks indicate complete replication of the genome), and viability is lost exponentially. My *dnaC*^{ts} data indicates that contrary to previous models, parental DNA is just as susceptible to DNA degradation at the origin of replication as is nascent DNA (Figure 6.1).

The cell only needs one whole chromosome to remain viable, however starving cells which are in the process of actively replicating their chromosome must either degrade all nascent DNA, or in the case of cells with multiple forks, degrade DNA from futile replication forks to regenerate nucleotide for use in viable replication reactions. Any mutation that stimulates this process without losing the integrity of at least one chromosome per cell by the end of the starvation should have a rescuing effect. It is plausible that RecF, either through its interaction with RecA or due to its activity at the fork, interferes with such degradation, resulting in lower internal pools of dTTP and accelerated killing (Figure 6.10).

6.2.3. Future Directions

My results imply that replication restart is the culprit behind much of the loss of viability in thymine-starved cells. This is a difficult place from which to carry on research. Replication restart is difficult to study *in vivo,* and although it is known that replication restart occurs in healthy growing cells (Cox, 2001), the majority of work done on replication restart has utilized UV-irradiated cells (which differs significantly from thymine starvation), and most of what we understand about restart stems from experiments reconstituted *in vitro.* Many of the structures that have been seen in *in vitro* experiments in *E. coli* have yet to be observed in living cells. Besides this, the role of replication restart in UV-irradiation and thymine starvation may be quite different as the two types of DNA damage have proven to be quite different in terms of actual DNA damage and the effects of repair processes.

Nevertheless, there are some experiments which could help better understand the role of replication initiation as well as the role of RecF protein. The DNA in the 'dip' surrounding the origin is not single-stranded in character, however it is uncertain whether the formation of this 'dip' was preceded by formation of single-stranded DNA. Using the ExoIII/S1 nuclease assay described in chapter 3 of this thesis throughout starvation and comparing it to comparative genomic hybridization data would help answer this question.

Due to the possibility that some initiation events never result in viable replication forks which can complete replication, it is important to determine whether initiation events or replication fork number are correlated with loss of viability. One possible way to address this is the use of fluorescently-tagged DnaA protein incorporated into the genome or expressed on a plasmid transformed into *thyA*$^-$ cells. DnaA protein oligomerizes at the origin of replication in *E. coli*¸ and would appear as a foci using fluorescence microscopy. A *dnaA*-GFP fusion expressed from a low but constitutively expressing plasmid results in a cell with two bright foci on polar opposites of the *E. coli* cell with several small punctate dots on other parts of the nucleoid. This correlates well with the role of DnaA as both an initiation protein (large foci at poles) and as a transcription factor (small punctate dots around the nucleoid). The number of initiation events attempted could be counted as the number of large foci present at the time cells are treated with replication run-out, and the results of replication run-out would show the number of viable replication forks that resulted from those initiation events.

The observation that *recF*$^-$ cells are able to maintain their 'older' forks later into thymine starvation seems to indicate that RecF has a detrimental effect at those forks later in starvation in *recF*$^+$ cells. One idea is that DNA synthesis becomes discontinuous in both strands during thymine starvation as the concentration of dTTP decreases over time (Figure 6.9) This could generate stretches of single-stranded DNA as has been seen to occur in yeast (Lopes et al., 2006), and such DNA would be a ready target for both RecF protein, and particularly sensitive to breakage. For whatever reason, it appears that newer forks are more susceptible to degradation than older forks. This implies that newly initiated replication forks are somehow different than older forks during thymine starvation, and the quality of the DNA there is quite poor. Once the newer forks have been compromised and degraded, older forks may become

susceptible to the same processes. Chromatin-immunoprecipitation analysis hybridized to DNA microarray (ChIP-chip) could show whether RecF associates preferentially to newer or older forks (those forks closer to the origin and those further away from the origin on the chromosome). Doing ChIP-chip with an HA-tagged RecF as bait coupled with a ChIP-chip experiment utilizing 5'-bromouracil to determine areas of new DNA incorporation in thymine starved cells could further illuminate whether RecF is associating with actively replicating forks in thymine starvation. I have already made a *thyA*$^-$ strain of *E. coli* with a genomic copy of HA-tagged *recF*, and my lab has done work previously using HA-targeting antibodies to test the binding sites of globally binding transcription factors. A similar experimental set-up could be used to determine the binding sites of RecF with and without thymine starvation.

Understanding the answers to these questions could help elucidate the mechanism by which the cells degrade their DNA during thymine starvation, whether single-strand or double-strand nucleases are involved, and thus what coping mechanism the cell is employing to deal with the damage.

Thymineless death can only be studied *in vivo,* and as this work and others have shown, thymineless death touches nearly all metabolic processes involving DNA in the cell. One of the difficulties in working with an *in vivo* system is the number of unknowns which are difficult to isolate and account for. Working with *E. coli* as a model system, I have come to appreciate its robustness for analyzing the intricacies of basic DNA replication and initiation. There are many aspects to replication and repair, especially replication initiation that we still do not understand but I think thymineless death may actually prove useful in better understanding these processes in a living cell.

Figure 6.1. (Derived from Figures 4.4 and 4.8)Replication initiation events do not necessarily result in viable replication forks. An initiation event has taken place after between 0 minutes 20 minutes return to permissive temperature in PC1 cells as evidenced by an increase in gene copy number near the origin of replication in CGH analysis (0e+00)(a.), however the major peak in replication run-out representing the number of viable replication forks at that time does not shift to the right between 0 and 20 minutes return to permissive temperature. The initiation event that resulted in an increase of gene copy number as measured by comparative genomic hybridization does not produce robust replication forks that complete the replication of an additional chromosome as evidenced by replication run-out.

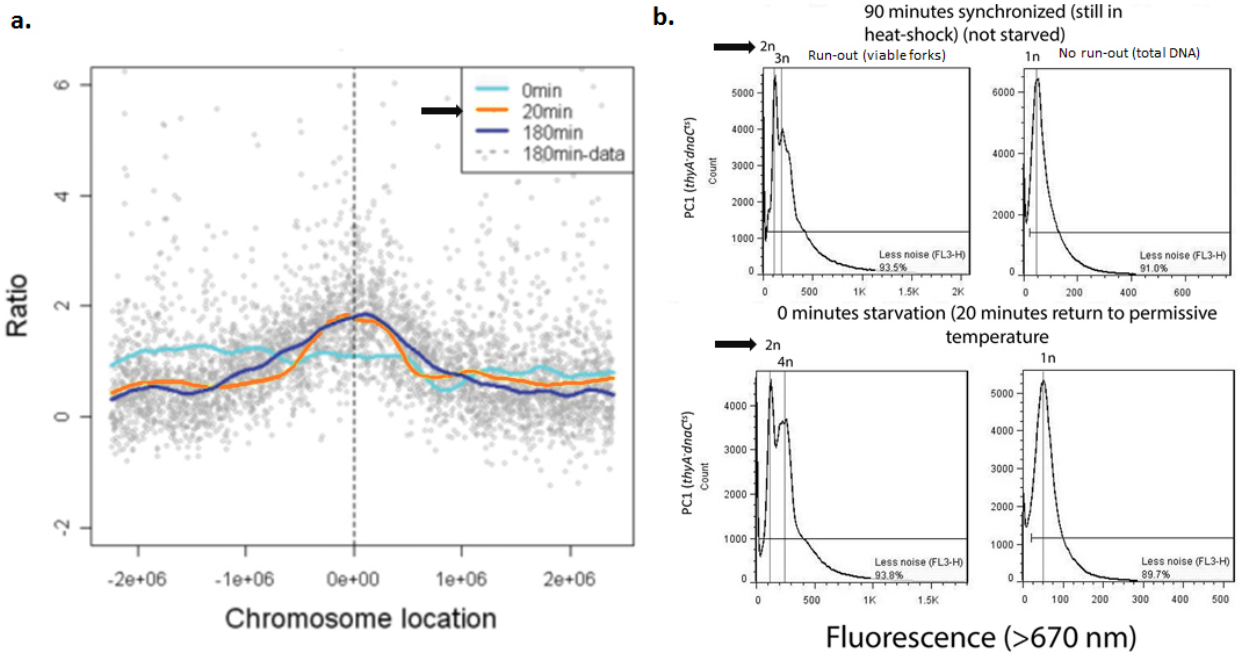

Figure 6.2. There is an increase in number of run-out chromosomes between 60 and 120 minutes starvation in *thyA*⁻ strains **A.** (derived from Figure 5.5) When averaging the mode of the peaks with the highest number of 'cell events' in them, the average number of viable replication forks increases steadily over time in all replicates in CL001 (*thyA*⁻) cultures **B**. The total DNA content remains relatively steady over time until approximately 120 minutes starvation correlating well with the beginning of DNA loss as measured by CGH array (**C**), and viability (**D**)(Derived from Figures 4.4 and 4.8 respectively).

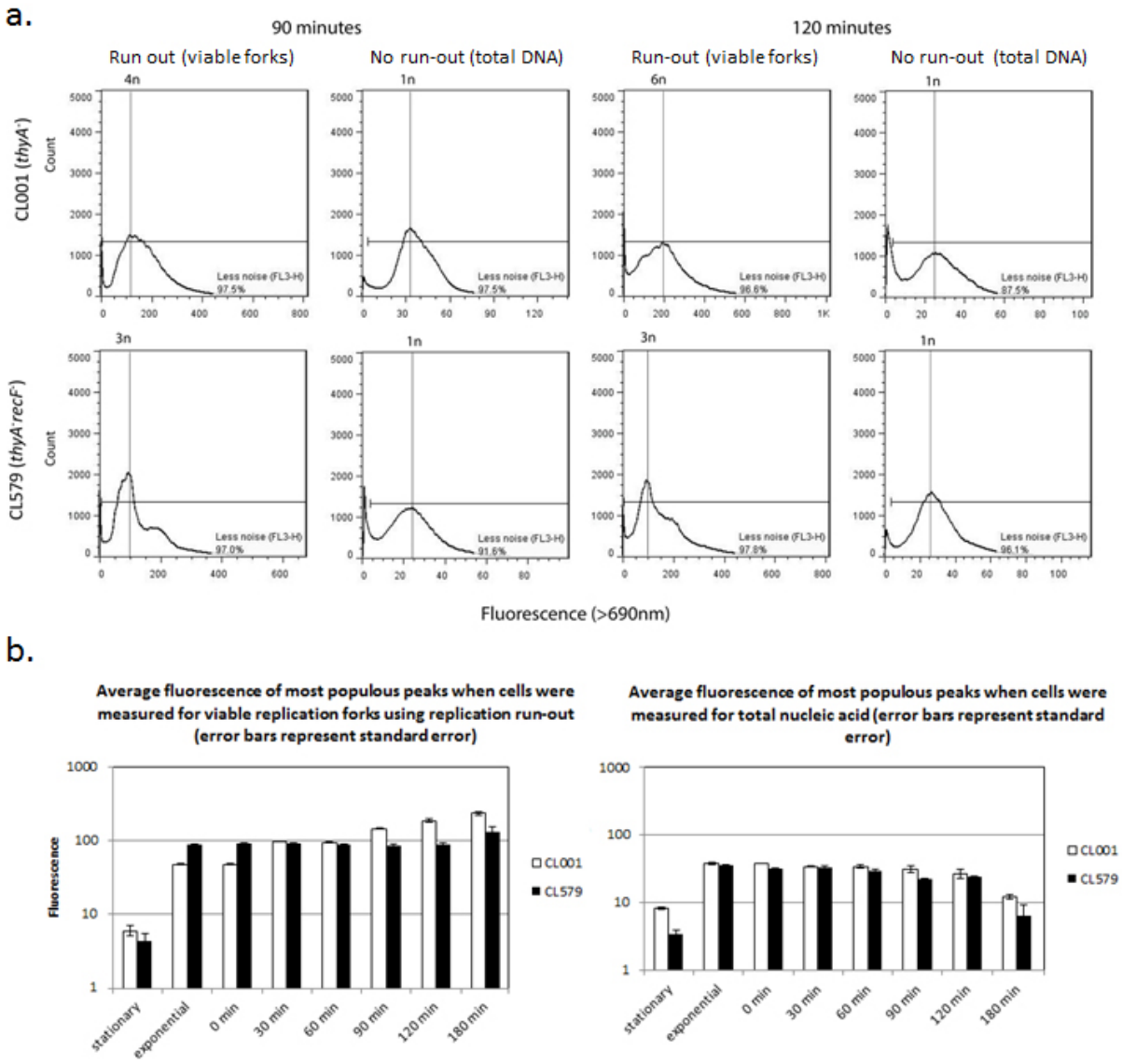

c.

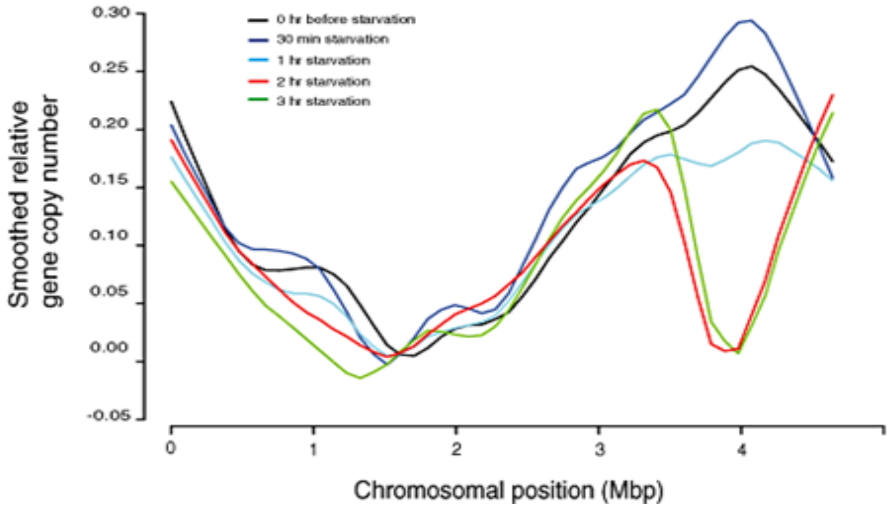
0 hr before starvation
30 min starvation
1 hr starvation
2 hr starvation
3 hr starvation
Smoothed relative gene copy number
0.30
0.25
0.20
0.15
0.10
0.05
0.00
-0.05
0
1
2
3
4
Chromosomal position (Mbp)

d.

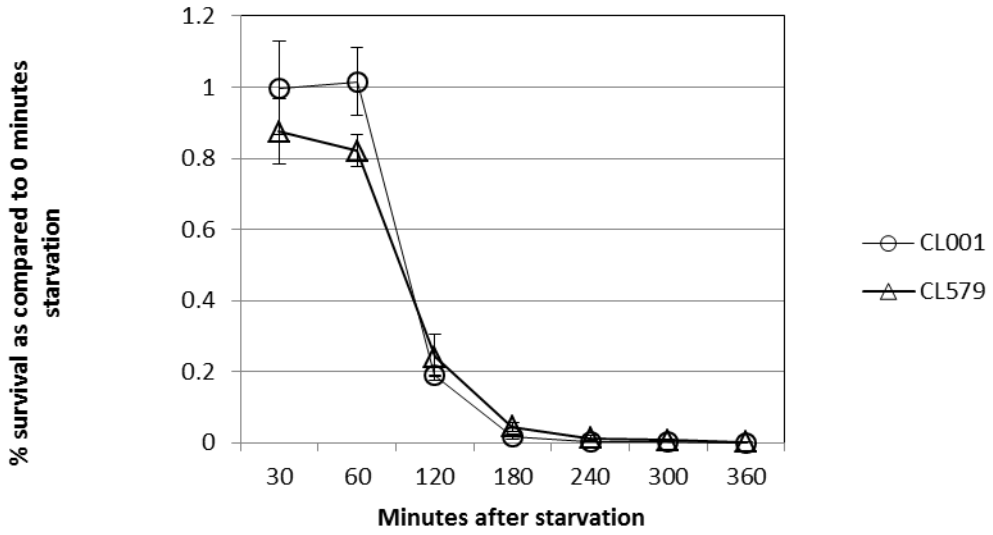
% survival as compared to 0 minutes starvation
1.2
1
0.8
0.6
0.4
0.2
0
30
60
120
180
240
300
360
Minutes after starvation
CL001
CL579

Figure 6.3 (D erived from Figure 4.8)Flow cytometric analysis of fluorescence of cells treated with propidium iodide nucleic acid stain with (a.) and without (b.) replication run-out. Both *dnaA*^{ts} and *dnaC*^{ts} cells have additional viable replication forks after synchronization by heat-shock when starved of thymine in heat-shock as compared to cells synchronized in the presence of adequate thymine. This indicates thymine starvation induces replication initiation events outside the space of normal replication regulation.

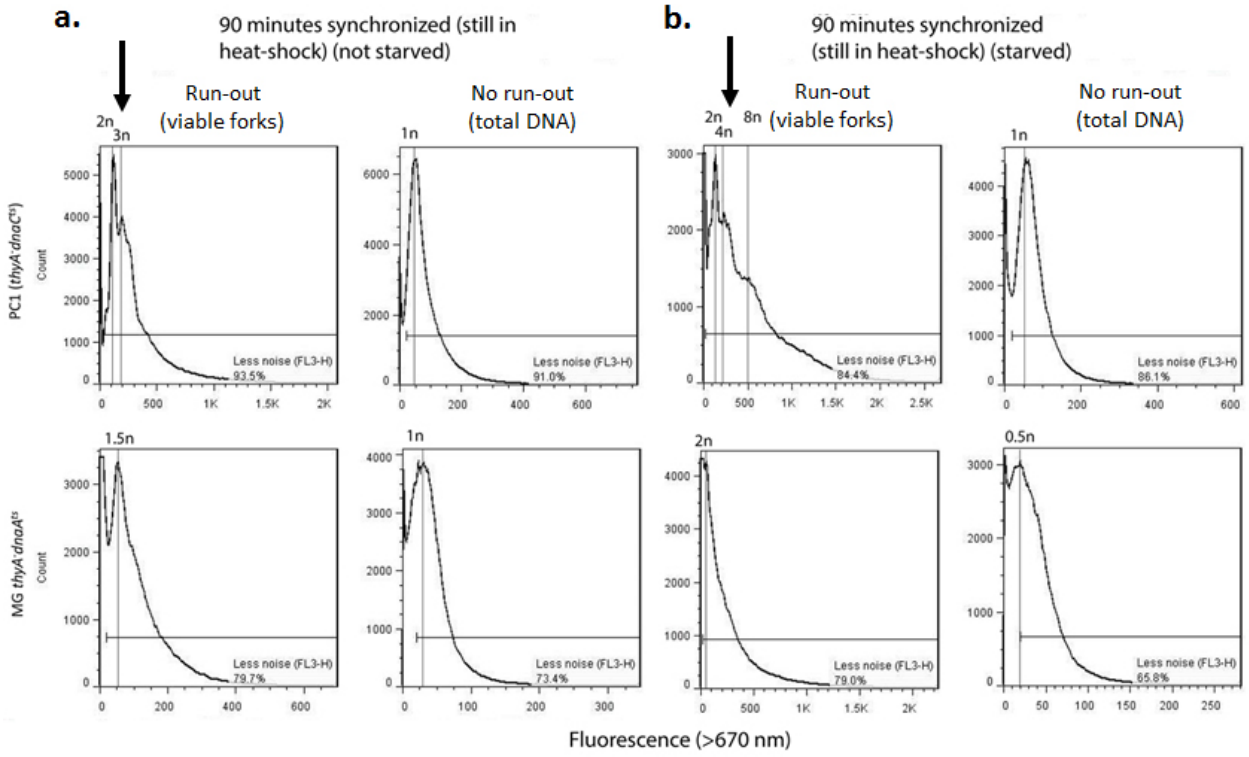

Figure 6.4 (Derived from Figure 4.7). Replication initiation is required for DNA degradation at the origin in MG *thyA*$^{-}$*dnaA*^{ts} cells. MG*thyA*$^{-}$*dnaA*^{ts} cells which have been synchronized in heat-shock and starved but never allowed to return to permissive temperature for DnaA-dependent replication initiation do not have DNA degradation events at the origin of replication, unlike the case where cells are returned to permissive temperature during starvation.

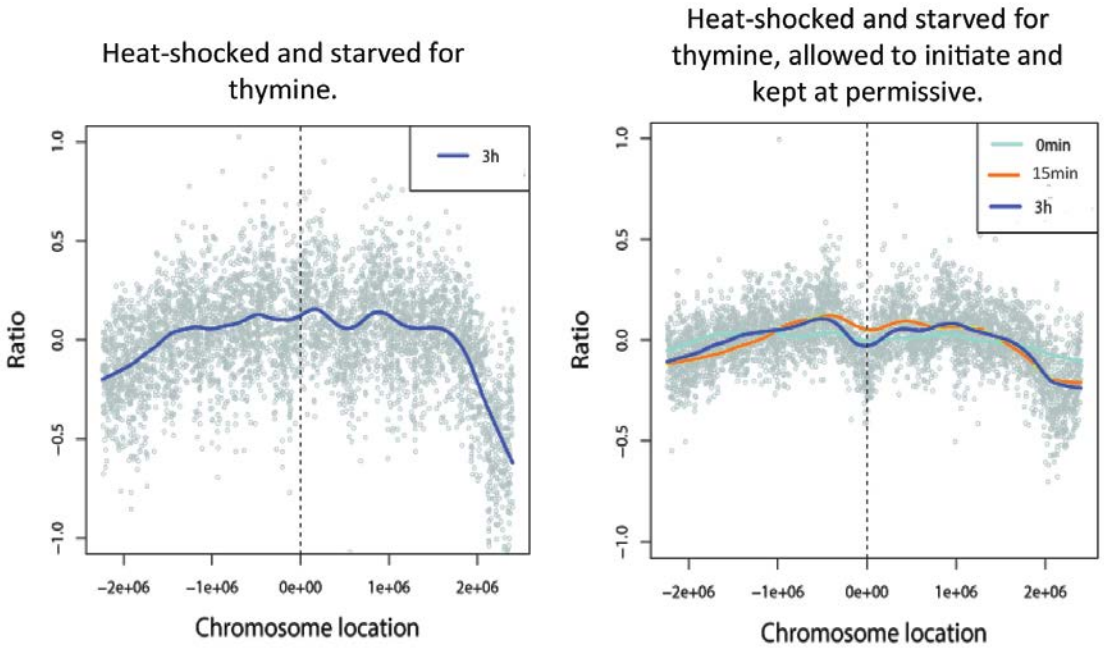

Figure 6.5. (Derived from Figure 4.4). In *thyA*$^{-}$*dnaC*^{ts} cells upon return to permissive temperature after synchronization by heat-shock for 90 minutes, both parental (present at 0 minutes permissive temperature) and nascent strands of DNA (present at 20 minutes permissive temperature) are degraded at the origin of replication by 180 minutes after return to permissive temperature.

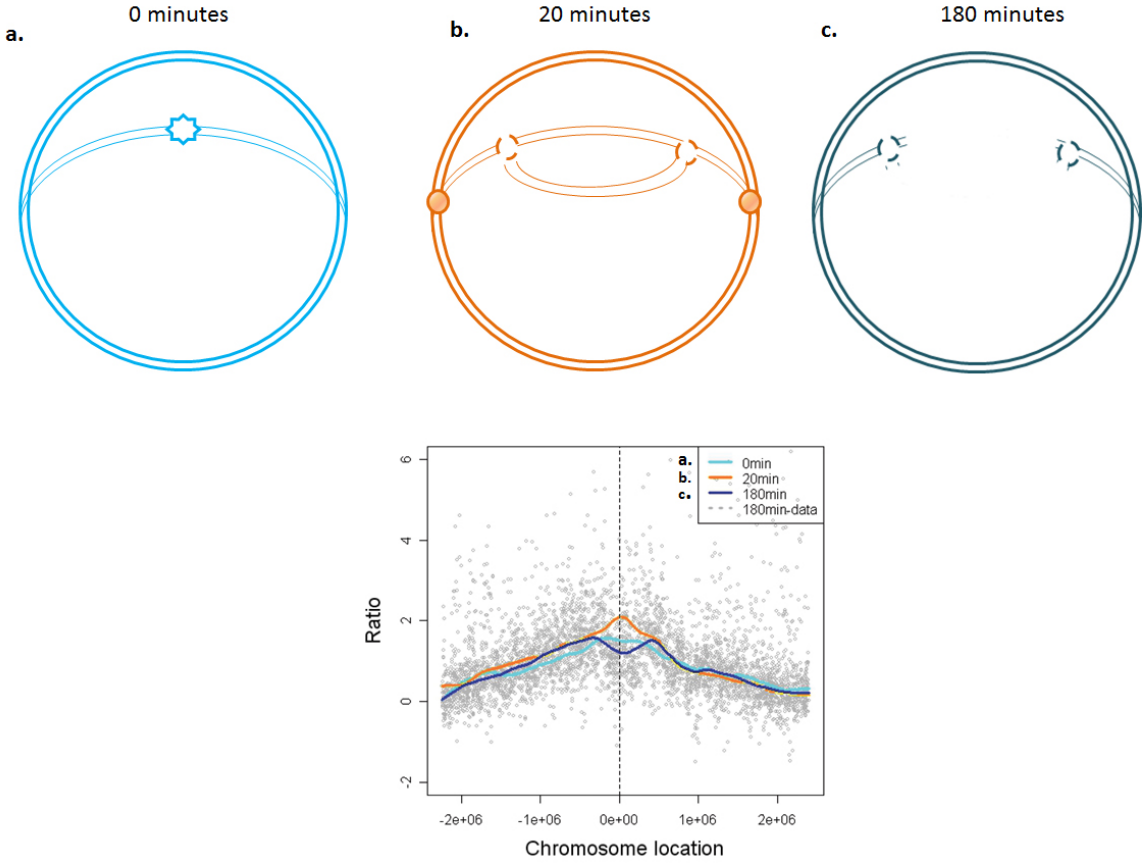

Figure 6.6. (Derived from Figure 4.10). Strains of *thyA*$^{-}$ *E. coli* that contain temperature sensitive alleles for either DnaC helicase loader (in PC1 cells, which is required for all replication initiation or restart), or DnaA initiator protein (in MG*thyAdnaA* cells, which is required for replication initiation at the origin, were synchronized for replication initiation in heat-shock. During starvation in heat-shock, cells that were replication-restart-competent (*dnaA*^{ts} mutants) had a much lower viability than cells which were deficient in only origin-specific-replication-initiation (PC1 cells) (a). After return to permissive temperature, the strain which had more viable replication forks upon return to permissive temperature (PC1 cells) had a much lower viability (b).

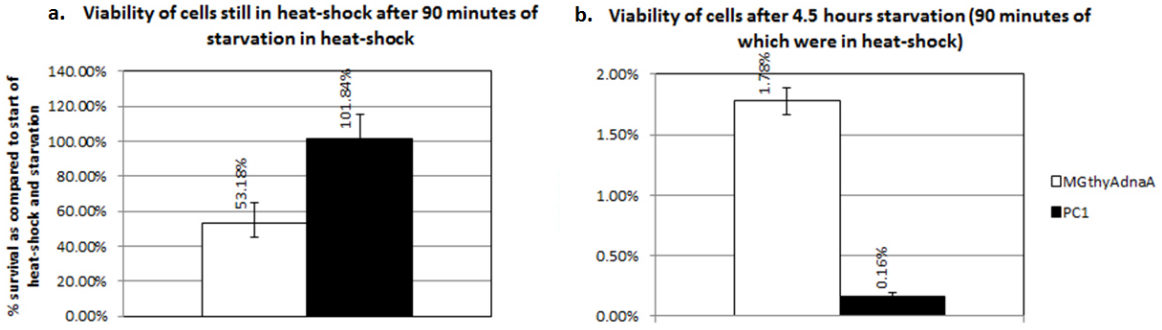

Figure 6.7. (Derived from Figure 4.4, 4.7-4.8) Single chromosomal equivalents in *dnaA*^{ts} and *dnaC*^{ts} (PC1) cells were determined by observing the mode of fluorescence of cells in replication run-out which had been synchronized in heat-shock for replication (90 minutes with thymine), and for which comparative genomic hybridization showed a flat line indicating a single gene copy number across the chromosome (a). That value was used to determine chromosomal equivalents in other samples. During starvation and heat-shock, RecF^{+} *dnaA*^{ts} cells have less than a whole chromosome's worth of DNA as compared to replication restart-deficient *dnaC*^{ts} cells in the same condition (b). This indicates that some portion of *dnaA*^{ts} DNA is single-stranded in character.

a.

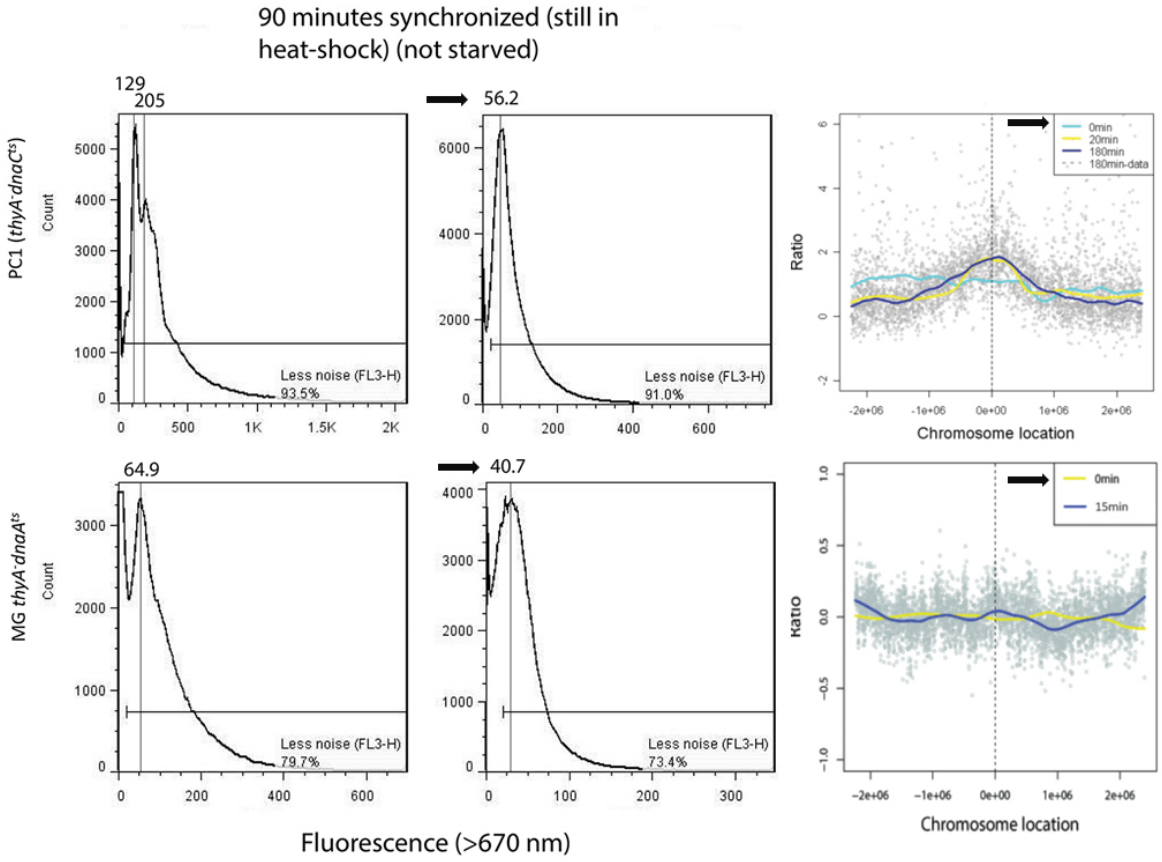

b.

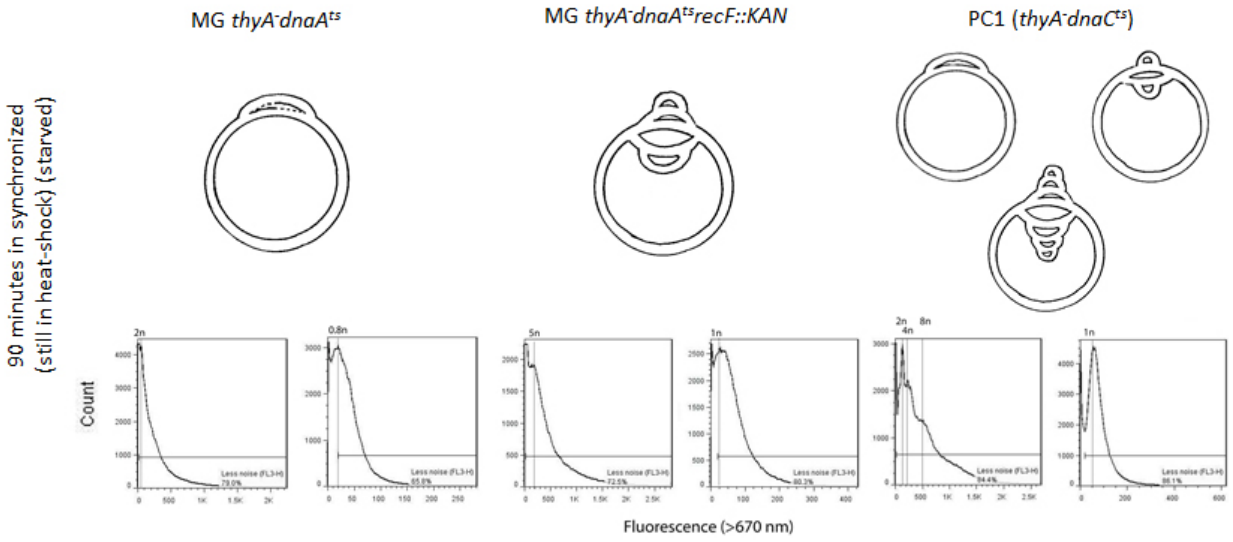

Figure 6.8 (Derived from Figure 5.5). W3110 cells with a functional RecF protein gradually accumulate viable replication forks over the course of thymine starvation (**A**), however *recF*$^{-}$ cells have trouble maintaining viable replication forks over starvation (**B**). In W3110*thyA*$^{-}$*recF*$^{-}$ cells it appears that between 0 and 30 minutes, either DNA degradation has occurred (based on decrease in total DNA content) while replication forks remained static, or rather replication completed between 0 and 30 minutes, and new initiation events occurred. Either scenario is different in W3110*thyA*$^{-}$ cells. In the replication run-out of CL579 cells, the transition from the 60 minute time point to the 120 minute time point is unclear, as the two populations of cells merge more or less into one. It is unclear whether the cell population with a single chromosome with three pairs of forks simply degrades one of the replication forks (i), or whether the new replication forks stall, and the older replication forks continue resulting in a poorly replicated chromosome which may be subjected to degradation (ii). The cells containing a single chromosome with 1 pair of viable replication forks may initiate a new round of replication on one chromosomal arm to obtain an additional set of viable forks(iii). Either way, by 120 minutes a single chromosome with two pairs of replication forks remain (iv). It is unknown whether CL579 cells undergo the same initiation events as CL001 cells, but if they do, they are unable to maintain the new replication forks. After replication initiation is synchronized by heat-shock, *dnaA*^{ts} (with or without functional RecF protein), where most cells in the population have one chromosome per cell, there is a large increase in viable replication fork number (**C**&**D**). The consistently odd number of chromosomes in *recF::KAN* cells implies that RecF is involved in either replication initiation itself or in maintenance of new replication forks since in wild-type cells replication initiation is symmetric. Both strains in **C** & **D** seem to continue to have high numbers of viable forks well into starvation as compared to those strains shown in **A** & **B**.

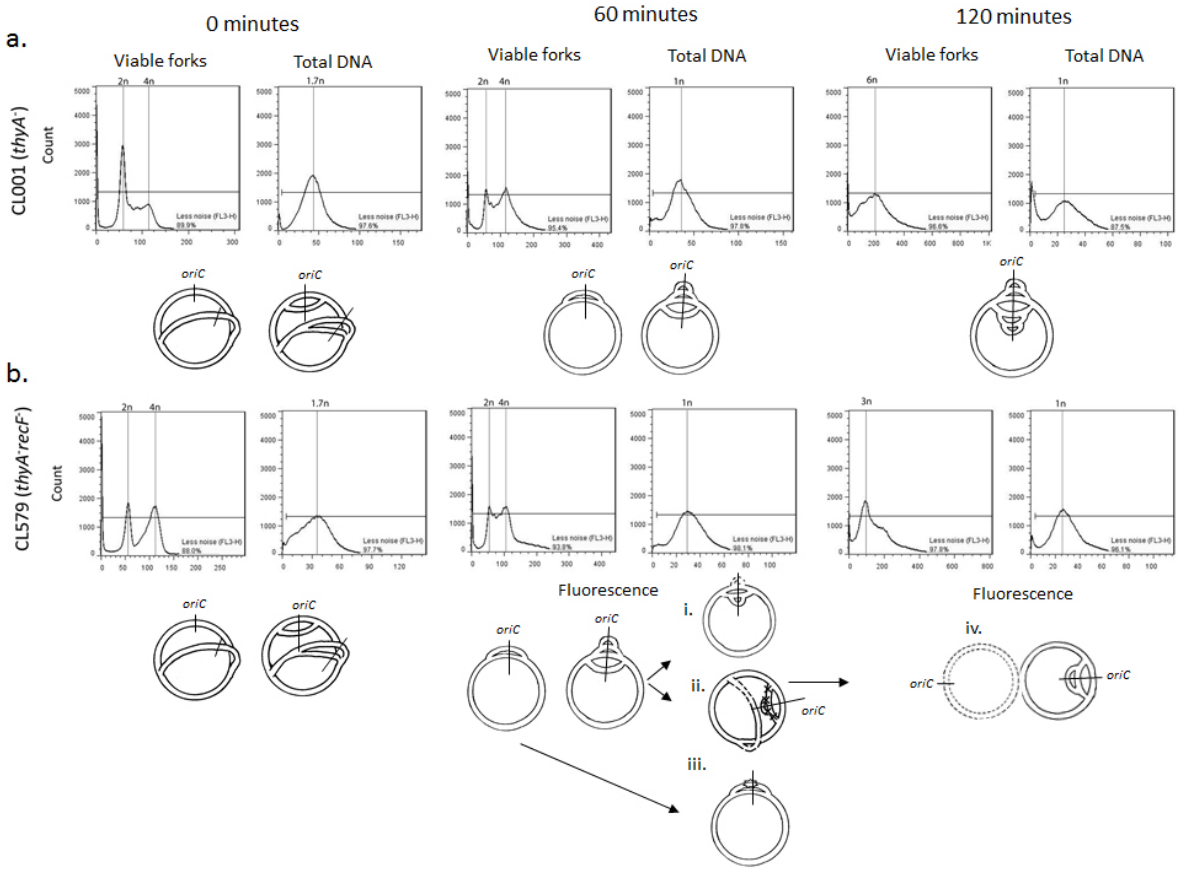
a.
0 minutes
60 minutes
120 minutes
Viable forks
Total DNA
Viable forks
Total DNA
Viable forks
Total DNA
CL001 (thyA⁻)
Count
2n 4n
1.7n
2n 4n
1n
6n
1n
oriC
oriC
oriC
oriC
oriC
b.
CL579 (thyA⁻recF⁻)
Count
2n 4n
1.7n
2n 4n
1n
3n
1n
oriC
oriC
Fluorescence
oriC
oriC
i.
ii.
oriC
iii.
Fluorescence
iv.
oriC
oriC

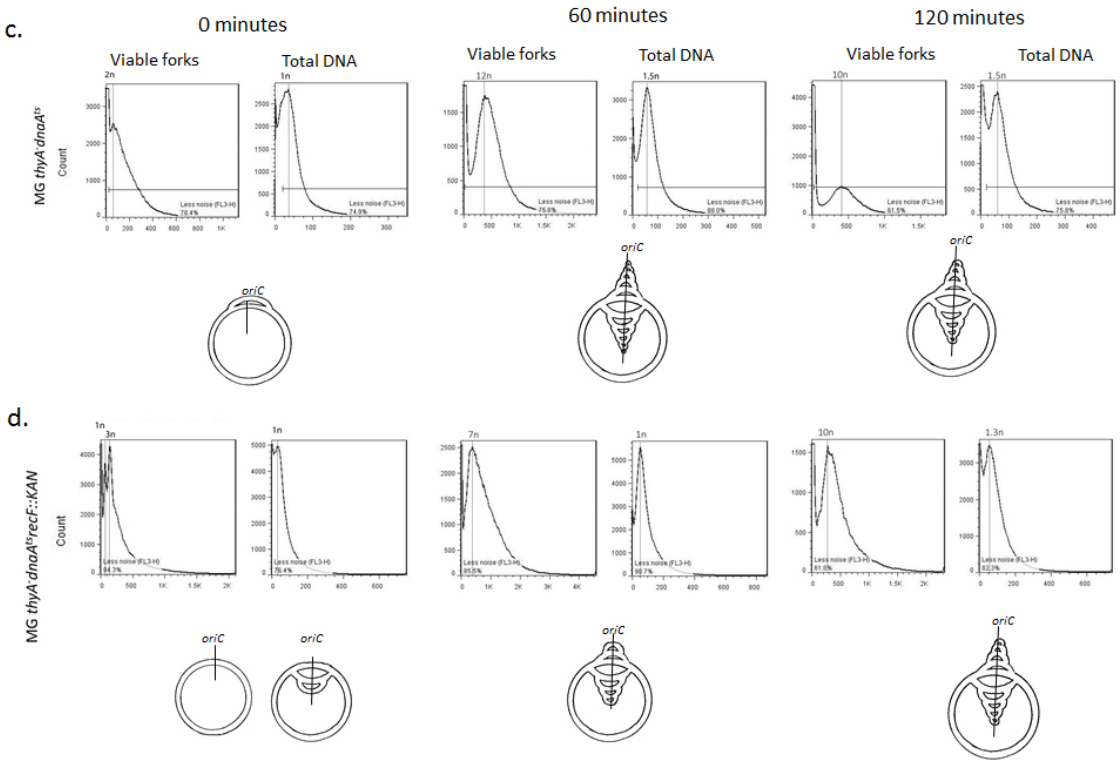
c.
0 minutes
60 minutes
120 minutes
Viable forks
Total DNA
Viable forks
Total DNA
Viable forks
Total DNA
MG thyA dnaA^ts
Count
2n
1n
12n
1.5n
10n
1.5n
oriC
oriC
oriC
d.
MG thyA dnaA^ts recF::KAN
Count
1n
3n
1n
7n
1n
10n
1.3n
oriC
oriC
oriC
oriC

Figure 6.9 Model of events at replication forks during thymine starvation. At a typical replication fork, the leading strand polymerase synthesizes DNA as fast as the helicase unwinds the parental duplex DNA and extrudes single-stranded template, while the lagging strand is extruded in a loop that allows the lagging strand polymerase to bind and synthesize in a 5'->3' direction (a). During thymine starvation, the polymerases slow or stall due to too low a concentration of thymine, but helicase may continues to unwind parental duplex DNA (b). Polymerases could then jump to the next available RNA primer to prevent uncoupling and subsequent fork collapse. In doing so, many single-strand gaps may be generated on either nascent strand (c).

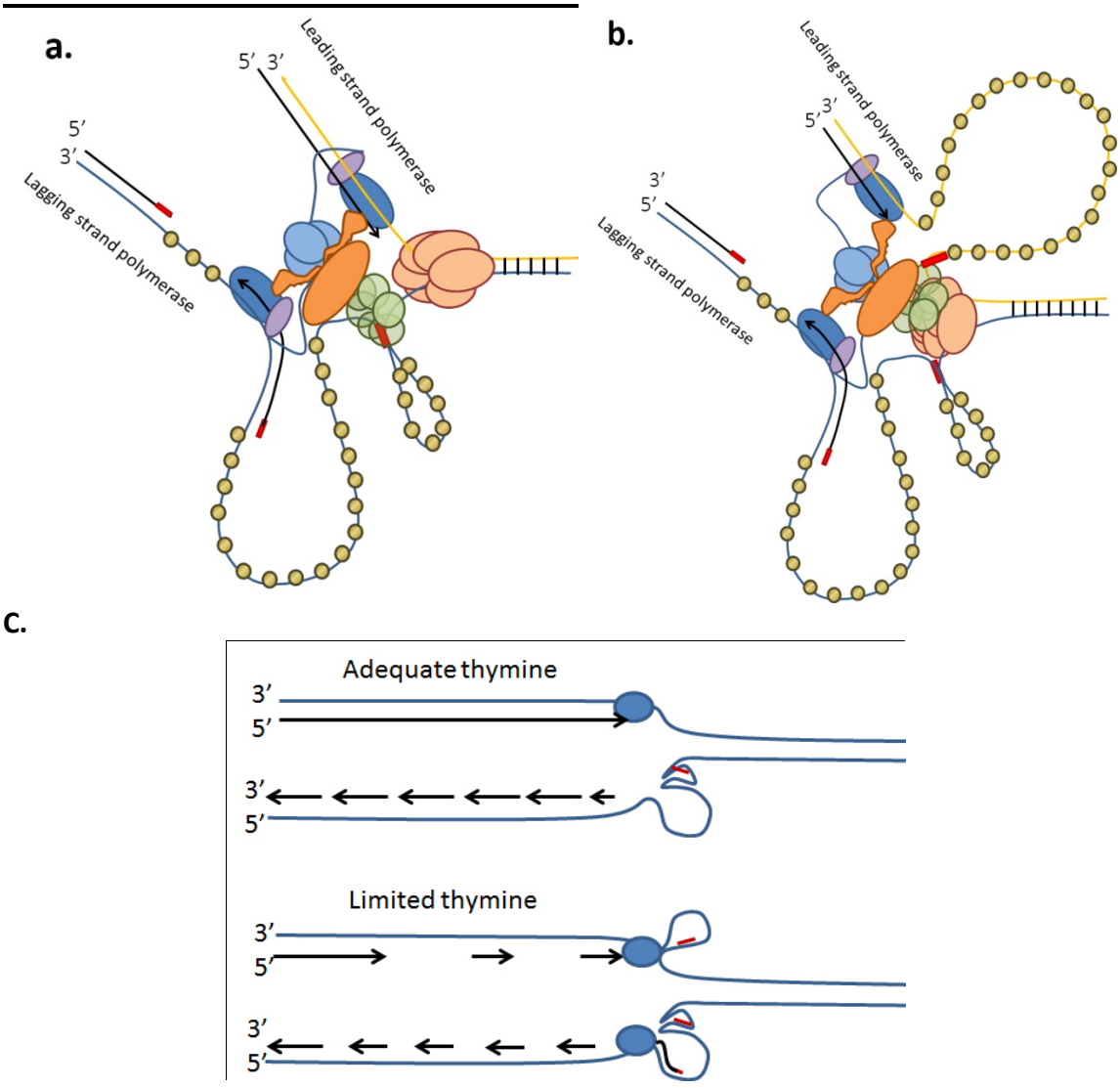

Figure 6.10 Model showing possible progression of replication fork and initiation-related events over time in thymine starvation. At the onset of starvation both strains likely have several active replication forks which stall within a few minutes of thymine starvation (a black 'x' represents replication forks present before the onset of starvation). In early starvation, *thyA*$^-$ cells (**A**) continue to initiate new rounds of replication resulting in new viable replication forks (represented by an open 'x'), perhaps maintained with the aid of RecF protein, and these forks make some progress away from the origin of replication. The quality of the DNA at those new forks may be gapped and full of uracil. By mid-phase thymine starvation, these cells continue to initiate new rounds of replication, however the parental template from the previous round of replication is compromised likely resulting in highly gapped duplex DNA that is prone to nuclease attack. By late phase starvation, these cells have degraded most of the DNA proximal to the origin of replication, and 'older' replication forks begin to collapse, perhaps due to issues in replication restart. In early starvation of *thyA*$^-$*recF*$^-$ cells (**B**) the same arrest of 'older' forks occurs as well, but without functional RecF protein, new rounds of replication fail to occur or result in inviable replication forks. Later initiation events continue to have poor probabilities of forming viable replication forks, and DNA at the origin is less likely to be targeted for degradation. RecF may also play a role at the older replication forks as *recF*$^-$ cells are able to retain viable replication forks several minutes longer than RecF$^+$ cells.

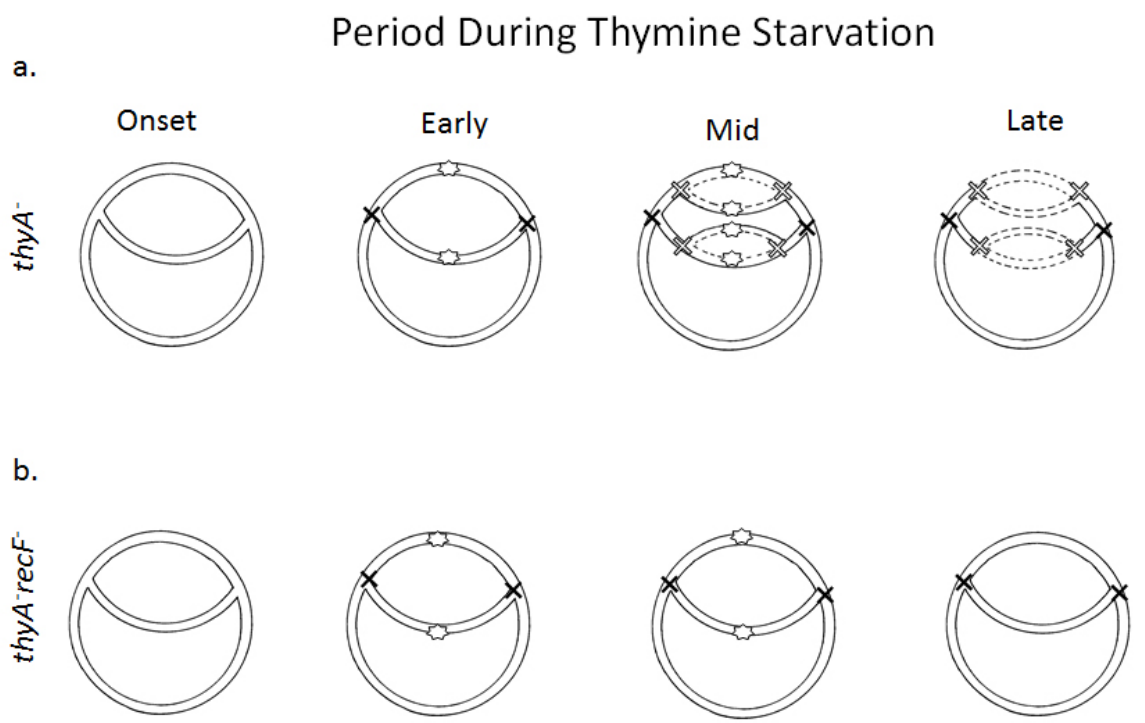

Figure 6.11 A comparison of viable replication forks over time (resulting in full chromosomes after replication run-out), to DNA content and survival during thymine starvation in K-12 strains. In (**A**), filled marks represent chromosomal number after replication run-out, open markers represent chromosomal number present at the start of replication run-out. The genotype of CL001 is *thyA*$^-$ and the genotype of CL579 is *thyA*$^-$*recF*$^-$. Viability over time is shown in (**B**) for the strains described in A. By two hours starvation (the onset of rapid loss of viability) strains with higher numbers of viable replication forks suffer higher losses of viability between 2 and 3 hours.

a.

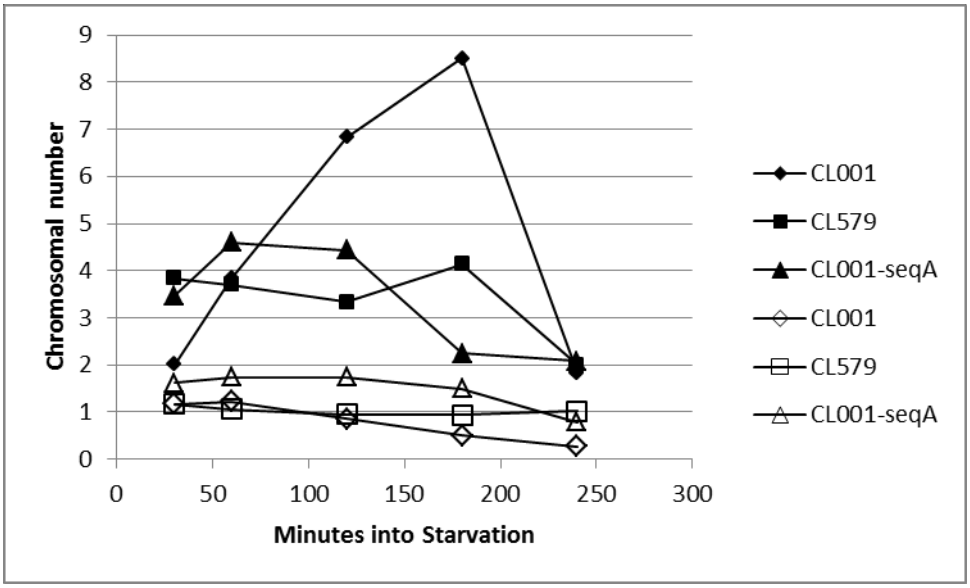

b.

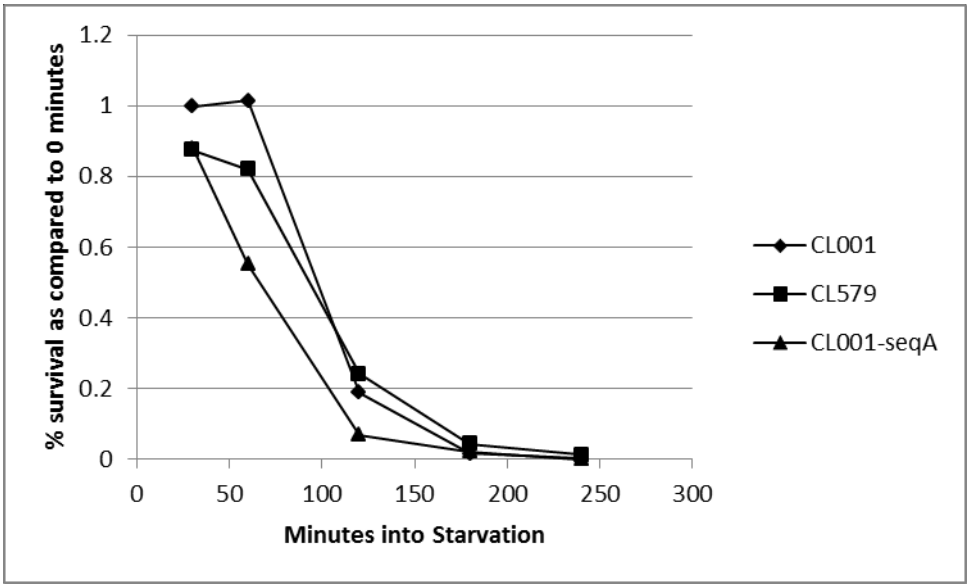

Bibliography

1. Ahmad, S. I., Kirk, S. H., & Eisenstark, A. (1998). Thymine metabolism and thymineless death in prokaryotes and eukaryotes. *Annual review of microbiology, 52*: 591–625.
2. Adelberg, E.A., and Coughlin, C.A. (1956). Bacterial mutation induced by thymine starvation. *Nature*. *178:* 531-532.
3. Allen, G. C., & Kornberg, A. (1991). Fine balance in the regulation of DnaB helicase by DnaC protein in replication in Escherichia coli. *The Journal of Biological Chemistry*, *266*(33): 22096–101.
4. Amyes, S.G., and Smith, J.T. (1974). Trimethoprim action and its analogy with thymine starvation. *Antimicrob. Agents. Chemother. 5*: 169-178
5. Anderson, J.A., and Barbour, S.D. (1973). Effect of thymine starvation on deoxyribonucleic acid repair systems of *Escherichia coli* K-12. *J. Bacteriol*. *113*: 114-121.
6. Atlung, T., & Hansen, F. G. (1993). Three distinct chromosome replication states are induced by increasing concentrations of DnaA protein in *Escherichia coli*. *Journal of Bacteriology*, *175*(20): 6537–45.
7. Ayusawa, D., Shimizu, K., Koyamas, H., & Takeishi, K. (1983). Accumulation of DNA Strand Breaks during Thymineless Death in Thymidylate Synthase-negative Mutants of Mouse FM3A Cells . *Journal of Biological Chemistry*, *258*(20): 12448–12454.
8. Baba, T., Ara, T., Hasegawa, M., Takai, Y., Okumura, Y., Baba, M., Datsenko, K., Tomita, M., Wanner, B., and Mori, H. (2006). Construction of Escherichia coli K-12 in-frame, single-gene knockout mutants: the Keio collection. *Molecular Systems Biology*, *2*: 1-11.
9. Barner, H. D., & Cohen, S. S. (1957). The isolation and properties of amino acid requiring mutants of a thymineless bacterium. *Journal of Bacteriology*, *74*(3), 350–5.
10. Bazill, G.W. (1967). Lethal unbalanced growth in bacteria. *Nature. 216:*346-349.

11. Beacham, I. R., Beacham, K., Zaritsky, a, & Pritchard, R. H. (1971). Intracellular thymidine triphosphate concentrations in wild type and in thymine requiring mutants of Escherichia coli 15 and K12. *Journal of Molecular Biology*, *60*(1): 75–86.

12. Belle, J.J., Casey, A., Courcelle, C.T., and Courcelle, J. (2007) Inactivation of the DnaB helicase leads to the collapse and egradation of the replication fork: a comparison to UV-induced arrest. *J. Bacteriol. 189*: 5452-5462.

13. Berger, F. G., & Berger, S. H. (2006). Thymidylate Synthase as a Chemotherapeutic Drug, *Cancer Biology & Therapy,* 5(9): 1238–1241.

14. Bernander, R., Stokke, T., & Boye, E. (1998). Flow cytometry of bacterial cells: comparison between different flow cytometers and different DNA stains. *Cytometry, 31*(1): 29–36.

15. Blanche, F., B. Cameron, F.-X. Bernard, L. Maton, B. Manse, L. Ferrero, N. Ratet, C. Lecoq, A. Goniot, D. Bisch, and J. Crouzet. (1996). Differential behaviors of *Staphylococcus aureus* and *Escherichia coli* type II DNA topoisomerases. *Antimicrob. Agents Chemother. 40***:**2714-2720.

16. Bliska, J. B., and N. R. Cozzarelli. (1987). Use of site-specific recombination as a probe of DNA structure and metabolism *in vivo*. *J. Mol. Biol. 194***:**205-218.

17. Carr, K.M., Kaguni, J.M. (1996). The A184V missense mutation of the *dnaA5* and *dnaA46* alleles confers adefect in ATP binding and thermolability in initiation of *Escherichia coli* DNA replication. *Mol. Microbiol. 20*(6): 1307-18.

18. Champoux, J. J. (2001). DNA topoisomerases: structure, function, and mechanism. *Annu. Rev. Biochem. 70***:**369-413.

19. Cheung, K. J., V. Badarinarayana, D. W. Selinger, D. Janse, and G. M. Church. (2003). A microarray-based antibiotic screen identifies a regulatory role for supercoiling in the osmotic stress response of *Escherichia coli*. *Genome Res. 13***:**206-215.

20. Cohen, S.S., and Barner, H.D. (1954). Studies on unbalanced growth in *Escherichia coli. PNAS. 40*: 885-893.

21. Courcelle, C.T., Chow, K.H., Casey, A., and Courcelle, J. (2006). Nascent DNA processing by RecJ favors lesion repair over translesion synthesis at arrested replication forks in *Eschericia coli. PNAS. 103*: 9154-9159.

22. Chow, K.H., & Courcelle, J. (2004). RecO acts with RecF and RecR to protect and maintain replication forks blocked by UV-induced DNA damage in Escherichia coli. *The Journal of Biological Chemistry, 279*(5): 3492–6.

23. Clark, A. J., Chamberlin, M., Boyce, R. P., & Howard-Flanders, P. (1966). Abnormal metabolic response to ultraviolet light of a recombination deficient mutant of Escherichia coli K12. *Journal of Molecular Biology, 19*(2): 442–454.

24. Clark, D. J., & Felsenfeld, G. (1991). Formation of nucleosomes on positively supercoiled DNA. *The EMBO Journal, 10*(2): 387–95.

25. Cohen, S. S., & Barner, H. D. (1953). The induction of thymine synthesis by T2 infection of a thymine requiring mutant of Escherichia coli. *Journal of Bacteriology, 68*(1): 80–88.

26. Cohen, S. S., & Barner, H. D. (1956). Studies on the induction of thymine deficiency and on the effects of thymine and thymidine analogues in Escherichia coli. *Journal of Bacteriology, 71*(5): 588–97.

27. Courcelle, J., Crowley, D. J., & Hanawalt, P. C. (1999). Recovery of DNA Replication in UV-Irradiated Escherichia coli Requires both Excision Repair and RecF Protein Function Recovery of DNA Replication in UV-Irradiated Escherichia coli Requires both Excision Repair and RecF Protein Function. *Journal of Bacteriology, 181*(3):916.

28. Courcelle, J., & Hanawalt, P. C. (2003). RecA-dependent recovery of arrested DNA replication forks. *Annual Review of Genetics, 37*: 611–46.

29. Cox, M. M. (2001). Recombination DNA Repair of Damaged Replication Forks in *Escherichia coli. Annual Review of Genetics*, 35: 53–82.

30. Cummings, D. J., & Kusy, a R. (1970). Thymineless death in Escherichia coli: deoxyribonucleic acid replication and the immune state. *Journal of Bacteriology, 102*(1): 106–17.

31. Datsenko, K. a, & Wanner, B. L. (2000). One-step inactivation of chromosomal genes in Escherichia coli K-12 using PCR products. *PNAS*, *97*(12): 6640–5.

32. Drlica, K., and M. Malik. (2003). Fluoroquinolones: action and resistance. *Curr. Top. Med. Chem. 3*:249-282.

33. Faith, J.J., Hayete, B., Thaden, J.T., Mogno, I., Wierzbowski, J., Cottarel, G., *et al.* (2007). Large-scale mapping and validation of *Escherichia coli* transcriptional regulation from a compendium of expression profiles. *PLoS Biol. 5*: e8.

34. Ferrero, L., B. Cameron, B. Manse, D. Lagneaux, J. Crouzet, A. Famechon, and F. Blanche. (1994). Cloning and primary structure of *Staphylococcus aureus* DNA topoisomerase IV: a primary target of fluoroquinolones. *Mol. Microbiol. 13***:**641-653.

35. Ferullo, D. J., & Lovett, S. T. (2008). The stringent response and cell cycle arrest in Escherichia coli. *PLoS Genetics, 4*(12): 1-15.

36. Flatman, R. H., A. J. Howells, L. Heide, H. P. Fiedler, and A. Maxwell. (2005). Simocyclinone D8, an inhibitor of DNA gyrase with a novel mode of action. *Antimicrob. Agents Chemother. 49***:**1093-1100.

37. Fonville, N. C., Bates, D., Hastings, P. J., Hanawalt, P. C., & Rosenberg, S. M. (2010). Role of RecA and the SOS response in thymineless death in Escherichia coli*. PLoS Genetics*, 6(3): 1-10.

38. Fonville, N. C., Vaksman, Z., DeNapoli, J., Hastings, P. J., & Rosenberg, S. M. (2011). Pathways of resistance to thymineless death in Escherichia coli and the function of UvrD. *Genetics, 189*(1): 23–36.

39. Freifelder, D., and MaalØe, O. (1964). Energy requirement for thymineless death in cells of *Escherichia coli. J. Bacteriol. 88*: 987-990.

40. Freifelder, D. (1967). Lack of a Relation Between Deoxyribonucleic Acid Methylation and Thymineless Death in Escherichia coli. *Journal of Bacteriology*, *93*(5): 1732–1733.

41. Freifelder, D. (1969). Single-strand Breaks in Bacterial DNA Associated with Thymine Starvation. *Journal of Molecular Biology, 45*(1909): 1–7.

42. Fukui, K. (2010). DNA mismatch repair in eukaryotes and bacteria. *Journal of Nucleic Acids*, 1–16.

43. Gallant, J., & Suskind, S. R. (1961). Relationship between thymineless death and ultraviolet inactivation in *Eschericia coli*, *J. Bacteriol*. *82*:187-194.

44. Gallant, J., and Suskind, S.R. (1962). Ribonucleic synthesis and thymineless death. *Biochi.m Biophys. Acta. 55*: 1591-1598.

45. Gallant, J., an dSpottswood, T. (1964). Measurement of the stability of the repressor of alkaline phosphatase synthesis in *Escherichia coli. PNAS. 52*: 1591-1598.

46. Gayama, S., Kataoka, T., Wachi, M., Tamura, G., & Nagai, K. (1990). Periodic formation of the oriC complex of *Escherichia coli. The EMBO Journal, 9*(11): 3761–5.

47. Georgescu, R. E., Kurth, I., & O'Donnell, M. E. (2012). Single-molecule studies reveal the function of a third polymerase in the replisome. *Nature Structural & Molecular Biology, 19*(1): 113–6.

48. Gmeiner, W. H. (2005). Novel chemical strategies for thymidylate synthase inhibition. *Current Medicinal Chemistry, 12*(2): 191–202.

49. Gmuender, H., K. Kuratli, K. Di Padova, C. P. Gray, W. Keck, and S. Evers. (2001). Gene expression changes triggered by exposure of *Haemophilus influenzae* to novobiocin or ciprofloxacin: combined transcription and translation analysis. *Genome Res. 11*:28-42.

50. Guarné, A., Brendler, T., Zhao, Q., Ghirlando, R., Austin, S., & Yang, W. (2005). Crystal structure of a SeqA-N filament: implications for DNA replication and chromosome organization. *The EMBO Journal*, *24*(8): 1502–11.

51. Guarino, E., Salguero, I., Jimenez-Sanchez, A., and Guzman, E.C. (2007). Double-strand break generation under deoxyribonucleotide starvation in *Escherichia coli. J. Bacteriol. 189*: 5782-5786.

52. Hanawalt, P. C. (1963). Involvement of Synthesis of RNA in Thymineless Death. *Nature.* 168: 286

53. Hanawalt, P.C., MaalØe, O., Cummings, D.J., and Schaechter, M. (1961). The normal DNA replication cycle. II. *J. Mol. Biol. 3:* 156-165.

54. Handa, N., Morimatsu, K., Lovett, S. T., & Kowalczykowski, S. C. (2009). Reconstitution of initial steps of dsDNA break repair by the RecF pathway of *E. coli. Genes & Development, 23*(10): 1234–45.

55. Hardy, C. D., and N. R. Cozzarelli. (2003). Alteration of *Escherichia coli* topoisomerase IV to novobiocin resistance. *Antimicrob. Agents Chemother. 47*:941-947.

56. He, X. M., & Liu, H.-W. (2002). Formation of unusual sugars: mechanistic studies and biosynthetic applications. *Annual Review of Biochemistry, 71*: 701–54.

57. Heller, R. C., & Marians, K. J. (2006). Replisome assembly and the direct restart of stalled replication forks. *Nature reviews: Molecular Cell Biology*, 7(12): 932–43.

58. Hiasa, H. 2002. The Glu-84 of the ParC subunit plays critical roles in both topoisomerase IV-quinolone and topoisomerase IV-DNA interactions. Biochemistry 41**:**11779-11785.

59. Hiasa, H., R. J. DiGate, and K. J. Marians. (1994). Decatenating activity of *Escherichia coli* DNA gyrase and topoisomerases I and III during *oriC* and pBR322 DNA replication *in vitro. J. Biol. Chem. 269:*2093-2099.

60. Hiasa, H., and M. E. Shea. (2000). DNA gyrase-mediated wrapping of the DNA strand is required for the replication fork arrest by the DNA gyrase-quinolone-DNA ternary complex. *J. Biol. Chem. 275***:**34780-34786.

61. Hiasa, H., M. E. Shea, C. M. Richardson, and M. N. Gwynn. (2003). *Staphylococcus aureus* gyrase-quinolone-DNA ternary complexes fail to arrest replication fork progression *in vitro*: effects of salt on the DNA binding mode and the catalytic activity of *Staphylococcus aureus* gyrase. *J. Biol. Chem. 278***:**8861-8868.

62. Hill, C. W., & Harnish, B. W. (1981). Inversions between ribosomal RNA genes of Escherichia coli. *PNAS*, *78*(11): 7069–72.

63. Hill, W. E., & Fangman, W. L. (1973). Single-strand breaks in deoxyribonucleic acid and viability loss during deoxyribonucleic acid synthesis inhibition in *Escherichia coli. Journal of Bacteriology, 116*(3): 1329–35.

64. Hoffmann, J. S., Pillaire, M. J., Lesca, C., Burnouf, D., Fuchs, R. P., Defais, M., & Villani, G. (1996). Fork-like DNA templates support bypass replication of lesions that block DNA synthesis on single-stranded templates. *PNAS*, *93*(24): 13766–9.

65. Holzenkämpfer, M., M. Walker, A. Zeeck, J. Schimana, and H.-P. Fiedler. (2002). Simocyclinones, novel cytostatic angucyclinone antibiotics produced by *Streptomyces antibioticus* Tü 6040. II. Structure elucidation and biosynthesis. *J. Antibiot. 55***:**301-307.

66. Holzenkämpfer, M., and A. Zeeck. (2002). Biosynthesis of simocyclinone D8 in an $^{18}O_2$-rich atmosphere. *J. Antibiot.* 55**:**341-342.

67. Ippen-Ihler, K. A., & Minkley, Jr., E. G. (1986). The Conjugation System of F, the Fertility Factor of *Eschericia coli. Annual Review of Genetics, 20*: 593–624.

68. Jensen, P. R., C. C. van der Weijden, L. B. Jensen, H. V. Westerhoff, and J. L. Snoep. (1999). Extensive regulation compromises the extent to which DNA gyrase controls DNA supercoiling and growth rate of *Escherichia coli*. *Eur. J. Biochem*. *266*:865-877.

69. Jeong, K.S., Xie, Y., Hiasa, H., and Khodursky, A.B. (2006). Analysis of pleiotropic transcriptional profiles: a case study of DNA gyrase inhibition. *PLoS Genet. 2*: e152.

70. Jonsson, J. (1996). The evolutionary transition from uracil to thymine. *Journal of Chemometrics*. *10*: 163–170.

71. Kaguni, J. M. (2006). DnaA: controlling the initiation of bacterial DNA replication and more. *Annual Review of Microbiology, 60*: 351–75.

72. Kahlmeter, G. (2002). An international survey of the antimicrobial susceptibility of pathogens from uncomplicated urinary tract infections: the ECOmiddle dotSENS Project. *Journal of Antimicrobial Chemotherapy, 51*(1): 69–76.

73. Katayama, T., Ozaki, S., Keyamura, K., & Fujimitsu, K. (2010). Regulation of the replication cycle: conserved and diverse regulatory systems for DnaA and oriC. *Nature reviews: Microbiology. 8*(3): 163–70.

74. Kerr, M. K., M. Martin, and G. A. Churchill. (2000). Analysis of variance for gene expression microarray data. *J. Comput. Biol*. *7*:819-837.

75. Khodursky, A.B., Peter, B.J., Schmid, M.B., DeRisi, J., Botstein, D., Brown, P.O., and Cozzarelli, N.R. (2000). Analysis of topoisomerase function in bacterial replication fork movement: use of DNA microarrays. *PNAS. 97*: 9419-9424.

76. Khodursky, A.B., Bernstein, J.A., Peter, B.J., Rhodius, V., Wendisch, V.F., and Zimmer, D.P. (2003). *Escherichia coli* spotted double-strand DNA microarrays. RNA extraction, labeling, hybridization, quality control, and data management. *Methods Mol. Biol. 224*: 61-78.

77. Khodursky, A. B., E. L. Zechiedrich, and N. R. Cozzarelli. (1995). Topoisomerase IV is a target of quinolones in *Escherichia coli*. *Proc. Natl. Acad. Sci. USA 92*:11801-11805.

78. Klug, A. (1968). Rosalind Franklin and the Discovery of the Structure of DNA. *Nature*. *219*: 808–810, 843–844.

79. Kohanski, M.A., Dwyer, D.J., Hayete, B., Lawrence, C.A., and Collins, J.J. (2007). A common mechanism of cellular death induced by bactericidal antibiotics. *Cell. 130*: 797-810.

80. Kogoma, T. (1997). Is RecF a DNA replication protein? *PNAS*, *94*(8): 3483–4.

81. Kornberg, A., and Baker, T.A. (1992). *DNA replication,* 2nd edn. New York: Freeman.

82. Kubitschek, H. E., & Freedman, M. L. (1971). Chromosome Replication and the Division Cycle of *Escherichia coli* B / r. *Journal of Bacteriology, 107*(1): 95–99.

83. Kunzt, B. A., Glickmant, B. W., & Carolina, N. (1985). Mechanism of mutation by thymine starvation in *Escherichia coli* : Clues from Mutagenic Specificity. *Journal of Bacteriology.* 162(3):859.

84. Kuong, K. J., & Kuzminov, A. (2009). Cyanide, Peroxide and Nitric Oxide Formation in Solutions of Hydroxyurea Causes Cellular Toxicity and May Contribute to its Therapeutic Potency. *Journal of Molecular Biology. 390*(5): 845–862.

85. Kuong, K. J., & Kuzminov, A. (2010). Stalled replication fork repair and misrepair during thymineless death in *Escherichia coli*. *Genes to Cells. 15*(6), 619–34.

86. Kuong, K. J., & Kuzminov, A. (2012). Disintegration of nascent replication bubbles during thymine starvation triggers RecA- and RecBCD-dependent replication origin destruction. *The Journal of Biological Chemistry. 287*(13): 23958-23970.

87. Kurokawa, K., Nishida, S., Emoto, a, Sekimizu, K., & Katayama, T. (1999). Replication cycle-coordinated change of the adenine nucleotide-bound forms of DnaA protein in *Escherichia coli. The EMBO Journal*, *18*(23): 6642–52.

88. Kuzminov, A. (1999). Recombinational repair of DNA damage in Escherichia coli and bacteriophage lambda. *Microbiology and Molecular Biology Reviews : MMBR. 63*(4), 751–813.

89. Kuzminov, A., & Stahl, F. W. (1999). Double-strand end repair via the RecBC pathway in Escherichia coli primes DNA replication. *Genes Dev. 13:* 345–356.

90. Lark, K. G., & Afol, J. (1972). Evidence for the Direct Involvement of RNA in the Initiation DNA Replication in Escherichia coli UT- in in the absence of further protein was a gift from, 47–60.

91. Lark, K. G., Repko, T., Hoffman, E. J. (1963). The effect of amino acid deprivation on subsequent deoxyribonucleic acid replication. *Biochim. Biophys. Act. 76*: 9–24.

92. Lau, I. F., Filipe, S. R., Søballe, B., Økstad, O.-A., Barre, F.-X., & Sherratt, D. J. (2004). Spatial and temporal organization of replicating Escherichia coli chromosomes. *Molecular Microbiology, 49*(3): 731–743.

93. Lee, M. S., & Garrard, W. T. (1991). Positive DNA supercoiling generates a chromatin conformation characteristic of highly active genes. *PNAS*. *88*(21): 9675–9.

94. Little, J.G., and Hanawalt, P.C. (1973). Thymineless death and ultraviolet sensitivity in *Micrococcus radiodurans. J. Bacteriol. 113*:233-240.

95. Livak, K. J., and T. D. Schmittgen. (2001). Analysis of relative gene expression data using real-time quantitative PCR and the $2_T^{-\Delta\Delta C}$ method. *Methods 25*:402-408.

96. Longley, D.B., Harkin, D.P., and Johnston, P.G. (2003). 5-fluorouracil: mechanisms of action and clinical strategies. *Nat. Rev. Cancer. 3:* 330-338.

97. Lopes, M., Foiani, M., & Sogo, J. M. (2006). Multiple mechanisms control chromosome integrity after replication fork uncoupling and restart at irreparable UV lesions. *Molecular Cell. 21*(1): 15–27.

98. Low, K. B. (2010). Hfr Strains of *Eschericia coli* K-12. In *Eschericia coli* and *Salmonella*, 2nd Edition.

99. Maaløe, O., and Hanawalt, P.C. (2961). Thymine deficiency and the normal DNA replication cycle. I. *J. Mol. Biol. 3*: 144-155.

100. Maisnier-Patin, S., Nordström, K., & Dasgupta, S. (2001). Replication arrests during a single round of replication of the Escherichia coli chromosome in the absence of DnaC activity. *Molecular Microbiology, 42*(5): 1371–82.

101. Marszalek, J., & Kaguni, J. M. (1994). DnaA protein directs the binding of DnaB protein in initiation of DNA replication in Escherichia coli. *The Journal of Biological Chemistry*. *269*(7): 4883–90.

102. Martín, C. M., & Guzmán, E. C. (2011). DNA replication initiation as a key element in thymineless death. *DNA repair*. *10*(1): 94–101.

103. Maxwell, A. (1999). DNA gyrase as a drug target. *Biochem. Soc. Trans. 27*:48-53.

104. Mccarty, M., Avery, O. T., & MacLeod, C. M. (1944). Studies on the chemical nature of the substance inducing transformation of pneumococcal types: Induction of transformation by a deoxyribonucleic acid fraction isolated from *Pneumococcus* Type II. *The Journal of Experimental Medicine. 79*(2): 137–158.

105. McFall, E., and Magasanik, B. (1962). The effects of thymine deprivation on the synthesis of protein in *Escherichia coli. Biochim Biophys Acta. 55:* 920-928.

106. McInerney, P., & O'Donnell, M. (2007). Replisome fate upon encountering a leading strand block and clearance from DNA by recombination proteins. *The Journal of Biological Chemistry*, *282*(35): 25903–16.

107. Menzel, R., and M. Gellert. (1983). Regulation of the genes for *E. coli* DNA gyrase: homeostatic control of DNA supercoiling. *Cell 34***:**105-113.

108. Meselson, B. Y. M., & Stahl, F. W. (1958). The Replication of DNA in *Escherichia coli. PNAS*. *44*: 671–682.

109. Meyer, R.R., and Laine, P.S. (1990). The single-stranded DNA-binding protein of *Escherichia coli. Microbiol. Rev. 54:* 342-380.

110. Morganroth, P. A, & Hanawalt, P. C. (2006). Role of DNA replication and repair in thymineless death in *Escherichia coli. Journal of Bacteriology*. *188*(14): 5286–8.

111. Morimatsu, K., Wu, Y., & Kowalczykowski, S. C. (2012). RecFOR proteins target RecA protein to a DNA gap with either DNA or RNA at the 5' terminus: implication for repair of stalled replication forks. *The Journal of Biological Chemistry*. *287*(42): 35621–30.

112. Murakami, S., R. Nakashima, E. Yamashita, and A. Yamaguchi. (2002). Crystal structure of bacterial multidrug efflux transporter AcrB. *Nature 419***:**587-593.

113. Nakayama, H, & Hanawalt, P. (1975). Sedimentation analysis of deoxyribonucleic acid from thymine-starved *Escherichia coli. Journal of Bacteriology. 121*(2): 537–47.

114. Nakayama, Hiroaki. (2005). Escherichia coli RecQ helicase: a player in thymineless death. *Mutation Research. 577*(1-2): 228–36.

115. Nakayama, K., Kusano, K., Irino, N., & Nakayama, H. (1994). Thymine starvation-induced structural changes in Escherichia coli DNA. Detection by pulsed field gel electrophoresis and evidence for involvement of homologous recombination. *Journal of Molecular Biology. 243*(4): 611–20.

116. Nakayama, H., Nakayama, K., Nakayama, R., and Nakayama, Y. (1982). Recombination-deficient mutations and thymineless death in *Escherichia coli* K12: reciprocal effects of *recBC* and *recF* and indifference of *recA* mutations. *Canadian Journal of Microbiology. 28*: 425-430.

117. Nakayama, H., Nakayama, K., Nakayama, R., Irino, N., Nakayama, Y., and Hanawalt, P.C. (2984). Isolation and genetic characterization of a thymineless death-resistant mutant of *Escherichia coli* K12: identification of a new mutation (*recQ1*) that blocks the RecF recombination pathway. *Mol. Gen. Genet. 195:* 474-480.

118. Nakayama, K., Shiota, S., Nakayama, H. (1988) Thymineless Death in *Escherichia coli* mutants deficient in the RecF recombination Pathway. *Canadian Journal of Microbiology. 34*(7): 905-907.

119. Neddermann, P., & Jiricny, J. (1994). Efficient removal of uracil from G.U mispairs by the mismatch-specific thymine DNA glycosylase from *HeLa* cells. *PNAS. 91*(5): 1642–6.

120. Neuhard, J. (1966). Studies on the acid-soluble nucleotide pool in thymine-requiring mutants of *Escherichi coli* during thymine starvation. 3. On the regulation of the deoxyadenosine triphosphate and deoxycytidine triphosphate pools of *Escherichia coli. Biochim Biophys Act. 129*: 104-115.

121. Nguyen, D., Joshi-Datar, A., Lepine, F., Bauerle, E., Olakanmi, O., Beer, K., McKay, G., Siehnel, R., Schafhauser, J., Wang, Y., Britigan, B., Singh, P. K. (2011). Active starvation responses mediate antibiotic tolerance in biofilms and nutrient-limited bacteria. *Science. 334*(6058): 982–6.

122. Nikaido, H., and H. I. Zgurskaya. (2001). AcrAB and related multidrug efflux pumps of *Escherichia coli*. *J. Mol. Microbiol. Biotechnol. 3*:215-218.

123. O'Reilly, E.K., and Kreuzer, K.N. (2004). Isolation of SOS constitutive mutants of *Escherichia coli* K12. *Eur. J. Biochem. 60*: 57-66.

124. Odsbu, I., Morigen, & Skarstad, K. (2009). A reduction in ribonucleotide reductase activity slows down the chromosome replication fork but does not change its localization. *PloS One*, 4(10): 1-13.

125. Ohkawa, T. (1975). Studies of Intracellular Thymidine Nucleotides: Thymineless Death and the Recovery after Re-addtion of Thymine in *Eschericia coli* K12. *Eur. J. Biochem*. *60*: 57–66.

126. Olins, D. E., & Olins, A. L. (2003). Chromatin history: our view from the bridge. *Nature reviews: Molecular Cell Biology. 4*(10): 809–14.

127. Pan, X.-S., and L. M. Fisher. (1997). Targeting of DNA gyrase in *Streptococcus pneumoniae* by sparfloxacin: selective targeting of gyrase or topoisomerase IV by quinolones. *Antimicrob. Agents Chemother. 41*:471-474.

128. Pan, X.-S., and L. M. Fisher. (1999). *Streptococcus pneumoniae* DNA gyrase and topoisomerase IV: overexpression, purification, and differential inhibition by fluoroquinolones. *Antimicrob. Agents Chemother. 43*:1129-1136.

129. Pauling, C., and Hanwalt, P. (1965). Nonconservative DNA replication in bacteria after thymine starvation. *PNAS. 54*: 1728-1735.

130. Peng, H., and K. J. Marians. (1993). *Escherichia coli* topoisomerase IV. Purification, characterization, subunit structure, and subunit interactions*. J. Biol. Chem. 268*:24481-24490.

131. Peter, B. J., J. Arsuaga, A. M. Breier, A. B. Khodursky, P. O. Brown, and N. R. Cozzarelli. (2004). Genomic transcriptional response to loss of chromosomal supercoiling in *Escherichia coli*. *Genome Biol. 5*:R87.

132. Petit, C., & Sancar, A. (1999). Nucleotide excision repair: from *E. coli* to man. *Biochimie*. *81*(1-2): 15–25.

133. Pfeiffer, E. S., and H. Hiasa. (2004). The replacement of the α4 helix of ParC with that of GyrA increases the stability and the cyototoxicity of topoisomerase IV-quinolone-DNA ternary complexes. *Antimicrob. Agents Chemother. 48*:608-611.

134. Pohlhaus, J. R., Long, D. T., O'Reilly, E., & Kreuzer, K. N. (2008). The epsilon subunit of DNA polymerase III Is involved in the nalidixic acid-induced SOS response in *Escherichia coli. Journal of Bacteriology*. *190*(15): 5239–47.

135. Poole, K. (2001). Multidrug efflux pumps and antimicrobial resistance in *Pseudomonas aeruginosa* and related organisms. *J. Mol. Microbiol. Biotechnol*. 3:255-264.

136. Postow, L., C. D. Hardy, J. Arsuaga, and N. R. Cozzarelli. (2004). Topological domain structure of the *Escherichia coli* chromosome. *Genes Dev. 18*:1766-1779.

137. Possoz, C., Filipe, S. R., Grainge, I., & Sherratt, D. J. (2006). Tracking of controlled *Escherichia coli* replication fork stalling and restart at repressor-bound DNA in vivo. *The EMBO Journal. 25*(11): 2596–604.

138. Ramos, J. L., E. Duque, M. T. Gallegos, P. Godoy, M. I. Ramos-Gonzalez, A. Rojas, W. Teran, and A. Segura. (2002). Mechanisms of solvent tolerance in gram-negative bacteria. *Annu. Rev. Microbiol. 56***:**743-768.

139. Reiter, H., and Ramareddy, G. (1970). Loss of DNA behind the growing point of thymine-starved *Bacillus subtilis* 168. *J. Mol. Biol. 50*: 533-548.

140. Reyes-Lamothe, R., Sherratt, D. J., & Leake, M. C. (2010). Stoichiometry and architecture of active DNA replication machinery in *Escherichia coli. Science*. *328*(5977): 498–501.

141. Roberts, L., and S. Simpson. (2008). Deadly defiance. *Science 321***:**355.

142. Robertson, A. B., Klungland, A., Rognes, T., & Leiros, I. (2009). DNA repair in mammalian cells: Base excision repair: the long and short of it. *Cellular and Molecular Life Sciences. 66*(6): 981–93.

143. Rudolph, C. J., Upton, A. L., & Lloyd, R. G. (2007). Replication fork stalling and cell cycle arrest in UV-irradiated Escherichia coli. *Genes & Development. 21*(6): 668–81.

144. Sakai, A., & Cox, M. M. (2009). RecFOR and RecOR as distinct RecA loading pathways. *The Journal of Biological Chemistry. 284*(5): 3264–72.

145. Sandler, S J, Marians, K. J., Zavitz, K. H., Coutu, J., Parent, M. a, & Clark, a J. (1999). *dnaC* mutations suppress defects in DNA replication- and recombination-associated functions in *priB* and *priC* double mutants in *Escherichia coli* K-12. *Molecular Microbiology*. *34*(1): 91–101.

146. Sandler, S. J. (2005). Requirements for replication restart proteins during constitutive stable DNA replication in *Escherichia coli K-12*. *Genetics. 169*(4): 1799–806.

147. Sander, S.J. (2005) Chapter 2: Post-Replication Repair. From *DNA Damage and Repair*, *Vol. 3: Advances from Phage to Humans*. Humana Press Inc., Totowa, NJ.

148. Sangurdekar, D.P., Srienc, F., and Khodursky, A.B. (2006). A classification based framework for quantitative description of large-scale microarray data. *Genome Biol. 7*: R32.

149. Sangurdekar, D. P., Hamann, B. L., Smirnov, D., Srienc, F., Hanawalt, P. C., & Khodursky, A. B. (2010). Thymineless death is associated with loss of essential genetic information from the replication origin. *Molecular microbiology*. *75*(6): 1455–67.

150. Sangurdekar, D. P., Zhang, Z., & Khodursky, A. B. (2011). The association of DNA damage response and nucleotide level modulation with the antibacterial mechanism of the anti-folate drug trimethoprim. *BMC Genomics. 12*(1): 583.

151. Sassanfar, M., Roberts, J.W. (1990) Nature of the SOS-inducing Signal in *Escherichia coli* – the Involvement of DNA Replication. *Journal of Molecular Biology. 212*(1):79-96.

152. Sat, B., Reches, M., and Engelberg-Kulka, H. (2003). The *Escherichia coli mazEF* suicide module mediates thymineless death. *J. Bacteriol. 185*: 1803-1807.

153. Satoh, K., Kikuchi, M., Ishaque, A. M., Ohba, H., Yamada, M., Tejima, K., Onodera, T., Narumi, I. (2012). The role of *Deinococcus radiodurans* RecFOR proteins in homologous recombination. *DNA repair*. *11*(4): 410–8.

154. Schimana, J., H.-P. Fiedler, I. Groth, R. Süssmuth, W. Beil, M. Walker, and A. Zeeck. (2000). Simocyclinones, novel cytostatic angucyclinone antibiotics produced by *Streptomyces antibioticus* Tü 6040. I. Taxonomy, fermentation, isolation and biological activities. *J. Antibiot. 53***:**779-787.

155. Sclafani, R. A, & Holzen, T. M. (2007). Cell cycle regulation of DNA replication. *Annual Review of Genetics*. *41*: 237–80.

156. Sekimizus, K., Bramhillq, D., & Kornberg, A. (1988). Sequential Early Stages in the in Vitro Initiation of Replication at the Origin of the *Escherichia coli* Chromosome. *Journal of Biological Chemistry*. *263*(15): 7124–7130.

157. Sicard, N., & Bouvier, F. (1975). Interference of *dna* ^{ts} Mutations of *Escherichia coli* with Thymineless Death. *Journal of Bacteriology. 124*(3): 1198–1204.

158. Skarstad, K., & Boye, E. (1988). Perturbed chromosomal replication in *recA* mutants of *Escherichia coli*. *Journal of Bacteriology. 170*(6): 2549–54.

159. Skarstad, K., & Boye, E. (1993). Degradation of individual chromosomes in *recA* mutants of *Escherichia coli. Journal of Bacteriology. 175*(17), 5505–9.

160. Sklar, L. (2005). *Flow Cytometry for Biotechnology,* 1st edn. Oxford University Press, USA.

161. Stuger, R., C. L. Woldringh, C. C. van der Weijden, N. O. E. Vischer, B. M. Bakker, R. J. M van Spanning, J. L. Snoep, and H. V. Weterhoff. (2002). DNA supercoiling by gyrase is linked to nucleoid compaction. *Mol. Biol. Rep. 29***:**79-82.

162. Tanaka, M., K. Sato, Y. Kimura, I. Hayakawa, Y. Osada, and T. Nishino. (1991). Inhibition by quinolones of DNA gyrase from *Staphylococcus aureus*. *Antimicrob. Agents Chemother. 35*:1489-1491.

163. Taubes, G. (2008). The bacteria fight back. *Science 321*:356-361.

164. Theobald, U., J. Schimana, and H.-P. Fiedler. (2000). Microbial growth and production kinetics of *Streptomyces antibioticus* Tü 6040. *Antonie van Leeuwenhoek 78*:307-313.

165. Tikhonova, E. B., and H. I. Zgurskaya. (2004). AcrA, AcrB, and TolC of *Escherichia coli* form a stable intermembrane multidrug efflux complex. *J. Biol. Chem. 279*:32116-32124.

166. Tusher, V. G., R. Tibshirani, and G. Chum. (2001). Significance analysis of microarrays applied to the ionizing radiation response. *Proc. Natl. Acad. Sci. USA 98*:5116-5121.

167. Tusher, V.G., Tibshirani, R., and Chu, G. (2001). Significance of microarrays applied to the ionizing radiation response. *PNAS. 98*: 5116-5121.

168. Wahles, E., Laskenb, R. S., & Kornberg, A. (1989). The *dnaB-dnaC* Replication Protein Complex of *Escherichia coli.* II. Role of the complex in mobilizing *dnaB* functions. *Journal of Biological Chemistry. 264*(5): 2469–2475.

169. Walker, J. R. (1970). Thymine Starvation and Single-Strand Breaks in Chromosomal Deoxyribonucleic acid of *Escherichia coli. Journal of Bacteriology*. *104*(3): 1391–2.

170. Wang, J. C. (2002). Cellular roles of DNA topoisomerases: a molecular perspective. *Nat. Rev. Mol. Cell Biol. 3*:430-440.

171. Wang, X., Lesterlin, C., Reyes-Lamothe, R., Ball, G., & Sherratt, D. J. (2011). Replication and segregation of an *Escherichia coli* chromosome with two replication origins. *PNAS*. *108*(26): 243–50.

172. Warner, H.R., Duncan, B.K., Garrett, C., and Neuhard, J. (1981). Synthesis and metabolism of uracil-containing deoxyribonucleic acid in *Escherichia coli. J. Bacteriol. 145*: 687-695.

173. Warners, H. R. (1978). Uracil incorporation : A source of pulse-labeled DNA fragments in the replication of the *Escherichia coli* chromosome. *PNAS.* 75(1): 233–237.

174. Watson, J., & Crick, F. (1953). Molecular structure of nucleic acids. *Nature*. *171*(4356): 737–738.

175. Webb, B. L., Cox, M. M., & Inman, R. B. (1997). Recombinational DNA repair: the RecF and RecR proteins limit the extension of RecA filaments beyond single-strand DNA gaps. *Cell. 91*(3): 347–56.

176. Wechsler, J A. (1975). Genetic and phenotypic characterization of *dnaC* Genetic and Phenotypic Characterization of *dnaC* Mutations. *Journal of Bacteriology. 121*(2):594

177. Wechsler, James A., & Gross, J. D. (1971). *Escherichia coli* Mutants Temperature-Sensitive for DNA Synthesis. *Molecular & General Genetics. 284*(3): 273–284.

178. Withers, H. L., & Bernander, R. (1998). Characterization of *dnaC2* and *dnaC28* Mutants by Flow Cytometry. *Journal of Bacteriology. 180*(7): 1624-31.

179. Wu, H., Kerr, M.K., Cui, X., and Chruchill, G.A. (2003). MAANOVA: a software package for the analysis of spotted cDNA microarray experiments. In: *The Analysis of Gene Expression Data: Methods and Software.* Parmigiani, G., Garrett, E.S., Irizarry, R.A., and Zeger, S.L. (eds). New York, NY: Springer, pp. 313-341.

180. Wus, C. A., Zechnero, E. L., & Marians, K. J. (1992). Coordinated Leading- and Lagging-strand Synthesis at the *Escherichia coli* DNA Replication Fork. *Journal of Biological Chemistry.* 267(6): 4030–4044.

181. Yoshinaga, K. (1973). Double-strand scission of DNA involved in thymineless death of *Escherichia coli* 15 TAU. *Biochim. Biophys. Acta. 294*: 204-213.

182. Zahradka, K., Buljubasić, M., Petranović, M., & Zahradka, D. (2009). Roles of ExoI and SbcCD nucleases in “reckless” DNA degradation in *recA* mutants of *Escherichia coli*. *Journal of Bacteriology. 191*(5): 1677–87.

183. Zaritsky, A., Woldringh, C. L., Einav, M., & Alexeeva, S. (2006). Use of Thymine Limitation and Thymine Starvation To Study Bacterial Physiology and Cytology. *Journal of Bacteriology. 188*(5): 1667.

Appendix

A1. Interpretation of Flow Cytometry Data.

Flow cytometry data acquisition is set by the user of the flow cytometer, and in my case included forward scatter, side scatter (both involved in size determination), and readings from all three fluorescence filters. For the FACSCalibur this included FL1 (530±30nm), FL2 (585±42nm), and FL3 (≥670nm)filters). I did not set thresholds on data acquisition for any of those parameters during acquisition and instead chose to set thresholds after acquisition during data analysis. The downside to this approach is that a number of 'events' measured by the machine may simply be noise, and can take up valuable data space in the 100,000 event quota I set, however I tried to overcome this limitation by working with multi-filtered running buffer so that over the course of two minutes, I had fewer than 5000 events with buffer plus dye. Since most of my experimental runs lasted less than 60 seconds, less than 2.5% of the events could be attributed to noise for the flow experiments, and this could be parsed out by gating.

I used FlowJo 7.6 software to visualize and examine data from flow cytometry experiments. Since 'gating' or selecting which part of the data to consider significant is a highly subjective process, I describe my methodology below (which is illustrated in Figure A1.1). The data was visualized with at least two parameters. In the top graph I have the data shown with side-scatter on the y-axis and forward-scatter on the x-axis to differentiate between cell events and non-cell events by size. Because the difference was relatively clear I could create a large gate that eliminated a large part of the buffer 'noise' based on size. Taking the events within that gate I could discriminate cells based on propidium iodide fluorescence which measured nucleic acid content. The bulb used in the FACSCalibur for these experiments emits at a 488nm wavelength which can excite a number of nucleic acid staining dyes. Since propidium iodide has an increased fluorescence of at least 50 –fold upon binding the minor groove of duplex nucleic acids (Sklar, 2005), and propidium iodide emits in the 615nm wavelength, it was much easier to collect only the most fluorescent events (which appeared the ≥690nm filter range),resulting in much cleaner peaks. While thymine starvation results in a number of anucleate cells which can convolute data analysis, I removed the effects of auto-fluorescence by gating between stained

and unstained cells. These gates were used for all samples in the experiment for which they were collected so that I could have a reference for a consistent comparison based on gating.

When I started working with propidium iodide, I encountered difficulties finding the optimal concentration of RNase A to use and for what time period to RNase treat my samples as I tended to get varying results depending on time of RNase treatment. I finally settled on a 2 hour treatment as it resulted in the greatest reduction in peak noise (the peaks became tighter and more pronounced), and treating past 2 hours did not improve peak quality. Overnight treatment resulted in some degradation of the DNA in the cells (resulting in broad, or non-existent peaks upon staining and measurement by flow cytometry). I found this to be an improvement in my work as compared to other published experimental set-ups which use RNase treatment for only 10-20 minutes before staining for flow cytometry work (Bernander et al., 1998; Skarstad & Boye, 1993).

I also encountered problems when displaying overlapping samples in the FlowJo 7.6 software. While the program would allow direct overlapping of samples, the program would not stretch or shrink the data of sample 2 to match the access of the data from sample 1, it would over-write the axis of sample 1 (Figure A.2). Therefore I displayed data in this thesis on a linear scale, although sometimes doing so made direction comparison difficult.

A2. Casamino acid supplementation results in higher numbers of viable replication forks per cell

For the 2010 Molecular Microbiology publication I grew my W3110 background strains in a minimal media that was supplemented with 0.4% glucose, but not casamino acids. Later as I began working with temperature-sensitive *thyA*- strains, I found that these strains grew very slowly unless they were supplemented with casamino acids. This is a problem because slow-growing cells tend to escape thymine starvation more readily than faster growing cells. Other groups studying thymine-less death also used casamino acids in concentrations ranging from 0.2-0.5% (in the same M9 minimal media, usually supplemented with 0.4 % glucose). When I grew my original W3110 background strains in M9 media of the some composition but supplemented with 0.2% casamino acids, not only did they spend a shorter period in lag phase

before entering exponential growth, but they suffered a greater loss in viability when starved of thymine. This was true of K-12 strains whether they had a mutation in the *deo* operon (which reduced the thymine requirement for the strain) or not (Figure A.1). While the doubling time of cells supplemented with the casamino acids was half that of cells grown in the same media except without casamino acids, the difference in viability was several fold greater than the fold-change in growth rate.

To see if something other than growth rate was responsible for the difference in viability I used replication run-out to measure the number of viable replication forks in each growth medium. I used the MG1655 background *thyA*$^-$ strain for replication run-out as it does not have a *deo* mutation. *Deo* mutations lower the thymine requirement of a strain (Ahmad et al., 1998). Replication run-out of these cells grown and starved of thymine with and without casamino acid supplementation shows that not only do cells grown in the presence of casamino acids have more viable replication forks per cell than those not supplemented (Figure A.2 exponential), but cells not supplemented with casamino acids also maintain viable replication forks as well as nucleic acid content later into thymine starvation. It is possible that since there are fewer replication forks at the beginning of thymine starvation, there are fewer locations for incorporation of thymine, and so it is more likely that those cells with fewer forks will reach completion of replication than in cells which have more replication forks progressing simultaneously.

Figure A.1 How control samples were gated in FlowJo 7.6 software

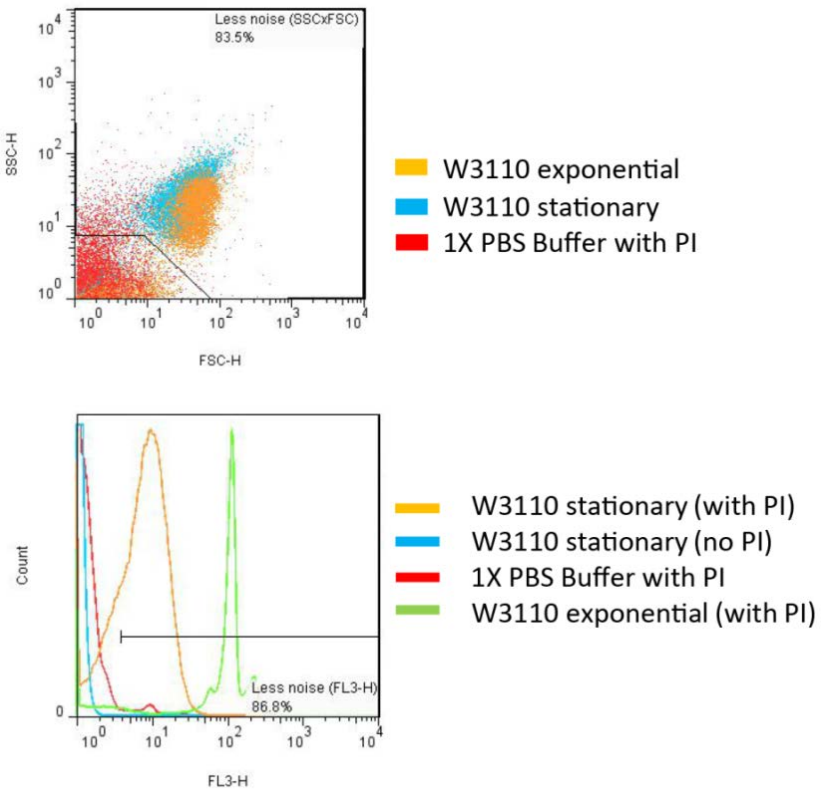

Figure A.2 FlowJo 7.6 output when data is overlapped. A.) Individual samples graphed on a linear scale have their own individual x-axis values. B.) Overlapping the linear scale graphs results not only in adjustment of the x-axis in the overlapping graph but *also of the individual graphs* even though the data hasn't been altered (compare to data in A). C.) Individual samples graphed on a log scale have similar x-axis values. D.) Overlapping log-scale samples results in no alteration of the data or x-axis values-I used this method for displaying data in chapters 3 and 4 of this thesis.

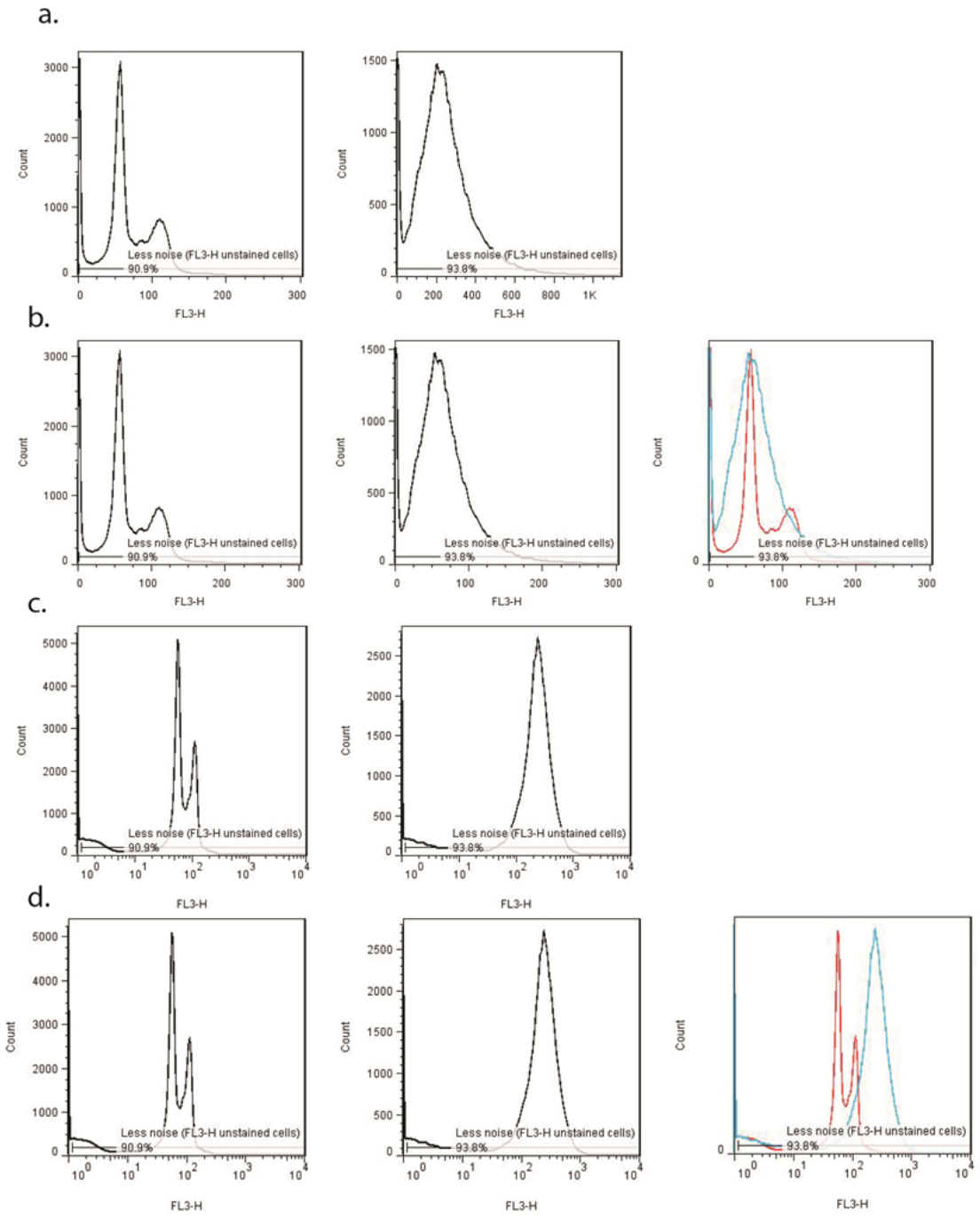

Figure A.3. Percent survival as compared to 0 minutes starvation of *thyA*⁻ strains when starved of thymine for three hours in M9 media (0.4% glucose, 10µ/mL thiamine, 5µg/mL uracil) with and without 0.2% casamino acids. A. MG1655 background (Δ*thyArecF::KAN*) B. W3110 background (*thyA*36, *deoC*2 with or without *recF*6206) C. Viability of W3110 background strain CL001 after three hours starvation as compared to the same strain where the *thyA36* allele (point mutation) has been replaced with a kanamycin resistance cassette to form a complete knock-out/gene replacement showing that knock-out and point mutation result in an indistinguishable loss of viability.

a.

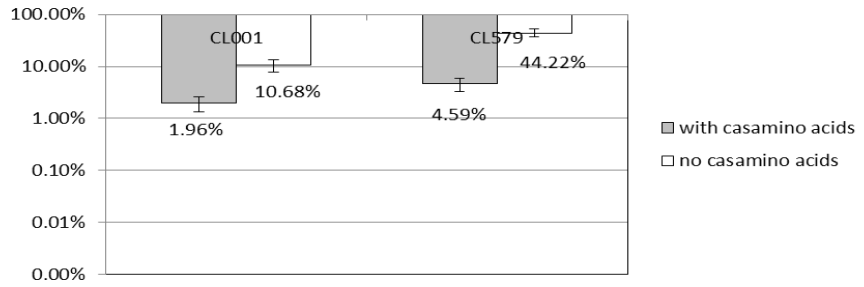

b.

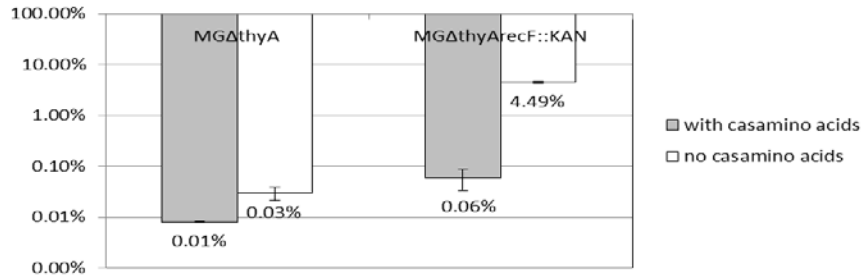

c.

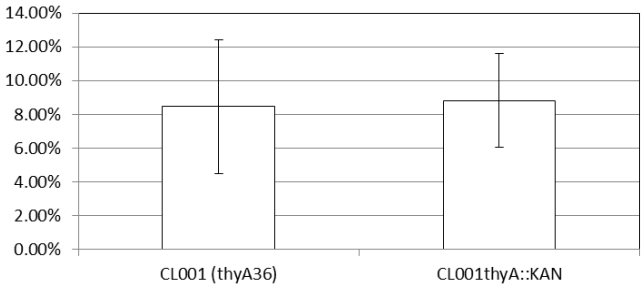

Figure A.4. Replication run-out of MG1655 Δ*thyA* cells grown with and without casamino acids to exponential growth in M9 minimal media with glucose, and starved for thymine in exponential growth. Higher fluorescence indicates more chromosomal equivalents in that population of cells.